Formules infantiles modèles : Relation entre structures protéiques et comportement en digestion Modification du profil protéique, de la teneur en matière sèche et de la température de traitement

Amira Halabi

▶ **To cite this version:**

HAL Id: tel-03340179

https://hal.inrae.fr/tel-03340179v1

Submitted on 24 Nov 2020 (v1), last revised 10 Sep 2021 (v2)

THESE DE DOCTORAT DE

AGROCAMPUS OUEST

Par

Amira HALABI

Formules infantiles modèles :
Relation entre structures protéiques et comportement en digestion
Modification du profil protéique, de la teneur en matière sèche et de la température de traitement

Rapporteurs avant soutenance :

Claire BOURLIEU-LACANAL	Chargée de Recherche, INRAE, Montpellier, France
Paul MENUT	Professeur, AgroParisTech, Paris, France

Composition du Jury :

Président:	Paul MENUT	Professeur, AgroParisTech, Paris, France
Examinateurs:	Lotti EGGER	Biochemistry teamleader, Agroscope, Suisse
	Marieke VAN AUDENHAEGE	Responsable Pôle technologie laitière, SODIAAL, Rennes, France
Directeur de thèse	Thomas CROGUENNEC	Professeur, Institut Agro, Rennes, France
Co-directrice de thèse	Amélie DEGLAIRE	Maître de conférences, Institut Agro, Rennes, France

Titre : Formules infantiles modèles : relation entre structures protéiques et comportement en digestion

Mots clés : formules infantiles modèles ; lactoferrine ; traitement thermique ; structure protéique ; digestion *in vitro*

Résumé : Les traitements thermiques appliqués pendant la fabrication des préparations pour nourrissons (PPNs) peuvent altérer les structures des protéines et donc leur comportement au cours de la digestion. L'objectif de ce projet de thèse était d'étudier la relation entre la structure des protéines au sein de PPNs modèles et leur comportement au cours de leur digestion *in vitro*.

Trois PPNs modèles ont été développées, se différenciant par leur profil en protéines du lactosérum (PS) afin de se rapprocher du profil protéique du lait maternel. Les PPNs, avec différentes teneurs en matière sèche et donc concentration protéique (1.3% ou 5.5%), ont été traitées thermiquement entre 67.5°C et 80°C. La cinétique de dénaturation thermique des PS a été étudiée puis les structures protéiques générées ont été caractérisées pour un même taux de dénaturation des PS (65%). La cinétique de digestion protéique a été évaluée en digestion *in vitro* statique puis dynamique, simulant les conditions physiologiques du nourrisson.

Les résultats ont montré que la cinétique de dénaturation des PS était ralentie pour la PPN proche du lait maternel de par l'absence de β-LG, et ce indépendamment de la teneur en matière sèche. Pour un même taux de dénaturation des PS, la structure protéique des PPNs variait selon la composition protéique des PPNs, leur teneur en matière sèche et les conditions thermiques, ce qui, *in fine*, impactait le devenir des protéines au cours de la digestion *in vitro*.

La structure des protéines pourrait donc être un levier pour l'optimisation des PPNs. Ces résultats doivent être complétés par l'évaluation de l'impact physiologique de ces différentes structures.

Title: Model infant milk formulas: relationship between protein structures and digestive behaviour

Keywords: model infant milk formulas; lactoferrin; heat treatment; protein structures; *in vitro* digestion

Abstract : The heat treatments applied during the manufacture of infant milk formulas (IMFs) may alter the protein structures and so their behaviour during digestion. The aim of this PhD project was to study the relationship between protein structure within model IMFs and their behaviour during *in vitro* digestion.

Three model IMFs were formulated, differing only in their whey protein (WP) profile to be as close as possible to the protein profile of human milk. The IMFs, with different dry matter contents and therefore protein concentration (1.3% or 5.5%), were heat-treated between 67.5°C and 80°C. The kinetics of heat-induced WP denaturation were studied, then the protein structures generated were characterised for an identical extent of WP denaturation (65%). The kinetics of protein hydrolysis were evaluated using static then dynamic *in vitro* digestion methods at the infant stage.

The results showed that the denaturation kinetics of WPs were slowed down for IMF close to human milk due to the absence of β-LG, regardless of the dry matter content. For an identical extent of WP denaturation, the heat-induced protein structures varied according to the protein profile, the dry matter of IMFs, and the heating conditions, which ultimately impacted the protein behaviour during *in vitro* digestion.

The protein structure could therefore be a lever for the IMF optimisation. These results must be complemented by the evaluation of the physiological impact of these different structures.

Acknowledgments

A l'issue de ces trois années riches au sein du STLO, voici le temps des remerciements. J'espère n'oublier personnes, et si c'est le cas, je m'en excuse par avance. Je tiens à remercier chaleureusement toutes les personnes qui, de près ou de loin, ont contribué à l'accomplissement de ce travail de thèse.

Dans un premier temps, je remercie les membres du jury, **Claire Bourlieu-Lacanal**, **Lotti Egger**, **Marieke Van Audenhaege** et **Paul Menut**, pour avoir accepté de juger mes travaux de thèse.

J'exprime mes profonds remerciements à **Thomas** et **Amélie**. Vous avez été d'un soutien indéniable au cours de ces trois années, aussi bien scientifiquement qu'émotionnellement. Merci pour votre confiance et vos précieux conseils. Votre expertise, votre disponibilité et votre gentillesse ont été des éléments clés pour le bon déroulement de ce projet.

Je remercie également **Yves**, pour m'avoir accueilli au sein du STLO, **Said** et **Didier**, pour nos discussions très intéressantes qui m'ont permis d'aborder ce projet sous différents angles de vue. C'est également grâce à vous que j'ai eu l'occasion de participer à plusieurs congrès à l'international, qui ont été de supers expériences.

Un grand merci aux collaborateurs de ce projet. Merci à **Marie Hennetier** et **Frédéric Violleau** ainsi que leur équipe d'ingénieurs pour leur formidable accueil dans leurs locaux à Purpan (Toulouse) et pour la qualité de leur formation sur la technique d'AF$_4$. Merci également à **Agnès Burel** pour la formation à la microscopie électronique.

Juliane et **Lucie L.**, mes encadrantes de stage de fin d'étude, merci à vous pour m'avoir encouragé à poursuivre dans la recherche. Ce stage aura été un élément déclencheur pour que je me décide à continuer dans la recherche.

Je remercie également tous les permanents du STLO pour leur accueil et leur bonne humeur. Je tiens particulièrement à adresser mes remerciements à **Pascaline** et **Fabienne** pour avoir été les Mme Bricoleuse de la RP-HPLC, à **Arlette** pour ton aide pour la quantification des minéraux, **Olivia**, « Mme Digestion », pour ton aide précieuse pour mes expériences de digestion et, au-delà, pour ta constante bonne humeur. Merci à **Gwen** pour les analyses d'acides aminés et à **Yann** et **Jordane** pour les analyses en microscopie confocale. Je tiens particulièrement à remercier les équipes ISF et BN ; merci pour les petites douceurs au cours de nos réunions d'équipe et pour les discussions et conseils scientifiques, qui m'ont permis de prendre du recul sur ma thèse.

Je tiens également à remercier les personnes qui contribuent tous les jours à la bonne gestion du laboratoire : **Nathalie L., Laurence, Danielle, Jessica, Michel, Sébastien, Sylvie, Anne G.** et **Rachel**.

J'ai eu la chance d'avoir plusieurs collègues de bureau au cours de ces trois années. Merci **Xiaoxi** pour les nombreuses manips reprises en relai, **Catherine** pour ton sourire permanent et ta joie de vivre, **Aurélie**, pour tes astuces informatiques et **Nathalie**, pour tes conseils « comment prendre une pause pour être plus efficace ».

Merci à tous les doctorants, post-doctorants, stagiaires et autres que j'ai eu la chance de rencontrer au cours de ces trois années. Je tiens également à remercier mes amies rencontrées au cours de mes études d'ingé, **Dahlia, Mélissa, Mélanie** : bon courage pour la suite de votre doctorat.

Et enfin, le meilleur pour la fin : ma famille. Tout simplement, merci ! Merci pour votre soutien, vos encouragements et votre patience. Plus particulièrement, à mes parents, merci pour tous les sacrifices que vous avez faits pour que l'on devienne les personnes d'aujourd'hui. Je tiens également à dédicacer ce manuscrit à **Henna Zahra** (Allah y Rahma), qui me demandait toujours « L'école, ça va ? ».

List of contents

List of abbreviations

α-LA: α-lactalbumin

AF_4: asymmetric flow field flow fractionation

ARA: arachidonic acid

β-LG: β-lactoglobulin

CPP: casein phosphopeptide

d_f: fractal dimension

DH: degree of hydrolysis

DHA: docosahexaenoic acid

D-value: decimal reduction time

Ea: activation energy

ESPGHAN: European Society for Paediatric Gastroenterology Hepatology and Nutrition

FDA: Food and Drug Administration

FOS: fructo-oligosaccharide

GMP: glycomacropeptide

GOS: galacto-oligosaccharide

HTST: high-temperature short-time

Ig: immunoglobulin

IMF: infant milk formula

k: reactive rate constant

k_0: denaturation/aggregation frequency factor

kDa: kiloDalton

LCPUFA: long-chain polyunsaturated fatty acid

LF: lactoferrin

MALS: multi-angle light scattering

M_w: molecular weight

n: reaction order

OPA: *o*-phtalaldehyde

Pan: pancreatin

pI: isoelectic point

PPN: préparation pour nourrissons

R: universal gas constant

R_h: hydrodynamic radius

R_g: gyration radius

RP-HPLC: reverse phase-high performance liquid chromatography

SDS-PAGE: sodium dodecyl sulfate-polyacrylamide gel electrophoresis

SGF: simulated gastric fluid

SIF: simulated intestinal fluid

SMP: Skim milk powder

TAME: Tail-Associated Muralytic Enzyme

TEM: transmission electronic microscopy

UHT: ultra-high temperature

UNICEF: United Nations Children's Fund

WHO: World Health Organisation

WPI: whey protein isolate

WPNI: whey protein nitrogen index

Figure contents

Table contents

Supplementary material contents

General introduction

The World Health Organisation (WHO) recommends exclusive breastfeeding for the first six months of life and partial breastfeeding for up to 2 years. Indeed, human milk is recognised as the «gold standard» for infant nutrition due to its adequate composition of essential nutrients and specific bioactive components only available in human milk (Alles et al., 2004).

In France, in 2011, 70% of infants were breastfed during the first days of life, while only 20% were exclusively fed human milk at three months of life (Wagner et al., 2015). The decision to breastfeed is personal but can be influenced by socio-economic, cultural, religious and health factors (Maharlouei et al., 2018). When breastfeeding is not an option or a desire, infant formulas constitute an adequate human milk substitute.

Infant formulas are defined as a breastmilk substitute specially manufactured to meet the nutritional requirements of infants during the first months of life up to the introduction of an appropriate complementary feeding. Thus, the main objective of infant formula manufacturers is to attempt to mimic the composition and the performance of human milk. Infant formulas are available in powdered or liquid forms, with a prevalence for the powdered form in France. In 2017, the French market of powdered infant formulas represented 141 531 T (i.e. 1061 M of L) compared to 96 M of L for liquid infant formulas (FranceAgriMer, 2018). Powdered infant formulas are easy to transport and to store, while liquid infant formulas are more convenient to use. Currently, infant formulas are mostly formulated based on bovine milk, which is different in composition from human milk. Every effort has been made to develop infant formulas mimicking as close as possible the nutrition profile of human milk. Particularly, one possibility of infant formula optimisation is to mimic the protein profile of human milk. Proteins influence major functions of the body like growth, body composition, neurodevelopment, appetite and hormonal regulation (Michaelsen & Greer, 2014). By simulating the protein profile of human milk, the protein content of infant formulas could be reduced while respecting the regulatory aminogram of human milk. The reduction of protein content of IMFs could prevent health issues for infants, as the risk of overweight and obesity later in life (Michaelsen & Greer, 2014).

The processing technology for infant formulas consists of a succession of steps during which heat treatments are applied to guarantee the microbiological safety and to extend the shelf life. Depending on the heating conditions, the extent of whey protein denaturation and the structure of milk proteins are differently affected, varying potentially the functional properties and nutritional value of infant formulas. Many studies have been conducted on the denaturation kinetics of whey proteins (Douglas G. Dalgleish et al., 1997; Dannenberg & Kessler, 1988; Oldfield et al., 1998; Sánchez et al., 1992), on the properties of the heat-induced protein structures (Anema & Klostermeyer, 1997; Patel et al., 2006; Sutariya et al., 2017; Vasbinder & de Kruif, 2003) and on the heating effects on digestibility (Tunick et

al., 2016; Ye et al., 2017). Nevertheless, these studies cannot be extrapolated to infant formulas as the milk protein behaviour during heating depends on many factors such as protein content (Muditha Dissanayake et al., 2013), protein profile (Beaulieu et al., 1999; Crowley et al., 2016; Oldfield et al., 1998), heating temperature, holding time (Qian et al., 2017) and pH (Vasbinder & de Kruif, 2003). To our knowledge, only a few studies have been conducted on infant formulas (Buggy et al., 2017; Crowley et al., 2016), and even less on those mimicking the protein profile of human milk. To fill the gap, the objective of the present thesis was to answer to the question:

What are the protein structures generated during the heating of model infant formulas and how do they impact the digestion kinetics of milk proteins at the infant stage?

The present work is divided into eight chapters. **Chapter 1** is dedicated to the current knowledge about the bovine-based infant formulas, their manufacture, the denaturation mechanism of milk proteins during heating and the protein digestion by infants. **Chapter 2** describes the objectives and strategies of the thesis. **Chapter 3** presents the material and methods used during the thesis. **Chapters 4-7** address the main results of the work, which are concomitantly discussed. In **chapter 4**, the kinetics of whey protein denaturation are described, the heat-induced protein structures are characterized in **chapter 5**, and the influence of the latter on the infant gastrointestinal digestion based on *in vitro* study is investigated under static conditions in **chapter 6** or dynamic conditions in **chapter 7**. Finally, **chapter 8** presents a general discussion and the main lines of research to be pursued to complete the present work.

Chapter 1 - Literature review

1. Bovine milk based-infant formulas, a substitute of human milk

1.1. Infant nutritional recommendations

The development of infants during the first 2 years of life require specific nutritional needs. The adequate supply of nutrients (in terms of quantity and quality) during early life modulates the differentiation of tissues and organs, and has short- and long-term consequences for lifelong health and well-being (Koletzko, 2008). Human milk is recognised as the gold standard for infant nutrition thanks to its nutritional composition and bioactive factors, allowing the suitable physiological development of infants during the first months of life.

Various health organisations such as the World Health Organization (WHO), the UNICEF, the American Academy of Pediatricians and the European Society for Paediatric Gastroenterology Hepatology and Nutrition (ESPGHAN) recommend exclusive breastfeeding for the first six months of life, followed by breastfeeding along with appropriate complementary foods up to 2 years old and beyond (Agostoni et al., 2009; World Health Organization & UNICEF, 2003). Many benefits are associated to breastfeeding, for both the infant and the mother. The benefits of breastfeeding for the infant are the lower risk of necrotising enterocolitis and diarrhoea, allergy and asthma, inflammatory bowel and cardiovascular diseases, and in the long term, a lower risk of type II diabetes and obesity (Turck et al., 2013; Victora et al., 2016). The benefits of breastfeeding for the mother are a reduction of postpartum maternal bleeding, an easier postpartum weight loss and a potential risk reduction for type II diabetes, cardiovascular disease or breast cancer (Godfrey & Lawrence, 2010).

However, despite the WHO recommendation, about 40% of infants under 6 months of age are exclusively breastfed worldwide (UNICEF & WHO, 2017). More precisely, UNICEF pointed the disparity of breastfeeding practices amongst countries. In 2017, 1 in 5 infants were never breastfed in high-income countries, compared to 1 in 25 in low- and middle-income countries, with sociocultural and economic factors influencing the breastfeeding decisions (UNICEF, 2018). At a national scale, the proportion of breastfed infants at 6 months of life (approximatively 20%) is among the lowest across European and North American countries (Cattaneo et al., 2010; Wagner et al., 2015). As a consequence, a large proportion of the French infants are fed with infant formulas (80% at 3 months of age; Wagner et al., 2015).

1.2. Infant formulas

Infant formulas are defined as a food intended for use by infants during the first months of life and satisfying by itself the nutritional requirements of such infants until the introduction of appropriate complementary feeding (European Commission, 2006).

1.2.1. History

During the 19th century, a wet nurse was the safest alternative to breastfeeding, particularly if the birth mother could not breastfeed the infant. Nevertheless, by 1860, the German chemist Justus von Leibig developed the first commercial infant food, a powdered formula made from bovine milk, wheat flour, malt flour, and potassium bicarbonate. In the late 19th century, many scientists believed that infant formulas were nutritionally inadequate and therefore inappropriate for infants. The American paediatrician Thomas Morgan Rotch developed in the 1890's the "percentage method", based on the disparity of casein amount between human and bovine milks. The dilution of bovine milk aimed to lower the casein amount, but, at the same time, it decreased the sugar and fat content to less than that of human milk. To correct these deficiencies, cream and sugar were added in precise amounts (Apple, 1988). In the same time, dairy industries began to develop adequate sterilisation and pasteurisation techniques, which improved handling and storage conditions for milk (Obladen, 2014). In the early 20th century, the focus of nutrition scientists shifted from modifying the protein content of infant formulas to making their carbohydrate and fat contents closer to those of human milk. Today, the composition of infant formulas is strictly regulated, and each manufacturer must follow established guidelines set by government agencies.

1.2.2. Regulations

There is currently a large offer of infant formulas, with nearly 148 references listed for the French market (Bocquet et al., 2015). Infant formulas can be classified according to different criteria, according to the European Union (2016):

- the age of infants:
  - first-stage formula (1st age): from birth to 6 months
  - follow-on formula (2nd age): 6-12 months of age, in complement to dietary diversification
  - growing-up formula (3rd age): 12-36 months of age
- the nature of protein source:
  - bovine milk proteins (used in most infant formulas)
  - goat milk proteins
  - soy protein isolates

For the rest of the manuscript, the term "infant formulas" or "infant milk formulas" corresponds to 1st age bovine milk-based infant formulas. Regulations are adapted for each category of infant formulas in order to provide appropriate intake of nutrients during infancy. By 1980, the first Codex Alimentarius standard for infant formulas was published, which outlined the nutritional requirements (Codex Alimentarius Commission, 1981) (Figure 1). Since then, the European Commission regulates the minimum and maximum levels of energy, proteins, macro- and micro-nutrient contents, as well as the authorised/approved ingredients in infant formulas (Table 1). Currently, these products are specifically covered by the Commission Directive 2006/141/EC (European Commission, 2006). The Commission delegated Regulation (EU) 2016/127 (European Union, 2016) was adopted on 25 September 2015 and is effective since February 2020. This last regulation mainly indicates a reduction of protein content to prevent from potential "metabolic stress" such as obesity, the source of hydrolysed proteins limited to bovine proteins, and the mandatory addition of docosahexaenoic acid (DHA), in a range of 13-32.5 mg/100 mL, to ensure a proper infant neurodevelopment. Some other nutritional changes include an increase in the maximum levels for alpha-linolenic acid, and small increase in the minimum levels of copper, iodine, selenium, sodium, potassium, chloride, vitamin A, vitamin D and folic acid.

Historical and regulatory evolution

Dairy fat

1867 — **First infant formulas** based on wheat flour, bovine milk, malt flour and potassium carbonate (J. Von Liebig)

1890 — **Pasteurisation technique**

Vegetable fat

1971 — First Codex Alimentarius standard for infant formulas

1976 — First European decree on infant food

1980 — Infant formula act, greater regulatory control over the formulation and production of infant formula

1991 — EC directive 1999/21/EC: definition and composition of 1st age infant formulas and follow on infant formulas

Proteins:
Min: 1.2 g/100 mL
Max: 2.0 g/100 mL

Lipids:
Min: 2.3 g/100 mL
Max: 3.9 g/100 mL

2006 — EC directive 2006/141/EC: lower protein content and new recommandations on LC-PUFAs

Lipids:
Min: 2.9 g/100 mL
Max: 3.9 g/100 mL

2007 — Directive 2007/1441: bacteriologic criteria

2016 — EC directive 2016/127/EC (applicable since February 2020): reduction of protein content and recommendations on DHA content

Proteins:
Min: 1.2 g/100 mL
Max: 1.6 g/100 mL

DHA:
Min: 13 mg/100 mL
Max: 32.5 mg/100 mL

Scientific evolutions

1838: determination of human milk composition (Simons)

1915: fat content adapted to resemble human milk

1961: first whey-dominant infant formulas (Lien et al., 2003)

1974: ESPGHAN creation

1986: first infant formulas enriched with lactoferrin (Tomita et al., 2002)

2000: infant formulas enriched with LF-PUFAs

2013: Interest of dairy fat for DHA brain accumulation (Delplanque et al., 2013)

Figure 1. Important historical and regulatory evolutions as well as scientific evolutions that have influenced infant formula production
(Adapted from Bourlieu et al., 2017)
[1] Lien, 2003; [2] Tomita et al., 2002; [3] Delplanque et al., 2013.

Table 1. European regulation on the macronutrients and mineral contents in infant formulas (Adapted from European Union, 2016)

	Minimum (per 100 mL)	Maximum (per 100 mL)
Energy (kcal)	60	70
Proteins (g)	1.2	1.6
Lipids (g)	2.6	4.2
Carbohydrates (g)	5.4 (with lactose: 2.7)	9.8
Calcium (mg)	30	98
Chloride (mg)	36	112
Iron (mg)	0.18	0.91
Phosphorus (mg)	15	63
Potassium (mg)	48	112
Sodium (mg)	15	42
Magnesium (mg)	3	10.5
Zinc (mg)	0.3	0.7

Ideally, both breastfed infants and formula-fed infants should show similar growth and development patterns (Lönnerdal, 2014). To achieve this goal, infant formulas are formulated, usually based on a bovine milk, in such a way as to mimic the composition of macro- (protein, fat, and carbohydrates) and micro-nutrients (vitamins and minerals) of human milk (Lönnerdal, 2014).

1.3. Human milk *vs.* bovine milk

Milk is defined as a natural oil-in-water emulsion composed of native milk fat globules dispersed in an aqueous phase containing a colloidal suspension of proteins (caseins, whey proteins) and other soluble components, such as carbohydrates and minerals. The composition of human and bovine milks varies with the course of lactation, the diet, the genotype and length of gestation.

Three fluids are produced during the lactation period. Colostrum, the first fluid produced after delivery (one day to five days postpartum), supports the immature immune system of infants in the first days of life (Castellote et al., 2011). Colostrum is replaced by transitional milk (from 5 days to two weeks postpartum) then by mature human milk, which will support the nutritional and developmental needs of the rapidly growing infant. The mature human milk also presents some nutritional variations over the course of lactation, with a slight decrease in protein content and a slight increase in lipid content, the latter nutrient being the most variable across human milk. The term "human milk" refers in all the manuscript to the mature human milk. Human and bovine milks contain a wide variety of macro- (proteins, lipids, carbohydrates) and micro- (vitamins, minerals and/or bioactive molecules) nutrients (Table 2). The milk composition is unique to each specie. In general terms, bovine milk contains higher protein content and must therefore undergo a series of modifications to more closely mimic human milk composition for the infant formula production. In contrast, lactose, the main carbohydrate in milk, is at a lower content in bovine milk compared to human milk.

Table 2. Overview of compositional differences between human milk and bovine milk
(Adapted from Ahern et al., 2019)

Elements	Human per 100 ml	Bovine per 100 ml	References
Energy (kcal)	71	60–70	(1)
Protein (g)	0.90–1.2	1.8–2.0	(1)
Whey (g)	0.72	0.6	(1)
Casein (g)	0.31	2.6	(1)
Casein:whey	40:60	80:20	
α-Lactalbumin (g)	0.15	0.12	(1)
β-Lactoglobulin (g)	Trace	0.2–0.4	(2)
α_{s1}-Casein (g)	n.d.	1.2–1.5	(2)
α_{s2}-Casein (g)	n.d.	0.3–0.4	(2)
β-Casein (g)	0.26–0.44	0.9–1.1	(3); (2)
K-Casein (g)	0.09–0.13	0.2–0.4	(3); (2)
Lactoferrin (g)	0.15	Trace	(1)
Lysozyme (mg)	50	Trace	(1)
Immunoglobulin A (µg)	26.2 (mg)	0.1	(4); (5)
Immunoglobulin G (µg)	2.1 (mg)	0.3–0.6	(4); (5)
Immunoglobulin M (µg)	3.8 (mg)	0.4–1.0	(4); (5)
Fatty acids (% mol and g/100 g)			
Fats (g)	3.8	3.7	(1)
Butyric acid (C4:0)	n.d.	3.3%	(1)
Caproic acid (C6:0)	Trace	1.6%	(1)
Caprylic acid (C8:0)	Trace	1.3%	(1)
Capric acid (C10:0)	1.3%	3.0%	(1)
Lauric acid (C12:0)	3.1%	3.1%	(1)
Myristic acid (C14:0)	5.1%	14.2%	(1)
Palmitic acid (C16:0)	20.2%	42.9%	(1)
Stearic acid (C18:0)	4.8%	5.7%	(1)
Myristoleic acid (C14:1)	Trace	1.4%	(1)
Palmitoleic acid (C16:1)	3.1%	2.5%	(1)
Oleic acid (C18:1)	46.4%	16.7%	(1)
Linoleic acid (C18:2)	13.0%	1.6%	(1)
Linolenic acid (C18:3)	1.4%	1.8%	(1)
Eicosenic acid (C20:1)	1.0%	Trace	(1)
Arachidonic acid (C20:4)	0.5%	Trace	(6)
Docosahexaenoic acid (C22:6)	0.3%	n.d.	(6)
Carbohydrate (g)			
Lactose (g)	7	4.8	(1)
Minerals (mg)			
Iron	70	50	(1)
Calcium	33	120	(1)
Phosphorous	95	15	(1)
Magnesium	3	12	(1)
Manganese	0.0025–0.003	0.025–0.1	(1)
Fluoride	0.005–0.01	0.022–0.007	(1)
Iodine	7	n.d.	(1)
Selenium	16.3 (ng)	0.0155	(7); (8)
Copper	39	20	(1)
Zinc	0.16	0.38	(1)
Sodium	15	50	(1)
Potassium	55	150	(1)
Vitamins			
Fat soluble			
Vitamin A (µg)	53	34	(1)
Vitamin E (mg)	0.66	0.1	(1)
Vitamin D (IU)	42	36	(1)
Vitamin K (µg)	1.5	5.8	(1)
Water soluble			
Ascorbic acid (mg)	43	48	(1)
Thiamine (µg)	16	42	(1)
Riboflavin (µg)	42.6	175	(1)
Niacin (µg)	172	85	(1)
Pantothenic acid (µg)	196	350	(1)
Cobalamin B12 (µg)	Trace	0.46	(1)

(1) Thompkinson & Kharb, 2007; (2) Farrell et al., 2004; (3) Cuillière et al., 1999 ; (4) Butler, 1994 ; (5) Goldsmith et al., 1983 ; (6) Brenna et al., 2007 ; (7) Givens et al., 2004 ; (8) Smith et al., 1982

1.3.1. Lipids

The lipid fraction of human milk is the primary source of energy for infants, contributing to ~ 50% of the total energy need (Koletzko et al., 2011). Human and bovine milks contain almost the same amount of lipids (~ 3.8 g/100 mL) (Thompkinson & Kharb, 2007), for which the triglycerids are the major fraction (in most cases > 95%) . Some differences between the lipids in human milk and bovine milk concerns the type of fatty acids esterified to the glycerol backbone (Table 2).

Human milk contains 3-times more long-chain polyunsaturated fatty acids (LCPUFAs) than bovine milk. They are essential for the retina and brain development (Bindels, 1992). Human milk is a particularly rich source of essential LCPUFAs such as DHA and arachidonic acid (ARA) (Innis, 1993). Their supplementation in infant formulas is important since endogenous synthesis is insufficient for a similar growth and development compared to breastfed infants. Hence, European regulation (European Union, 2016) states that from February 2020, all infant formulas marketed in the European Union must contain 20-50 mg DHA/100 kcal (the equivalent of 0.5-1% of total fatty acids). This level of DHA is higher than that typically reported in human milk and found in current infant formula products. ARA remains an optional ingredient and there is no requirement to add it to the finished product.

Currently, the lipid source of the majority of infant formulas consists of a blend of vegetable oils. The most commonly used vegetable oils are coconut oil, corn oil, soybean oil, palm oil (palm olein, palm kernel oil), (high oleic) sunflower oil, high oleic safflower oil, peanut oil, and, in Europe, low-erucic acid rapeseed oil (Berger et al., 2000). Vegetable oils do not share the same specificities of fatty acids than both human and bovine milks. In particular, the short chain fatty acids and the regiodistribution of the fatty acids on the glycerol backbone for the vegetable oils is different to that found in human and bovine milks, in which the palmitic acid is located in the sn-2 position and the oleic acid in sn-1 and sn-3 positions unlike that in vegetable oils (Innis, 2011). Previous studies have shown that the partial replacement of vegetable oils by dairy lipids or MFGM has health benefits for infants, like the prevention of infections (Le Huërou-Luron et al., 2018; Timby et al., 2015) or the beneficial impact on intestinal immune function (Lemaire et al., 2018). Indeed, bovine milk contains cholesterol, phospholipids and sphingolipids, that are absent from vegetable oils.

In addition, the lipid droplets in infant formulas are smaller than in human milk (0.3 – 0.8 μm *vs* 0.1 – 15 μm, respectively) (Bourlieu et al., 2015; Michalski et al., 2005) (Figure 2). They are composed of submicronic droplets stabilized by a neoformed membrane mainly based on milk proteins. Non-dairy surfactants (mainly functionalised lecithins or esters of partial glycerides from plants) are usually added to help stabilising the emulsion (Bourlieu et al., 2015). Recently, infant formulas with large fat droplets

(3 - 5 μm) mimicking the milk fat globule have been developed and patented (Nuturis®, Danone Nutrica Research EP2825062A1).
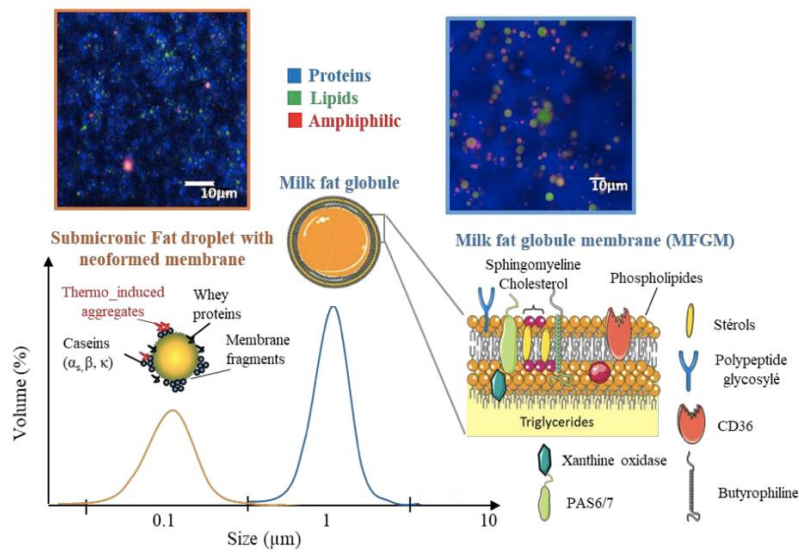
Figure 2. Comparison between lipid structure in human milk (milk lipid globule) and infant formulas (submicronic lipid droplet)
(Adapted from Bourlieu et al., 2015; Michalski, 2009)

1.3.2. Carbohydrates

Carbohydrates of human milk are the second most important source of energy for infants after lipids, contributing to ~ 40% of the total energy intake (Senterre et al., 2010). According to the European Commission (2016/127), the authorized sources of carbohydrates for bovine-milk based infant formulas are lactose, maltose, glucose syrup (with a dextrose equivalent inferior to 32), maltodextrins, precooked or gelatinised starch.

1.3.2.1. Lactose

Lactose is the main carbohydrate in milk with ~ 6-7 g/100 mL in human milk (Bindels, 1992; Bosscher et al., 2000; Newburg & Neubauer, 1995) and ~ 4.5 g/100 mL in bovine milk (Fox & McSweeney, 1998). Lactose can be used as a sole carbohydrate source in infant formulas and the amount of lactose supplement should not exceed the recommended total carbohydrates for infant formulas (European Union, 2016).

Lactose is a slow digestible sugar that is partially hydrolysed in the small intestine by the lactase enzyme. The remaining lactose is fermented in the large intestine, which contributes to maintain an acidic pH (5.5-6.0) that is beneficial for protecting infants from infections (Thompkinson & Kharb, 2007). Lactose also helps increase the absorption of some minerals in the human body such as calcium, sodium, and iron (Koletzko et al., 2005; Thompkinson & Kharb, 2007).

1.3.2.2.   Oligosaccharides

Oligosaccharides are complex carbohydrates with length ranges from 3-10 monosaccharide residues. While human milk is a rich source of oligosaccharides (0.5-2 g/100 mL), the oligosaccharide content is at very low level in bovine milk (Bode, 2012; Engfer et al., 2000; Rudloff & Kunz, 1997). About 200 different human milk oligosaccharides have been characterised and classified into 13 groups according to their core structure (Wu et al., 2011). Most of the oligosaccharides in human milk are resistant to digestion and absorption within the small intestine and act as prebiotics in the infant's colon (Engfer et al., 2000; Gnoth et al., 2000). Indeed, oligosaccharides promote the growth of bifidus microflora in the gut (Goedhart & Bindels, 1994; Rudloff & Kunz, 1997) and inhibit bacterial adhesions to epithelial surfaces (Kunz et al., 2000), thereby preventing gastrointestinal infections of breastfed infants.

Based on their beneficial effect on the infant gastrointestinal tract, oligosaccharides are expected to be included in infant formulas. However, due to the complexity of the human milk oligosaccharides, the production of synthetic oligosaccharide-like structures is challenging and is still very expensive. Consequently, many infant formulas are supplemented with non-human oligosaccharides, such as galacto-oligosaccharides (GOS) and fructo-oligosaccharides (FOS). The maximal amount of oligosaccharides that can be added in infant formulas is 0.8 g/100 mL respecting a GOS:FOS ratio of 90:10 (European Union, 2016). A recent European decision (2016/376) has authorised the addition of 2'fucosyllactose (0.12 g/100 mL) combined with lacto-N-neotetraose (0.06 g/100mL) respecting a ratio 2:1. Alliet et al. (2016) showed that the global microbiota composition of infants fed formulas supplemented with 2'fucosyllactose and lacto-N-neotetraose was close to that of breastfed infants at 3 months of life.

1.3.3. Proteins

Human milk provides nitrogen and the essential amino acids required for protein synthesis, allowing the maintenance of body protein equilibrium, the infant growth and the synthesis of non-protein nitrogenous compounds (neurotransmitters, hormones, vitamin B3, etc).

The total protein content of human milk ranges from 0.9–1.2 g/100 mL, ~ 3-times lower than that of bovine milk (3.4 g/100 mL) (Jensen & Thompson, 1995). In addition to the protein content, the protein profile of human and bovine milks differs. Milk proteins are classified into two groups, caseins and whey proteins. They have recently expanded to include a third group, the mucins. Mucins are found within the milk fat globule membrane and represent less than 1% of total proteins (Ballard & Morrow, 2013). While the casein:whey protein ratio in human milk is usually considered as 40:60, the proportion in bovine milk is about 80:20 (Chatterton et al., 2013; Lönnerdal, 2003). Besides, the nature of the whey

proteins and the caseins are very different between the two milks (Table 3). This will be discussed in detail below.

Table 3. Protein composition of human milk and bovine milk
(Adapted from Chatterton et al., 2013)

Fraction	Human milk (per L)	Bovine milk (per L)
Whey proteins (g)	5.3 – 6.6	5.0 – 7.0
α-lactalbumin (g)	2.5	1.0-1.5
β-lactoglobulin (g)	0	3.0-4.0
Lactoferrin (g)	1.5	0.01-0.1
Immunoglobulins (g)	1.2	0.6-1.0
Serum albumin (g)	0.4[1]	0.3[2]
Osteopontin (mg)	138	18
Lactoperoxidase (mg)	5.7	13-30
Caseins (g)	3.5 – 4.4	30
α_{S1}-casein (g)	0.6	12-15
α_{S2}-casein (g)	0	3-4
β-casein (g)	2.7	9-11
κ-casein (g)	0.9	3-4
MFGM proteins (mg)	50 – 100	28.2-48.4

[1] Lönnerdal & Atkinson, 1995; [2] Fox et al., 2015
MFGM: milk fat globule membrane

1.3.3.1.   Caseins

Based on the amino acid sequence, four caseins can be distinguished: α_{s1}-casein, α_{s2}-casein, β-casein, and κ-casein. Caseins belong to a large family of secretory proteins, characterised by a loose tertiary, and highly hydrated structure with phosphoserine residues that strongly bind polyvalent cations such as calcium. In human and bovine milks, the majority of caseins (90–95%) are present in a micellar form, but the casein micelles in human milk (30–75 nm in diameter; Calapaj, 1968) are smaller in size than those in bovine milk (100-200 nm in diameter; Lin et al., 1971). These structures are characterised by a central hydrophobic core made of calcium-sensitive α_S- and β-caseins, and a peripheral hydrophilic layer of κ-caseins (Figure 3) (Qi, 2007). The main function of casein micelles is to maintain in suspension calcium phosphate that is at saturation in milk (Farrell et al., 2002).
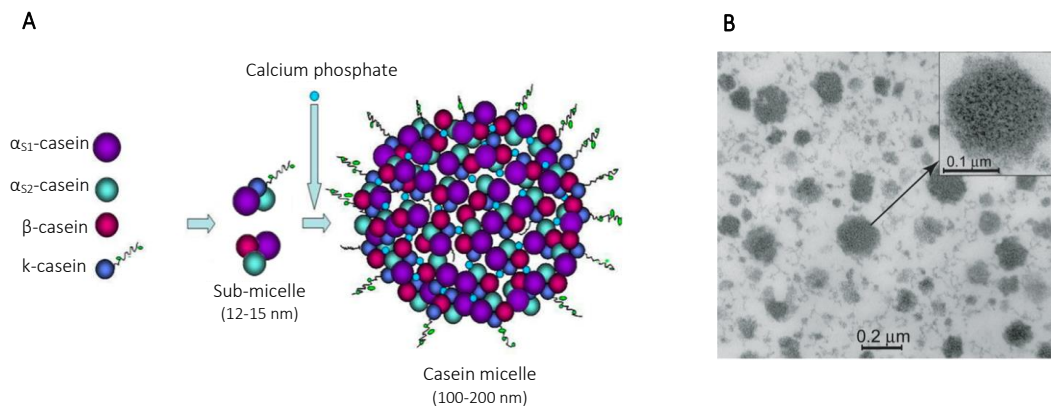
Figure 3. Structure (A) and transmission electron micrograph (B) of bovine casein micelles
(Qi, 2007; Villa et al., 2018)

In human milk, β-casein is the main casein, making up over 70% of total caseins, with α_{s1}-casein and κ-casein representing the remaining amount (O'Callaghan et al., 2011). Human milk is α_{s2}-casein free. In bovine milk, α_{s1}-casein, α_{s2}-casein, β-casein and κ-casein represent about 40%, 12.5%, 35%, and 12.5% of the casein fraction, respectively (Wal, 2002). While both human and bovine milks contain β-casein and κ-casein, the amino acid sequence of the proteins differ between the species. Particularly, human and bovine β-caseins have only ~ 50% of homology (Jenkins et al., 2007; Villa et al., 2018).

β-casein is a highly phosphorylated protein. During digestion, the degradation of β-casein leads to the formation of peptides rich in phosphorylated amino acid residues, called casein phosphopeptides (CPPs). By keeping calcium soluble, CPPs contribute to the high bioavailability of human milk calcium (Sato et al., 1986). CPPs may also affect the absorption of other divalent cations (Hansen et al., 1996). Commercial fraction of purified β-casein may be added in infant formulas to increase the β-casein content. However, clinical studies related to β-casein enriched-formulas are still limited (O'Callaghan et al., 2011).

K-casein is largely glycosylated and it is present in very small amounts in human milk. Glycomacropeptide (GMP) (or caseinomacropeptide) corresponds to the fragment 106-169 of κ-casein that is obtained after κ-casein hydrolysis by chymosin during cheese making or by pepsin during the digestion process. GMP is characterised by many biological properties such as antibacterial, prebiotic, remineralising, modulatory of digestion process and metabolism, anti-tumoral and immune-modulatory activities (Córdova-Dávalos et al., 2019). It is often recovered in the whey protein ingredients used to formulate infant milk formulas.

1.3.3.2.   Whey proteins

The whey protein fraction contains more than 100 proteins. Although whey protein amount is nearly similar between human and bovine milks (~ 0.6 g/100 mL), the main whey proteins largely differ between bovine and human milks, as indicated in Table 3.

1.3.3.2.1.   α-lactalbumin

In human milk, α-LA is the main protein and accounts for ~ 22% of total proteins and 36% of whey proteins (Heine et al., 1996; Kunz & Lönnerdal, 1992), while in bovine milk, α-LA accounts for only 3.0-3.5% of total proteins (Heine et al., 1991). α-LA is synthesised by the mammary gland and plays an important role during milk synthesis and secretion. Combined with the enzyme β-1,4-galactosyltransferase, α-LA forms lactose synthase that converts glucose and galactose into lactose (Ebner et al., 1966).

Human α-LA has a very high content of essential amino acids (63.2% of the total amino acid content), with a high content of lysine and cysteine and a remarkably high content of tryptophan (5.9% of total amino acid content) (Table 4) (Heine, 1999). Tryptophan is a precursor of serotonin, a neurotransmitter that regulates the sleep-wake rhythm, the response to stress and other physiologic processes (Yogman et al., 1982). Cysteine is the precursor of taurine, an amino acid involved in brain development (Sturman, 1988). Due to the low proportion of α-LA in bovine milk, its tryptophan and cysteine contents are approximately one-half of those of human milk, when related to the total amino acid content (Heine et al., 1991). To balance this disparity, infant formulas usually contain a higher protein amount (~ 1.3 g of proteins/100 mL) than that of human milk. However, some studies have reported that plasma tryptophan level in infants fed with high protein-infant formulas were still lower than that for breastfed infants (Hanning et al., 1992). The blood-brain transfer of tryptophan follows the same pathways as other apolar neutral amino acids. In human milk, the blood-brain transfer of tryptophan is optimal due to the high tryptophan to other apolar neutral amino acids ratio. In contrary, in infant formulas, the tryptophan to other apolar neutral amino acids ratio is lower. Thus, the blood-brain transfer of tryptophan is less optimal and therefore the tryptophan plasma amount of formula-fed infants is lower than that of breastfed infants (Heine, 1999). Moreover, the high-protein content in infant formulas may be at the origin of overweight and obesity predispositions of infants in later life (Koletzko et al., 2019).

When lowering the protein content of infant formulas, the first limiting amino acid is tryptophan (Lönnerdal, 2003). One approach to compensate the lack of tryptophan is to add free tryptophan during infant formula processing (Fazzolari-Nesci et al., 1992). However, the metabolic consequences of the tryptophan fortification of infant formulas is poorly known. Another approach is to increase the α-LA

content in infant formulas (Davis et al., 2008). Recent advances in dairy technology have enabled the commercialisation of α-LA enriched whey protein concentrate. Bovine α-LA may be an excellent substitute for human α-LA in infant nutrition as the amino acid sequences of human and bovine α-LA are very similar (72% of homology; Heine et al., 1991). Clinical studies have shown that lowering the protein amount in infant formulas coupled with an increased proportion of α-LA results in plasma tryptophan contents similar to those in breastfed infants (Davis et al., 2008; Sandström et al., 2008).

Table 4. Amino acid composition of human and bovine forms of α-lactalbumin, β-lactoglobulin and lactoferrin

Amino acids (residue)	α-LA		β-LG	LF	
	Human[1]	Bovine[2]	Bovine[2]	Human[1]	Bovine[3]
Essential amino acids					
Cys	8	8	5	32	28
His	2	3	2	9	10
Ile	12	8	10	16	17
Leu	14	13	22	61	61
Lys	12	12	15	46	42
Met	2	1	4	6	4
Phe	4	4	4	31	25
Thr	6	7	8	31	39
Tyr	4	4	4	20	19
Trp	3	4	2	11	9
Val	2	6	10	49	43
Non-essential amino acids					
Ala	6	3	14	63	59
Arg	1	1	3	46	32
Asp + Asn	17	21	16	71	71 (Asp)
Glu + Gln	15	13	25	70	61 (Glu+Asn)
Gly	6	6	3	56	43
Pro	2	2	8	35	31
Ser	7	7	7	50	45

[1] Lönnerdal & Atkinson, 1995; [2] Fox et al., 2015; [3] Castellino et al., 1970

1.3.3.2.2. β-lactoglobulin

β-LG is absent in human milk while it is the dominant whey protein in bovine milk, accounting for 10-12% of the total proteins and 50% of the total whey proteins in bovine milk (Creamer et al., 2011). The exact biological function of β-LG is unclear. It has nutritional benefits due to its amino acid profile, and it can play a role in the metabolism of phosphate in mammary gland (Farrell et al., 1987). β-LG is a retinol-binding protein and may play a role in the retinol transport (Puyol et al., 1991). It is supposed to bind, protect and transport other small hydrophobic ligands such as vitamin D, fatty acids, cholesterol and curcumin (Pérez & Calvo, 1995).

As β-LG is the major whey protein in bovine milk, it is the most dominant whey proteins in the current infant formulas. Moreover, the removal of β-LG from bovine milk or bovine whey without altering the functional properties of the other whey proteins is costly and complex to design (Lucena et al., 2006). β-LG is considered as one of the major allergen to infants (Matsumoto, 2011; Wal, 2002). To prevent

early allergy manifestation, hydrolysed infant formulas can be an alternative (Nasirpour et al., 2006), although additional clinical studies are required to confirm this (Osborn & Jones, 2018).

1.3.3.2.3. Lactoferrin

In human milk, LF is the second most abundant whey protein (~ 0.15 g/100 mL), representing 10-15% of the total proteins, while the LF amount is considerably lower in bovine milk (1-10 mg/100 mL) (Table 3). LF plays an important role as an iron carrier, mucosal proliferation stimulant and has antibacterial effect (Chierici & Vigi, 1994; Iyer & Lonnerdal, 1993; van de Looij et al., 2014) (Figure 4). In 2000, LF was recognised as a Generally Recognized as Safe (GRAS) ingredient by FDA for different food categories (Franco et al., 2018).
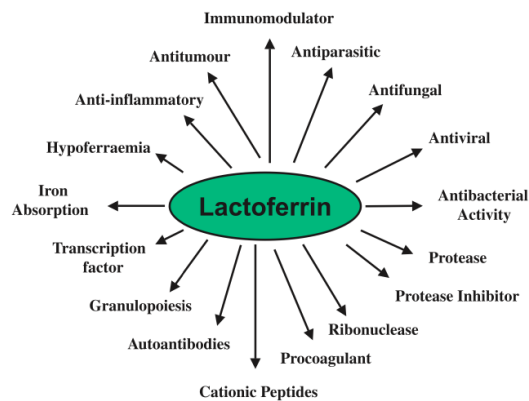
Figure 4. Possible functions of lactoferrin
(As proposed by Brock, 2002)

Infant formulas were supplemented with LF in Japan for the first time in 1986 (Ben, 2008; Tomita et al., 2002). LF is Generally Recognised As Safe by the FDA (Office of Food Additive Safety, 2016), and the European Food Safety Authority recommends intakes of 200 mg of LF per kg bodyweight (or 1.2 g bovine LF per day) for infants aged from 0–6 months (European Food Safety Authority, 2012). Clinical studies indicate that LF enriched infant formulas lead to the increase of haematocrits and the decline of respiratory illnesses (O'Callaghan et al., 2011). However, clinical studies on bovine LF added to infant formulas have not shown any enhancing effect on iron absorption because bovine LF is not recognised by human LF receptors (Chierici et al., 1992; Davidson & Lonnerdal, 1988; Fairweather-Tait et al., 1987). This could be explained by the fact that human and bovine LF have only 69% amino acid homology (Pierce et al., 1991).

Due to the high cost of LF as ingredient and the difficulty in preserving the LF bioactivity during infant formula production, the enrichment of infant formulas with LF is still limited (O'Callaghan et al., 2011). Currently, bovine LF is added as a supplement to infant formulas in only few countries such as Indonesia,

South Korea, Spain, Japan (Conesa et al., 2010; Wakabayashi et al., 2006) and the United States (Johnston, 2015).

1.3.3.2.4. Serum albumin

Human and bovine milks contain a near akin amount of serum albumin (10-40 mg/100 mL) (Fox et al., 2015; Lönnerdal & Atkinson, 1995). Human and bovine serum albumins share 76% of homology (Peters, 1985). Serum albumin is described as a multifunctional protein with high ligand binding capacity, which facilitates the transfer of fatty acids, calcium, hormones and drugs into blood (Kinsella & Whitehead, 1989). In addition, serum albumin is a source of essential amino acids. However, its biological function in human milk remains unknown (Lönnerdal et al., 2017), and a limited number of studies have investigated its therapeutic potential as functional ingredient (Krissansen, 2007).

1.3.3.2.5. Immunoglobulins

The major classes of Ig in human and bovine milks are IgA, IgM, IgG. IgG exists as IgG_1 and IgG_2. In human milk, the largest class is IgA (90% of total Igs), while in bovine milk, IgGs are dominant (80-90% of total Igs) (Lönnerdal, 2013; Stelwagen et al., 2009). At birth, infants are susceptible to infectious agents due to the immaturity of their immune system. Thus, Igs of human milk play a role in immune development and serve to protect infants from early infection (Hurley & Theil, 2013). Attempts have been made to increase the Ig amount in infant formulas. Some clinical studies showed that bovine colostrum-enriched infant formulas are beneficial for the protection of infants against rotavirus infections (Davidson et al., 1989; Ebina et al., 1985) or for necrotising enterocolitis resistance in preterm piglets (Møller et al., 2011). Recent studies have suggested bovine colostrum as a relevant alternative to human milk for preterm infants when human milk is not available (Jensen et al., 2013). However, other studies have demonstrated contradictory results (Aunsholt et al., 2014; Turner & Kelsey, 1993).

1.3.3.3. Non-protein nitrogen

In human milk, 20-25% of the nitrogen is present as non-protein nitrogen, while only 5% of the nitrogen in bovine milk is non-protein (Hambraeus & Lonnerdal, 2003; Jenness, 1979). Non-protein nitrogen fraction consists of more than 200 compounds, including urea, free amino acids, ammonia, carnitine, choline, taurine, amino sugars, amino alcohols, nucleic acids, nucleotides, polyamines, peptides, and other biologically active compounds such as growth factors (Atkinson & Lönnerdal, 1995; Brown, 2016).

Many of these components, such as taurine, choline and nucleotides, are considered conditionally essential for infants. For example, human milk is a source of purine and pyrimidine bases as well as nucleotides necessary for *de novo* synthesis of nucleotides by infants (Donangelo & Trugo, 2003). Furthermore, nucleotides are known to be beneficial for the development and maturation of the gastrointestinal tract, as well as for the development of the microbiota and immune function (Gutiérrez-Castrellón et al., 2007; Singhal et al., 2008; Uauy et al., 1994).

Urea of human milk, as well as some peptides and free amino acids, contribute to infant protein metabolism. Urea nitrogen is a significant part (30–50%) of total non-protein nitrogen in human milk, while free amino acids represent 3–5% of the total non-protein nitrogen in human milk. Glutamate/glutamine and taurine, a non-protein sulfonic acid, are the predominant free amino acids in human milk. Taurine, in its conjugated form with bile acids, is important for lipid absorption (Lombardini & Azuma, 1992). Taurine also supports the appropriate development of the brain and retina. Since 1980's, infant formulas are supplemented with taurine as bovine milk contains a lower amount (0.1-0.7 mg/100 mL; Atkinson & Lönnerdal, 1995) than human milk (3.3 mg/100 mL; Packard, 1982). Owing to the relative lack of evidence that taurine supplementation of infant formulas has beneficial clinical effects, recommendations for the nutrient contents of infant formulas do not include a minimum content of taurine. However, a maximum amount of 7.8 mg/100 mL is specified (European Union, 2016).

1.3.3.4.   Minerals

The total mineral content of human milk (~ 2.0 g/L) is considerably lower than that of bovine milk (~ 7.3 g/L) (Table 2) (Thompkinson & Kharb, 2007). Among the main minerals of human milk, calcium is an important mineral for the formation and maintenance of bone mass, as well as for normal activities of nerves and muscles. Sodium and potassium significantly contribute to osmotic pressure in cells. Iron is an important element for synthesis of haemoglobin (Aumeistere et al., 2017). Iron deficiency results in anemia, the most frequent nutritional deficiency of essential elements for infants. Anemia is characterised by a reduction of the work capacity of infants and a delayed psychomotor development, coupled with cognitive deficit (Wang, 2016). Due to the mineral content dissimilarities between human and bovine milks, demineralised whey protein powders are used during infant formula manufacturing to help standardise the mineral content (de Wit, 1998).

Beyond fine nutritional and structural differences between human milk and infant formula, another large difference is that infant formulas have to be produced at industrial scale and stored for long time. The steps used to reach this goal may affect the nutritional and functional properties of the components.

2. Infant formula processing

As human and bovine milk compositions differ in many points, the manufacture of bovine milk based-infant formulas requires a number of adjustments in order to meet the nutritional requirements of infants. As previously stated, powdered infant formulas are much easier to transport and store compared to the liquid infant formulas, but the latter are more convenient to use as they require no reconstitution. Moreover, while liquid infant formulas are commercially sterile, powdered infant formulas are not. The manufacture of infant formulas consists of a succession of processing steps that differ between powdered and liquid infant formulas.

2.1. Powdered infant formulas

Two different processes are generally used for the manufacture of powdered infant formulas: a dry mix process or a wet mix process (or a mix of both) (Montagne et al., 2009). The wet mix process (i.e. blending of ingredients in a liquid phase) has many advantages compared to the dry mix process (i.e. dry-blending of ingredients): a better uniformity of nutrient distribution in the product, a better control of the microbiological safety thanks to pasteurisation/sterilisation steps during the manufacturing process and a better solubility of the powder during reconstitution provided by a well-controlled spray drying process. As the wet mix process is the most widely used process, the subsequent section will only describe this process (Figure 5).
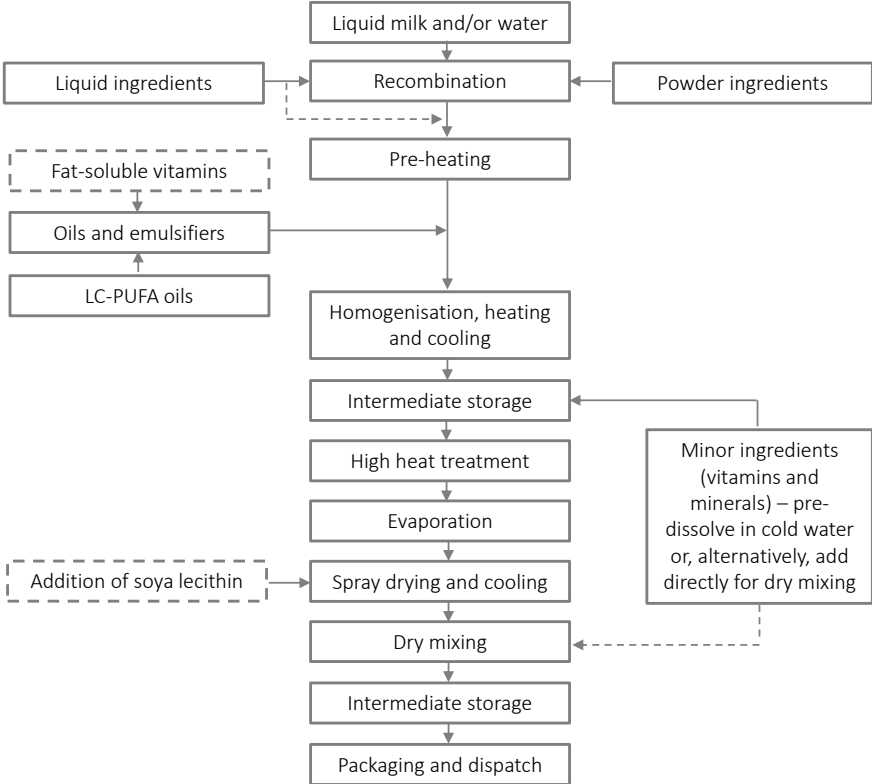
Figure 5. The manufacturing steps of powdered infant formulas (Montagne et al., 2009)
Dotted lines are alternative processing route.

2.1.1. Raw materials

The authorised raw ingredients used during the infant formula manufacturing are listed by the European Commission (2006) (Table 5). All ingredients have to meet quality specifications to ensure their suitability for incorporation into infant foods. These specifications are registered in the Code of Federal Regulations (21 CFR 110.80).

Table 5. Typical raw materials used for infant formula manufacture
(European Union, 2016)

Milk	Skimmed or full fat, liquid or powder, from bovine or goat origin
Casein	Acid casein or sodium/calcium/potassium caseinate
Whey protein	Concentrate, isolate, partially demineralised, partially hydrolysed
Alternative protein source	Isolated soya protein
Carbohydrates	Lactose, maltose, glucose-syrup (with a dextrose equivalent inferior to 32), maltodextrins, precooked or gelatinised starch, FOS/GOS
Lipids	Vegetable oils, butter oil, cream, alpha-linolenic acid, linoleic acid, DHA, other polyunsatured fatty acids
Functional ingredients	Emulsifiers/stabilisers as soya lecithin, mono- and di-glycerides
Major minerals	Calcium carbonate, calcium phosphate, magnesium phosphate, potassium citrate, magnesium chloride
Oligo-elements	Potassium iodide, ferrous sulphate, manganese sulphate, copper sulphate, zinc sulphate
Vitamins	Vitamin A, D, E, K, B3 (niacin), B9 (folic acid), B5 (pantothenic acid)
Other ingredients	Biotine, choline, inositol, free amino acids (L-carnitine, taurine), nucleotids (for example, 5'-cytidylic acid)

The quality and pre-treatment of raw ingredients used for infant formula production influence the physical properties of the wet-mix. For example, skim milk powder (SMP) is classified as high, medium and low heat, according to the severity of heat treatment undergone during its manufacture (Martin et al., 2007) (Table 6). This classification, based on the whey protein nitrogen index (WPNI), gives an indirect indication of the level of whey protein denaturation. The heat treatment intensity has an impact on the functional properties of the SMP (Lin et al., 2017).

Table 6. Characteristics of the skim milk powder
(Adapted from Kelly et al., 2003)

SMP classification	Typical heat treatment	WPNI [1]	Functional properties
Low heat	70°C/15 s	> 6.0	Solubility, lack of cooked flavor
Medium heat	85°C/ 1 min; 90°C/30 s; 105°C/30 s	1.5-6.0	Emulsification, foaming, water absorption, viscosity, color, flavor
High heat	90°C/5 min; 120°C/1 min; 135°C/30 s	< 1.5	Heat stability, gelation, water absorption

[1] The whey protein nitrogen index (WPNI) is a measure of undenatured whey protein nitrogen content (expressed as mg of whey protein nitrogen/ g of SMP).

In the same way, the functional and nutritional properties of infant formulas depend on the extent of whey protein denaturation of the whey-based ingredients (de Wit, 1998; Lorenzen & Schrader, 2006; Zhang et al., 2016).

2.1.2. Preparation of the mix

Two systems are separately prepared: a water-soluble system and an oil-soluble system. The water soluble-ingredients are rehydrated in fresh skim milk or a mixture of water and SMP to the desired composition regarding macro-elements (Montagne et al., 2009). The mixture is stored to ensure complete powder hydration. The minerals are dissolved separately in hot water are then added to the mixture. If necessary, the pH of the mix is adjusted by addition of an alkali (potassium hydroxide or sodium hydroxide) or a citric acid solution (Bylund, 1995). Then the water-soluble system is heat-treated. Heat sensitive micro-ingredients (vitamins) may be added at a later stage to limit their degradation. They can be added to the water-soluble system before drying or mixed as a dry premix to the spray dried powder. Some other ingredients can be added at different stages according to their functional properties. For example, starches are often sprayed with infant formulas directly in the chamber of the spray dryer in order to limit the viscosity increase during the steps prior to drying (Blanchard et al., 2013).

2.1.3. Pasteurisation

Pasteurisation is a process that consists in the heating of a medium over 60°C during an appropriate time, with the aim to eliminate the vegetative forms of bacteria, viruses, protozoa, moulds and yeasts. The temperature/time combinations for pasteurisation in dairy industry are low temperature pasteurisation (60-65°C/15-30min), high temperature pasteurisation (70-75°C/15-40s) and flash pasteurisation (85-95°C/1-2s) (Jeantet et al., 2016).

Previous studies have shown that standard pasteurisation treatment during infant formula manufacturing is effective for the inactivation of *Enterobacter sakazakii* (Iversen & Forsythe, 2004; Nazarowec-White & Farber, 1999). Indeed, the heat treatments applied during infant formula manufacturing are theoretically sufficient to ensure the destruction of at least 8-log units of *Enterobacteriaceae*, including *Salmonella* and *E.sakazakii*, as well as other microorganisms as *Listeria monocytogenes* or *Streptococcus aureus* (World Health Organization, 2006). Depending on the processing conditions, spore-formers such as *Bacillus cereus* and *Clostridium botulinum* are partly inactivated.

A joint FAO/WHO consultation group (2004-2006) identified *E.sakazakii* and *Salmonella enterica* as the pathogens of most concern in powdered infant formulas, associated with serious infant illness and death (WHO, 2007). These microorganisms can survive (but not grow) in powdered infant formulas for a long period of time. Therefore, once the product is rehydrated, microorganisms can develop and be at risk for the infant safety, depending on the temperature of rehydratation water and the time between the product rehydration and its administration. *E.sakazakii* is a Gram negative, non-spore forming

bacterium. It can lead to infections that constitute an important cause of life-threatening meningitis, septicaemia and necrotizing enterocolitis in infants (Lai, 2001). To reduce the risk of infection in infants fed powdered infant formulas, recommendations have been made for its preparation and storage. *Salmonella* are Gram negative, facultative anaerobic bacteria. The symptoms of *Salmonella* contamination include acute enterocolitis, abdominal pain, diarrhoea, nausea, vomiting and fever (Jones et al., 2006). In some cases, *Salmonella* infection lead to more serious consequences such as bacteraemia, septic arthritis, pneumonia and meningitis (Kent et al., 2015).

2.1.4. Homogenisation

The oil-soluble phase, composed of a mixture of oils, fat and lipophilic vitamins, is generally mixed with the water-soluble system after pasteurisation to form a pre-emulsion. The pre-emulsion is homogenised in order to decrease the lipid droplet size and increase their creaming stability. Homogenisation is usually carried out by using two-stage valve type homogenisers. The pre-emulsion is forced through the homogeniser in order to break down the lipid droplets into submicronic droplets. Consequently, the total surface of the lipid droplets increases, which enable milk proteins, and emulsifiers if present, to adsorb on the newly formed surface. The affinity of proteins to adsorb at the oil-water interface depends on many factors such as the nature (caseins, whey proteins) and physical form (native, denatured) of proteins (Dickinson, 2013).

2.1.5. Evaporation and spray drying

Evaporation of the emulsion is often employed to remove water prior to spray drying, as evaporation requires lower energy compared to spray drying. Evaporation is carried out under vacuum at temperature 50-70°C. In addition to the increase of viscosity due to the concentration of the wet-mix, evaporation can affect the physico-chemical properties of the constituents such as the casein micelle hydration, the size of lipid droplets and the amount of calcium associated with the casein micelles (Liu et al., 2012). Moreover, the formation of calcium phosphate during evaporation can reduce the pH of the concentrate (Singh, 2007).

The concentrated emulsion is then dehydrated by spray drying to produce powdered infant formulas. Powdered infant formulas are generally produced using two or three stage spray drying. It consists of a large drying chamber in which the bulk water is removed, followed by supplementary drying using an internal and/or an external fluidized bed. Previous study has shown that varying concentrate heating temperature (65–74 °C) and inlet/outlet air dryer temperature (200/101 °C–160/89 °C) does not impact whey protein denaturation for bovine milk, in contrary to the pre-heating step (Oldfield et al., 2005; Harjinder Singh & Creamer, 1991).

2.2. Liquid infant formulas


```
                        ┌──────────────────────────┐
                        │  Liquid milk and/or water │
                        └──────────────────────────┘
                                     │
┌────────────────────┐   ┌──────────────────────────┐   ┌────────────────────┐
│ Liquid ingredients │──▶│      Recombination        │◀──│ Powder ingredients │
└────────────────────┘   └──────────────────────────┘   └────────────────────┘
                                     │
                         ┌──────────────────────────┐
                         │       Pre-heating         │
                         └──────────────────────────┘
┌ ─ ─ ─ ─ ─ ─ ─ ─ ─ ┐
  Fat-soluble vitamins
└ ─ ─ ─ ─ ─ ─ ─ ─ ─ ┘
                                     │
┌────────────────────┐   ┌──────────────────────────┐   ┌──────────────────────────┐
│ Oils and emulsifiers│──▶│ Homogenisation, heating  │◀──│     Minor ingredients     │
└────────────────────┘   │      and cooling          │   │  (vitamins and minerals)  │
┌────────────────────┐   └──────────────────────────┘   └──────────────────────────┘
│    LC-PUFA oils    │
└────────────────────┘                │
                         ┌──────────────────────────┐
                         │  Standardisation and      │
                         │  intermediate storage     │
                         └──────────────────────────┘
                                     │
┌────────────────────┐   ┌──────────────────────────┐
│     Packaging      │   │  UHT treatment,           │
└────────────────────┘   │  homogenisation and       │
                         │  cooling                  │
                         └──────────────────────────┘
                                     │
┌────────────────────┐   ┌──────────────────────────┐
│ Retort sterilisation│   │  Aseptic intermediate     │
│    and cooling      │   │       storage             │
└────────────────────┘   └──────────────────────────┘
                                     │
                         ┌──────────────────────────┐
                         │    Aseptic packaging      │
                         └──────────────────────────┘
                                     │
                         ┌──────────────────────────┐
                         │  Incubation of packaged   │
                         │  product for sterility    │
                         │        testing            │
                         └──────────────────────────┘
                                     │
                         ┌──────────────────────────┐
                         │   Storage and dispatch    │
                         └──────────────────────────┘
```

Figure 6. The manufacturing steps of liquid infant formulas
(Montagne et al., 2009)
Dotted lines are alternative processing route.

Unlike powdered infant formulas, liquid infant formulas are manufactured to be sterile (destruction of both vegetative and sporulated forms of the microorganisms) in order to be stored at ambient temperature between 6 months to 1 year without undergoing spoilage or textural changes. Thus, liquid infant formulas are generally subjected to more severe heat treatments than those intended for powdered infant formulas, meaning UHT processing followed by aseptic packaging (Figure 6).

A sterilisation treatment is applied to the liquid infant formulas before commercialisation to guarantee its safety. It is defined in D-values for specific heat-resistant spores. An international standard for the temperature 121°C is a minimal of 12 decimal reductions for *Clostridum botulinum* spores. In the ultra-high temperature (UHT) range of 140-150°C, *Bacillus stearothermophilus* spores are generally used as the reference.

Two types of sterilisation can be applied during the manufacture of liquid infant formulas: the retort sterilisation or the UHT sterilisation. The retort sterilisation consists of the heating at high temperature

(118-122°C) during a long time (15-20 min) of the sealed final product. This high temperature/long time treatment can alter some properties of liquid infant formulas such as the colour, the taste or the nutritional value (Montagne et al., 2009). Retort sterilisation is mainly used in hospitals to feed premature infants. In contrary to the retort sterilisation, UHT sterilisation minimizes the browning reactions and the modification of nutritional quality of liquid infant formulas (Y. J. Jiang & Guo, 2014). During the UHT sterilisation, liquid infant formulas are pre-heated in-line in a plate heat exchanger to ∼ 80°C, followed by a very fast temperature increase to 140–150°C by direct steam injection and kept at this temperature for a few seconds. Afterwards, cooling down to ∼ 80°C is done instantaneously using a vacuum vessel. During this so-called flash cooling, the product is completely deaerated and the initially injected steam is removed.

Heat treatment is a critical control point in order to ensure microbiological quality of infant formulas. However, depending on the processing conditions, heat treatment can result in irreversible changes in milk component structure, particularly on protein fraction, which can modify the functional and nutritional properties of the final product. The heat-induced protein modifications will be discussed in the next section.

3. Heat treatment and protein structure

In contrast to caseins, whey proteins are globular proteins with high levels of secondary and tertiary structures which make them susceptible to denaturation during heat treatments. Briefly, protein denaturation is defined as an irreversible conformational change of the native protein structure. It occurs through the unfolding of the native protein structure and the subsequent aggregation of unfolded proteins through intermolecular interactions. Aggregation reactions may also involve other milk components such as lactose. The unfolding/aggregation of whey proteins is an important factor affecting their functional properties such as emulsifying, thickening, gelling and foaming properties (Boye et al., 2004; Poon et al., 2001) and potentially their nutritional properties. Furthermore, whey protein denaturation can lead to the fouling of heat exchangers during processing (Bansal & Chen, 2006) and the formation of cooked flavour (Al-Attabi et al., 2014).

For over 60 years, the denaturation kinetics of whey proteins has been studied under various medium conditions. The majority of these studies were based on β-LG, the most abundant whey protein in bovine milk. Overall, there is very limited information in the literature on the heat denaturation of whey proteins in infant formulas and even less on the heat-induced protein structures.

3.1. Whey protein denaturation

3.1.1. Heat-induced unfolding and aggregation of β-lactoglobulin

Bovine β-LG is a globular protein of 162 amino acids, characterised by a molecular mass of 18.4 kDa and a radius of ∼ 2 nm (Sawyer, 2013). Its isoelectric point (pI) is ~ 5.3 (Rene & Lalande, 1988) and its denaturation temperature is estimated at ~ 78°C (Brodkorb et al., 2016). Depending on the environment conditions (pH, temperature and ionic strength), β-LG can exist as a monomer, dimer, or octamer (Kumosinski & Timasheff, 1966; McKenzie & Sawyer, 1967; Sakurai et al., 2001). Under physiological conditions (neutral pH and β-LG > 50 μM), β-LG is predominantly dimeric (de Wit, 2009; Verheul et al., 1998). The secondary structure of β-LG monomer consists of nine antiparallel β-strands, eight of which forming two perpendicular β-sheets, and one C-terminal α-helix (Figure 7) (Townend et al., 1969). Each monomer contains two disulfide bonds (Cys66-Cys160 and Cys106-Cys119) and one free thiol group (Cys121), hidden within the protein structure (McKenzie et al., 1972). The secondary and tertiary structures of β-LG are stabilised by the two disulfide bonds as well as hydrophobic, ionic and hydrogen bonds (de Wit, 2009). Nine different genetic variants of bovine β-LG exist (A to H), the most common of which are A and B.
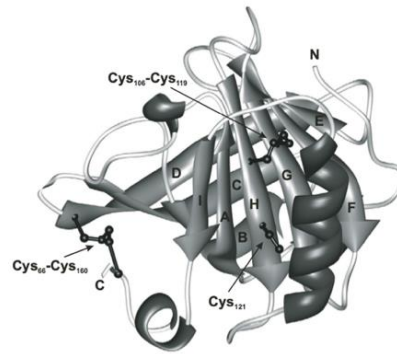
Figure 7. Molecular structure of bovine β-lactoglobulin monomer
(Tolkach & Kulozik, 2007)
Eight antiparallel β-strands (A-H) form the central β-sheet calyx. The ninth β-strand I and the AB loop are involved in dimer structure formation. The β-lactoglobulin structure is stabilised by two disulfide bonds (Cys66-Cys160 and Cys106-Cys 119). One free thiol group (Cys121) is hidden by the α-helix in the native state.

3.1.1.1.   Mechanism of heat-induced β-lactoglobulin denaturation

The widely accepted model regarding the heat-induced denaturation of β-LG consists of a multistage process (Figure 8) (Mulvihill & Donovan, 1987; Tolkach & Kulozik, 2007). At ambient temperature and physiological pH, β-LG exists as a native dimer which dissociates into two native monomers above 40°C (Kim & Lund, 1998; Rene & Lalande, 1988). At temperatures 40-55°C, the tertiary structure of β-LG slightly changes to form the R-state, characterised by a very weak aptitude for aggregation (Mulvihill & Donovan, 1987; Tolkach & Kulozik, 2007). The increase of temperature to 60-70°C leads to reversible β-LG unfolding, corresponding to the breakage of non-covalent bonds and thus alteration of its tertiary structure and the exposition of its free thiol group to the solvent. This phenomenon, called the Tanford transition, leads to the formation of a «molten globule» state that is reactive for aggregation reactions with the participation of the exposed free thiol (Delplace et al., 1997; Santos et al., 2006). As covalent bonds are not altered, the molten globule structure is temperature reversible, and β-LG can refold with the temperature decrease. The formation of the molten globule state ends at 80-90°C. Finally, at temperatures 130-140°C, the secondary structure of β-LG is completely altered, leading to irreversible protein denaturation. β-LG in its R-, molten globule and denatured states are able to aggregate.

$$N_2$$
$$\sim\!40\ °C\ \updownarrow$$
$$2N$$
$$\sim\!40\text{–}55\ °C\ \updownarrow$$
$$2N_R$$
$$\sim\!60\text{–}70\ °C\ \updownarrow$$
$$2U_{MG} \longrightarrow U_n \longrightarrow U_m$$
$$\sim\!130\text{–}140\ °C\ \downarrow$$
$$2U_D \qquad n = 2,3,4,5$$
$$m \gg n$$
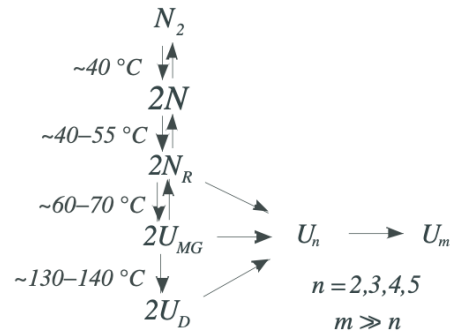
Figure 8. Mechanism of the heat-induced denaturation and aggregation of β-lactoglobulin (Tolkach & Kulozik, 2007)

N_2: native dimer state; N: native monomer state; N_R: R-state; U_{MG}: molten globule state; $U_{n,m}$: polymer and aggregate states; U_D: irreversible denatured state.

3.1.1.2. Kinetics and thermodynamics of heat-induced denaturation of β-lactoglobulin

One common method to investigate the kinetics of β-LG denaturation is to study the disappearance of the native protein over time. The heat-induced β-LG denaturation is usually modelled by supposing a two-stage process (Figure 9) (Tolkach & Kulozik, 2007; Verheul et al., 1998), while it is well known that the denaturation process is more complex (Figure 8). The first stage consists of the unfolding step: the native non-covalent protein dimer dissociates into two native monomers that unfold, leading to the exposure of one free thiol group per monomer, each of them available for reaction. During the unfolding step, β-LG is in equilibrium between its native form and non-native monomer forms (i.e. R-, molten globule, denatured forms). The second stage consists of the aggregation step: by the exposition of the free thiol group, the activated monomers participate to several irreversible aggregation reactions leading to the formation of β-LG aggregates *via* thiol–disulfide interchange reactions. Although this model was comprehensive, it does not take into account non-covalent interactions and it concerns a solution of purified β-LG at relatively low heating temperatures (65-70°C) and neutral pH. Thus, Oldfield et al. (1998) improved the previous model by adding the contribution of the hydrophobic groups exposed during the whey protein unfolding. These latter participate to non-covalent interactions between unfolded proteins. These hydrophobic aggregates are rapidly converted into disulfide bound aggregates upon heating at temperatures higher than 75 °C (Wijayanti et al., 2014).
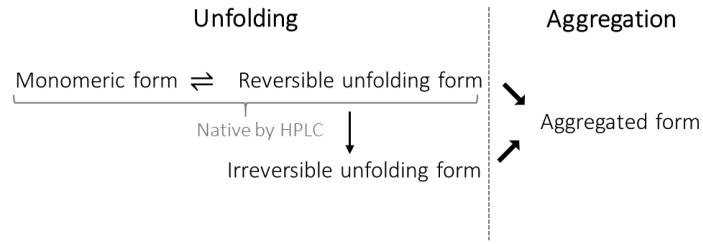
Figure 9. Two-stage process for the modelisation of the heat-induced β-lactoglobulin denaturation (Adapted from Tolkach & Kulozik, 2007)
k_1 is the denaturation rate constant and k_{agg} is the aggregation rate constant.

The heat-induced denaturation process of β-LG can be summarised by the Equation 1:

Equation 1

$$-\frac{dC}{dt} = k.\,C^n$$

With C the native protein amount, k the reactive rate constant and n the reaction order. After integration of Equation 1, and for n ≠ 1:

Equation 2

$$\left(\frac{C_t}{C_0}\right)^{1-n} = 1 + (n-1).\,k.\,t$$

With C_t (g.L^{-1}) the native protein amount at holding time t (min) and C_0 (g.L^{-1}) the initial protein amount.

The relationship between the reactive rate constant and heating temperature can be mathematically expressed by the Arrhenius equation (Equation 3).

Equation 3

$$\ln(k) = \ln(k_0) - \frac{E_a}{R.\,T}$$

with k_0 (g^{1-n}·L^{n-1}·min^{-1}) the denaturation frequency factor, E_a (kJ.mol^{-1}) the activation energy, R the universal gas constant (8.314 J·mol^{-1}·K^{-1}) and T the heating temperature (K).

The reaction order for β-LG denaturation mechanism has been estimated at 1.5 (S.G. Anema, 2000; Dannenberg & Kessler, 1988; Oldfield et al., 1998). The reaction order is 1.0 if the unfolding step is rate-limiting, which is observed at low heating temperatures, at pH close to the pI or at high ionic strength. Conversely, the reaction order is 2.0 if the aggregation process is the rate-limiting step, which is observed at high heating temperatures, at pH away from the pI or at low ionic strength. This two-stage process is illustrated by a slope break on the Arrhenius plot of β-LG denaturation, which delimits two temperature ranges (Figure 10). Below the critical temperature (78°C), the denaturation reaction is

limited by the unfolding reaction, while above the critical temperature, β-LG denaturation is limited by the aggregation reaction.
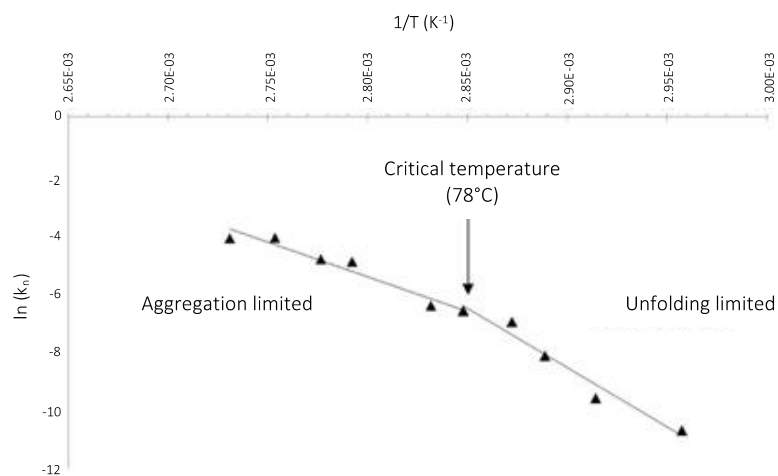
Figure 10. Arrhenius plot of β-lactoglobulin denaturation
(de Guibert et al., 2020)

In addition to heating temperature, the β-LG denaturation reaction is influenced by many parameters such as pH and ionic environment.

3.1.1.3.   Effect of pH on β-lactoglobulin denaturation

The mechanism of β-LG denaturation is pH-dependent. The denaturation temperature of β-LG decreases with increasing pH (Gotham et al., 1992). Moreover, β-LG free thiol group has higher availability for intermolecular disulfide bond formation above pH 7.0 (Watanabe & Klostermeyer, 1976). The aggregate size is also influenced by the pH. At pH above ~ 6.4, small aggregates (40 nm) are formed due to increasing reactivity of free thiol groups and increasing repulsions between unfolded proteins while, at lower pH (i.e. pH below ~ 6.4), a secondary aggregation takes place leading to larger aggregates (~ 100 nm) (Hoffmann et al., 1996; Zúñiga et al., 2010).

3.1.1.4.   Effect of calcium on β-lactoglobulin denaturation

The presence of ionic calcium affects β-LG denaturation. Firstly, calcium ions stabilise the unfolded state of β-LG, leading to the exposition of its free thiol group, which promotes the formation of intermolecular disulfide bonds. This effect is concomitant with an increase in β-LG hydrophobicity, which further increases the β-LG tendency to aggregate (Jeyarajah & Allen, 1994). Secondly, calcium favours the aggregation of β-LG by neutralising the protein surface charges and thus reducing Coulombian repulsion (Schmitt et al., 2007; Verheul et al., 1998). Thirdly, calcium contributes to β-LG complex formation through formation of non-covalent bridges by its fixation to the negative groups of β-LG which

strengthens the aggregates (Britten et al., 1988; Mulvihill & Donovan, 1987). Consequently, the aggregates formed in calcium-rich solutions are larger and denser. Thus, it is expected that the lower amount of calcium in infant formulas (30-98 mg/100 mL according to European regulation) (Table 1) compared to bovine milk (120 mg/100 mL) (Table 3) will impact the heat denaturation of β-LG during infant formula heating.

3.1.2. Heat-induced denaturation of other whey proteins
3.1.2.1. α-lactalbumin

Bovine α-LA, the second major protein in bovine milk, consists of 123 amino acids forming a compact globular structure stabilized by four disulfide bonds (Cys6-Cys120, Cys61-Cys77, Cys73-Cys91 and Cys28-Cys111). α-LA does not contain free thiol group (Brew, 2013). α-LA is a calcium metalloprotein with a pI of 4.2-4.5 and a molecular weight of 14.2 kDa (Brew & Grobler, 1992; Farrell et al., 2004). Under native conditions, the bilobal tertiary structure of α-LA consists of one lobe composed by α-helices (large α-domain), while β-sheets and unordered structures make up the other lobe (short β-domain) (Figure 11). The two lobes are connected by a calcium binding loop (Brew, 2011, 2013).
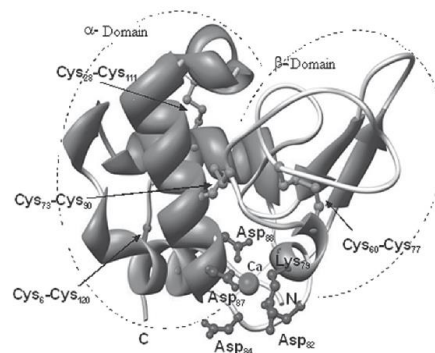
Figure 11. Molecular structure of bovine α-lactalbumin
(Jakopovic et al., 2016)
The tertiary α-LA structure, composed by two domains (α- and β-domains), is stabilized by four disulfide bonds (Cys6 –Cys120, Cys61 –Cys77, Cys73 –Cys91 and Cys28 –Cys111). The calcium binding site is formed by oxygen ligands of carboxyl group of three aspartic acid residues (Asp82, Asp87 and Asp88), two carbonyl bonds between Lys79 and Asp84 and one or two water molecules.

The denaturation temperature, meaning the temperature at which 50% of proteins are in their denatured form, of α-LA (68°C; Nielsen et al., 2018) is lower than that of β-LG (78°C; Brodkorb et al., 2016). α-LA is strongly affected by the presence of calcium in its structure, with a lower denaturation temperature for the apo-form (calcium free) compared to the holo-form (calcium bound) (35°C *vs.* 68°C, respectively) (Boye & Alli, 2000). Moreover, at temperatures below 80°C and in the absence of other whey proteins, the heat-induced unfolding of α-LA is largely reversible. More than 90% of the protein

refold to a native state upon cooling after a heat treatment at 77°C/15 min, while 40% of the protein refold to its native structure when heated at 95°C/15 min (Chaplin & Lyster, 1986). The reversible denaturation of α-LA is explained by the lack of free thiol group in the native protein structure. However, when the temperature is high enough, one or more of the four disulfide bonds of α-LA disrupt and release highly reactive free thiol groups that initiate and propagate irreversible aggregation reactions following a mechanism similar to that described for β-LG (Chaplin & Lyster, 1986). In the absence of disulfide bond disruption, α-LA is unable to initiate disulfide-bond interchanges with other proteins (Calvo et al., 1993). All studies to date have reported a first-order reaction for the denaturation of α-LA (Dannenberg & Kessler, 1988; Kessler & Beyer, 1991).

3.1.2.2. Lactoferrin

Bovine LF is a globular protein whose primary structure consists of a single polypeptide chain of 689 amino acid residues, including 17 intramolecular disulfide bonds, but no free thiol group (Pierce et al., 1991). Based on its peptide sequence, the molecular mass of the LF is ~ 80 kDa. LF is a highly basic protein with a pI of 8.0-9.0 (Groves, 1960; Shimazaki et al., 1993). The secondary structure of the LF consists of 41% α-helix and 24% β-sheet. The conformation of the LF comprises two lobes (N- and C-lobes) connected by a short α-helix (Moore et al., 1997) (Figure 12). Each lobe is further divided into two similarly sized sub-domains: N1, N2 and C1, C2, respectively. The two sub-domains of each lobe form a deep cavity, the interdomain cavity, in which a ferric ion (Fe^{2+} or Fe^{3+}) can bind in synergy with a carbonate ion (CO_3^{2-}) (Baker & Baker, 2005). The two lobes of LF are similar in conformation and have ~ 40% homology in their primary sequence (Baker & Baker, 2005; Baker et al., 2002).
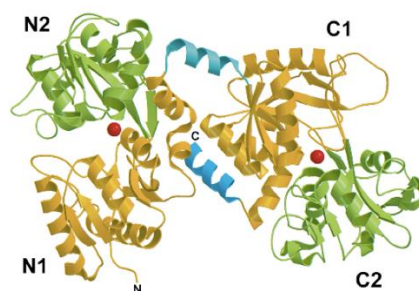
Figure 12. Molecular structure of bovine lactoferrin
(Baker et al., 2002)
For each lobe, sub-domain 1 is coloured in yellow and sub-domain 2 in green. The α-helix that joins the two lobes is coloured in blue. The two iron atoms are shown as red spheres.

Depending on the iron-saturation levels, LF can exist in three different forms: the holo-LF form, saturated with iron in both sites; the apo-LF form, devoid of iron; the partially iron saturated form, which contains iron only in either of the two lobes. In its native form, LF is partially saturated with iron, with

5%-30% saturation rate for bovine LF (Deeth & Bansal, 2019). The binding of iron to LF gives salmon pink colour to the protein solution. The affinity of LF for iron is very high, with an affinity constant of ~ 10^{20} and 10^3 for Fe^{3+} and Fe^{2+}, respectively (Baker, 1994; Harris, 1986).

Like other whey proteins, LF is a globular protein that is sensitive to heat treatment. However, iron binding alters LF conformation, which influences its heat stability. The apo-LF denaturation presents a single endothermic transition at temperature 60-65°C, while the holo-LF is much more heat stable and exhibits a main denaturation peak at ~ 90°C, and a minor endothermic transition at a lower temperature (70-75°C) (Rüegg et al., 1977; Sánchez et al., 1992). These two transitions for the holo-LF may be related to a difference of heat stability between the C- and N-lobes of the protein. When saturated with iron, the C-lobe is more compact than the N-lobe and therefore is more heat stable (Sánchez et al., 1992). Consequently, the native LF has two endothermic transitions. The first transition corresponds to the denaturation peak of the apo-form (~ 65°C) and the second, at higher temperature, corresponds to the denaturation of the holo-form (~ 90°C).

Heat-induced changes of LF are similar to those observed for α-LA, as both proteins have only disulfide bonds but no free thiol groups. Upon heating, the cleavage of intramolecular disulfide bonds induces the exposition of free thiol groups, which initiates thiol/disulfide interchange reactions, resulting in the formation of aggregates. The accessibility of newly formed free thiol groups is dependent on the iron saturation level of LF. The apo- and native-LF are more susceptible to disulfide bond cleavage than holo-LF. The more compact structure of the latter could stabilise LF disulfide bonds. Non-covalent interactions are also involved in the formation of large insoluble aggregates of LF due to the heat-induced exposition of sites normally buried inside the molecule. The few studies on the heat-denaturation of LF reported a first-order reaction (Kussendrager, 1994; Sánchez et al., 1992).

3.1.3. Heat-induced denaturation of whey proteins in presence of caseins

Caseins account for 80% of total proteins in bovine milk, where they are dispersed as large colloidal protein-mineral complexes called casein micelles. The low level of secondary and tertiary structures of caseins and the high electrosteric repulsions between casein micelles explain their remarkable heat stability. At temperatures up to 100°C, no modification of the casein micelle structure occurs in the absence of whey proteins (Anema & Li, 2003). However, the casein micelle structure is sensitive to environmental changes that can lead to irreversible structural changes, affecting many of its properties (e.g. heat stability and rennet coagulation properties).

Heat treatment of bovine milk (mixture of whey proteins and casein micelles) leads to the formation of casein-whey protein complexes (Anema & Klostermeyer, 1997; Sutariya et al., 2017; Vasbinder et al.,

2003; Vasbinder & de Kruif, 2003). The interactions between whey proteins and casein micelles are non-covalent (e.g., ionic and/or hydrophobic interactions) and/or covalent, depending on the heating conditions (Jang & Swaisgood, 1990; Mulvihill & Donovan, 1987; Vasbinder et al., 2003; Vasbinder & de Kruif, 2003). A majority of non-covalent interactions are formed during the early stages of heating and covalent interactions in the later stages (Mulvihill & Donovan, 1987). The covalent interactions occur *via* thiol/disulfide interchange reactions between mainly unfolded β-LG and κ-casein and α_{s2}-casein that exist as small polymers and disulfide bound dimers in casein micelles, respectively (Farrell et al., 2004; Hill, 1989; Jang & Swaisgood, 1990). Heat induced-denatured whey proteins are either associated to the casein micelle surface as casein micelle-bound complexes or dispersed as soluble whey protein/κ-casein complexes in the soluble phase. There is still some debates over the sequence of interaction reactions between the denatured whey proteins and κ-casein (Figure 13). Oldfield et al. (1998) proposed that, under rapid heating rates, whey proteins initially aggregate in the soluble phase and then associate with κ-casein at the casein micelle surface on prolonged heating (Corredig, Dalgleish, 1999). At slower heating rates, unfolded β-LG monomers or small whey protein aggregates interact with the casein micelles, and then the whey protein/κ-casein complexes dissociate from the casein micelle surface (Figure 13). Another mechanism suggested that κ-caseins are dissociated from the casein micelle at an early stage of heating, and they interact subsequently with denatured whey proteins in the soluble phase. This mechanism is supported by the fact that κ-casein dissociation occurs at temperatures lower than the denaturation temperatures of whey proteins and that the denatured whey protein:κ-casein ratio in the soluble phase is high (Anema, 2007; Anema & Klostermeyer, 1997; Guyomarc'h, Queguiner, et al., 2003).
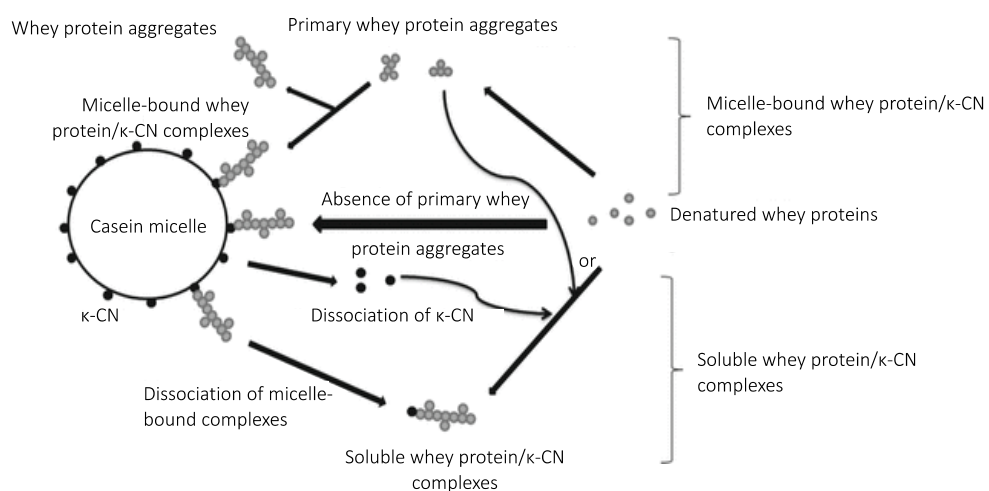
Figure 13. Pathways of formation of the heat-induced whey protein/κ-casein complexes in heated skim bovine milk
(As proposed by Donato & Guyomarc'h, 2009)
κ-CN: κ-casein

3.2. Other heat-induced modifications of proteins

3.2.1. Protein lactosylation

Maillard reaction, also known as non-enzymatic browning, is another heat-induced modification affecting protein structure in heated milk and milk products. The chemistry of the Maillard reaction is very complex, and the mechanism is usually divided into three stages: the early, advanced, and final stages. The early stage consists of the condensation reaction of the carbonyl group from a reducing sugar such as lactose with a primary amine, coming from the α-amino group of the free amino acids or at the terminal position of peptides or proteins or from the ε-amino group of the lysine residues within proteins such as caseins and whey proteins (Van Boekel, 1998). As a result, a Schiff's base forms and then rearranges to produce the more stable Amadori product (i.e. lactulosyl lysine). The condensation reaction between lactose and milk proteins is greatly accelerated by heat. Under severe heat treatments, the Amadori products further undergo a complex series of condensation, rearrangement and fragmentation reactions, a.k.a Strecker degradation, forming a vast array of degradation products named the advanced glycation end products, such as N ε-(carboxymethyl)lysine, diketones, etc.

Direct nutritional effects due to Maillard reaction are therefore mainly related to the impairment of the bioavailability of lysine from milk proteins (ALjahdali & Carbonero, 2019; Zenker et al., 2020). Protein intra- and inter-molecular cross-linking by advanced products of Maillard reactions can alter the functional properties of milk powder (Fan et al., 2018) or reduce the protein digestibility (Corzo-Martínez et al., 2010). In addition, the formation of volatile compounds such as aldehydes or aminoketones can lead to cooked flavours into infant formulas (Nunes et al., 2019).

3.2.2. Protein-lipid interaction

Native milk fat globules are surrounded and stabilised by a specific membrane (milk fat globule membrane: MFGM), which contains mainly phospholipids, proteins (glycoproteins, enzymes), glycolipids and other minor compounds (Keenan 2006). During heating of bovine milk, α-LA and β-LG associate with MFGM proteins mainly *via* covalent disulfide interactions. The interaction between whey proteins and MFGM is enhanced with the temperature increase up to 80 °C (Ye et al., 2004). Whey proteins can also displace the original membrane material by competition with native compounds of the MFGM or insert the gaps left after its heat-induced break down (Dalgleish & Banks, 1991). In addition, κ-casein can interact directly with MFGM components or *via* κ-casein/β-LG polymers through sulfydryl-disulfide interchange reactions during heating (Houlihan et al., 1992). The association of α-LA and β-LG with MFGM strongly affect the functional properties of MFGM, such as their emulsifying properties (Corredig & Dalgleish, 1999). The MFGM is also modified during intense shearing (homogenisation, spray-drying); the increase of the fat surface allows milk proteins (casein micelles,

free caseins and whey proteins) to absorb to newly formed oil/water interface, which can alter the milk properties (Michalski et al., 2002).

3.3. Factors influencing the heat-induced protein structures
3.3.1. Protein profile

Although whey protein aggregation is commonly associated to the heat destabilisation of β-LG, other proteins such as α-LA and BSA have also been recovered in whey protein aggregates. Due to the absence of free thiol group, α-LA is not able to initiate heat-induced covalent aggregates. However, in the presence of β-LG, α-LA denaturation is enhanced (Calvo et al., 1993) and unfolded α-LA is incorporated into heat-induced aggregates though covalent and hydrophobic interactions (Schokker et al., 2000). The presence of α-LA decreases the proportion of smaller aggregates and increases the number of very large aggregates (Schokker et al., 2000).

In contrast to α-LA, β-LG denaturation is not affected by the presence of α-LA (Hines & Foegeding, 1993). This indicates that the mechanism of aggregation in mixture of α-LA and β-LG is governed by β-LG. The free thiol group exposed during β-LG unfolding interacts with accessible disulfide bonds on β-LG and on α-LA to initiate intermolecular thiol/disulfide interchange reactions (Figure 14) (Livney et al., 2003; Schokker et al., 2000). The heat-induced aggregates consist of a mixture of β-LG aggregates, α-LA aggregates and β-LG/α-LA aggregates (Vardhanabhuti & Foegeding, 1999).
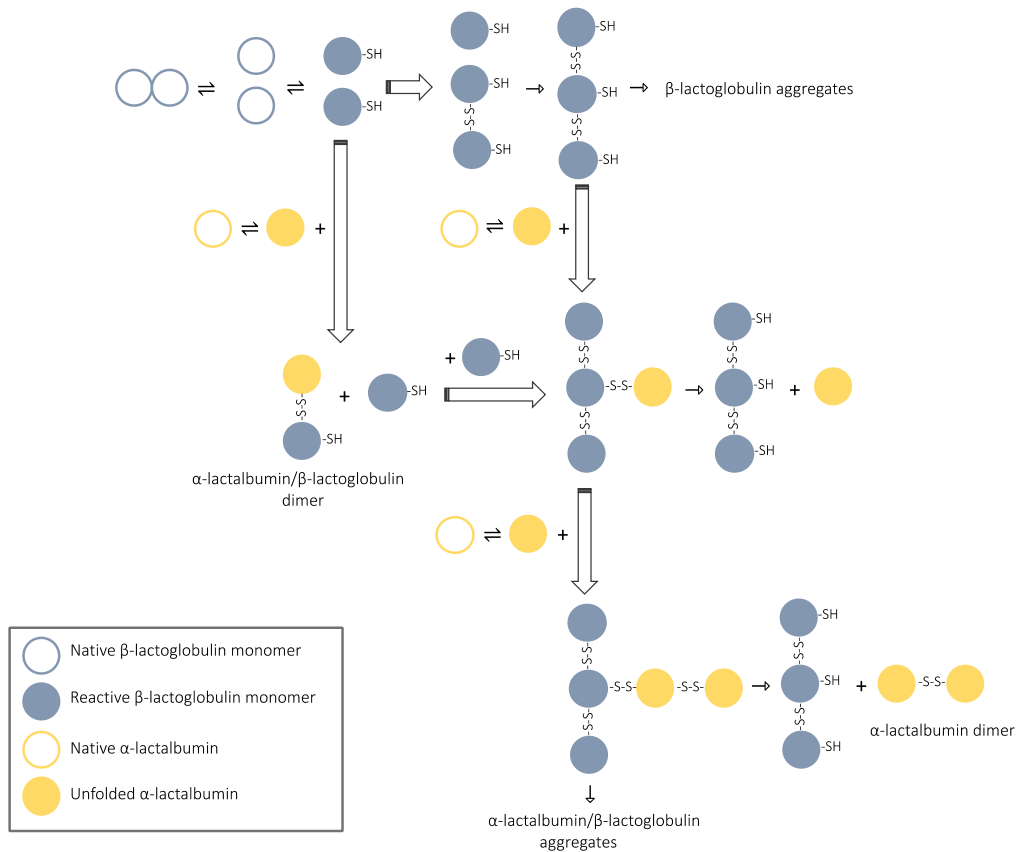
Figure 14. Mechanism of α-lactalbumin and β-lactoglobulin aggregation
(As proposed by Schokker et al., 2000)

Heat-induced interactions of LF with whey proteins have received little attention due to its low amount in bovine milk. Heat-induced unfolding of LF has been reported to occur faster in the presence of bovine whey proteins (Paulsson et al., 1993). In addition, the type of interactions between LF and whey proteins in heat-induced aggregates depends on the pH. At pH 6.7, mainly hydrophobic interactions and disulfide bonds are formed, while at pH 5.8, attractive electrostatic and hydrophobic interactions dominate (Li & Zhao, 2018).

In addition, although κ-casein interacts mainly with β-LG, denatured α-LA and LF can also be involved in thiol/disulfide exchange reactions with κ-casein and therefore be incorporated in heat-induced protein aggregates (Anema, 2008). The interactions between α-LA and κ-casein occur only if β-LG (or another whey protein with a free thiol group) is present during heating, and this may require the initial formation of β-LG/α-LA complexes, which subsequently interact with κ-casein (Baer et al., 1976; Elfagm & Wheelock, 1978).

The initial amount of the different milk proteins (for example β-LG, α-LA, κ-casein and α-casein) affect the structure and kinetics of formation of heat-induced aggregates. As β-LG plays a major role in the formation of the heat-induced aggregates, the decrease of β-LG:α-LA ratio at constant total protein

content increases the heat stability of model infant formulas due to the decrease of covalent interactions between proteins (Crowley et al., 2016).

Moreover, the casein:whey protein ratio can have a significant impact on the heat-induced protein changes, such as the size of the generated aggregates or the viscosity and the heat stability of the dairy products (Beaulieu et al., 1999; Donato & Guyomarc'h, 2009; Harjinder Singh, 2004, McSweeney et al., 2004). More precisely, modification of the casein:whey protein ratio can alter the whey protein denaturation kinetics (Anema et al., 2006). Caseins improve the heat stability of whey protein solutions (Patocka et al., 1993). They exhibit a protective chaperone-like effect by blocking the hydrophobic surfaces exposed during the denaturation of whey proteins (Morgan et al., 2005; Mounsey & O'Kennedy, 2010; Zhang et al., 2005), resulting in the prevention of irreversible whey protein denaturation and aggregation during heat processing (Liyanaarachchi & Vasiljevic, 2018; O'Kennedy & Mounsey, 2006). It has been proposed that this chaperone-like mechanism is related to the higher charge density of casein/whey protein aggregates compared to native whey proteins, thereby limiting interactions with other proteins (Gaspard et al., 2017).

3.3.2. Dry matter content

Powdered infant formulas are manufactured at relatively low dry matter contents (20-40%) prior to concentration by evaporation up to 50-58% of dry matter and finally spray-dried. Previous studies (Table 7) have shown that the increase of dry matter content delays β-LG denaturation (Anema, 2000; Hillier et al., 1979; McKenna & O'Sullivan, 1971). Nevertheless, this effect decreases with the increase of heating temperature and it becomes negligible above 100°C (Anema, 2000). The inhibition of β-LG denaturation at increasing dry matter content in the low temperature range is due to a stabilisation of the native β-LG conformation by the environmental medium (Plock et al., 1998). Lactose content may prevent transition of β-LG from dimeric to monomeric form and then delays β-LG unfolding. At temperature above 80°C, the aggregation reaction is the limiting step of β-LG denaturation and is not affected by lactose content. In contrast, lactose and dry matter does not affect α-LA denaturation kinetics (Anema, 2001) as, α-LA being a monomeric protein, no rate-determining shift in molecular transition and association occurs.

Table 7. Effects of dry matter on whey protein denaturation
(Adapted from Fenelon et al., 2019)

Reference	Protein System	Protein content	Heating temperature Holding time	Conclusion
Harland et al., 1952	Whey In skim milk	9%-36% (w/w)	Not available As reported by Anema (2000)	Protein content had little effect on whey protein denaturation
Guy et al., 1967	Whey In cottage cheese whey	5%-40% (w/w)	87°C; 84.5°C; 74°C For up to 30 min	Whey protein denaturation was at a minimum at 20% (w/w)
McKenna & O'Sullivan, 1971	Whey In skim milk	9%-44% (w/w)	75°C; 80°C For from 5 to 20 min	Whey protein denaturation decreased with protein content
Hillier et al., 1979	α-LA and β-LG In cheese whey	1.9-11.4 g/L	From 70°C to 130°C No heating times mentioned	Denaturation of α-LA increased with protein content; Denaturation of β-LG decreased with protein content
Oldfield, 1996	α-LA and β-LG In skim milk	6%-13% (w/w)	110°C in a direct steam injection plant	Whey protein denaturation increased with protein content
Anema, 2000	β-LG In skim milk	9.6%-38.4% (w/w)	From 75°C to 100°C For up to 15 min	β-LG denaturation decreased with increasing protein content; effect of protein content decreased with increased heating temperatures—at 100°C there was no affect
Anema, 2001	α-LA In skim milk	9.6%-38.4% (w/w)	From 75°C to 100°C For up to 15 min	α-LA denaturation was not affected by protein content

3.3.3. Temperature/time combination

Heating is the processing of milk that most promotes the whey protein denaturation and their interaction with casein micelles. Generally, two types of heat treatment are used in the dairy and infant formula industry: (i) indirect heating, where heat is transferred across a physical barrier which separates product from a heating medium (e.g., plate or tubular heat exchangers) and (ii) direct heating, where the product and heating medium are in contact (e.g. steam injection or infusion). With direct heat treatments, the heat load transfers to the product is lower than with indirect treatments (Lewis & Deeth, 2009) and the target temperature (140-150°C) is achieved after as little as 1 s, compared to more than 10 s for indirect treatments. As a result, the denaturation level of β-LG and α-LA is lower after direct UHT treatment compared to indirect UHT treatment (Tran et al., 2008). Whey protein denaturation is stabilised at ~ 88% following an indirect UHT heat treatment of bovine milk (149°C /10 s) (Labropoulos et al., 1981).

Compared to UHT treatment, the extent of whey protein denaturation in bovine milk is lower after HTST pasteurisation at 72°C/15 s , with about 20% of extent of whey protein denaturation (Lee et al., 2017). Moreover, most of the secondary protein structures of the whey proteins are preserved (Bogahawaththa et al., 2017). In addition, HTST pasteurisation (70.8°C/42 s) has a limited effect on the LF denaturation (about 95% remained in the native form after heating), as well as on its iron-binding

capacity and storage stability (Wazed et al., 2020). Nevertheless, the lower unfolding transition of native LF is affected (Paulsson et al., 1993).

3.3.4. Ionic environment

The ionic strength and the type of ions influence the heat-induced aggregation of the whey proteins. Increasing ionic strength increases the denaturation temperature of whey proteins due to the reduction of the intramolecular repulsions which stabilise the native protein structure. Simultaneously, the intermolecular repulsions are reduced, promoting protein aggregation (de la Fuente et al., 2002). Moreover, aggregate size increases as a function of salt amount (Marangoni et al., 2000). Specific salt effects on protein stability depends on their ability to bind to proteins and change their hydration properties. Salts that enhance protein hydration and weakly bind to proteins stabilise proteins while salts that reduce protein hydration and strongly bind to proteins destabilise them. Salts might also destabilise hydrophobic interactions inside proteins and/or stabilise unfolded protein structure (Dey, 2011). Divalent cations (such as calcium) promote protein aggregation *via* electrostatic shielding, ion-specific hydrophobic interactions and salt bridges by cross-linking anionic groups on adjacent proteins (Havea et al., 2002). Monovalent cations compete with divalent cations for interaction with proteins and reduce the effect of divalent cations (Havea et al., 2002).

Heat treatments can affect protein structure, which can in turn affect protein digestibility. Moreover, during digestion, protein structure can be modified by the acidic conditions in the stomach and are hydrolysed by the digestive enzymes, which have specific cleavage sites. These latter can be chemically or physically blocked by structural constrains, such as after protein aggregation through non-covalent or covalent bonds or by modification of the amino acid residues due to Maillard-type reactions. Heat-induced protein structural changes can lead to proteins that become either more susceptible or more resistant to proteolysis during digestion. The digestion process in infants will be described on the next section, as well as the consequences of heat processing on milk protein digestion.

4. Protein structure and infant digestion

In the first days of life, infants are recognised to have an immature digestive system, which can impact their ability to digest and absorb nutrients (Bourlieu et al., 2014; Poquet & Wooster, 2016). This section aims to present the key parameters of the infant digestion, with a focus on the gastrointestinal digestion of proteins.

4.1. Specificities of infant digestion

4.1.1. Anatomy and function

The main characteristics of the developing digestive system of infants are summarised in Figure 15. Digestive immaturity at birth is mainly linked to secretory functions, motility and immature digestive tract. Infant digestion process includes a limited oral phase due to the milk-based liquid meals rapidly transiting through the oral cavity (5-10 s) (Shani-Levi et al., 2017), although the swallowed saliva can interact with the meal during the gastric phase (mainly glycoproteins and salivary amylase) (Bourlieu et al., 2014). Consequently, the stomach is considered as the first main digestive compartment in infants, which stores, mixes, initiates the hydrolysis and regulates the emptying of the bolus toward the small intestine. Gastric juice, secreted by the epithelial cells of the gastric mucosa, contains mainly enzymes (pepsins, human gastric lipase), hydrochloric acid, sodium bicarbonate, as well as mucins that form a protective barrier for the gastric mucosa. Most of the hydrolysis and absorption of nutrients take place in the duodenum and jejunum, and the large intestine is mostly in charge of the absorption of water and electrolytes. Other accessory organs are crucial to the digestive process, i.e. pancreas (production of the alkaline pancreatic secretion containing lipases, proteases and amylase), liver (production of bile, metabolism of lipids and proteins, storage of glycogen and vitamins) and gallbladder (storage and release of bile toward the duodenum) (Berseth, 2006).
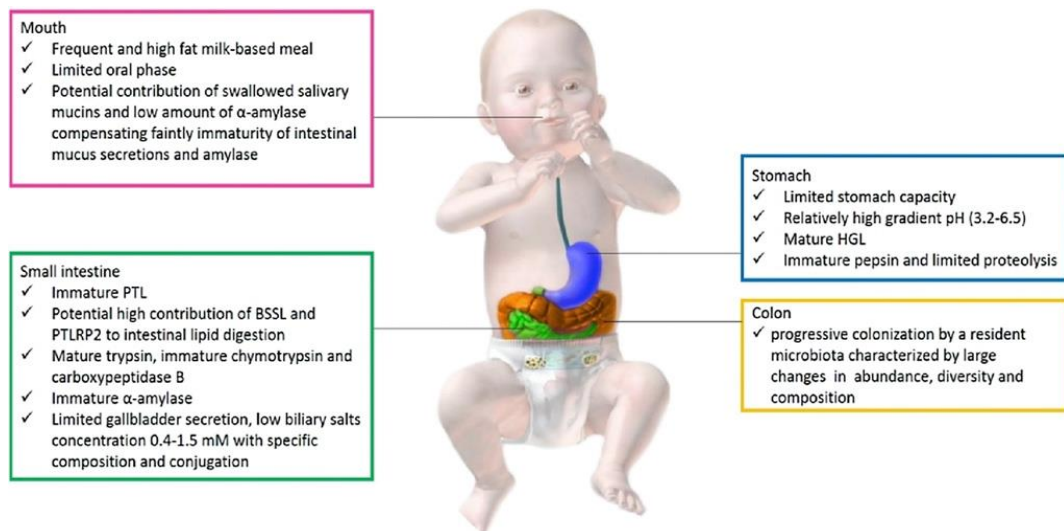
Figure 15. Summary of the developing digestive physiology in infant
(Shani-Levi et al., 2017)

Abbreviations are HGL, Human Gastric Lipase; PTL, pancreatic triglyceride lipase; BSSL, bile salt-stimulated lipase; PTLRP2, pancreatic triglyceride lipase-related protein 2.

Figure 16 illustrates the maturity of the main enzymes acting in gastric and intestinal digestion from 10 weeks of gestation to 24 months after birth compared to older infants or the fully mature adult digestive system. At birth, the pepsin activity is reported to be at 18% of the adult level (Henderson et al., 2001; Shani-Levi et al., 2017), while trypsin activity reaches almost 90% of the adult level (McClean & Weaver, 1993). However, the trypsin activity for neonates previously referenced is generally expressed in µg and the conversion into U is not straightforward and/or not necessarily reliable (Cleghorn et al., 1988; Lieberman, 1966). To our knowledge, there are no data available in the literature regarding the trypsin activity (U) within the neonate duodenal content. In addition, chymotrypsin and carboxypeptidase activities in intestinal fluid of neonates only reach 50-60% and 25% of the level of infants aged of 2 years and above, respectively (Lebenthal & Lee, 1980). In contrary, gastric lipase activity is akin at birth and at adult age (Sarles et al., 1992), while pancreatic lipase activity varies. Pancreatic triglyceride lipase (PTL), the key enzyme in intestinal lipid digestion in adults, is immature at birth (Delachaume-Salem & Sarles, 1970) and the bile salts, required for the lipase adsorption onto the hydrophobic surface of the lipid droplet, are secreted in low amount (Norman et al., 1972). Instead, the bile salt-stimulated lipase (BSSL) and the pancreatic lipase-related protein 2 (PLRP2) are the main lipases expressed in infant pancreas at birth. The exact activity of these lipases in the intestinal compartment is unknown. BSSL is also found in human milk (3.6–5.3 U/mL of milk; Shani-Levi et al., 2017), which compensates the low endogenous lipid digestion capacity (Andersson et al., 2007).
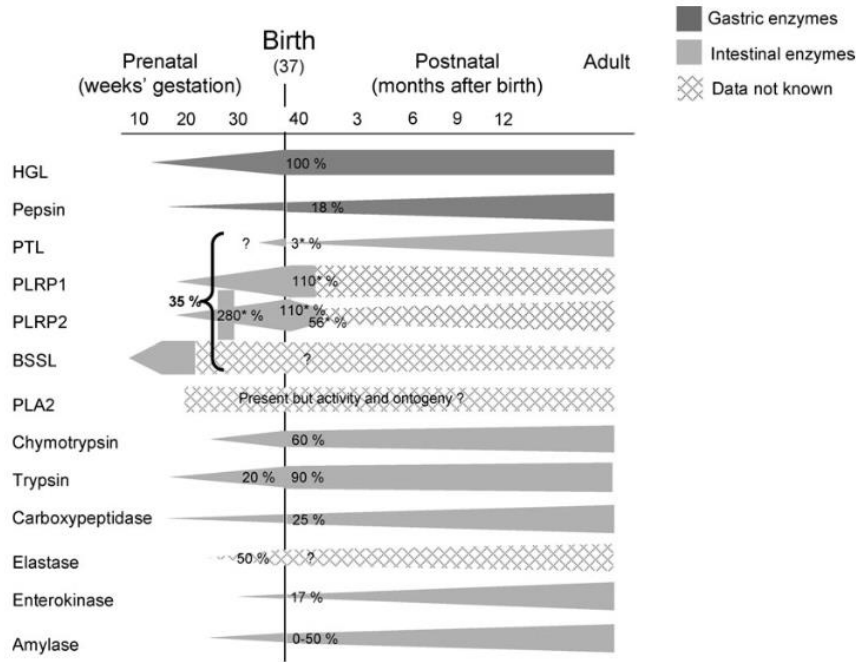
Figure 16. Ontogeny, levels of activity or of mRNA expression (*) of the main digestive enzymes in infants (Bourlieu et al., 2014)

Figure refers to the values at birth or at a given postnatal age for term infants. Abbreviations are HGL: human gastric lipase, PTL: pancreatic triglyceride lipase, PLRP1: pancreatic lipase-related protein 1; PLRP2: pancreatic lipase-related protein 2; BSSL: Bile salt-dependent lipase; PLA2: phospholipase A2

4.1.2. Focus on protein digestion

4.1.2.1. Gastric protein hydrolysis

The initial stage of protein degradation occurs in the acidic environment of the stomach by the action of pepsin, an endopeptidase activated from pepsinogen by selective cleavage of a 7.5 kDa basic peptide. Pepsin activity is influenced by pH. A relatively high gastric pH in infants (pH 3.2-6.5) has been reported (Bourlieu et al., 2014), which is higher than the optimum pH usually reported for pepsin activity (pH 1.5-2.2). However, the latter has been determined on serum albumin by Piper & Fenton (1965) and the pH-depend activity of pepsin may be linked to the protein substrate. Ménard et al. (2018) has shown that in static gastric digestion using an infant model (pH 5.3), intact caseins were almost totally hydrolysed (less than 10% of residual intact caseins) after 60 min of gastric digestion. α-LA or β-LG were resistant to digestion at pH 5.3 (infant model) but were almost fully hydrolysed at pH 3 and with a higher level of pepsin (adult model).

The postpandrial gastric acidification capacity of infants and adults is illustrated in Figure 17. Because of the buffering capacity of human milk or infant formulas, the gastric pH gradually decreases. Thus, the combination of these two factors (reduced pepsin secretion and limited acidification in infants) explains the limited proteolysis reported during the gastric phase in infants compared to in adults (Chatterton et

al., 2004; Henderson et al., 2001). The major gastric proteolysis products are polypeptides with N-terminal amino acids including aromatic amino acids and leucine, corresponding to the cleavage sites of pepsin (Keil, 1992). This results in degree of hydrolysis inferior to 5% at the end of *in vitro* gastric digestion of infant formulas (Le Roux et al, 2020a; Le Roux et al., 2020b) or degree of hydrolysis of 18-20% at the end of *in vivo* gastric digestion of infant formulas by piglets (Lemaire et al., 2018). Kinetics of gastric proteolysis determines the state of the proteins arriving in the small intestine.
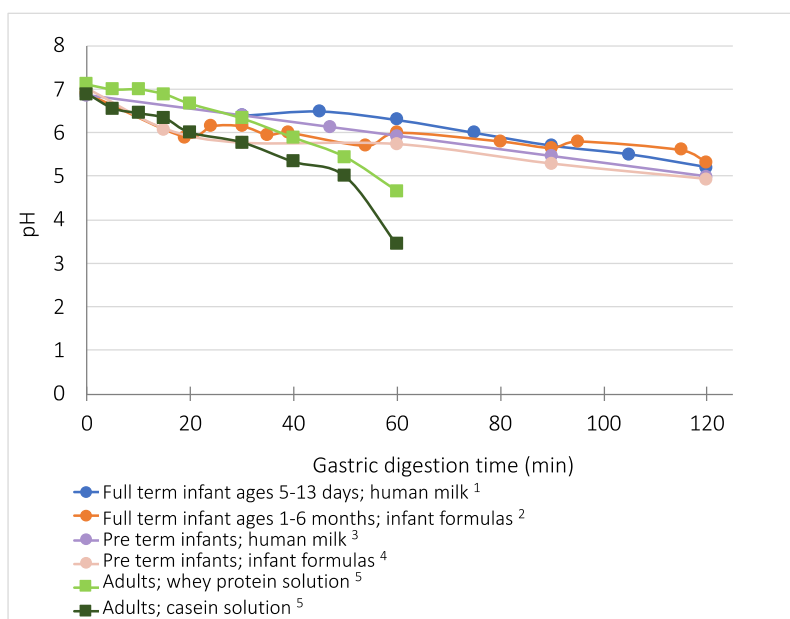
Figure 17. Postprandial gastric pH of infants and adults
[1]Mason, 1962; [2] Cavell, 1983; [3] De oliveira (2016); [4] Roman et al., 2007; [5] Calbet & Holst, 2004.

4.1.2.2.   Intestinal proteolysis

Intestinal proteolysis occurs through the combined actions of pancreatic and brush border enzymes. The key pancreatic proteases are trypsin, chymotrypsins (A, B and C variants), elastase and carboxypeptidases (A and B variants). In addition, enterokinase, a protease secreted from intestinal epithelial cells in response to food stimulation (Neu, 2007), is required to activate the conversion of trypsinogen to trypsin (Britton & Koldovsky, 1989). Then, trypsin activates the conversion of chymotrypsinogen to chymotrypsin, proelastase to elastase and procarboxypeptidase to carboxypeptidase (Lebenthal et al., 1983). Trypsin cleaves peptides at the carboxyl side of the basic amino acids that are lysine and arginine (Leiros et al., 2004). Chymotrypsin mainly cleaves peptides on the carboxyl side of aromatic amino acids (i.e. tyrosine, tryptophan or phenylalanine) (Appel, 1986). Elastase cleaves peptides at the carboxyl side of neutral amino acids such as glycine, alanine, serine and valine. Carboxypeptidase B cleaves the basic amino acids arginine and lysine from the carboxyl-terminal ends of intermediate peptides resulting from the protein hydrolysis by the endopeptidases (i.e. pepsin, trypsin and chymotrypsin endopeptidases) (Kim et al., 1972).

The products of protein hydrolysis are further degraded by brush border peptidases, which hydrolyse the peptide fragments into di- and tri-peptides and free amino acids (Auricchio et al., 1981), which can be absorbed into the enterocyte. Substantial quantities of brush border peptidases, including γ-glutamyl-transpeptidase, oligoaminopeptidase and dipeptidylaminopeptidase IV are present since 22 weeks of gestation (Lebenthal et al., 1983). The enzymatic activity depends on the individual brush border enzymes. For example, the activity of dipeptyl peptidase IV is akin for infants at birth and for adults (Auricchio et al., 1981). In addition, some intestinal brush border enzymes are proline-specific aminopeptidases such as the dipeptidyl aminopeptidase IV, carboxypeptidase P and angiotensin-converting enzyme.

The di- and tri-peptides are absorbed at the apical membrane of enterocytes through the H^+-coupled peptide transporter PEPT-1, which is the main absorption mode of products of protein digestion in infants (Daniel, 2004). Peptides are then hydrolysed by peptidases within enterocytes before being released into the portal blood through amino acid transporters at the basolateral membrane (Boudry et al., 2010). The absorption of free amino acids in the enterocytes involves an active transport system. Many amino acid transporters are coupled with Na^+ or K^+ pumps, and they are not specific to each amino acid but to groups of amino acids that are structurally similar, such as cationic, anionic, neutral amino acids (Boudry et al., 2010).

4.2. Models used to study infant protein digestion

The use of simple *in vitro* digestion models to simulate the gastrointestinal tract have been proposed as alternatives to the use of *in vivo* models because it does not suffer of ethical restrictions and presents other advantages such as a better control, a higher reproducibility, a lower cost and a shorter experimental phase (Bohn et al., 2018). *In vitro* models allow the study of the digestion kinetics, eventually the determination of the protein digestibility and the observation of the structural changes during digestion (Brodkorb et al., 2019; Gouseti et al., 2019; Hur et al., 2011). The development of *in vitro* models for infant gastrointestinal digestion has been allowed thanks to recent reviews on specific infant physiological parameters (Abrahamse et al., 2012; Bourlieu et al., 2014; Poquet & Wooster, 2016). Particularly, Bourlieu et al. (2014) have reviewed studies that characterised gastrointestinal conditions in preterm and full-term infants from birth to six months.

4.2.1. *In vivo* digestion models

Human clinical trials remain the best approach to study food digestion (Deglaire et al., 2009). However, for evident ethical reasons, infant digestion studies are difficult to conduct. This was made possible on

preterm neonates, as those infants have a nasogastric tube for their feeding, which allows gastric digestion collection (de Oliveira et al., 2016). However, intubating infants for a digestion study is not ethically acceptable. Alternatively, animal *in vivo* models, particularly piglet model, can be used to study the digestion of infant formulas (Bouzerzour et al., 2012; Lemaire et al., 2018; Rutherfurd et al., 2006) or of human milk (Darragh & Moughan, 1998). Indeed, pig is considered as the best model to mimic the upper part (stomach and small intestine) of the human gastrointestinal tract (Deglaire & Moughan, 2012; Rowan et al., 1994). Digesta can be collected after piglet slaughtering at specific time points after food ingestion. Intestinal cannulas are difficult to use at this age because the piglet is still sensible and fragile.

4.2.2. *In vitro* digestion models

Different *in vitro* digestion models have been developed to study infant digestion: static (Chatterton et al., 2004; Ménard et al., 2018; Nguyen et al., 2015; Wada & Lönnerdal, 2015), semi-dynamic (Amara et al., 2014; Bourlieu et al., 2015) or dynamic (Maathuis et al., 2017; Ménard et al., 2014; Passannanti et al., 2017; Shani-Levi et al., 2013; Zhang et al., 2014) models. These models have rarely used similar parameters to mimic the infant digestions, which makes difficult the result comparison among studies (Table 8 and Table 9).

Table 8. Literature review of the infant gastrointestinal parameters for *in vitro* static digestion models

References	Physiological state	Meal	Gastric digestion				Intestinal digestion				
			pH	Duration (min)	Meal:secretion ratio (v/v)	Pepsin content [2]	pH	Duration (min)	Meal:secretion ratio (v/v)	Intestinal enzymes [3]	Bile
Fogleman et al., 2012	Preterm newborn	Human milk	5	120	66:34	40 mg/mL of SGF	7.0	120	40:60	Pancreatin: 2 mg/mL of SIF	12 mg/mL of SIF
Vincent et al., 2020			5.3	60	63:37	126 U/mL of gastric content	6.6	60	39:61	Porcine pancreatin: 59 U of lipase/mL of intestinal content	1.6 mM
Wada & Lönnerdal, 2014		Bovine milk	4	15	/	1:12.5 pepsin:protein	7.0	5	/	1:62.5 pancreatin:protein	/
Sun et al., 2019		Goat milk (colostrum)	/	180	/	22.75 U/mg of protein	6.5	60	/	Porcine trypsin: 3.45 U/mg of proteins; Bovine chymotrypsin: 0.04 U/mg of proteins	1 mM sodium taurocholate; 1 mM sodium glycodeoxycholate
Luo et al., 2020 [1]		Yak milk	6.5 - 6.0 - 5.5 - 5.0	120	/	100 U/mL of SGF	7.0	120	50:50 chyme:SIF	Porcine pancreatin:1.6 mg/mL of SIF	5 mg/mL of SIF
Liu et al., 2016		Protein solution	3	60	50:50	113.8 U/mL of SGF	6.5	60	25:75	Bovine trypsin: 8.6 U/mL of SIF	2 mM sodium taurocholate; 2 mM sodium glycodeoxycholate
Torcello-Gómez et al., 2020	Term newborn	Infant formulas	5.3	120	63:37	272 U/mL of gastric content	6.6	60	39:61	Porcine pancreatin: 16 U of trypsin/mL of intestinal content	3.1 mM
Lueamsaisuk et al., 2014			2 - 3.5 - 4.5 - 5.5	120	28:72	5346 U/mL of gastric content				/	
Prakash et al., 2014			1.5	60	50:50	2640 U/mL of gastric content	7.0	120	25:75	Porcine pancreatin: 1.6 mg/mL of solution	5 mg/mL of solution
Nguyen et al., 2015			4	60	65:35	22.75 U/mg of protein	8.0	60	/	Bovine trypsin: 3.45 U/mg of proteins; Bovine chymotrypsin: 0.04 U/mg of proteins	2 mM sodium taurocholate; 2 mM sodium glycodeoxycholate
Ménard et al., 2018			5.3	60	63:37	268 U/mL of gastric content	6.6	60	39:61	Porcine pancreatin: 90 U of lipase and 16 U trypsin /mL of intestinal content	3.1 mM
Le Roux et al., 2020			5.3	60	63:37	270 U/mL of gastric content	6.6	60	39:61	Porcine pancreatin: 16 U of trypsin/mL of intestinal content	3.1 mM
Zenker et al., 2020			5.3	60	63:37	269 U/mL of gastric content	6.6	60	39:61	Porcine pancreatin: 90 U of lipase/mL of intestinal content	3.1 mM
Chatterton et al., 2004		Human milk	2 - 3 - 3.5 - 4 - 5 - 6.5	60	99:1	/				/	
Xavier et al., 2019			5.3	60	63:37	268 U/mL of gastric content	6.6	60	39:61	Porcine pancreatin: 90 U of lipase/mL of intestinal content	3.1 mM
Su et al., 2017		Human milk; Infant formulas	4	120		100 U/mg of protein	6.5	120	/	Pancreatin: 34.5 U/mg of protein	4 mM sodium taurocholate; 4 mM sodium glycodeoxycholate
Yuan et al., 2020 [1]			At 30 min: 5.5	30	/	450 U/mL	6.5	120	/	Porcine pancreatin: 90 U of lipase/mL	1 mM
Dupont et al., 2010	Infant	Protein solution	3	60	85:15	22.75 U/mg of protein	6.5	30	76:24	Porcine trypsin: 34.5 U/mg of protein - Bovine chymotrypsin: 0.4 U/mg of protein	4 mM sodium taurocholate; 4 mM sodium glycodeoxycholate

[1] Gastric pH was controlled to decrease during the gastric digestion; [2] SGF: simulated gastric fluid; [3] SIF: simulated intestinal fluid

Table 9. Literature review of the infant gastrointestinal parameters for *in vitro* dynamic digestion models

References	Physiological state	Meal	Model	Gastric digestion						Intestinal digestion							
				pH	Duration (min)	Pepsin	Flow (mL/min)	$t_{1/2}$ (min)	β	pH	Duration (min)	Bile	Flow (mL/min)	Pancreatin	Flow (mL/min)	$t_{1/2}$ (min)	β
de Oliveira et al., 2016	Preterm newborn	Human milk	DIDGI	- 0.0155 x time + pH_{milk}	180	120 U/mL of gastric content	0-10 min: 1 10-180 min: 0.5	36	1.2	6.2	180	1.6 mmol/L of intestinal content	0.5	59 U lipase/mL of intestinal content	0.25	200	2.2
Nebbia et al., 2020			DIDGI	8.10^{-5} x time² − 0.031 x time + 6.80	180	120 U/mL of gastric content	0-10 min: 1 10-180 min: 0.5	36	1.2	6.2	180	1.6 mmol/L of intestinal content	0.5	1.52 U trypsin/mL of intestinal content	0.25	200	2.2
Yuan et al., 2020			/	- 0.0155 x time + pH_{milk}	120	8.6 U of RGL²/mL of SGF	0-10 min: 1 10-120 min: 0.5	36	/	6.2	120	1.6 mmol/L of SIF	0.5	/	/	200	/
Le Roux et al., 2020	Term newborn	Infant formulas	DIDGI	- 0.0155 x time + pH_{milk}	180	268 U/mL of SGF [3]	0-10 min: 1 10-180 min: 0.5	78	1.2	6.2	180	3.1 mM	0.5	90 U lipase/mL of SIF	0.25	200	2.2
de Oliveira et al., 2016		Human milk	DIDGI	- 0.0155 x time + pH_{milk}	180	268 U/mL of SGF	0-10 min: 1 10-180 min: 0.5	47	0.9	6.2	180	3.1 mM	0.5	90 U lipase/mL of SIF	0.25	200	2.2
Passannanti et al., 2017	Infant at 6 months of life	Rice based food	MIDA¹ system	/	120	1000 U/mL of gastric content	/	/	/	No intestinal digestion							
Ye et al., 2019		Infant formulas	Human gastric simulator	6.6 - 5.6 - 4.5 - 3	240	1050 U/mL of solution	SGF: 0.6 Pepsin: 0.15	/	/	No intestinal digestion							

[1] Model of an Infant Digestive Apparatus; [2] RGL: rabbit gastric lipase; [3] SGF: simulated gastric fluid

4.2.2.1. *In vitro* static and semi-dynamic models

Static model is widely used as it is easy to set up and do not require specific tools. This model consists of a succession of bioreactors mimicking the gastrointestinal environment. In each compartment (mouth, stomach, duodenum), a specific set of parameters (pH, meal dilution, enzyme concentration, mixing) is set up at the start of the digestion, without any pH adjustment or modifications of enzyme flow or emptying during the digestion time. This model can be used for studying the digestion of purified molecules to assess the potential allergenicity of proteins, for example, or for screening different food matrices (Ménard & Dupont, 2014). In addition, compared to the static digestion model, the semi-dynamic model takes into account the gradual acidification during the gastric digestion, the fluid and enzyme secretion flow and the gastric emptying (Mulet-Cabero et al., 2020).

While the INFOGEST network has developed an international consensus for a standardised static model (Brodkorb et al., 2019; Minekus et al., 2014), and recently a semi-dynamic model (Mulet-Cabero et al., 2020), to mimic digestion at the adult stage, to date, there is no such consensus reached for the infant model. Lastly, a physiologically relevant harmonised model of *in vitro* static digestion at the infant stage (28 days of life; gestation age from 38 to 42 weeks) was developed within our laboratory (Ménard et al., 2018) using *in vivo* data of infant physiology for setting model parameters (Bourlieu et al., 2014) (Figure 18). The oral phase has been omitted due to the very short residence time in the mouth for liquid products.
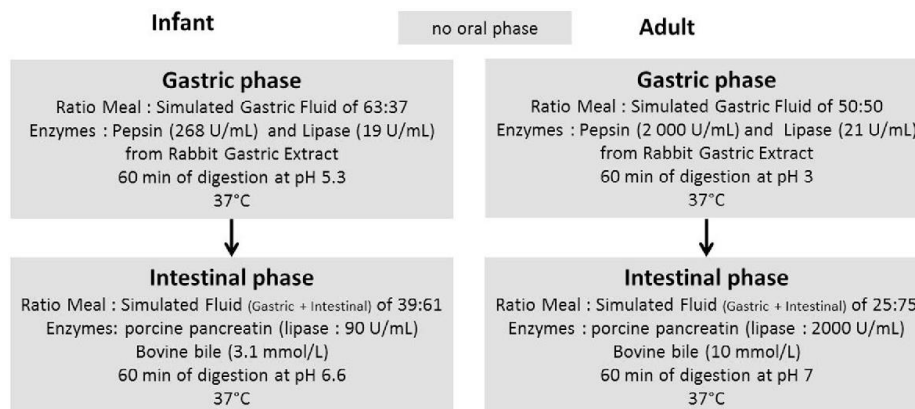
Figure 18. Infant and adult digestive conditions used in the static *in vitro* digestion models (Ménard et al., 2018)

Parameters (meal:secretion ratio, pH) have been determined based on the infant gastric conditions occurring at half-time emptying, assumed to be more representative than the final time point. The half-time gastric emptying has been reported to be at 78 min for infant formulas (Bourlieu et al., 2014). The meal:gastric secretion ratio has been determined following the simulation of secretion flows in the

dynamic digestion model DIDGI® validated for infant formula digestion (Ménard et al., 2014), in which the mean flow rate of secretions is 0.25 mL/min. At 78 min after the start of meal ingestion, the meal:gastric secretion ratio (v/v) was 63:37. The simulated gastric fluid (SGF) composition has been determined based on a study on 30 full-term infants (Hyde, 1968).

The compilation of *in vivo* data of gastric pH in preterm infants during digestion allowed the determination of a linear regression describing the gastric acidification curve (Equation 4). Even if the gastric pH of term infants is less documented, it is considered to be similar to that of preterm infants (Figure 17). Considering a half-time gastric emptying of 78 min and a meal pH of 6.52, gastric pH in the static model was set up at 5.3.

<div align="right">Equation 4</div>

$$pH = -0.0155 \times t + pH_{meal}$$

with t the digestion time (min).

The determination of postprandial enzyme activities for preterm infants resulted in average values of 63 U of pepsin and 4.5 U of lipase per mL of gastric content and per kg of body weight (Armand et al., 1996; Roman et al., 2007). These data have been adapted to term infants by considering a mean body weight of 4.25 kg for a 1-month old infant (de Oliveira et al., 2016). Thus, 268 U of pepsin and 19 U of lipase per mL of gastric content have been set up, corresponding to 13% and 90% of the pepsin and lipase activity, respectively, in the adult static model. This is in accordance with the enzyme ontogeny data for newborns (18% and 100%, respectively; Figure 16).

For the intestinal phase, the meal:gastrointestinal secretion ratio (39:61) has been determined according to the simulation of secretion flows in the DIDGI® model with an overall mean secretion flow rate of 0.85 mL/min at 78 min of digestion (Ménard et al., 2014). The composition of simulated intestinal fluid (SIF) is based on the characterisation of duodenal fluid of 1-week-old full-term infants (Zoppi et al., 1973). Calcium chloride (3 mM) is added separately before the beginning of the intestinal phase (Zoppi et al., 1973). Bovine bile extract concentration (3.1 mM bile salts) has been fixed based on the average postprandial value for 2 week-old infants (Signer et al., 1974). Pancreatin, a mixture of several digestive enzymes composed of amylase, trypsin, lipase, ribonuclease and protease, is added to cover the intestinal lipase activity of infants (90 U/mL of intestinal content, Norman et al., 1972). To our knowledge, there are no data available in the literature regarding the trypsin activity (U/mL) within the neonate duodenal content as discussed previously (Chapter 1 - section 4.1.1).

As already mentioned, *in vitro* static model is simple, easy to use but is not so relevant on a physiological point of view since it is difficult to recreate the complexity of the gastrointestinal tract in a series of beakers. For this reason, dynamic model has been developed to take into account the dynamic of the digestion.

4.2.2.2. *In vitro* dynamic model

Recent gastrointestinal dynamic model gives a more realistic representation of the digestive tract than the static model since they simulate the dynamic changes of pH, the enzymatic flow and activity, the emptying rate, and the flux between gastric and intestinal compartments. Collection of samples from the different digestive compartments over the digestion permits the study of kinetics of disintegration and hydrolysis for example. Different dynamic models have been developed to mimic one or several compartments (de Oliveira et al., 2016; Kong & Singh, 2010; Ménard et al., 2014; Minekus et al., 1999; Molly et al., 1993; Passannanti et al., 2017; Shani-Levi et al., 2013; Zhang et al., 2014).

The most popular gastrointestinal dynamic model is the TIM-1 (TNO gastrointestinal model 1), which consists of stomach and the three parts of the small intestine (duodenum, jejunum, ileum) (Minekus, 2015). Controlled by a computer, this model takes into account parameters such as human temperature, gastric pH decrease, digestive secretions, emptying rates, peristaltic movements and nutrient absorption in the intestine by a dialysis system (Guerra et al., 2012). More recently, a TIM-2 model was developed from TIM-1, which additionally mimics the microbiota (Ji & Xiao, 2006). Another complete *in vitro* dynamic model and adapted to older infants is the Model of Infant Digestive Appartus (MIDA). It mimics the physiology of the gastrointestinal tract (i.e. the oesophagus, the stomach, the pyloric sphincter and the intestine) of 6-month-old infants (Passannanti et al., 2017). Recently, a "near-real" dynamic *in vitro* human stomach system has been developed, simulating the morphology, dimension and wrinkled inner structure of stomach (Wang et al., 2019). It is manufactured with silicone using 3D-printing technology. It is able to generate consistent gastric emptying ratio of both solid and liquid food fractions.

A more simplified gastrointestinal dynamic system, named DIDGI® (INRAE, France), has been developed in our laboratory (Ménard et al., 2014). It contains two successive compartments simulating the stomach and the small intestine controlled by the SToRM® software (Stomach regulation and monitoring) (Figure 19). It simulates the flow of ingested food and within each compartment, the digestive secretions, the gastric pH decrease, the emptying rates, and the temperature (Ménard et al., 2014).

pH probe
Gastric compartment
Gastric emptying pump
Control system
STORM® software
Intestinal compartment
Intestinal emptying pump
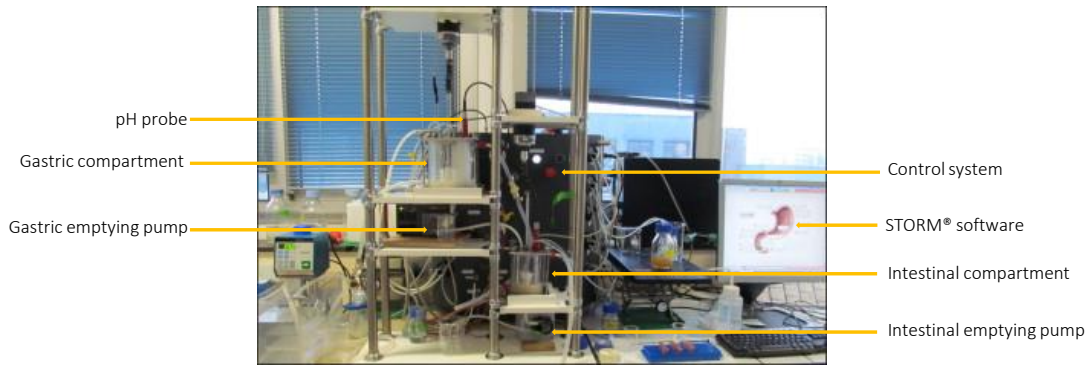
Figure 19. The *in vitro* gastrointestinal dynamic digestion system DIDGI®
(Ménard et al., 2015)

An *in vitro* dynamic digestion protocol using the DIDGI system has been developed to closely mimic the digestive conditions of term infants at the postnatal age of four weeks (Ménard et al., 2014). This protocol has been used within our laboratory in several studies dealing with the digestion of human milk (de Oliveira et al., 2016; Nebbia et al., 2020) and infant formulas (Le Roux et al., 2020b).

According to *in vivo* data (Bourlieu et al., 2014), the pH curve in the gastric compartment follows the linear regression reported in Equation 4. The transit time in the gastric and intestinal compartments are controlled according to the exponential mathematical equation (Equation 5), as described by Elashoff et al. (1982).

Equation 5

$$F(t) = 2^{-\left(t/t_{1/2}\right)^{\beta}}$$

with F the fraction of meal delivered, t the digestion time (min), $t_{1/2}$ the gastric emptying half-time (min) and β the coefficient describing the curve shape.

The $t_{1/2}$ and β values for the gastric and intestinal digestion have been fixed based on reported data in the literature for formula fed-full term infants (Bourlieu et al., 2014). The gastric $t_{1/2}$ is set at 78 min [*vs.* 48 min for human milk; Cavkll (1981)] and the gastric β at 1.2. The intestinal $t_{1/2}$ and β are 200 min and 2.2, respectively. The flow rates of secretion were fixed based on previous studies (Blanquet et al., 2004; Minekus et al., 1995). The enzyme activity and bile targets used in the DIDGI® system is similar as those presented above for the static model (Chapter 1-section 4.2.2.1). Table 10 summarises the gastrointestinal digestion parameters to mimic the digestion of full-term infant at 28 days of life, using *in vitro* static and dynamic models.

Table 10. Parameters for *in vitro* static and dynamic digestion of infant formulas for full-term infants 28 days of life (4.25 kg)

Adapted from de Oliveira et al. (2016) and Ménard et al. (2018)

Gastric conditions (37°C)		
Simulated gastric fluid	Na^+	94 mM
	K^+	13 mM
	Cl^-	122 mM
Gastric pH	Static	5.3
	Dynamic	pH = - 0.0155 x time + pH $_{meal}$
Enzyme	Pepsin	268 U/mL of total gastric content
Gastric emptying parameters	$t_{1/2}$	78 min
	β	1.2
Meal:secretion ratio	Static	63:37
	Dynamic	Meal: 10 mL/min for 10 min
		Secretions: 1 mL/min from 0-10 min
		0.5 mL/min from 10-180 min
Duration	Static	60 min
	Dynamic	Up to 180 min
Intestinal conditions (37°C)		
Simulated intestinal fluid	Na^+	164 mM
	K^+	10 mM
	Ca^{2+}	3 mM
Intestinal pH		6.6
Bile salts		3.1 mmol/L
Pancreatic lipase		90 U/mL of total intestinal content
Intestinal emptying parameters	$t_{1/2}$	200 min
	β	2.2
Meal:secretion ratio	Static	60 min
	Dynamic	180 min

Although *in vitro* digestion systems have substantial advantages, there are still limitations and challenges for the future to better mimic the gastrointestinal digestion mechanism. Indeed, the functions of the mucosal barrier with all its regulatory processes, particularly hormonal and nervous control, the feedback control mechanisms, the mucosal cell activity, the complexity of peristaltic movements, the action of local immune system and the effects of the intestinal microflora and the liver metabolism are neglected in *in vitro* digestion models (Alegría et al., 2015). The absence of hormonal feedback, as the mediation by cholecystokinin (CCK) of the secretion of pancreatic enzyme and bile in response to the entry of chyme in the duodenum (Guilloteau et al., 2006), can make difficult the extrapolation from *in vitro* to *in vivo* data (de Oliveira et al., 2016). Moreover, the brush border peptidases, which play a key physiological role *in vivo* by hydrolysing the peptides at the end-point of digestion into di- and tri-peptides and free amino acids (Chapter 1 - section 4.1.2.2), have been omitted in the majority of *in vitro* digestion models. The reason lies in the difficulty to define the appropriate parameters of the brush border peptidase activity as very few *in vivo* data is available and the commercial availability of the peptidases is limited (Picariello et al., 2016). Porcine brush border

peptidases have been used to simulate the intestinal step within an *in vitro* static digestion of skim milk powder (Picariello et al., 2015). Authors showed that, at the end of duodenal digestion, the degree of protein hydrolysis was significantly higher with brush border peptidases (57%) than without (38%) (Picariello et al., 2015).

4.2.2.3. Other *in vitro* models

Microfluidic devices can be used to simulate digestion. Marze et al. (2014) have developed lipid droplet microfluidic digestion system and, recently, de Haan et al. (2019) have devised a miniaturised digestive system composed by three micromixers coupled in series to a gut-on-a-chip to provide a continuous flow of digested materials.

In vitro digestion models can be combined with human intestinal cell culture such as Caco-2 cells (Andersson et al., 2011; Lipkie et al., 2014; Vors et al., 2012), which integrates brush border enzyme activities as well as active and facilitated transport processes (Abrahamse et al., 2012; Poquet & Wooster, 2016). However, their use for quantitative evaluation remains difficult.

4.3. Impact of protein structures on digestion

Infant formula processing (heat treatments, for example) can change the structure of the milk proteins in several ways, depending on the conditions under which it has been processed (as mentioned in Chapter 1 - section 3). These heat-induced protein modifications may change the digestion kinetics as well as the protein digestibility.

4.3.1. Infant digestion of milk protein

During digestion, the behaviour of caseins and whey proteins differs markedly. The gastric acidification of milk destabilises the casein micelle structure by affecting the internal structure of the casein micelles as well as its external surface layer. The net charge of caseins decreases with the bovine milk acidification and causes the solubilisation of colloidal calcium phosphate (CCP) from the micelles (McMahon et al., 2009). As CCP acts as a bridge connecting the casein micelles, its removal is accompanied by the shrinkage of the casein micelles and the release of individual caseins from micelles (Dalgleish et al., 1989). CCP is fully removed from casein micelles when the pH is inferior to 4.9 (i.e. the pI of casein micelles for raw bovine milk) (Ye et al., 2020). Acidification also causes collapse of the hairy surface layer of the casein micelles. At neutral pH, this layer is negatively charged, and charge repulsions maintain the C-terminal part of k-casein extended in the solvent. As the charges are reduced with acidification, this hair layer is less extended and therefore offers less stabilisation (de Kruif, 1997). This

collapse of the hairy layer has been suggested by the decrease in the hydrodynamic radius of the casein micelles during acidification (Alexander & Dalgleish, 2005).

In addition, caseins are sensitive to pepsin action because the flexible and open structure of casein micelles facilitates the access of cleavage sites on caseins for pepsin (Morell et al., 2017). Bouzerzour et al. (2012) have shown that 23% of intact caseins were remaining after 30 min of gastric digestion of milk-based infant formulas using piglets and 11% of caseins were remaining at 60 min of static gastric digestion of infant formulas (Ménard et al., 2018).

In contrast to casein micelles, whey proteins, because of their globular structure, are known to be extremely resistant to gastric hydrolysis. Previous studies of static digestion of infant formulas have shown that β-LG and α-LA remained intact at the end of gastric digestion (Ménard et al., 2018; Nguyen et al., 2015). In the same way, *in vivo* studies have shown that, during the first days of life, 2-6% of LF consumed by infants during breastfeeding is excreted in the faeces per day (Davidson & Lönnerdal, 1987). This indicates that native LF is resistant to gastrointestinal hydrolysis, as observed for the digestion of human milk using *in vitro* dynamic model (Nebbia et al., 2020).

The analysis of peptides released from human milk and infant formulas during gastrointestinal digestion by infants have been investigated using *in vivo* (Beverly et al., 2019; Dallas, Guerrero, Khaldi, et al., 2014) and *in vitro* (Deglaire et al., 2019; Hernández-Ledesma et al., 2007; Su et al., 2017) models and showed the highest number of peptides came from β-casein hydrolysis. Among the identified functional peptides, some of them are common to human milk and infant formula digestion and have antibacterial, immunomodulatory, antihypertensive, opioid antagonist and/or opioid agonist activities (Su et al., 2017).

4.3.2. Effect of heat-induced protein denaturation on digestion

Firstly, heat treatment of bovine milk leads to the increase of pH at which the caseins coagulated from pH ~ 4.9 to ~ 5.4 (Graveland-Bikker & Anema, 2003; Guyomarc'h et al., 2003; Heertje et al., 1985; Lucey, Tamehana, et al., 1998). This is attributed to the coating of the casein micelles with whey proteins, which modify the casein micelle surface properties (Donato & Guyomarc'h, 2009). The isoelectric pH of whey proteins is at pH 5.2. Therefore, surface-coated casein micelles flocculate at higher pH, resulting in a clear shift in gelation pH (Lucey, Teo, et al., 1998). In addition, the heat-induced whey protein/κ-casein complexes in the soluble phase are also involved in the casein micelle coagulation as they can bind to the surface of casein micelles prior to destabilisation of the casein micelles by acidification (Alexander & Dalgleish, 2005; Donato, Alexander, et al., 2007; Guyomarc'h et al., 2009).

Moreover, many studies have investigated the impact of heat treatment on milk protein digestion at the adult stage. Impacts of heat treatment on casein hydrolysis during digestion was less studied compared to on whey proteins. The heating of skimmed bovine milk increases casein resistance to gastric hydrolysis for adults (Sánchez-Rivera et al., 2015) and infants (Dupont, Boutrou, et al., 2010), probably due to the formation of casein/whey protein aggregates. Regarding whey proteins, it has been shown that holder (de Oliveira et al., 2016) and HTST (Nebbia et al., 2020) pasteurisation treatments of human milk promote the gastric hydrolysis of LF under infant digestion conditions, while the protein is defined as resistant to pepsin hydrolysis in its native form (Britton & Koldovsky, 1989; Davidson & Lönnerdal, 1987; Furlund et al., 2013). In the case of bovine milk, the impact of heat treatment on whey protein digestion is still controversial. Carbonaro et al. (1997) have shown that UHT and sterilisation treatments of bovine milk decrease the whey protein digestibility compared to pasteurisation. In contrary, other studies have shown an increase in the digestibility and susceptibility to hydrolysis of whey proteins after various heat treatments, despite the formation of whey protein/k-casein (Singh & Creamer, 1993) and whey protein/whey protein (O'Loughlin et al., 2012) complexes.

Only a few studies have directly linked the heat-induced protein structures to protein digestion kinetics (Leeb et al., 2015; Zhang & Vardhanabhuti, 2014), and even less for the specific infant formula environment. The *in vitro* studies that investigate the effects of heat treatment on bovine milk protein digestion usually focus on β-LG hydrolysis. *In vitro* studies on the enzymatic hydrolysis of β-LG in bovine milk (Mulet-Cabero et al., 2019, p.; Tunick et al., 2016; Wada & Lönnerdal, 2014), β-LG pure solution (Guo et al., 1995; Rahaman et al., 2017) or WPI solution (Wang et al., 2018) have shown that heat treatments enhances β-LG hydrolysis by pepsin at the adult stage. Indeed, the compact native structure of β-LG makes it particularly resistant to proteolytic activities (Guo et al., 1995). The heat-denaturation of β-LG causes the opening of its 3D structure (as discussed in Chapter 1 - section 3.1.1) and increases the accessibility of the cleavage sites to digestive enzymes (Mullally et al., 1998). However, the susceptibility of β-LG to pepsin depends on the protein structures generated during the heat-treatment. Among the β-LG structures generated under heating, dimers formed at short heating times (i.e. 90°C/5 min) are mostly resistant to pepsin hydrolysis. At longer heating times (i.e. 90°C/60 to 120 minutes), large aggregates are formed that are rapidly digested by pepsin. Lastly, intermediate structures characterised by disulfide-linked β-LG monomers are slowly hydrolysed (Loveday et al., 2014; Peram et al., 2013). However, it remains to be explored whether these observations are similar for infants, for whom the gastric pH is higher and the pepsin activity is lower than for adults.

Thus, differences in product composition (type of protein, dry matter content, pH, etc.) and processing conditions (temperature/time) can lead to different protein structures that could alter protein digestion. The alteration of protein digestion can have further physiological consequences, as different kinetics of protein digestion can lead to different kinetics of peptide release and different postprandial absorption kinetics of amino acids. Released peptides can have effects on the gastrointestinal tract itself or the immune system (Nowak-Wegrzyn & Fiocchi, 2009). These considerations are especially relevant in early life for formula-fed infants, where bovine milk proteins are the unique source of food proteins.

To conclude the bibliographic review, infant formulas constitute an adequate substitute of human milk when breastfeeding is not a possibility or a wish, although human milk is considered as the ideal infant food for the first months of life. To ensure appropriate nutritional composition, infant formula composition is highly regulated. Current infant formulas are mainly based on bovine milk. However, human and bovine milks vary in terms of nutrient composition, particularly regarding the protein profile. Such differences are mainly corrected by controlling the casein:whey protein ratio and the aminogram of the infant formulas. Unfortunately, such approach leads to infant formulas that are more concentrated in proteins than human milk, with possible nutritional consequences later in life. This drawback could be solved by tuning the whey protein profile of infant formulas, especially its α-LA and LF content. Moreover, during the manufacturing of infant formulas, heat treatments are applied to ensure the microbiological safety. It is established that heat treatments above 60°C have irreversible consequences on the structure of whey proteins, mainly α-LA and β-LG, leading to their unfolding and aggregation. The behaviour of whey proteins under heating is governed by medium conditions, like the protein profile, the mineral and sugar contents of milk protein-based products. Depending on the environmental parameters, the heat-induced protein structure may change and alter the susceptibility to digestive enzymes. To date the protein structure generated during the heating of infant milk formulas is unknown especially those with an enrichment of α-LA and LF. Moreover, the studies dealing with the heating of infant formulas with a modified whey protein profile mainly focused on the technological properties of the heated infant formulas but not their nutritional properties. From the bibliographic review, it appears that a lack concerns the relationship between the heating conditions of the infant formulas, the generated protein structures and their digestion by infants. Due to ethical and technical constraints, *in vivo* infant digestion study can not be easily conducted. Thus, *in vitro* dynamic digestion model has been developed to simulate human digestion, and in particular infant digestion. The particularity of infant digestion conditions (gastric pH, enzyme activity) is an important factor to take into account for the study of protein digestion.

Chapter 2: Objectives and strategy

Infant formulas are intended to be an efficient substitute of human milk and every effort is made to mimic the nutritional profile of human milk for optimal infant growth and development. Although current infant formulas mimic the casein:whey protein ratio of human milk, α-LA and LF, the dominant whey proteins in human milk, are in low amounts, while β-LG, a protein that is absent of human milk, is usually the dominant whey protein in most infant formulas. Thus, supplementation of infant formulas with α-LA and LF constitutes a possible way to be closer to human milk protein profile.

Heat treatments used in the manufacture of infant formulas is the common process used to ensure their microbiological quality during long periods, but, in return, they modify the physicochemical and nutritional properties of infant formulas. Heat treatments induce the denaturation of whey proteins and the formation of aggregates whose structure depends on the physicochemical conditions of the medium such as its pH and ionic strength. Subsequently, these protein structural changes could alter the protein digestion behavior.

As shown in the literature review (chapter 1), the heat-denaturation kinetics of the whey proteins and the protein structures are well documented for bovine milk or purified milk protein solutions. However, the results of these studies cannot be extrapolated to infant formulas due to the different composition between bovine milk and infant formulas, in particular regarding the protein profile, the lactose amount and the mineral content. It is therefore relevant to study the heat-denaturation kinetics of the whey proteins and the protein structures within infant formulas, especially because the protein structure could impact the proteolysis kinetics, which, in turn, could modulate protein metabolism.

In this context, the present project aimed to better understand the behavior of the milk proteins during the heat treatment of model infant formulas (denaturation kinetics of the whey proteins, structure and physicochemical properties of protein aggregates), and their fate during simulated gastrointestinal digestion at the infant stage.

Thus, the main research question of this project was:

> **What are the protein structures generated during the heating of model infant formulas and how do they impact the digestion kinetics of the milk proteins at the infant stage?**

The general strategy of the PhD project is summarised in Figure 20. In a first part, three model infant milk formulas (IMFs) were developed in agreement with the European regulation (European Union, 2016) regarding the contents of protein, lactose and minerals. The IMFs were produced at 1.3% and 5.5% of total proteins, i.e. the protein contents at which are applied heat treatments during the manufacture of liquid or powdered infant formulas, respectively. The IMFs differed by their whey

protein profile (i.e. the α-LA:β-LG:LF ratio). The Control IMF had the same whey protein profile as bovine whey; the protein sources for the preparation of this IMF were skimmed bovine milk and WPI. The LF$^+$ IMF had the same LF amount than that of human milk; the protein sources for the preparation of this IMF were skimmed bovine milk, WPI and purified LF. The LF$^+$ α-LA$^+$ IMF had the same LF and α-LA amounts than those of human milk; this latter IMF was prepared using skimmed bovine milk, purified LF and purified α-LA.

In a second part, the kinetics of heat-induced denaturation of the major whey proteins (i.e. α-LA, β-LG and LF) in the IMFs (i.e. Control, LF$^+$, LF$^+$ α-LA$^+$ IMFs) at 1.3% or 5.5% of proteins were investigated in the temperature range from 67.5°C to 80°C by quantification of the residual native proteins after various heating times. The results and discussion section of this part are presented in **Chapter 4**.

The protein structures generated upon heating were investigated in a third part. For this, the IMFs (i.e. Control, LF$^+$, LF$^+$ α-LA$^+$ IMFs) at 1.3% or 5.5% of proteins were heated at 67.5°C or 80°C to reach an akin whey protein denaturation extent of 65%, value within the range found in commercial infant formulas. Protein structures were analyzed by asymmetrical flow field-flow fractionation coupled with multiangle light scattering and differential refractometer, transmission electron microscopy and electrophoresis. The unheated formulas were used as reference. The results and discussion section of this part are presented in **Chapter 5.**

In a fourth part, the IMFs (i.e. Control, LF$^+$ α-LA$^+$ IMFs) at 1.3% or 5.5% of proteins and akin whey protein denaturation extent of 65% were submitted to gastrointestinal digestion using *in vitro* static and dynamic models in order to investigate the relationship between the protein structure and protein digestion. Laser light scattering and confocal laser scanning microscopy (CLSM) were performed to analyse IMF destabilisation during digestion. SDS-PAGE, OPA (*o*-phthalaldehyde) assay, cation exchange chromatography and mass spectrometry were used to monitor the kinetics of proteolysis. The results and discussion section of this part are presented in **Chapters 6 and 7.**

1 **Development of model infant milk formulas**

In agreement with the European regulation (EU, 2016/127)

		Control IMF	LF⁺ IMF	LF⁺ α-LA⁺ IMF
Protein content		1.3% & 5.5%	1.3% & 5.5%	1.3% & 5.5%
Casein: whey protein		40:60	40:60	40:60
	α-LA	✖	✖	✖
Whey protein profile	β-LG	✖	✖	*Traces*
	LF	*Traces*	✖	✖

2 **Kinetics of heat-induced whey protein denaturation**

By reverse phase-high performance liquid chromatography

IMFs	⊗	Protein content of IMFs	⊗	Temperatures	⊗	Whey proteins
Control		1.3%		67.5°C − 80°C		α-LA
LF⁺		5.5%				β-LG
LF⁺ α-LA⁺						LF

4 **Kinetics of protein digestibility- *In vitro* static model**

By laser light scattering, electrophoresis, OPA assay and cation exchange chromatography

IMFs	⊗	Protein content of IMFs	⊗	Temperatures
Control		1.3%		Unheated
LF⁺ α-LA⁺		5.5%		67.5°C
				80°C

3 **Characterization of heat-induced protein structure**

By asymmetrical flow field-flow fractionation coupled with multiangle light scattering and differential refractometer, transmission electron microscopy and electrophoresis

IMFs	⊗	Protein content of IMFs	⊗	Temperatures
Control		1.3%		Unheated
LF⁺		5.5%		67.5°C
LF⁺ α-LA⁺				80°C

5 **Kinetics of protein digestibility- *In vitro* dynamic model**

By laser light scattering, confocal laser scanning microscopy, electrophoresis, OPA assay, cation exchange chromatography and mass spectrometry

IMFs	⊗	Protein content of IMFs	⊗	Temperatures
Control		1.3%		Unheated
LF⁺ α-LA⁺				80°C

Figure 20. General strategy implemented during the project

The Material & Methods of the present work is gathered in **chapter 3**. The results and discussion of the chapters 4, 5 and 6 for the IMFs processed at 1.3% proteins have been published in peer-reviewed journals[1]. Each chapter of results is divided into two sub-chapters, the first sub-chapter dealing with the results obtained for IMFs processed at 1.3% proteins and the second one those for IMFs processed at 5.5% proteins. The results obtained for IMFs processed at 5.5% proteins are briefly discussed and compared to those obtained for IMFs processed at 1.3% proteins.

---

[1] Halabi, A., Deglaire, A., Hamon, P., Bouhallab, S., Dupont, D., Croguennec, T. (2020). Kinetics of heat-induced denaturation of proteins in model infant milk T formulas as a function of whey protein composition. *Food Chemistry*, 302, 125296. https://doi.org/10.1016/j.foodchem.2019.125296

Halabi, A., Deglaire, A., Hennetier, M., Violleau, F., Burel, A., Bouhallab, S., Dupont, D., Croguennec, T. (2020). Structural characterization of heat-induced protein aggregates in model infant milk formulas. *Food Hydrocolloids*, 107, 105928. https://doi.org/10.1016/j.foodhyd.2020.105928

Halabi, A., Croguennec, T., Bouhallab, S., Dupont, D., Deglaire, A. (2020). Modification of protein structures by altering the whey protein profile and heat treatment affects *in vitro* static digestion of model infant milk formulas. *Food & function*, https://doi.org/10.1039/D0FO01362E

Chapter 3 - Material and methods

This section presents all the material and methods applied through the thesis project.

1. Infant formula ingredients

The low heat skimmed milk powder (SMP) was prepared by microfiltration of raw skimmed milk (1.4 μm cut-off) at Fromagerie Gillot (Saint-Hilaire-de-Briouze, France). Then, the microfiltered skimmed milk was concentrated in a two-stage falling film vacuum evaporator set on the first stage at 64°C. The concentrated milk temperature was 50°C at the outlet of the first stage and 38°C at the outlet of the evaporator. The concentrated milk was spray-dried with temperatures of inlet and outlet air of 240°C and 88°C, respectively. The temperature of the integrated fluid bed air was set at 75°C. Microfiltered skimmed milk evaporation and the subsequent spray-drying was conducted at the semi-industrial unit Bionov (Rennes, France). The SMP was characterised by a whey protein nitrogen index of 9 mg of nitrogen/g of SMP. The composition of SMP is described in Table 11.

Total nitrogen, non-protein nitrogen and non-casein nitrogen were quantified by the Kjeldahl method (International Dairy Federation, 1993). The total proteins, caseins and whey proteins were quantified by the Equation 6:

<div align="right">Equation 6</div>

$$\text{Total proteins} = (TN-NPN) \times 6.38$$

$$\text{Whey proteins} = (NCN-NPN) \times 6.38$$

$$\text{Caseins} = (TN-NCN) \times 6.38$$

With TN the content of total nitrogen, NPN the content of non-protein nitrogen and NCN the content of non-casein nitrogen. TN, NPN and NCN were expressed as g of nitrogen/100 g of IMFs. The contents of total proteins, whey proteins and caseins were expressed as g of proteins/100 g of IMFs.

Lactose content was quantified by refractometry after separation by high-performance liquid chromatography (HPLC) using a Aminex A-6 ion exchange column (Bio-Rad, Hercules, CA, USA) as described by Aburjaile et al. (2016). Calcium, iron, potassium and sodium contents were quantified by atomic absorption spectrometry as described by Brulé, Maubois, & Fauquant (1974). Inorganic phosphorus content was quantified by using the molybdenum blue method according to Jean (1969). Chloride was quantified with the Sherwood Scientific chloride analyzer (Modele 926, Sherwood Scientific Ltd, Cambridge, UK) as described by Berdagué, Grappin, & Duboz (1987).

Table 11. Composition of skim milk powder

	Composition	Quantity
g / 100 g of SMP	Total proteins	36
	Whey proteins	7
	Caseins	29
	Lactose	48
mg / 100 g of SMP	Calcium	1401
	Chloride	893
	Inorganic phosphorus	1014
	Magnesium	104
	Potassium	1616
	Sodium	382

Whey protein isolate (WPI; Prolacta®95) was purchased from Lactalis Ingredients (Bourgbarré, France). Bovine lactoferrin powder (LF - Prodiet Lactoferrin®), with an iron saturation level of 16% as determined by absorbance at 465 nm, was kindly provided by Ingredia Dairy Experts (Arras, France). Bovine α-lactalbumin powder (α-LA) was kindly supplied by Agropur Inc (Appleton, USA). Protein content of the WPI, LF and α-LA powders, as determined by Kjeldhal method with a nitrogen conversion factor of 6.38, was 88, 90 and 84% (w/w) respectively. The composition of major proteins in the SMP, WPI, LF and α-LA powders is illustrated in Figure 21 under both non-reducing and reducing conditions.

All protein powders were stored at -20°C until use. Lactose was supplied by Armor Proteines (Saint-Brice-en-Coglès, France). $CaCl_2 \cdot 2H_2O$ was from AnalaR (Leuven, Belgium), $FeSO_4 \cdot 7H_2O$ from Sigma-Aldrich (St-Louis, USA), KCl from Panreac (Barcelona, Spain), $Na_3PO_4 \cdot 12H_2O$ from Merck (Darmstadt, Germany), and $Na_3C_6H_5O_7 \cdot 2H_2O$ from Carlo Erba Reagents (Val-de-Reuil, France). Water was Milli-Q water.

Figure 21. Electrophoretic pattern of protein ingredients used for infant formula formulation under reducing and non-reducing conditions.
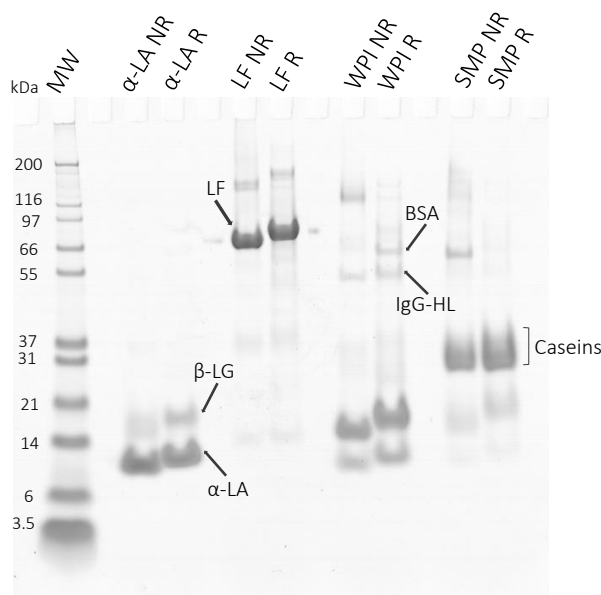
MW: Molecular weight marker; α-LA: α-lactalbumin; β-LG: β-lactoglobulin; IgG-HL: high chain of IgG; BSA: bovine serum albumin; LF: lactoferrin.
4 µg of proteins were deposited per well.

2. Chemicals

The standards of α-LA and β-LG were purchased from Davisco (MN, USA) LF Standard was from Ingredia Dairy Experts (Arras, France). Pepsin was from porcine gastric mucosa (P6887; 3075 U/mg). Pancreatin, a mix of pancreatic enzymes, was from porcine pancreas (P7545; trypsin activity of 6.7 U/mg; lipase activity of 85.2 U/mg). Bile extract was from bovine bile (B3883; 0.9 mmol/g). The enzyme activities and bile concentration were measured using the assays described in the harmonised INFOGEST protocol (Brodkorb et al., 2019). Enzymes and bile salts, as well as enzyme inhibitors, namely Pepstatin A (P5318) and Pefabloc® SC (76307), were purchased from Sigma-Aldrich (St. Quentin Fallavier, France).

3. Infant formula formulation and chemical characterisation

The IMFs were formulated in agreement with the European regulation (European Union, 2016) for the bovine-milk-based IMFs regarding the contents of protein, lactose and the principal minerals. The IMFs were prepared at 5.5% total proteins, as described in Figure 22, and with the ingredient quantities as referenced in Table 12. Briefly, lactose solution at approximatively 30% (w/w) was prepared at 50°C during 30 min and cooled at room temperature during 30 min. Then, WPI for the control IMF, WPI and LF powder for the LF[+] IMF, LF and α-LA powders for the LF[+] α-LA[+] IMF were rehydrated in the lactose solution at 24% (w/w), into which SMP was then added. Between each addition step, the solutions were magnetically stirred during 1h at room temperature. After dispersion, the solutions were supplemented

by minerals using $Na_3C_6H_5O_7 \cdot 2H_2O$, $Na_3PO_4 \cdot 12H_2O$, KCl, $CaCl_2 \cdot 2H_2O$ and $FeSO_4 \cdot 7H_2O$, as recommended by European Commission (2006) and stirred during 10 min at room temperature. Finally, the solutions were diluted with Milli-Q water at 1.3% of proteins. The IMFs at 1.3% and 5.5% proteins were adjusted at pH 6.8 with 1 M KOH and stored overnight at 4°C to ensure the complete rehydration and powder equilibration.
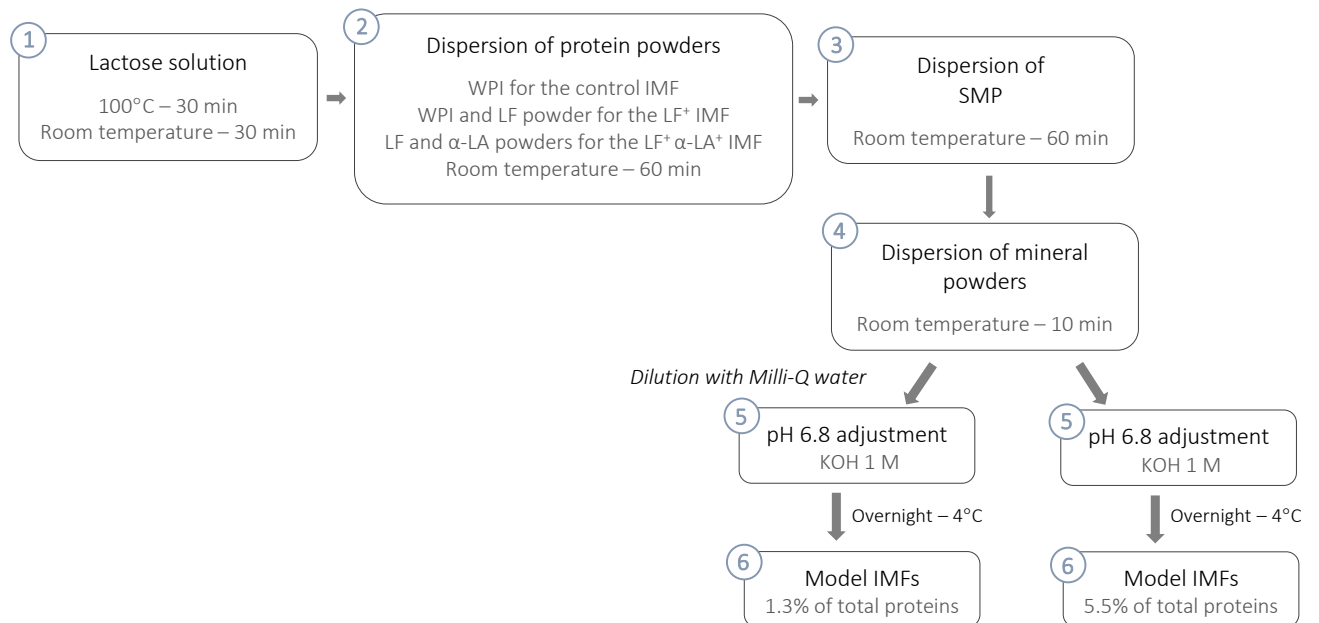
Figure 22. General scheme for the preparation of the infant milk formulas

Table 12. Ingredient amounts for the preparation of the infant milk formulas

	Step 1			Step 2			Step 3			Step 4		
	Control	LF⁺	LF⁺ α-LA⁺	Control	LF⁺	LF⁺ α-LA⁺	Control	LF⁺	LF⁺ α-LA⁺	Control	LF⁺	LF⁺ α-LA⁺
Lactose (g)	28.68	28.68	23.59									
Milli-Q (g)	91.32	91.32	76.41									
Lactose solution (g)				88.71	88.69	88.74						
WPI (g)				3.66	2.29	/						
LF (g)				/	1.34	1.34						
α-LA (g)				/	/	1.89						
SMP (g)							6.92	6.95	7.33			
$Na_3C_6H_5O_7{\cdot}2H_2O$ (mg)										127.3	129.7	160.1
$Na_3PO_4{\cdot}12H_2O$ (mg)										138.7	135	87.7
KCl (mg)										252.9	252	240.3
$CaCl_2{\cdot}2H_2O$ (mg)										183	203.7	206.9
$FeSO_4{\cdot}7H_2O$ (mg)										10.1	8.9	8.9

The steps correspond to those described in Figure 22.

The detailed composition of the IMFs at 1.3% or 5.5% proteins is presented on Table 13 or on Supplementary Table 1, respectively. As a reminder, the IMFs at 1.3% or 5.5% proteins differed by their total solid content. Protein, lactose and mineral contents in the IMFs were quantified as described previously (Chapter 3 - section 3). Ash content was determined by weighing the dry mineral residue after water and volatile vaporization, and organic matter oxidative burning at 550°C for 5h in a muffle furnace. The total amino acid content of each IMF was quantified as described previously (Davies & Thomas, 1973). Briefly, IMFs were chemically hydrolysed by 6 N HCl at 110°C for 24h and dried at 40°C under vacuum. Samples were re-dispersed in distilled water, filtered at 0.45 μm and diluted 3-times with 0.2 M lithium citrate buffer (pH 2.2). Samples (50 μL) were then injected in the cation exchange column of Biochrom 30 automatic amino acid analyser (Biochrom Ltd., Cambridge, UK) with post-column derivatisation with ninhydrin (EZ Nin Reagent™, Biochrom Ltd, Cambridge, UK), as described previously (Moore, Spackman & Stein, 1958). The ninhydrin derivative of proline was detected at 440 nm and the derivatives of other amino acids were detected at 570 nm. Lithium citrate buffers were used as eluents. Methionine and cysteine were determined separately after overnight cold performic acid oxidation followed by acid hydrolysis and were quantified as methionine sulfone and cysteic acid, respectively. Tryptophan was not quantified due to oxidative degradation during acid hydrolysis. The quantification of the total amino acids of IMFs was performed in at least two independent freshly prepared IMFs. The amino acid composition of the IMFs is presented on Table 14.

Table 13. Composition of the infant milk formulas at 1.3% proteins - Comparison with the European reglementation (EU 2016/127) and term human milk

Elements		Control IMF	LF[+] IMF	LF[+] α-LA[+] IMF	Reglementation[1]		Human milk[2]
					Min	Max	
Total proteins		1.33 ± 0.01	1.35 ± 0.01	1.31 ± 0.01	1.08	1.75	0.90
Whey proteins	*g / 100 g liquid meal*	0.83 ± 0.04	0.82 ± 0.00	0.75 ± 0.00			0.60
α-LA		0.14 ± 0.00	0.10 ± 0.00	0.39 ± 0.02			0.25
β-LG		0.51 ± 0.01	0.33 ± 0.00	0.06 [3]			Trace
LF		n.d.	0.17 ± 0.00	0.15 ± 0.01			0.15
Caseins		0.50 ± 0.03	0.53 ± 0.01	0.56 ± 0.01			0.40
Lactose		5.6 ± 0.4	5.8 ± 0.4	5.6 ± 0.2	2.7		7.6
Calcium	*mg / 100 g liquid IMF*	41.4 ± 0.7	41.1 ± 1.4	42.2 ± 0.7	30	98	27
Chloride		65.8 ± 1.7	69.6 ± 0.9	68.5 ± 0.4	36	112	40
Iron		0.42 ± 0.02	0.41 ± 0.02	0.43 ± 0.01	0.18	0.91	0.50
Inorganic phosphorus		21.1 ± 0.6	20.6 ± 0.6	20.8 ± 0.3	15	63	15
Potassium		60.2 ± 6.3	63.4 ± 1.3	62.4 ± 0.4	48	112	54
Sodium		21.5 ± 1.5	20.9 ± 1.2	25.0 ± 0.7	15	42	18
Ash	*%, w/w*	0.18 ± 0.04	0.17 ± 0.04	0.16 ± 0.03			n.d.

n.d: non determined

[1] European regulation for 1st age bovine milk-based infant formulas (European Union, 2016).

[2] Average value based on term human milk data from Lönnerdal, Forsum, & Hambraeus, 1976, Altomonte, Salari, Licitra, & Martini, 2019, Wack, Lien, Taft, & Roscelli, 1997.

[3] Value of β-LG content in the LF[+] α-LA[+] IMF was estimated by calculation from the amount of β-LG in SMP and the proportion of SMP in the IMF.

Table 14. Amino acid content of the infant milk formulas at 1.3% proteins - Comparison with the European reglementation (European Union, 2016) and term human milk

Amino acids (g/kg of liquid meal)	Control IMF [1]	LF+ IMF [1]	LF+ α-LA+ IMF [1]	Minimal reglementary value [2]	Human milk [3]
Cys	0.32 ± 0.00	0.34 ± 0.00	0.41 ± 0.01	0.23	0.24
His	0.32 ± 0.01	0.28 ± 0.01	0.32 ± 0.01	0.24	0.27
Ile	0.76 ± 0.01	0.64 ± 0.00	0.65 ± 0.01	0.54	0.55
Leu	1.56 ± 0.03	1.45 ± 0.01	1.35 ± 0.01	1.00	1.05
Lys	1.33 ± 0.01	1.25 ± 0.00	1.25 ± 0.01	0.68	0.69
Met	0.42 ± 0.00	0.36 ± 0.01	0.30 ± 0.01	0.14	0.17
Phe	0.58 ± 0.02	0.61 ± 0.02	0.64 ± 0.01	0.50	0.39
Thr	0.79 ± 0.01	0.74 ± 0.01	0.70 ± 0.02	0.50	0.47
Tyr	0.55 ± 0.00	0.56 ± 0.00	0.61 ± 0.03	0.46	0.50
Trp	0.19 [4]	0.16 [4]	0.30 [4]	0.19	0.20
Val	0.79 ± 0.02	0.79 ± 0.01	0.72 ± 0.00	0.53	0.58
Ala	0.58 ± 0.01	0.62 ± 0.00	0.48 ± 0.00		0.39
Arg	0.36 ± 0.02	0.45 ± 0.02	0.44 ± 0.01		0.37
Asp + Asn	1.38 ± 0.01	1.30 ± 0.01	1.50 ± 0.02		0.91
Glu + Gln	2.78 ± 0.01	2.54 ± 0.02	2.32 ± 0.04		1.89
Gly	0.27 ± 0.01	0.33 ± 0.00	0.35 ± 0.00		0.24
Pro	0.95 ± 0.02	0.90 ± 0.00	0.82 ± 0.01		0.95
Ser	0.68 ± 0.02	0.67 ± 0.01	0.64 ± 0.01		0.47
Total nitrogen	1.96 ± 0.01	1.92 ± 0.01	1.89 ± 0.08	1.73	1.90

[1] Data for IMFs are means ± SD (n = 2 or n = 3).

[2] European regulation for 1st age bovine milk-based infant formulas (European Union, 2016).

[3] The data of human milk are obtained from a systematic review derived from 13 countries of total amino acid for term human milk at 4 months of life (Zhang & Lyden, 2019).

[4] Tryptophan amount was not determined for IMFs due to oxidative degradation during acid hydrolysis of IMFs but it was estimated based on the amount of α-LA, β-LG and LF in the IMFs and the tryptophan amount for each protein (Castellino et al., 1970; Fox et al., 2015).

4. Heat treatment of infant formulas

4.1. Kinetics of whey protein denaturation

Glass capillary tubes (8 mm inner diameter and 40 mm length, Waters, USA), containing 800 µL of IMFs pre-heated at 30°C during 1h, were placed in a thermally controlled water bath (Fisherbrand™ Isotemp™ water bath, Thermo Fisher Scientific, Newington, USA) set at different temperatures ranging from 67.5°C to 80°C (by step intervals of 2.5°C). For each condition, the heating

ramp (i.e. the time to reach the target temperature) was controlled with a YC-747UD Data Logger Thermometer inserted in a reference tube. The heating ramp was converted into a heating time at target temperature (as explained in Chapter 3 - section 5.2.1). At various time intervals, tubes were removed and instantaneously chilled on ice bath to stop whey protein denaturation/aggregation reactions. The unheated IMFs were used as reference. Holding times for each heating temperature were chosen to scan the denaturation/aggregation of whey proteins up to a yield of 70% to 80%. Three independent experiments were performed for the heat treatment at 75°C, considering the standard deviation equivalents at all heating temperatures investigated.

4.2. Heating conditions to reach 65% of whey protein denaturation

For the studies of protein particle characterisation and *in vitro* static digestions, the same protocol than that described previously was applied, with some modifications. The water bath was set at 67.5°C or 80°C, and the holding times were fixed to reach an identical denaturation extent of total whey proteins of 65%, a value within the range found in commercial IMFs (Table 15). Each heat treatment was repeated on three freshly prepared IMFs (n = 3). Unheated and heated IMFs were stored at 4°C before further analysis.

Table 15. Holding times (in min) for the infant milk formulas at 1.3% and 5.5% proteins at 67.5°C and 80°C

	IMFs processed at 1.3% proteins			IMFs processed at 5.5% proteins		
	Control IMF	LF$^+$ IMF	LF$^+$α-LA$^+$ IMF	Control IMF	LF$^+$ IMF	LF$^+$α-LA$^+$ IMF
67.5°C	200	50	240	240	130	120
80°C	7	3	30	12	3.5	12

As the volume of IMFs needed for the *in vitro* dynamic digestion experiments (150 mL) was higher than the volume for the *in vitro* static digestion experiments (20 mL), a scale-up for the IMF heating was required. For this, IMFs were pre-heated at 53.5°C prior to heat treatment at 80°C to reduce the heating ramp. Glass tubes containing 10 mL of IMFs were pre-heated in a water bath to attempt 53.5°C, then placed in a water bath set at 80°C (Fisherbrand™ Isotemp™ water bath, Thermo Fisher Scientific, Newington, USA). The holding times (9 min for the control IMF and 30 min for the LF$^+$ α-LA$^+$ IMF) were fixed to reach an identical denaturation extent of total whey proteins of 65%. After heating, the IMF samples were cooled by immersion in an ice-water bath to stop the whey protein denaturation reaction. Each heat treatment was repeated three times on one freshly prepared IMF (n = 3). The unheated IMFs were used as reference. Unheated and heated IMFs were stored at 4°C before further analysis. Thereafter, IMFs heat-treated to a protein concentration of 1.3 or 5.5% are named « IMFs processed at 1.3% proteins » or « IMFs processed at 5.5% proteins », respectively.

5. Denaturation of whey proteins

5.1. Precipitation of caseins and denatured whey proteins, and quantification of native whey proteins

The caseins and denatured/aggregated whey proteins were precipitated by adding a sufficient volume of 1.4 M acetic acid/acetate buffer (pH 4.35) to 150 μL of unheated and heated IMFs to adjust the pH at 4.6. After heating at 40°C for 2 min, the proteins in the pH 4.6-soluble fraction were separated from the precipitate by centrifugation at 14,000*xg* for 20 min at 25°C using an Eppendorf Microcentrifuge MicroStar 17R (VWR, Leuven, Belgium). The supernatants of the IMFs were diluted 13-fold (or 58-fold for the IMFs processed at 5.5% of proteins) in Milli-Q water containing 0.106% (v/v) trifluoroacetic acid for analysis by RP-HPLC.

Native whey proteins were separated on a PLRP-S 300 Å, 8 μm, 150 x 3 mm separation column combined with a guard column (Agilent Technologies, UK) connected to a Dionex UltiMate 3000 HPLC System (Thermo Fisher, Dreieich, Germany), equipped with a detector VWD3400RS (Thermo Fisher, Dreieich, Germany) operating at 280 nm for the quantification of eluted proteins. Proteins were eluted at a flow rate of 0.2 mL/min and at 40°C, using a gradient of acetonitrile obtained by mixing the mobile phase A (0.106% (v/v) of trifluoroacetic acid in Milli-Q water) and the mobile phase B (0.1% (v/v) of trifluoroacetic acid in acetonitrile). The acetonitrile gradient started with a plateau of 35.2% of mobile phase B during 14 min, and then continued with successive increases of mobile phase B to 38.4% in 6 min, 40% in 7 min, 42.4% in 14 min, 49.6% in 1 min, and finally 80% in 4 min. Native whey proteins in unheated and heated samples were quantified using a calibration curve established by direct injection of standards of α-LA, β-LG and LF at 0.5 g/L of proteins. Chromatographs were analysed by Chromeleon® software (Version 7.2 SR4, Thermo Fisher, Waltham, USA). The term "native whey proteins" referred in the manuscript to the proteins in the pH 4.6-soluble fraction that have the same retention time in RP-HPLC than the whey protein standards. Consequently, the whey proteins still soluble at pH 4.6 but that underwent structural modifications during heat treatment in such a way that their RP-HPLC retention time was modified were not quantified as native proteins.

5.2. Kinetic parameters of individual whey protein denaturation

5.2.1. Calculation of D-values, Z-values, and the equivalent heating time

For each IMF and heating treatment, the equivalent time t_θ (min) was calculated, corresponding to the time required at the temperature θ (°C) to obtain the same rate of protein denaturation than the reference treatment [θ_{ref} (°C) at $t_{\theta ref}$ (min)]. T_θ was determined using the Equation 7, as follows:

Equation 7

$$t_\theta = t_{\theta ref} \cdot 10^{\frac{\theta ref - \theta}{z}}$$

with z (°C) corresponding to the mean of Z-values (i.e. temperature increase required to obtain a tenfold reduction of the whey protein denaturation time) estimated for each protein (Jeantet et al., 2016). Z-values were calculated from the Equation 8, as follows:

Equation 8

$$Z = \frac{T_2 - T_1}{\log(D_1) - \log(D_2)}$$

with D_1 and D_2 (min) the whey protein denaturation times for having 90% whey protein denaturation at heating temperature T_1 (°C) and T_2 (°C), respectively. The D-values were determined as the inverse of the slope of the linear regression of the logarithm of individual whey protein concentrations vs heating time.

5.2.2. Determination of the kinetic parameters for the heat denaturation/aggregation of whey proteins

The reaction orders n and the rate constants k_n were determined by the integration of the general rate equation (Equation 9) according to Croguennec et al. (2014), as follows:

Equation 9

$$-\frac{dC_t}{dt} = k_n \cdot C_t^{\,n}$$

which gives, for n ≠ 1:

Equation 10

$$\left(\frac{C_t}{C_0}\right)^{1-n} = 1 + (n-1) \cdot k_n \cdot C_0^{\,n-1} \cdot t$$

C_t (g/L) is the native whey protein concentration at holding time t (min), C_0 (g/L) the native whey protein concentration of the unheated sample and k_n (g^{1-n}/L^{1-n}/min) the rate constant.

The reaction order n was determined as the best fitting of experimental data by the Equation 10 considering different values of n. The rate constants k_n were determined from the linear regression slope of $\left(\frac{C_t}{C_0}\right)^{1-n}$ *vs.* holding time, as described by Dannenberg & Kessler (1988).

The Arrhenius representation, corresponding to the relationship between the logarithm of the rate constant k_n *vs.* the inverse of heating temperature, was plotted according to the Equation 11.

Equation 11

$$\ln(k_n) = \ln(k_{n,0}) - \frac{E_a}{R.T}$$

The activation energy E_a (kJ/mol) was obtained from the slope of the linear regression of the Arrhenius plot and the denaturation/aggregation frequency factor logarithm, $\ln(k_{n,0})$, from the y-intercept. R is the universal gas constant (8.314 J/mol/K) and T the heating temperature (K).

6. Protein particle characterisation

6.1. Asymmetric flow field flow fractionation coupled with multi-angle light scattering and differential refractometer

6.1.1. Principle

The field-flow fractionation (FFF) technique was originally developed by Giddings in 1966. The FFF technique allows the fractionation and characterisation of macromolecules and colloidal particles of size ranging from a few nanometers to about 100 µm with high resolution (Fraunhofer & Winter, 2004). In contrary to column-based separation methods as chromatographic techniques, the FFF systems are devoid of stationary phase, which limits the mechanical and shear stress during separation and so the alterations of the molecule conformation.

As chromatographic techniques, different FFF sub-techniques existed depending on the molecule properties (molecular size, charge, density, chemical structure). The most widely spread and commonly used FFF sub-technique is asymmetric flow field flow fractionation (AF4), developed by Grander in 1980. This sub-technique is characterised by the replacement of the bottom wall of the FFF system by a semi-permissive membrane with a specific cut-off size, placed above a frit, to allow the solvent penetration and the retention of specific sample components depending on their size (Figure 23).
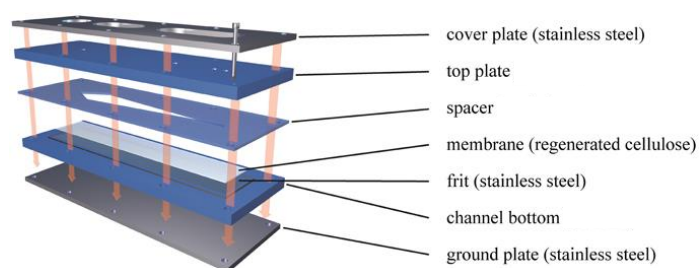
Figure 23. Schematic representation of the asymmetric flow field flow fractionation channel (Adapted from Müller et al., 2015)

Samples are injected during the focus stage, during which two parabolic laminar channel flows are generated in opposing directions to focus the samples in the accumulation wall (Figure 24.A).

Perpendicularly to the direction of the channel flows, an external field force (i.e. cross-flow) is applied to drive the accumulation of samples at the bottom wall. This external force is counteracted by Brownian diffusion of molecules resulting in their diffusion toward the inner channel. Smaller molecules, defined by a low hydrodynamic size and a high diffusion coefficient, are positioned in the higher laminar layers. By opposition, larger molecules are positioned near to the accumulation wall. Following the injection flow, a relaxation step marks the starting point of elution. The molecules are transported by the elution flow from the inlet to the outlet port. The trapezoidal channel geometry confers a laminar elution flow, with a higher velocity in the channel center than near to the accumulation wall (Figure 24.B). Thus, smaller molecules are eluted earlier as compared to larger molecules.
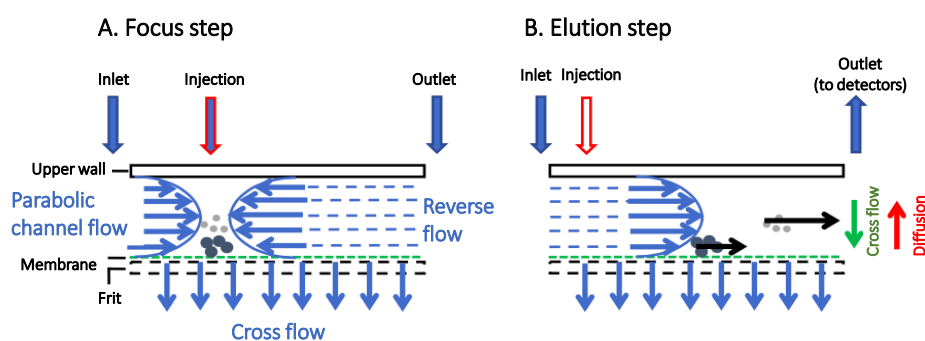
Figure 24. Separation principle in asymmetric flow field flow fractionation
(Adapted from Zhang & Lyden, 2019)

Coupled with online detectors as multi-angle light scattering (MALS), dynamic light scattering (DLS), or refractive index (RI), AF_4 provides a multitude of information about protein size and structure. The determination of the gyration radius (R_g), the hydrodynamic radius (R_h), the shape factor (R_g:R_h ratio) and the apparent fractal dimension (df_{app}) is possible with the light scattering detectors. The molecular weight (M_w) distribution can be determined by the combination of the protein concentration and the light scattering detector data.

6.1.1.1.   Determination of the R_g and M_w

The light scattering data obtained after the detection by MALS of the scattered intensity at different angles in relation to the incoming light are fitted to different models as the Debye (1944), Zimm (1948) and Berry (1966) models. The Berry's method has been used in the present study as it is adapted for molecules characterized by $R_g < 200$ nm. Briefly, the slope of the curve fitted to the angular dependence of the intensity of scattered light permits the R_g determination. Thus, the M_w average of each molecule

population is calculated from the intersection of the fitted curve, supposing that the refractive index increment (dn/dc) is known.

6.1.1.2. Determination of the diffusion coefficient and R_h

The molecule diffusion coefficients (D) are determined by the elution times. The R_h is determined by DLS instrument according to the Stokes-Einstein equation (Equation 12).

$$R_h = \frac{k_B T}{6\pi\eta D}$$

With R_h the hydrodynamic radius (m), k_B the Boltzmann constant ($m^2.kg.K/s^2$), T the temperature (K), η the viscosity (Pa.s) and D the diffusion coefficient (m^2/s).

6.1.1.3. Determination of the conformation properties

The apparent fractal dimension of the protein aggregates (df_{app}) are determined from the inverse of the slope of the log-log linear regression plot of R_g *vs.* M_w. A sphere conformation is characterised by a df_{app} = 3.0, while a random coil conformation is characterised by a df_{app} = 1.5-2.0 (Nilsson, 2013). In addition, the shape factor (R_g:R_h ratio) completes the conformational information. A shape factor of 0.775 traduced a compact spherical structure, values ranging from 1-2 characterise linear random coil structures, and values higher than 2 indicate anisotropic shapes (Adolphi & Kulicke, 1997; Glantz et al., 2010; Wittgren et al., 1998).

6.1.2. Practice

The AF_4 instrument was an Eclipse DualTec separation system (Wyatt Technology Europe, Dernbach, Germany), composed of a channel of trapezoidal geometry with a length of 19.5 cm, and from 1.65 to 0.27 cm in width. The channel spacer was made of polytetrafluoroethylene with a thickness of 250 µm. The ultrafiltration membrane was a regenerated cellulose membrane with a cut-off of 10 kDa (Wyatt Technology Europe, Germany). The eluent was a solution of 50 mM NaCl, 5 mM $CaCl_2$, 0.05% (w/v) of sodium azide in Milli-Q water (pH 7.6), filtered through 0.1 µm. Flows were controlled with an Agilent Technologies 1260 series isocratic pump (Agilent Technologies, Waldbronn, Germany) equipped with an in-line vacuum degasser. In order to prevent the separation system contamination, a filter holder with a 100 nm pore size polyvinylidene fluoride membrane (Millipore Corp, Darmstadt, Germany) was placed between the pump and the eclipse. Standards of α-LA, β-LG, LF and SMP as casein micelle standard were used for protein identification. Samples and standards were diluted in eluent at 1 g/L of

proteins. Injections of samples (20 µL) and standards (10 µL) were controlled with an Agilent 1260 Autosampler (Agilent Technologies, Waldbronn, Germany).

During the entire elution period, the channel flow was maintained at 1 mL/min, whereas the cross-flow gradient varied. Samples were injected during the focusing/injection step with a focus-flow rate of 1.5 mL/min and the focusing/relaxation step was performed for 5 min. The first step of the elution was the increase of the cross-flow at 4 mL/min then was set at this flow rate during 6 min. Thereafter, the cross-flow was decreased exponentially during 10 min to reach 0.1 mL/min, then was kept constant at 0.1 mL/min for 25 min. At the end of each run, the channel was rinsed with the eluent for 18 min to eliminate any contaminants prior to next injection.

The detection system consisted of four units: **(1)** An 18 angle Dawn Heleos II multiangle light scattering detector (Wyatt Technology, Santa Barbara, CA, USA) operating at a wavelength of 662 nm, calibrated with toluene and normalized with the interdetector delays and band broadening calculations with bovine serum albumin (M_w = 66.4 g/mol); **(2)** An Optilab T-Rex differential refractive index detector (Wyatt Technology, Santa Barbara, CA, USA) operating at a wavelength of 658 nm; **(3)** A UV-vis detector vWD 1260 Infinity Agilent Technologies operating at a wavelength of 280 nm; **(4)** A DynaPro NanoStar (Wyatt Technology Europe, Santa Barbara, CA, USA) connected online to the Dawn Heleos II on the angle 12.

Data were analysed with the Astra software (version 7.1.2, Wyatt Technology Corporation) as described by Loiseleux et al. (2018). The mean of the z-average R_g (nm) and the mean of the M_w (g/mol) were determined from the second-order polynomial fitting of the light scattering data obtained by MALS in the scattering angle range from 50-134°, using the Berry method with a refractive index increment of 0.185 mL/g (Wang & Lucey, 2003; Zhao, Brown, & Schuck, 2011). The z-average R_h (nm) was determined by the DLS instrument. The df_{app} and the shape factors were determined for conformation information.

6.2. Transmission electronic microscopy

The unheated and heated IMFs processed at 1.3% of proteins were analysed by transmission electronic microscopy (TEM) as described by Tercinier, Ye, Anema, Singh, & Singh (2014) with some modifications. Samples were concentrated using a 3 kDa Vivaspin® Polyethersulfone centrifugal filter (Vivaspin® 500, 3000K MWCO, PES, Sartorius AG, Goettingen, Germany) at 14,000x*g* during 20 min at 25°C. The concentrated phase was pipetted into a drop of 3.5% (w/v) low melting agar solution heated at 60°C and the mix was kept at room temperature until agar gelation. The agar block areas including the sample drops were cut and placed for 3h at room temperature in a 0.1 M sodium cacodylate buffer containing 2.5% (v/v) glutaraldehyde. The blocks were post-fixed for 1h in a 0.1 M sodium cacodylate buffer

containing 1% (v/v) osmium and 1% (v/v) ferrocyanide, then washed for 30 min in a 0.1 M sodium cacodylate buffer, and finally in distilled water for 20 min. Blocks were stained using an aqueous uranyl acetate solution at 1% (v/v) at 4°C overnight, and dehydrated into successive graded ethanol baths at 50%, 70%, 80%, 90% and 100% (v/v) during elapsed time per solution of at least 10 min. Blocks were impregnated in three mixtures of 1.6% (v/v) DMP-30 (2,4,6-Tris(dimethylaminomethyl)phenol) in Epon resin and ethanol having ratio 1:2, 1:1 and 2:1 (v/v) during elapsed time per mixture of 1h, then in 1.6% (v/v) DMP-30 in Epon resin for 2h, and finally polymerized in this Epon mixture at 60°C for 48h. Ultrathin sections (80 nm) of embedded samples were cut with a diamond knife using a Leica UC7 ultramicrotome (Leica Microsystems, Germany). The sections were placed on 200-mesh nickel grids. The TEM imaging was carried out using a JEM-1400 Transmission Electron Microscope (JEOL CO. Ltd, Tokyo, Japan) operating at 120 kV accelerating voltage. Images were acquired with a Gatan SC200 Orius® CCD camera at 50,000 magnification and set up with the imaging software Gatan DigitalMicrograph™ (Gatan, Pleasanton, USA). Images were recorded on at least two different regions of each sample.

6.3. Electrophoresis

The unheated and heated IMFs were analysed by sodium dodecyl sulphate-polyacrylamide gel electrophoresis (SDS-PAGE) under reducing and non-reducing conditions for both IMFs processed at 1.3 and 5.5% proteins and before and after ultracentrifugation (100,000xg; 1h; 25°C) only for the IMF processed at 1.3% proteins. The supernatant of ultrafiltration was collected and contained the soluble protein fraction; the pellet composed of the larger protein entities (intact and partially disintegrated casein micelles, whey protein aggregates, etc.) was discarded.

Samples were firstly diluted with distilled water (5.5- or 23-fold for IMFs processed at 1.3 and 5.5% proteins, respectively) and secondly 2-fold with the NuPAGE® LDS buffer (106 mM TRIS HCl; 141 mM TRIS Base; LDS 2 %; Glycerol 10 %; 0.51 mM EDTA; 0.22 mM SERVA® Blue G250; 0.175 mM Phenol Red; pH 8.5) (Invitrogen, Carlsbad, CA, USA). The samples for SDS-PAGE under reducing conditions were mixed with 0.5 M DTT (3 µL) and heated at 70°C for 10 min.

In order to identify the protein bands, a molecular weight marker ranging from 3.5 to 200 kDa (Mark 12 Unstained Standard; Novex® Life Technologies, California, USA) was used. Samples (20 µL) and the molecular weight marker (15 µL) were loaded in the wells of precast 4–12% polyacrylamide gels (NuPAGE® Novex® Bis-Tris gels, Invitrogen, Carlsbad, CA, USA). The gels were placed on the Hoefer™ miniVE vertical electrophoresis system (Pharmacia Biotech, Sweden) containing the MES SDS Running Buffer (Invitrogen, Carlsbad, CA, USA), and the electrophoresis migration was carried out at 200 V for 90 min. After migration, the proteins were precipitated by immersing the gel in aqueous solution of 30% (v/v) ethanol and 10% (v/v) acetic acid for 30 min, followed by coloration in Coomassie Biosafe (Bio-Rad

Laboratories) overnight. The gels were rinsed in distilled water for 90 min and scanned using an Image Scanner III LabScan 6.0 (GE Healthcare Europe GbmH, Velizy-Villacoublay, France).

7. *In vitro* digestions

7.1. Static model

In vitro gastrointestinal digestion of the unheated and heated IMFs processed at 1.3% or 5.5% proteins was carried out following a static model simulating the digestion conditions of a full-term infant at 28 days of life (Figure 25) (O. Ménard et al., 2018). The heated IMFs processed at 5.5% proteins were diluted with Milli-Q water at 1.3% proteins prior to digestion experiments.

Briefly, IMF was mixed with simulated gastric fluid (SGF), composed by 94 mM NaCl and 13 mM KCl (pH 6.6), and a sufficient volume of 1 M HCl to adjust the pH at 5.3. Freshly prepared pepsin solution in SGF (268 U/mL of total gastric volume) was finally added. The ratio of meal to gastric secretions was 63 to 37 (v/v). The solution was incubated for 60 min at 37°C in a water bath under stirring at 350 rpm. The pH was then increased to 7 by addition of 1 M NaOH in order to stop pepsin activity before further intestinal digestion.

Simulated intestinal fluid (SIF), composed by 164 mM NaCl, 10 mM KCl and 85 mM sodium bicarbonate (pH 6.6), bile extract solution in SIF (3.1 mmol/L of total intestinal volume) and $CaCl_2$ (1.1 mmol/L of total intestinal volume) were added to the previous solution. After pH adjustment to 6.6 with 1 M HCl, freshly prepared pancreatin solution in SIF (7.1 U trypsin activity/mL of total intestinal volume) was added. The ratio meal to gastrointestinal secretions was of 39 to 61 (v/v). The solution was incubated for 60 min at 37°C in a water bath under stirring at 350 rpm.

Samples were collected before digestion and during both gastric and intestinal digestions at 5, 15, 30 and 60 min. Except for particle size distribution analysis by laser light scattering performed immediately, proteolysis was inhibited by adding 10 µL of Pepstatin A (0.73 mM in methanol) per mL of gastric digesta or 50 µL of Pefabloc® SC (0.1 M in distilled water) per mL of intestinal digesta. Samples were stored at -20°C until analysis. *In vitro* digestion experiment was conducted on each triplicate of IMFs.
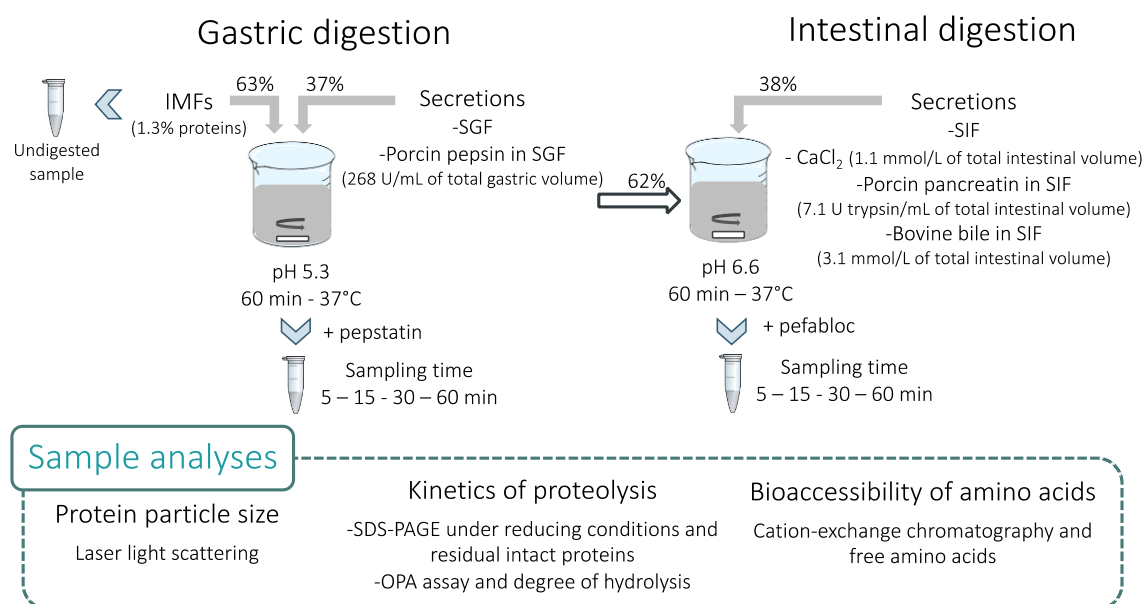
Figure 25. Illustration of the *in vitro* static digestion protocol simulating the digestion of full-term infant at 28 days of life, and recapitulation of sample analysis

7.2. Dynamic model

In vitro gastrointestinal digestion of the unheated and heated IMFs processed at 1.3% proteins was carried out following a dynamic model using the bi-compartmental system DIDGI® (Ménard et al., 2015) (Figure 26). The system was set up to simulate the gastrointestinal digestion conditions of term infants at the postnatal age of four weeks as described by de Oliveira et al. (2016), with some adaptation to the formula-fed infants. Fluid secretions, pH and compartment emptying were continuously controlled by the StoRM® software. The transit times in both gastric and intestinal compartments were set according to the exponential equation described by Elashoff et al. (1982). The gastric emptying coefficients ($t_{1/2}$ = 78 min; β = 1.2) and the intestinal emptying coefficients ($t_{1/2}$ = 200 min; β = 2.2) were fixed according to the review on human infant gastrointestinal physiological conditions (Bourlieu et al., 2014). The gastric pH followed a linear regression pH = - 0.0155 x t + pH$_{IMF}$ with t the digestion time (min) and pH$_{IMF}$ the pH of undigested IMF (6.82 ± 0.03). The intestinal pH was maintained at 6.6. The variation of gastric pH was controlled using 0.5 M HCl and the intestinal pH was neutralised using 0.5 M NaHCO$_3$. Pepsin was diluted in SGF to 268 U/mL of total gastric volume. Pancreatin and bile were diluted in SIF to 7.1 U of trypsin/mL of total intestinal volume and 3.1 mmol/L of total intestinal volume, respectively. After rehydration, pepsin and pancreatin solutions were kept on ice throughout the experiment to avoid autolysis. Pepsin solution was delivered in the gastric compartment at a constant flow rate of 0.5 mL/min. Pancreatin and bile solutions were delivered in the intestinal compartment at a constant flow rates of 0.25 mL/min and 0.5 mL/min, respectively. Table 16 summarises the parameters used for the *in vitro* dynamic digestion experiments.

Secretions
-Porcin pepsin in SGF
(0-180 min: 268 U/mL of total gastric volume)
-HCl (0.5 M)

pH electrode

Gastric digestion

IMFs
(1.3% proteins)

+ pepstatin

Sampling time
40 – 80 – 120 – 180 min

Undigested
sample

Stirrer
blade

$pH = -0.0155 \times time + pH_{IMF}$
180 min - 37°C

Secretions
-Porcin pancreatin in SIF
(Trypsine: 7.1 U/mL of total intestinal volume)
-Bovine bile in SIF
(3.1 mmol/L of total intestinal volume)
-NaHCO$_3$ (0.5 M)

Intestinal digestion

+ pefabloc

Sampling time
40 – 80 – 120 – 180 min

P

Pump

pH 6.6
180 min - 37°C

Sample analyses

Protein particle size
Laser light scattering

Structural analysis
Confocal laser scanning
microscopy

Kinetics of proteolysis
-SDS-PAGE under reducing conditions and
residual intact proteins
-OPA assay and degree of hydrolysis

Kinetics of amino acid release
Cation-exchange chromatography and
free amino acids

Kinetics of peptide release
Mass spectrometry

Figure 26. Illustration of the *in vitro* dynamic digestion protocol simulating the digestion of breastfed term infants at the postnatal age of four weeks, and recapitulation of sample analysis

Table 16. Gastrointestinal conditions for *in vitro* dynamic digestions
(Adapted from de Oliveira et al., 2016)

Gastric conditions (37°C)		
SGF	Na$^+$	94 mM
(stock solution adjusted at pH 6.5)	K$^+$	13 mM
	Cl$^-$	122 mM
Fasted state / initial conditions	SGF	2 mL
	pH	3.1
Milk ingested	Total volume	100 mL
	Flow rate	10 mL/min from 0 to 10 min
Gastric pH (acidification curve)	pH = -0.0155 x t + pH$_{IMF}$	
	with t: time after ingestion (min)	
SGF + Porcine pepsin	Pepsin	268 U/mL
	Flow rate	1 mL/min from 0 to 10 min
		0.5 mL/min from 10 to 180 min
Gastric emptying	t$_{1/2}$	78 min
(Elashoff fitting)	β	1.2
Intestinal conditions (37°C)		
SIF	Na$^+$	164 mM
(stock solution adjusted at pH 6.6)	K$^+$	10 mM
	Ca^{2+}	3 mM
Intestinal pH	6.6	
SIF + Bovine bile	Bile salts	3.1 mmol/L
	Flow rate	0.5 mL/min from 0 to 180 min
SIF + Porcine pancreatin	Pancreatin	7.1 U trypsin/mL
	Flow rate	0.25 mL/min from 0 to 180 min
Intestinal emptying	t$_{1/2}$	200 min
(Elashoff fitting)	β	2.2

Digestions were performed over 180 min. Samples were collected before digestion (undigested samples) and during both gastric and intestinal digestions at 40, 80, 120 and 180 min (G40, G80, G120 and G180 for the gastric samples, or I40, I80, I120 and I180 for the intestinal samples). Except for particle size distribution analysis by laser light scattering and structural analysis by confocal microscopy performed immediately after sampling, proteolysis was inhibited by adding 10 µL of Pepstatin A (0.73 mM in methanol) per mL of gastric digesta or 50 µL of Pefabloc® SC (0.1 M in distilled water) per mL of intestinal digesta. For spectrometry mass analysis, 50 µL of Pefabloc® SC PLUS (0.1 M in distilled water) per mL of intestinal digesta were added. Samples were stored at -20°C until analysis. Each *in vitro* digestion experiment was performed in triplicate for each type of IMF (n = 3).

8. Digesta characterisation
8.1. Particle size distribution

Particle size distribution of undigested IMFs and digesta was measured by laser light scattering using a Malvern Mastersizer 2000 (Malvern Instruments Ltd., Worcestershire, UK) with two laser sources at 633 and 466 nm. Samples were diluted in MilliQ-water in the measurement cell to reach between 3 and 7% of obscuration. The refractive index of protein and water were set at 1.45 and 1.33, respectively (Mulet-Cabero et al., 2019). Particle size measurement was performed in triplicate for each sample (n = 3).

8.2. Confocal laser scanning microscopy

The microstructure of the undigested IMFs and digesta was observed by confocal laser scanning microscopy (CLSM) using a ZEISS LSM880 inverted confocal microscope (Carl Zeiss AG, Oberkochen, Germany) at x20 magnification (Plan Apochromat objective, dry, NA 0.80). Samples (200 µL) were gently mixed with Fast Green aqueous solution (1% w/v; 6 µL) and the mixture was kept at room temperature for at least 10 min to label proteins. 20 µL of mixture was deposited on a glass slide in a spacer and a cover slip was placed on top of all samples. Fast green was excited using a He Ne laser system at a wavelength of 633 nm at a 1.72 µs pixel dwell scanning rate and detected using a PMT between 635 and 735 nm. Images were processed using confocal acquisition software ZenBlack and recorded in a panorama mode of 2 x 2 images at a resolution of 1024 × 1024 pixels each. Confocal analysis was performed for each *in vitro* digestion experiments (n = 3), with at least 10 micrographs recorded for each sample.

8.3. Electrophoresis and intact protein quantification

SDS-PAGE on undigested IMFs and digesta under reducing conditions was performed as described above (Chapter 3 - section 6.3). In order to identify the protein bands, a molecular weight marker ranging from 3.5 to 200 kDa was used (Mark 12 Unstained Standard; Novex® Life Technologies, California, USA). Pepsin and pancreatin solutions were loaded on the gels in amounts similar to those of the gastric or intestinal samples, respectively. After electrophoresis migration (90 min, 200 V), the proteins were precipitated by immersing the gel in aqueous solution of 30% (v/v) ethanol and 10% (v/v) acetic acid for 30 min, followed by coloration in Coomassie Biosafe (Bio-Rad Laboratories) during 120 min. The gels were rinsed in distilled water and scanned using an Image Scanner III LabScan 6.0 (GE Healthcare Europe GbmH, Velizy-Villacoublay, France).

Bands on SDS-PAGE gels were quantified by densitometry using the software Image Quant TL™ (GE Healthcare Europe183 GbmH, Velizy-Villacoublay, France) to study the kinetics of hydrolysis of α-LA, β-LG, LF and caseins during *in vitro* digestion (n = 3). Intact proteins remaining in the samples were quantified following the Equation 13 after taking into account the meal dilution by the secretions.

Equation 13

$$\text{Intact protein (\%)} = \frac{\text{Protein peak area}_{\text{digesta}}}{\text{Protein peak area}_{\text{undigested IMF}}} \times 100$$

Caseins were considered as a unique band due to the poor resolution of the individual casein bands.

8.4. Primary amino group quantification and degree of hydrolysis

The primary amino group quantification of undigested IMFs and digesta was performed using the OPA (*o*-phthalaldehyde) method (Church et al., 1983). Prior to analysis, samples were centrifuged at 10,000*xg* during 30 min at 4°C. Supernatants were diluted in distilled water, 10-times for the undigested IMFs and the gastric samples or 30-times for the intestinal samples, followed by a 3-fold dilution in OPA reagent. Samples were then incubated at 37°C for 10 min in a flat-bottom 96-well microliter plate (Greiner Bio-One, Courtaboeuf, France) and the absorbance was measured at 340 nm with a Multiskan™ GO Microplate Spectrophotometer (Thermo Fisher Scientific, Waltham, MA USA). The OPA reagent (pH 9.5) was composed of SDS (0.5% w/v), DTT (7 mM), OPA solution in ethanol (1.9 mM) and sodium tetraborate (18.9 mM). Primary amino groups were quantified using a methionine standard curve in a concentration range from 0 to 2 mM. The quantification of the primary amino groups was performed in triplicate for each sample (n = 3).

The degree of hydrolysis (DH), which corresponds to the proportion of the cleaved peptidic bonds within IMFs, was calculated using Equation 14, after taking into account the meal dilution by the gastrointestinal secretions:

<div align="right">Equation 14</div>

$$DH\ (\%) = \frac{[NH_{2\ digesta}] - [NH_{2\ secretions}] - [NH_{2\ undigested\ IMF}]}{[NH_{2\ total}] - [NH_{2\ undigested\ IMF}]}\ x\ 100$$

with [$NH_{2\ digesta}$] the primary amino group content in the digesta samples (mg/L of IMF), [$NH_{2\ secretions}$] the primary amino group content of bile and pancreatin solutions at the same concentrations than found in intestinal digesta (mg/L of IMF), [$NH_{2\ total}$] the total content of primary amino groups within the IMFs after acid hydrolysis by 6 N HCl at 110°C for 24h (mg/L of IMF). [$NH_{2\ undigested\ IMF}$] corresponded to the primary amino group content in the undigested IMFs (mg/L of IMF). For *in vitro* dynamic digestion study, [$NH_{2\ undigested\ IMF}$] was quantified after pH adjustment of the undigested IMFs to the different pH digesta samples, meaning pH 5.6 for G80 sample, pH 4.9 for G120 sample, pH 4.1 for G180 sample and pH 6.6 for intestinal samples for the *in vitro* dynamic digestions.

8.5. Total and soluble nitrogen quantification and *in vitro* protein digestibility

The contents of total nitrogen and of soluble nitrogen recovered in the 10 kDa-ultrafiltrate using a Vivaspin® 20 (10,000 K MWCO, PES, Sartorius Stedim Lab Ltd, Stonehouse, UK) operating at 9,000*xg* during 40 min at 4°C, were measured using the micro-Kjeldahl method (Miller & Houghton, 1945). They were determined in the intestinal compartment at 180 min (I180) and in the intestinal fraction emptied over 180 min (I180E). *In vitro* protein digestibility was calculated according to two calculations. The first calculation took into account the total nitrogen amount of the meal (Equation 15) to determine the true

in vitro protein digestibility, as described by Le Roux et al. (2020) except that the content of soluble N lower than 10 kDa was determined by the sum of peptide nitrogen and amino acid nitrogen.

$$\text{Overall } \textit{in vitro} \text{ protein digestibility (\%)} = \frac{[\text{Soluble N}_{\text{digesta}}] - [\text{Soluble N}_{\text{secretions}}]}{[\text{Total N}_{\text{undigested IMF}}]} \times 100$$

$$\text{Instantaneous } \textit{in vitro} \text{ protein digestibility (\%)} = \frac{[\text{Soluble N}_{\text{digesta}}] - [\text{Soluble N}_{\text{secretions}}]}{[\text{Total N}_{\text{digesta}}] - [\text{Total N}_{\text{secretions}}]} \times 100$$

[Total N$_{\text{digesta}}$] or [soluble N$_{\text{digesta}}$] is the nitrogen content in the total or soluble phase after a 10 kDa-ultrafiltration at 180 min of intestinal digestion (g of N/L of IMF). They correspond to the average of the [total N$_{\text{digesta}}$] or [soluble N$_{\text{digesta}}$] of I180 sample and the [total N$_{\text{digesta}}$] or [soluble N$_{\text{digesta}}$] of I180E sample weighted by the percentage of meal for each sample (g of N/L of IMF). [Total N$_{\text{secretions}}$] or [soluble N$_{\text{secretions}}$] is the nitrogen content in the total or soluble phase after a 10 kDa-ultrafiltration of the bile and pancreatin solutions at the same concentration than those found in the intestinal digesta samples (g of N/L of IMF). [Total N$_{\text{undigested IMF}}$] is the total nitrogen content in the IMFs before digestion (g of N/L of IMF).

8.6. Free amino acid quantification and amino acid bioaccessibility

The free AAs within digesta were quantified after deproteinisation by sulfosalicylic acid (Mondino et al., 1972). Digesta were mixed with sulfosalicylic acid solution (0.5 g/mL) and incubated for 60 min at 4 °C. The mixtures were centrifuged at 5,000*xg* for 15 min at 4 °C and the supernatants were filtered at 0.45 µm. The filtrate was 4-times diluted with 0.2 M lithium citrate buffer (pH 2.2) before injection. The amino acid analysis was carried out by cation-exchange chromatography as described previously (Chapter 3 - section 3). The amino acid bioaccessibility was calculated using the Equation 17:

$$\text{Amino acid bioaccessibility (\%)} = \frac{[\text{Free amino acid}]_{\text{digesta}} - [\text{Free amino acid}]_{\text{secretions}}}{[\text{Total amino acid}]_{\text{undigested IMF}}} \times 100$$

with [free amino acid$_{\text{digesta}}$] the content of free amino acids within digesta (g/kg of IMF), [free amino acid$_{\text{secretions}}$] the content of free amino acids of the bile and pancreatin solutions at the same concentrations than those found in intestinal digesta (g/kg of IMF) and [total amino acid$_{\text{undigested IMF}}$] the total amino acid content within IMFs (g/kg of IMF). The bioaccessibility of essential and non-essential amino acids was calculated as the ratio of the sum of corresponding free amino acids within the digesta *vs.* the sum of the corresponding amino acids within IMFs. The essential amino acids were cysteine, histidine, isoleucine, leucine, lysine, methionine, phenylalanine, threonine, tyrosine and valine. The non-

essential amino acids were alanine, arginine, aspartic acid, asparagine, glutamic acid, glutamine, glycine, proline and serine.

8.7. Mass spectrometry

8.7.1. Peptidomic profiling by LC–MS/MS

The undigested IMFs and digesta were analysed by mass spectrometry as described previously (Amélie Deglaire et al., 2019), using a nano-RSLC Dionex U3000 system coupled to a Q-Exactive mass spectrometer (Thermo Scientific, San Jose, USA) equipped with a nanoelectrospray ion source. Samples were normalised according to their protein content by dilution in the injection buffer and for each samples, 5 µL, containing 200 ng of proteins, was loaded onto a PepMap RSLC column (C18 column, 75 µm i.d. × 150 mm length, 3 µm particle size, 100 Å pore size; Dionex) equipped with a micro-precolumn pepMap100 (C18 column, 300 µm i.d. × 5 mm length, 5 µm particle size, 100 Å pore size; Dionex, Amsterdam, The Netherlands). Peptides were separated at a flow rate of 0.3 µL/min. Mobile phase A was 2% (v/v) acetonitrile, 0.08% (v/v) formic acid and 0.01% (v/v) TFA in HPLC gradient grade water and mobile phase B was 95% (v/v) acetonitrile, 0.08% (v/v) formic acid and 0.01% (v/v) TFA in HPLC gradient grade water. The elution gradient started with a plateau of 5% solvent B during 5 min, and then the mobile phase B gradually increased to 35% at 40 min, 85% solvent B at 42 min. Then, the gradient was maintained at 85% solvent B during 3 min, and decreased to 3% solvent B at 46 min and was constant during 9 min. Finally, the gradient increased to 5% solvent B at 55.1 min and was maintained during 10 min. The total run time was 65.1 min.

The mass spectra were recorded in positive mode using the m/z range 250–2,000. The resolution of the mass analyser at m/z of 200 amu (atomic mass unit) was set to 70,000 for MS and 17,500 for MS/MS. For each MS scan, the 10 most intense ions were selected for MS/MS fragmentation and excluded from fragmentation for 15 s.

8.7.2. Identification and quantification of peptides

Peptides were identified from the MS/MS spectra using the X!TandemPipeline C++ software (version 2017.2.1.4) against the protein database from "Bos Taurus" downloaded from Uniprot (https://uniprot.org; 6905 reviewed proteins). Serine or threonine phosphorylation, methionine oxidation and lysine or arginine lactosylation were selected as potential peptide modification. Peptides identified with an e-value < 0.01 were automatically validated.

Each identified peptide was quantified by label-free MS using the MassChroQ software (Valot et al., 2011). A m/z width of 10 ppm was used to perform extracted ion chromatograms (XIC) of peptides in time-aligned chromatograms and the area under the curve was then quantified. Peptides with a minimal

length of 6 amino acids were considered. When a peptide was measured with several charge states, all ion intensities were summed. Peptide number represented the number of unique peptide sequences identified despite sequence modifications. Abundance corresponded to the area under the curve of the eluted peak (ion intensity).

8.7.3. Peptidomic data analysis

Peptide data analysis was performed using the R software (version 3.6.1). Peptide identifications were considered for analysis if the peptides were detected in at least 2 out of 3 digestion replicates. Visualisation of the amounts of common or specific peptides among the IMFs was carried out using a Venn diagram (VennDiagram package).

The abundance of each peptide, determined at each digestion time, was log10-transformed [log10(abundance + 1)] and the maximum abundance was set to 1. Missing abundances were set at 0. Hierarchical clustering of the peptides identified in the undigested, gastric and intestinal samples (n = 3169) was realised, based on the minimum within-cluster variance Ward's agglomeration (*hclust* function; stats package). The number of clusters was determined thanks to the bar heights at one of the most marked jumps (6 clusters). The heatmap and its dendrogram were displayed (*heatmap.2* function; stats package). Each peptide cluster was characterised based on a number of qualitative and quantitative physicochemical characteristics (*catdes* function; FactoMiner package). The qualitative characteristics were the parent protein, the P1 and P1' cleavage sites. The quantitative characteristics were the molecular weight, the isoelectric point, the peptide length and the number of essential amino acids.

An in-house program allowed the peptide mapping on the parent protein sequence of α_{s1}-casein (CASA1), α_{s2}-casein (CASA2), β-casein (CASB), κ-casein (CASK), α-LA (LALBA), β-LG (LACB) and LF (TRFL) and their average cumulative abundances onto the parent protein. For each digestion replicate and each digestion phase (undigested, gastric or intestinal samples), abundances of the peptides were averaged over the different digestion times of the corresponding phase, summed amino acid by amino acid and log10-transformed [log10(abundance + 1)]. Missing abundances were set at 0. This mapping provides a visual overview by heatmap representation of the position of peptides released within the parent protein sequence (*heatmap.2* function; stats package).

Identified peptides in undigested, gastric or intestinal samples were examined for homology with literature-identified bioactive peptides using the Biopep Database (March 2020; 3897 sequences; Iwaniak et al., 2016) and the MBPDB Database for LF-derived peptides (July 2020; 65 sequences; Nielsen et al., 2017). Only exact matching between sequences was considered.

9. Statistical analysis

All data are reported as means ± standard deviation (SD). Data statistical analysis was performed using the R software (version 3.6.1). Residual intact protein, DH and amino acid bioaccessibility (dynamic digestion only) variables were analysed within the gastric or intestinal phase using a mixed linear model for repeated measures (nlme package). "Time", "Formula" (2 levels: control IMF − LF+ α-LA+ IMF) and "Treatment" nested within "Formula" (2 or 3 levels: unheated (− heated at 67.5°C) − heated at 80°C) were designated as fixed factors, and digestion replicates were designated as random factor. Residual normality and variance homogeneity for each factor were tested for all variable with Shapiro-Wilk test and Levene test, respectively (lawstat package). When data did not conform to the previous conditions, BoxCox-transformation was performed (MASS package).

Amino acid bioaccessibility variable for the study using *in vitro* static digestion model was investigated using a linear model with "Formula" and "Treatment" nested within "Formula" as fixed factors. When differences were significant (p < 0.05), pairwise multiple comparison of the means was carried out using Tukey's test (lsmeans package).

Chapter 4: Kinetics of heat-induced denaturation of proteins in model infant milk formulas as a function of whey protein composition

Based on the following publication for the IMFs processed at 1.3% proteins and on unpublished results for the IMFs processed at 5.5% proteins.

Kinetics of heat-induced denaturation of proteins in model infant milk formulas as a function of whey protein composition

Amira Halabi, Amélie Deglaire, Pascaline Hamon, Said Bouhallab, Didier Dupont, Thomas Croguennec*

UMR STLO, Agrocampus Ouest, INRA, 35000 Rennes, France

1. Abstract

The process of manufacturing IMFs involves heat treatments that can lead to whey protein denaturation. The objective of the study was to determine how protein profile and total solid of IMFs affects the denaturation kinetics of the major whey proteins (i.e. α-LA, β-LG and LF). Three model IMFs processed at 1.3% or 5.5% of proteins were produced with a casein:whey protein ratio of 40:60, differing only by the whey protein profile. The kinetics of heat-induced denaturation of α-LA, β-LG and LF were investigated between 67.5 °C and 80 °C by chromatographic quantification of the residual native proteins. Results showed that the heat-denaturation of α-LA was reduced when β-LG was absent. The heat-denaturation of LF was not affected by the composition of the IMFs but its presence enhanced the heat-denaturation of β-LG. This study revealed that, for higher heat treatments (90 °C/15 s, 75 °C/15 min), IMF processed at 1.3% proteins and containing α-LA and LF preserved a higher proportion of native whey proteins than IMFs containing β-LG. The increase of total solid of IMFs prior to heating slowed down the kinetics of whey protein denaturation for IMFs containing β-LG, explained by a reduced accessibility of the free thiol group of the protein, which is protected by lactose, at higher total solid.

2. Context and objectives

As discussed in chapter 1, heating of bovine milk at temperatures above 70°C can result in physicochemical changes including whey protein denaturation (Patel et al., 2006; Wijayanti et al., 2019). The extent of whey protein denaturation depends on environmental conditions such as the protein profile, the total solid or the heating temperature (Dissanayake et al., 2013; Hollar et al., 1995; Tolkach & Kulozik, 2007). Denaturation and aggregation of whey proteins have been extensively studied for bovine milk (Brodkorb et al., 2016; Dissanayake et al., 2013; Singh & Havea, 2003; Wolz & Kulozik, 2015), while there is very limited information in the literature for IMF environment, and even less for those that are mimicking the protein profile of human milk. Particularly, the heat denaturation of LF in bovine milk received very little attention compared to α-LA and β-LG, probably because of the very low LF quantity in bovine milk.

In this chapter, the aim was to investigate the kinetics of heat-induced denaturation of the major whey proteins (i.e. α-LA, β-LG and LF) of IMFs at temperatures from 67.5°C to 80°C. Three model IMFs were produced with a casein:whey protein ratio of 40:60, and differed by the whey protein profile (Table 13). The control IMF had the same whey protein profile as bovine whey, whereas the LF[+] IMF and LF[+] α-LA[+] IMF mimicked the quantity of LF or of both LF and α-LA in human milk, respectively. The IMFs were produced at 1.3% or 5.5% proteins (i.e. the protein content at which is applied the heat treatment during the manufacture of liquid or powdered IMFs, respectively). We assumed that the level of whey protein heat-denaturation was dependent on the whey protein composition of IMFs, since β-LG promotes whey protein denaturation (Elfagm & Wheelock, 1978) and LF is one of the most heat-sensitive protein in milk (Law, 1995). We also hypothesised that heat denaturation of whey proteins was affected by the total solid of the IMFs. The increased protein concentration probably enhanced collision between whey proteins (Wolz & Kulozik, 2015), the increased mineral content more efficiently screened charges on protein surface, affecting the protein unfolding and aggregation steps, and the increased sugar (lactose) content exerted a stabilising effect on proteins, even if the exact mechanism of protein stabilisation is still a matter of debate (Abriata et al., 2016; Kumar, 2009).

3. Infant milk formulas processed at 1.3% proteins

3.1. Results

The denaturation kinetics of the individual whey proteins α-LA, β-LG and LF in the IMFs were studied in the temperature range from 67.5 to 80°C by RP-HPLC quantification of the soluble protein fraction at pH 4.6. Solutions of α-LA and LF at identical concentration as found in the LF⁺ α-LA⁺ IMF and respecting the mineral and lactose contents of IMFs were investigated in the same conditions. These solutions were named "pure protein solution" in the following sections. This temperature range was selected from preliminary experiments. Heat treatments of the control IMF and LF⁺ IMF at temperatures higher than 80°C induced a very fast denaturation of the whey proteins preventing the precise determination of the whey protein denaturation kinetic parameters. In contrast, the very slow whey protein denaturation during the heating of LF⁺ α-LA⁺ IMF combined with the extensive lactosylation of the proteins for the longer holding times at temperatures lower than 67.5°C prevented the exact quantification of the proteins due to the elution of each protein as multi-peaks by RP-HPLC.

As expected, the increase of the heating temperature from 67.5 to 80°C or of the holding time at fixed temperature induced a higher decrease of the content of native whey proteins. To gain in clarity, only the whey protein denaturation kinetics at 70 and 75°C are presented. The whey protein denaturation kinetics at each temperature ranging from 67.5°C to 80°C are presented in Supplementary Figure 1. The reaction orders n and the rate constant k_n of the kinetics of denaturation of α-LA, β-LG and LF were calculated by the best fitting of the experimental data using Equation 10. The Arrhenius plots of α-LA, β-LG and LF were drawn using the values of rate constants of denaturation k_n of each individual whey protein at different temperatures. Each Arrhenius plot was best described by a linear regression, the slope of which gave the activation energies of the denaturation of the whey proteins Ea and the y-intercept the frequency factor logarithms ln ($k_{n,0}$).

3.1.1. Heat denaturation of α-lactalbumin

The kinetics of α-LA heat-denaturation were in the same range in the control and LF⁺ IMFs but they were systematically slower in the LF⁺ α-LA⁺ IMF (Figure 27.A). The reaction orders of the kinetics of denaturation of α-LA in both control and LF⁺ IMFs (n = 1.2 ± 0.2) and in the LF⁺ α-LA⁺ IMF (n = 1.5 ± 0.5) were higher than the one determined in the pure α-LA solution (n = 0.5 ± 0.3). At all heating temperatures, the rate constants k_n of α-LA were in the same range for the control and LF⁺ IMFs in one hand and for the LF⁺ α-LA⁺ IMF and the pure α-LA solution in the other hand (Figure 27.C). The k_n values obtained for the LF⁺ α-LA⁺ IMF and the pure α-LA solution were between 3-fold and 10-fold lower than those determined for the control and LF⁺ IMFs in the temperature range from 67.5°C to 80°C.

The thermodynamic parameters of the denaturation of α-LA (Ea and ln ($k_{n,0}$)) were highly dependent on the amount of β-LG in the IMFs. Indeed, Ea and ln ($k_{n,0}$) were similar between the control IMF (227 kJ.mol^{-1} and 75, respectively) and the LF$^+$ IMF (220 kJ.mol^{-1} and 73, respectively), which had higher content of β-LG (0.51% and 0.33% respectively). They were also in the same range for the LF$^+$ α-LA$^+$ IMF (110 kJ.mol^{-1} and 33 respectively) and the pure α-LA solution (100 kJ.mol^{-1} and 29), which contained traces or no β-LG.

Table C:

IMFs	Temperatures (°C)	k_n (10^{-2} $g^{1-n}.L^{n-1}.min^{-1}$)	R^2	D-value (min)	Ea (kJ.mol^{-1})	ln ($k_{n,0}$)
Control	67.5	0.5	0.994	421		
	70	1.3	0.968	161		
	72.5	1.9	0.953	113	227	75
$n = 1.2 \pm 0.2$	75	6.0 ± 1.0	0.994	36 ± 6		
Z-value = (8.0 ± 1.6)°C	77.5	6.7	0.988	32		
	80	7.9	0.997	27		
LF$^+$	67.5	0.7	0.980	338		
	70	2.4	0.993	96		
	72.5	3.3	0.972	70	220	73
$n = 1.2 \pm 0.2$	75	6.6 ± 0.4	0.996	35 ± 2		
Z-value = (7.8 ± 1.7)°C	77.5	8.8	0.999	26		
	80	12.5	0.965	19		
LF$^+$ α-LA$^+$	67.5	0.2	0.971	522		
	70	0.3	0.977	338		
	72.5	0.4	0.983	278	110	33
$n = 1.5 \pm 0.5$	75	0.6 ± 0.1	0.993	204 ± 20		
Z-value = (18.5 ± 2.7)°C	77.5	0.7	0.995	170		
	80	0.9	0.990	122		
Pure protein solution	67.5	0.3	0.975	1230		
	70	0.3	0.994	1019		
	72.5	0.5	0.997	672	105	31
$n = 0.5 \pm 0.3$	75	0.6	0.960	574		
Z-value = (23.4 ± 4.4)°C	77.5	0.9	0.990	380		
	80	0.9	0.978	369		

Figure 27. (A) Heat denaturation kinetics of α-LA for temperatures 70°C and 75°C (B) Arrhenius plots and (C) kinetic parameters associated, for the IMFs processed at 1.3% proteins and pure protein solution

(A) The pure protein solutions correspond to solution of α-LA at identical amount as found in the LF$^+$ α-LA$^+$ IMF and respecting the mineral and lactose contents of IMFs. Residual native fractions were calculated as a C_t/C_0 ratio. Ct (g.L^{-1}) is the native protein concentration at t holding time (min) and C_0 is the native protein concentration of unheated IMFs or protein solutions (g.L^{-1}). The results at 75°C represent means ± SD (n = 3). (B) K_n is the unfolding reaction rate constant (g^{1-n}.L^{n-1}.min^{-1}) and 1/T the inverse of the heating temperature (K^{-1}). The point at 75°C represents means ± SD (n = 3). (C) n is the reaction order and it is expressed as the average of the reaction orders determined at each heating temperature ± SD. K_n corresponds to the unfolding reaction rate constant (g^{1-n}.L^{n-1}.min^{-1}). Ea corresponds to the activation energy (kJ.mol^{-1}) and ln ($k_{n,0}$) represents the frequency factor logarithm, as determined by Arrhenius plots.

3.1.2. Heat denaturation of β-lactoglobulin

The kinetics of denaturation of β-LG in the control and LF$^+$ IMFs at 70 and 75°C are presented in the Figure 28.A. No data was recorded for the LF$^+$ α-LA$^+$ IMF because of the low amount of β-LG (0.06 %, w/w). At all heating temperatures, the heat-denaturation of β-LG was faster in the LF$^+$ IMF than in the control IMF. The reaction orders of the heat-denaturation of β-LG were similar for both IMFs (n = 1.5 - 1.6) (Figure 28.C).

The rate constants of β-LG denaturation in the control and LF$^+$ IMFs are presented in the Figure 28.C. The k_n-values were between 2-fold and 7-fold lower for the control IMF than for the LF$^+$ IMF in the studied temperature range. The k_n-values at 67.5°C were 0.3 x 10^{-2} g$^{-0.6}$.L$^{0.6}$.min^{-1} and 0.8 x 10^{-2} g$^{-0.5}$.L$^{0.5}$.min^{-1} for the control and LF$^+$ IMFs respectively, whereas they were 10.8 x 10^{-3} g$^{-0.6}$.L$^{0.6}$.min^{-1} and 70.9 x 10^{-2} g$^{-0.5}$.L$^{0.5}$.min^{-1} at 80°C, respectively. The activation energy and ln ($k_{n,0}$) of β-LG heat-denaturation determined from the Arrhenius plot were slightly lower in the control IMF (305 kJ.mol^{-1} and 102, respectively) compared to the LF$^+$ IMF (373 kJ.mol^{-1} and 126, respectively) (Figure 28.C).

IMFs	Temperatures	k_n	R^2	D-value	Ea	ln $(k_{n,0})$
	(°C)	(10^{-2} g^{1-n}.L^{n-1}.min^{-1})		(min)	(kJ.mol^{-1})	
	67.5	0.3	0.999	318		
Control	70	0.4	0.995	219		
	72.5	0.9	0.997	105		
$n = 1.6 \pm 0.1$	75	2.2 ± 0.1	0.999	42 ± 3	305	102
Z-value = (9.8 ± 2.7)°C	77.5	5.5	0.998	17		
	80	10.8	0.988	9		
	67.5	0.8	0.997	165		
LF$^+$	70	1.3	0.994	99		
	72.5	3.0	0.994	42		
$n = 1.5 \pm 0.2$	75	8.1 ± 0.8	0.997	16 ± 1	373	126
Z-value = (7.9 ± 1.7)°C	77.5	26.2	0.996	5		
	80	70.9	0.986	2		
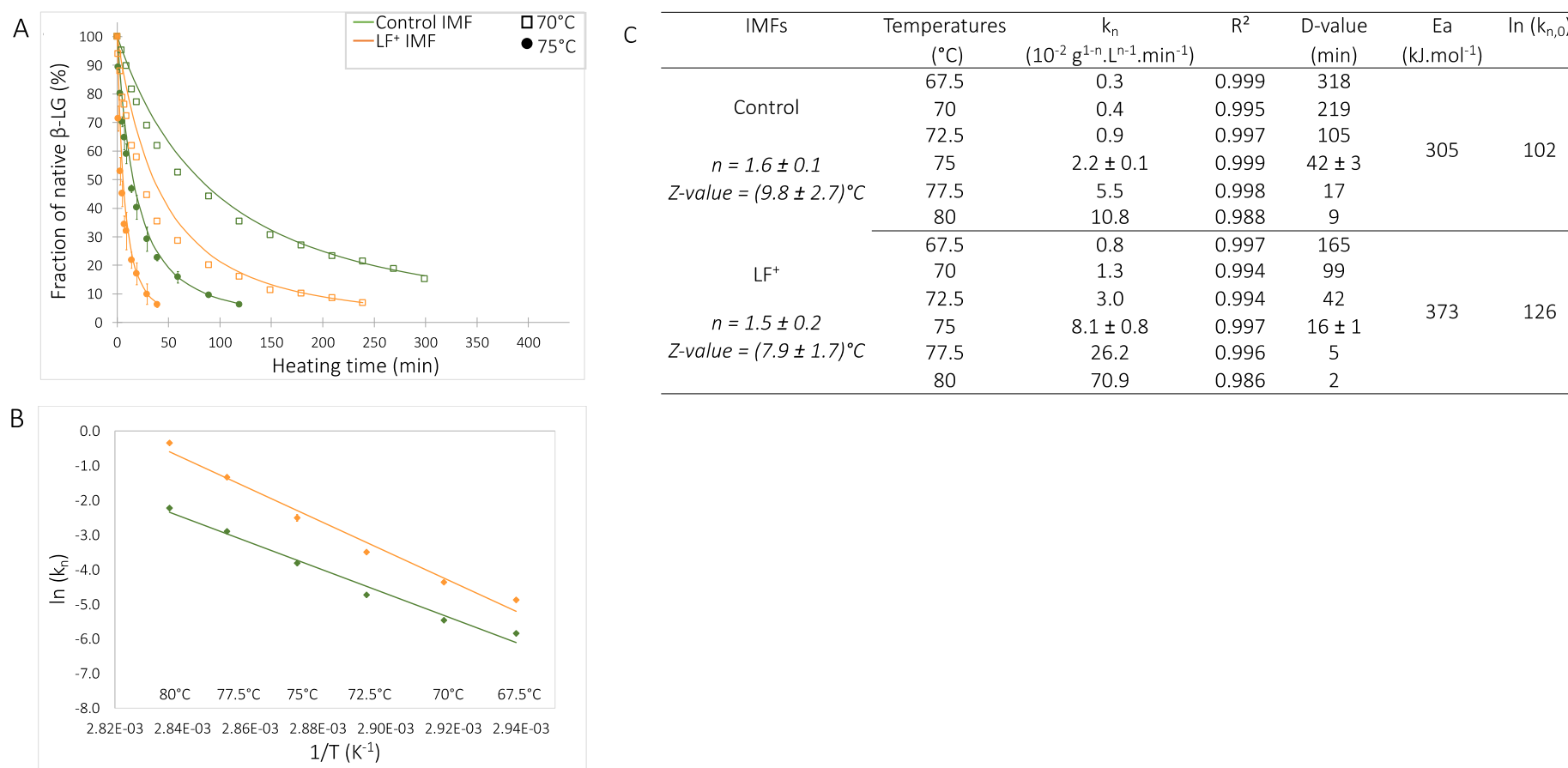
Figure 28. (A) Heat denaturation kinetics of β-LG for temperatures 70°C and 75°C (B) Arrhenius plots and (C) kinetic parameters associated, for the IMFs processed at 1.3% proteins

(A) Residual native fractions were calculated as a C_t /C_0 ratio. C_t (g.L^{-1}) is the native protein concentration at t holding time (min) and C_0 is the native protein concentration of unheated IMFs or protein solutions (g.L^{-1}). The results at 75°C represent means ± SD (n = 3). (B) K_n is the unfolding reaction rate constant (g^{1-n}.L^{n-1}.min^{-1}) and 1/T the inverse of the heating temperature (K^{-1}). The point at 75°C represents means ± SD (n = 3). (C) n is the reaction order and it is expressed as the average of the reaction orders determined at each heating temperature ± SD. K_n corresponds to the unfolding reaction rate constant (g^{1-n}.L^{n-1}.min^{-1}). Ea corresponds to the activation energy (kJ.mol^{-1}) and ln ($k_{n,0}$) represents the frequency factor logarithm, as determined by Arrhenius plots.

3.1.3. Heat denaturation of lactoferrin

The kinetics of LF heat-denaturation in the LF$^+$ and LF$^+$ α-LA$^+$ IMFs were compared (Figure 29.A). In the control IMF, the amount of LF was too low to quantify its heat-induced denaturation. Interestingly, the kinetics of heat-denaturation of LF were similar between the two IMFs at all studied temperatures. The reaction orders of LF heat-denaturation was 1.6 ± 0.2 and 1.8 ± 0.3 for the LF$^+$ and LF$^+$ α-LA$^+$ IMFs, respectively. A slightly lower reaction order (n = 1.4 ± 0.4) was obtained for the heat-denaturation of LF in the pure protein solution. The rate constants of LF denaturation were in the same range between the LF$^+$ and LF$^+$ α-LA$^+$ IMFs (Figure 29.C). In fact, in the temperature range between 67.5°C and 80°C, the rate constants of LF heat-denaturation varied between 3.6 x 10^{-2} to 42.8 x 10^{-2} $g^{-0.6}.L^{0.6}.min^{-1}$ for the LF$^+$ IMF and between 2.6 x 10^{-2} to 42.3 x 10^{-2} $g^{-0.8}.L^{0.8}.min^{-1}$ for the LF$^+$ α-LA$^+$ IMF. These values were higher than the rate constants determined for LF heat-denaturation in the pure LF solution at the same heating temperature (0.4 x 10^{-2} to 17.6 x 10^{-2} $g^{-0.4}.L^{0.4}.min^{-1}$). As expected, the activation energy of LF was similar in the LF$^+$ (202 kJ.mol^{-1}) and LF$^+$ α-LA$^+$ (215 kJ.mol^{-1}) IMFs. Likewise, the frequency factor logarithm of LF denaturation determined in the LF$^+$ IMF (68) was akin to the value determined for the LF$^+$ α-LA$^+$ IMF (73). Higher Ea and ln ($k_{n,0}$) values were determined for the pure LF solution compared to the LF$^+$ and LF$^+$ α-LA$^+$ IMFs (286 *vs.* 215 kJ.mol^{-1} and 96 *vs.* 70 kJ.mol^{-1}, respectively) (Figure 29.C).

C

IMFs	Temperatures (°C)	k_n (10^{-2} $g^{1-n}.L^{n-1}.min^{-1}$)	R^2	D-value (min)	Ea (kJ.mol^{-1})	ln ($k_{n,0}$)
LF$^+$	67.5	3.6	0.990	46		
	70	5.0	0.980	34		
	72.5	6.9	0.989	24		
$n = 1.6 \pm 0.2$	75	12.2 ± 1.8	0.998	14 ± 2	202	68
Z-value = (15.1 ± 3.0)°C	77.5	25.3	0.995	7		
	80	42.8	0.973	4		
LF$^+$ α-LA$^+$	67.5	2.6	0.969	63		
	70	8.1	0.988	20		
	72.5	16.9	0.972	10		
$n = 1.8 \pm 0.3$	75	21.3 ± 7.4	0.993	8 ± 3	215	73
Z-value = (8.2 ± 2.0)°C	77.5	36.7	0.982	5		
	80	42.3	0.993	4		
Pure protein solution	67.5	0.4	0.980	550		
	70	1.3	0.994	151		
	72.5	2.8	0.984	71		
$n = 1.4 \pm 0.4$	75	5.1	0.985	39	286	96
Z-value = (6.4 ± 1.4)°C	77.5	6.6	0.990	30		
	80	17.6	0.936	11		

Figure 29. (A) Heat denaturation kinetics of LF for temperatures 70°C and 75°C (B) Arrhenius plots and (C) kinetic parameters associated, for the IMFs processed at 1.3% proteins and pure protein solution

(A) The pure protein solutions correspond to solution of LF at identical amount as found in the LF$^+$ α-LA$^+$ IMF and respecting the mineral and lactose contents of IMFs. Residual native fractions were calculated as a C_t/C_0 ratio. Ct (g.L^{-1}) is the native protein concentration at t holding time (min) and C_0 is the native protein concentration of unheated IMFs or protein solutions (g.L^{-1}). The results at 75°C represent means ± SD (n = 3). (B) K_n is the unfolding reaction rate constant ($g^{1-n}.L^{n-1}.min^{-1}$) and 1/T the inverse of the heating temperature (K^{-1}). The point at 75°C represents means ± SD (n = 3). (C) n is the reaction order and it is expressed as the average of the reaction orders determined at each heating temperature ± SD. K_n corresponds to the unfolding reaction rate constant ($g^{1-n}.L^{n-1}.min^{-1}$). Ea corresponds to the activation energy (kJ.mol^{-1}) and ln ($k_{n,0}$) represents the frequency factor logarithm, as determined by Arrhenius plots.

3.1.4. Prediction of the amount of native whey proteins in infant milk formulas after pasteurisation treatments

Based on Equation 10 and the thermodynamic parameters calculated in this study (Figure 27.C, Figure 28.C and Figure 29.C), the proportion of native α-LA, β-LG and LF recovered in IMFs after the temperature/time conditions usually used to pasteurize milk can be predicted (Figure 30). A summary of the calculations is given in Supplementary Table 2. The whey protein denaturation yield simulated for the heat treatment 75°C/10 min was confirmed by RP-HPLC quantification.

The simulation of the holder pasteurisation (i.e. 62.5°C during 30 min) induced the denaturation of 4% of native whey proteins in the control IMF and of 13% and 15% in the LF$^+$ and LF$^+$ α-LA$^+$ IMFs, respectively. A standard HTST pasteurisation treatment (i.e. 75°C during 15 s) led to about the same total protein denaturation yield (between 1% and 4% of denatured proteins) in the three IMFs. Rising up the temperature of the pasteurisation treatment from 75°C to 90°C but keeping the holding time constant (15 s) resulted in a decrease of the fraction of native whey proteins in all IMFs, with 48%, 27% and 81% of residual native whey proteins in the control, LF$^+$ and LF$^+$ α-LA$^+$ IMFs, respectively. The native protein loss was mainly due to the heat-denaturation of β-LG and LF during the treatment at 90°C/15 s. A similar trend was observed when the holding time at 75°C was prolonged to 10 min but the proportion of the residual native proteins was slightly different: 61%, 32% and 71% of residual native whey proteins were calculated in the control, LF$^+$ and LF$^+$ α-LA$^+$ IMFs, respectively. The relative denaturation yield of α-LA and LF was higher after a heat treatment at 75°C/10 min compared to 90°C/15 s.
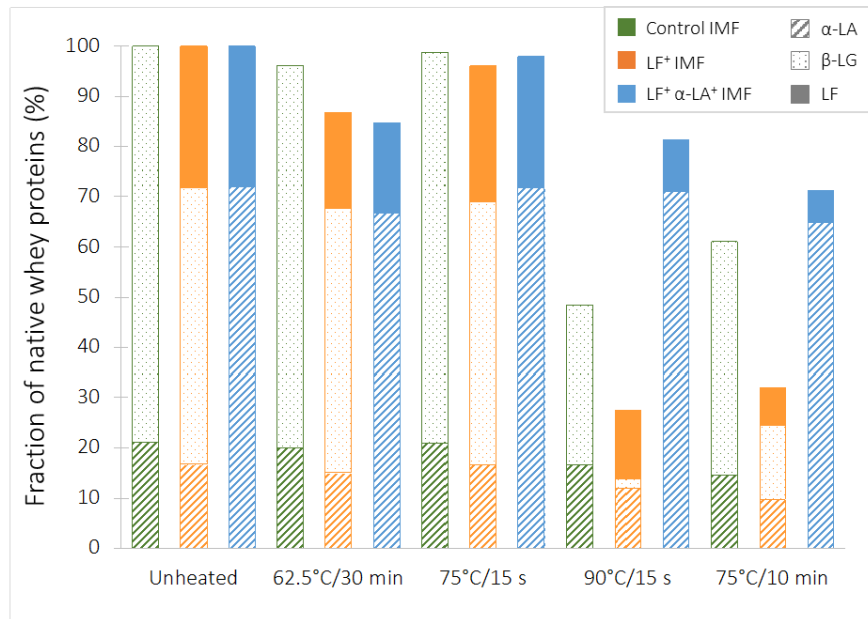
Figure 30. Whey protein contents and fractions of total native whey proteins for pasteurisation treatments of the IMFs processed at 1.3% proteins

The data are estimations from the equation $\frac{C_t}{C_0} = \sqrt[1-n]{\left(1 + (n-1) \times e^{\left(-\frac{E_a}{R} \times \frac{1}{T+273}\right)} \times k_{n,0} \times C_0^{n-1} \times t\right)}$, using the thermodynamic parameters (reaction orders n, activation energies E_a and frequency factors $k_{n,0}$) as referenced previously. C_t (g.L^{-1}) corresponds to the protein content at holding time t (min), C_0 is the protein content in the unheated IMFs (g.L^{-1}). T corresponds to the heating temperature (°C).

3.2. Discussion

The present paper evidences that the kinetics of whey protein denaturation depend on both the whey protein profile of IMFs and the heating conditions (i.e. temperature/time combination).

3.2.1. The heat-denaturation of lactoferrin is independent of the amount of α-lactalbumin and β-lactoglobulin in the infant milk formulas

The reaction orders of LF determined for the LF$^+$ and LF$^+$ α-LA$^+$ IMFs and in the pure LF solution are in accordance with the one previously determined for the thermal denaturation of the recombinant human LF (Castillo, Pérez, Franco, Calvo, & Sánchez, 2012). These authors determined a reaction order of 1.5, independently of the iron saturation level of LF.

The present results show that LF heat-denaturation kinetics are independent of the change of α-LA and β-LG amounts in the IMFs in the whole range of the studied heating temperatures. Since LF is one of the most heat-sensitive protein in milk with a reported denaturation temperature around 60°C (Bengoechea, Peinado, & McClements, 2011), it is assumed that its denaturation occurs before the heat-denaturation of α-LA and β-LG with denaturation temperatures of about 68°C (Nielsen et al., 2018) and 78°C (Brodkorb et al., 2016), respectively. Consequently, these latter have no or very little influence on the heat-denaturation of LF explaining that the rate constants and the activation energy of the heat-

denaturation of LF are similar in the LF[+] and LF[+] α-LA[+] IMFs, in spite of different contents in α-LA and β-LG.

Interestingly, the LF heat-denaturation rate constants were lower and the activation energy was higher in the pure LF solution compared to those obtained in the LF[+] and LF[+] α-LA[+] IMFs, indicating that the physicochemical environment in the IMFs favours the denaturation of LF during heating. LF is able to bind to casein micelles mainly by electrostatic interactions (Anema & de Kruif, 2012) and this was confirm in this study since 43% of LF was recovered with the casein micelle fraction in the ultracentrifugation pellet (100,000xg - 1h - 25°C) of the LF[+] and LF[+] α-LA[+] IMFs. The binding of LF to caseins is facilitated by heating and results in the formation of LF-casein complexes (Li & Zhao, 2018). This binding is susceptible to modify the heat-stability of LF and can be an explanation for the faster heat-denaturation of LF in the IMFs compared to the pure protein solution.

Casein micelles also have the ability to bind various types of cations such as iron ions (Fe^{2+} and Fe^{3+}). This binding was observed in a suspension of casein micelles (Philippe, Legraet, & Gaucheron, 2005) and in bovine milk (Broyard & Gaucheron, 2015). The binding of iron to casein micelles could reduce the amount of iron bound to LF, and therefore accelerate its heat-denaturation kinetics because LF heat-stability is dependent on the iron saturation level (Brisson et al., 2007; Sánchez et al., 1992). However, the quantification of LF and iron in the supernatant after ultracentrifugation of unheated LF[+] and LF[+] α-LA[+] IMFs (iron:LF molar ratio of 3.7; data not shown) indicated that LF was fully saturated with iron considering a binding constant of about $10^{22} - 10^{24}$ M[-1] (Majka et al., 2013). Therefore, the faster heat-denaturation of LF in IMFs compared to pure LF solution was rather a consequence of the binding of LF to casein micelles than a reduction of the iron saturation level of LF.

3.2.2. The heat-denaturation of α-lactalbumin is enhanced in the presence of β-lactoglobulin

The reaction orders of α-LA determined for the three IMFs (n = 1.2-1.5) were higher than the one reported in the literature for the heat-denaturation of α-LA in bovine milk (n = 1.0; Anema et al., 2006; Dannenberg & Kessler, 1988; Oldfield et al., 1998) and the value determined in the pure α-LA solution (n = 0.5). This could be a consequence of the different protein content (Wehbi et al., 2005) and/or distinct medium conditions between bovine milk, the pure α-LA solution and the IMFs.

The denaturation kinetics of α-LA in the different IMFs revealed that α-LA was more rapidly denatured in the control and LF[+] IMFs that contain 0.51 g and 0.33 g of β-LG/100 g of liquid IMF, respectively. When the β-LG content is as low as in the LF[+] α-LA[+] IMF, the denaturation rate constant of α-LA is comparable to that of α-LA in the pure solution. These results are in agreement with published data showing that the denaturation of α-LA is promoted by the presence of β-LG (Wehbi et al., 2005). In the absence of β-

LG, α-LA reversibly unfolds on heating but does not form irreversible aggregates (Nielsen et al., 2018). The aggregation of α-LA is enhanced in the presence of unfolded β-LG molecule that exposes its free thiol group to the solvent, making it available to react with unfolded α-LA *via* thiol-disulfide interchanges (Dalgleish et al., 1997). This covalent cross-link between β-LG and α-LA traps α-LA in an irreversibly unfolded structure in the formed aggregates. The irreversible denaturation of α-LA induced by addition of thiol reagents (Nguyen et al., 2018) confirms that the presence of available thiol groups cleaving intramolecular α-LA disulfide bonds is necessary to promote α-LA denaturation/aggregation .

To the best of our knowledge, the effect of LF on the heat-denaturation of α-LA was less studied than that of β-LG. The similarities of the activation energies of α-LA in the LF$^+$ α-LA$^+$ IMF and in the pure α-LA solution, both containing the same quantities of α-LA and the same lactose and mineral contents, demonstrate that LF does not interfere with the mechanism of heat-denaturation of α-LA. LF has 34 cysteine residues in its structure, all involved in intramolecular disulfide bonds, but no free thiol group (Pierce et al., 1991). The absence of a free thiol group in the structure of LF is a plausible explanation for the absence of LF effect on α-LA heat-denaturation that is promoted by thiol containing molecules. However, the profile of the α-LA denaturation kinetics in the LF$^+$ α-LA$^+$ IMF and the pure α-LA solution differs due to the variation of the reaction order (n = 1.5 ± 0.5 and n = 0.5 ± 0.3, respectively). The higher reaction order in the LF$^+$ α-LA$^+$ IMF could be a consequence of the presence of other proteins (LF, caseins, β-LG traces) facilitating the aggregation of denatured α-LA.

3.2.3. The heat-denaturation of β-lactoglobulin is enhanced in the presence of lactoferrin

The reaction orders of the heat-denaturation of β-LG determined for the control and LF$^+$ IMFs (n = 1.5-1.6) are in adequacy with the reaction order widely reported in the literature for the heat-denaturation of the protein in bovine milk (Anema & McKenna, 1996). The heat-denaturation of β-LG was faster in the LF$^+$ IMF (containing LF protein) than in the control IMF (lacking of LF protein), with the rate constants of denaturation of β-LG being 2 to 6-times higher in the LF$^+$ IMF than in the control IMF, and the denaturation activation energy being higher in the LF$^+$ IMF than in the control IMF (373 *vs* 305 kJ.mol^{-1}, respectively).

The mechanism of heat-denaturation of β-LG has been well-described (de Wit, 2009). Upon heating, the dimer/monomer equilibrium of native β-LG is shifted to the monomeric form that unfolds and exposes its free thiol group and hydrophobic patches to the solvent. This reactive entity aggregates with proteins in its close surrounding mainly *via* disulfide interchange reactions, but also by hydrophobic driven association reactions. β-LG reacts rapidly with proteins having exposed disulfide bonds such as α-LA (Dalgleish et al., 1997) or LF (Brisson et al., 2007). Among these proteins, LF is particularly rich in

disulfide bonds (17 disulfide bonds) and is already unfolded when β-LG starts to denature. This could facilitate the formation of intermolecular disulfide bonds between LF and β-LG supporting the hypothesis of Brisson et al. (2007), who showed that upon heating, LF aggregates with proteins containing cysteine residues such as β-LG to form disulfide bound aggregates.

3.2.4. The impact of the pasteurisation treatments is dependent on the whey protein composition of infant milk formulas

The simulation of the heat treatments at 90°C/15 s and 75°C/10 min revealed a lower content of native whey proteins in the pasteurized LF+ IMF than in the control and LF+ α-LA+ IMFs, explained by the simultaneous presence of LF that rapidly denatures on heating and β-LG that initiates covalent cross-links between unfolded whey proteins. Surprisingly, the decrease of the native whey protein fraction in the control and LF+ IMFs heat-treated at 90°C/15 s is mainly explained by the heat-denaturation of β-LG, and to a lesser extent by the heat-denaturation of LF. However, it is probable that the fraction of native β-LG in these heated IMFs is underestimated because the Arrhenius plot of β-LG exhibits a specific profile with a change of the denaturation activation energy around 80°C. In the aggregation-limited domain (temperatures above 80°C), the denaturation activation energy is between 2 and 3-times lower than in the unfolding-limited domain (temperatures below 80°C) (Petit et al., 2011). As the denaturation of the whey proteins in IMFs was not studied above 80°C for the reasons presented previously, the change of the denaturation activation energy at temperature higher than 80°C cannot be taken into account for the estimation of the residual native β-LG after heating the IMFs at 90°C. Consequently, the rate constant used to calculate the fraction of residual native β-LG is likely overestimated, thus potentially explaining the lower amount of native whey protein fractions in the control and LF+ IMFs heat-treated at 90°C/15 s than at 75°C/10 min.

Almost all whey proteins remained native after simulation of HTST treatment (75°C/15 s) for the three IMFs. This is consistent with previous work that showed that HTST treatment of human (Cavallarin, 2011) and bovine (Douglas et al., 1981) milks did not significantly denature whey proteins. Moreover, the lower native whey protein quantity for the LF+ and LF+ α-LA+ IMFs after the holder pasteurisation simulation, a classical heat treatment used in human milk bank to ensure the sanitary quality before feeding infants, is due to the denaturation of LF, which is more heat-sensitive at low temperature than other whey proteins (Law, 1995). This confirms previous experiments showing that the holder pasteurisation of human milk mainly lead to the LF denaturation, whereas α-LA was not affected (Deglaire et al., 2019).

4. Infant milk formulas processed at 5.5% proteins

Results and discussion

As indicated previously for the IMFs processed at 1.3% proteins, only the whey protein denaturation kinetics at 70°C and 75°C are presented to gain in clarity. The whey protein denaturation kinetics at each temperature ranging from 67.5°C to 80°C are presented in Supplementary Figure 2. The reaction orders n, the rate constant k_n, the activation energy Ea and the y-intercept the frequency factor logarithms ln $(k_{n,0})$ were determined as previously described.

The reaction order of β-LG (n = 1.7 ± 0.2) and LF (n = 1.6 ± 0.1) were near identical to those for IMFs processed at 1.3% proteins (n = 1.6 ± 0.1 and n = 1.7 ± 0.1, respectively) (Figure 28.B and Figure 29.B). Only the reaction order of α-LA (n = 0.7 ± 0.1) was ~ 2-times lower than those for the IMFs processed at 1.3% proteins (n = 1.3 ± 0.2), meaning that the mechanism of denaturation of α-LA is affected by the total solid content of the IMFs. The reaction order of the α-LA heat-induced denaturation for the IMFs processed at 5.5% proteins and the pure α-LA solution at 1.3% and 5.5% proteins are close together (between 0.5 and 0.8).

A detailed analysis of the kinetics of whey protein heat-induced denaturation for the IMFs processed at 5.5% proteins reinforced previous observations made for IMFs processed at 1.3% proteins, but also gave new insights on the heat denaturation of whey proteins within IMFs. The effects of the protein profile of IMFs on the heat denaturation kinetics of α-LA and β-LG were similar in the IMFs processed at 1.3% or 5.5% proteins, meaning the slowdown of the heat denaturation kinetics of α-LA in the absence of β-LG (Figure 31) and the acceleration of the heat denaturation kinetics of β-LG in presence of LF (Figure 32).

The rate constants for heat denaturation of α-LA were higher in the IMFs and the pure α-LA solution processed at 5.5% than at 1.3% proteins, meaning that the conditions in the concentrated solutions were favourable to α-LA heat denaturation. The kinetics of α-LA heat denaturation was also faster in the IMFs containing β-LG than in absence of β-LG, supporting the observation that α-LA denaturation was enhanced in the presence of β-LG. However, β-LG contribution to the heat-induced denaturation of α-LA was reduced. The heat denaturation rate constants of α-LA were only 1.5- to 2-times higher in the β-LG-containing IMFs processed at 5.5% than at 1.3% proteins *vs.* 10-times in the β-LG-free IMF and pure α-LA solution. This suggested that β-LG still influenced the denaturation of α-LA in the IMFs processed at 5.5% proteins but to a lesser extent than in the IMFs processed at 1.3% proteins because the kinetics of β-LG denaturation was reduced (decreased accessibility of β-LG free thiol group in the presence of lactose; Anema, 2000). However, other favourable conditions promoting α-LA heat-denaturation in the concentrated IMFs counterbalanced the lower β-LG contribution. This was also in

accordance with the modification of the reaction order and the mechanism of the heat-denaturation of

α-LA in the concentrated IMFs.

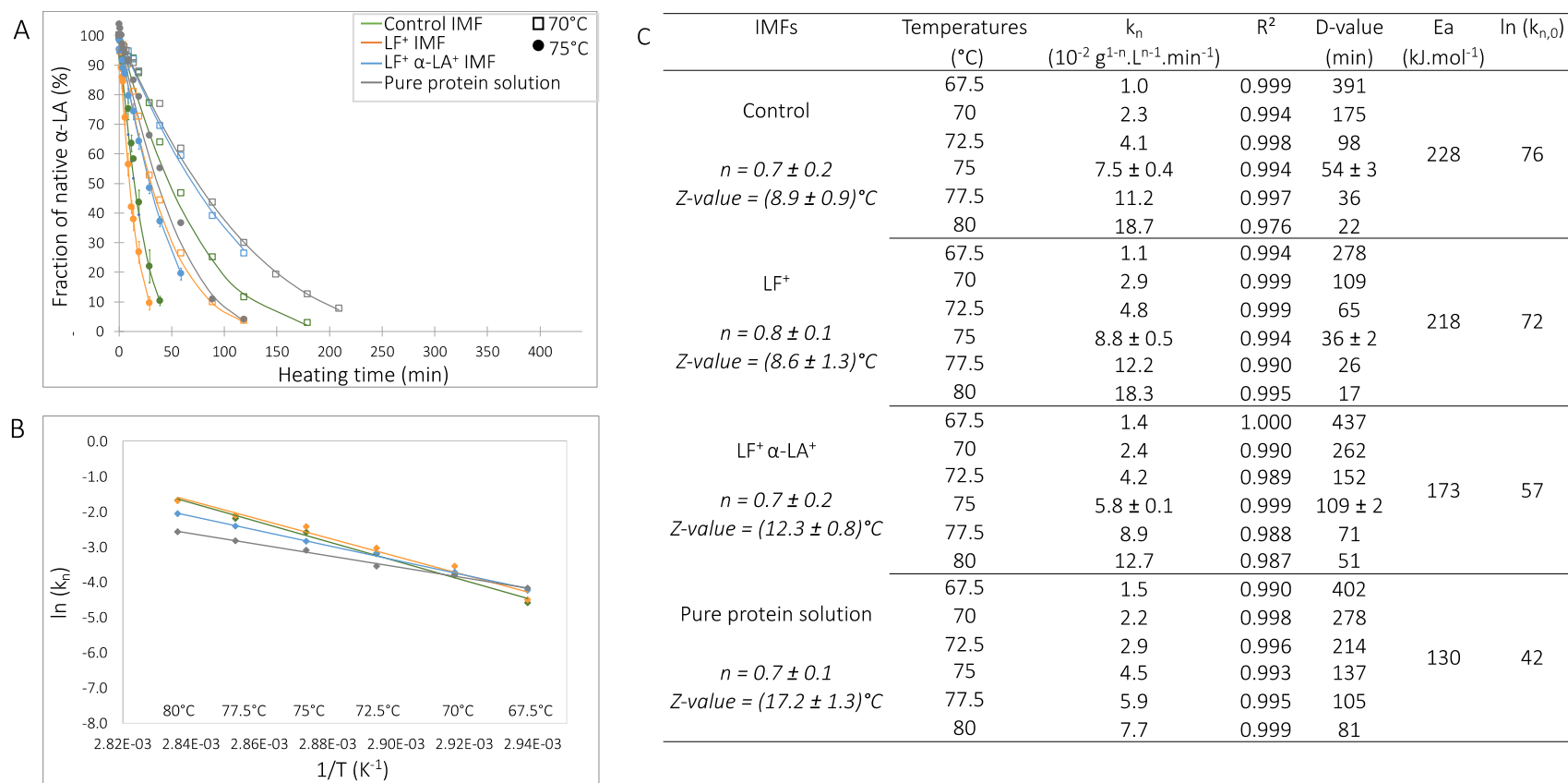| IMFs	Temperatures	k_n	R^2	D-value	Ea	ln $(k_{n,0})$
	(°C)	(10^{-2} $g^{1-n}.L^{n-1}.min^{-1}$)		(min)	(kJ.mol^{-1})	
Control	67.5	1.0	0.999	391		
	70	2.3	0.994	175		
	72.5	4.1	0.998	98		
n = 0.7 ± 0.2	75	7.5 ± 0.4	0.994	54 ± 3	228	76
Z-value = (8.9 ± 0.9)°C	77.5	11.2	0.997	36		
	80	18.7	0.976	22		
LF⁺	67.5	1.1	0.994	278		
	70	2.9	0.999	109		
	72.5	4.8	0.999	65		
n = 0.8 ± 0.1	75	8.8 ± 0.5	0.994	36 ± 2	218	72
Z-value = (8.6 ± 1.3)°C	77.5	12.2	0.990	26		
	80	18.3	0.995	17		
LF⁺ α-LA⁺	67.5	1.4	1.000	437		
	70	2.4	0.990	262		
	72.5	4.2	0.989	152		
n = 0.7 ± 0.2	75	5.8 ± 0.1	0.999	109 ± 2	173	57
Z-value = (12.3 ± 0.8)°C	77.5	8.9	0.988	71		
	80	12.7	0.987	51		
Pure protein solution	67.5	1.5	0.990	402		
	70	2.2	0.998	278		
	72.5	2.9	0.996	214		
n = 0.7 ± 0.1	75	4.5	0.993	137	130	42
Z-value = (17.2 ± 1.3)°C	77.5	5.9	0.995	105		
	80	7.7	0.999	81		

Figure 31. (A) Heat denaturation kinetics of α-LA for temperatures 70°C and 75°C (B) Arrhenius plots and (C) kinetic parameters associated, for IMFs processed at 5.5% proteins and pure protein solution

(A) The pure protein solutions correspond to solution of α-LA at identical amount as found in the LF⁺ α-LA⁺ IMF and respecting the mineral and lactose contents of IMFs. Residual native fractions were calculated as a C_t / C_0 ratio. Ct (g.L^{-1}) is the native protein concentration at t holding time (min) and C_0 is the native protein concentration of unheated IMFs or protein solutions (g.L^{-1}). The results at 75°C represent means ± SD (n = 3). (B) K_n is the unfolding reaction rate constant ($g^{1-n}.L^{n-1}.min^{-1}$) and 1/T the inverse of the heating temperature (K^{-1}). The point at 75°C represents means ± SD (n = 3). (C) n is the reaction order and it is expressed as the average of the reaction orders determined at each heating temperature ± SD. K_n corresponds to the unfolding reaction rate constant ($g^{1-n}.L^{n-1}.min^{-1}$). Ea corresponds to the activation energy (kJ.mol^{-1}) and ln $(k_{n,0})$ represents the frequency factor logarithm, as determined by Arrhenius plots.

The rate constants for heat denaturation of β-LG were lower in the IMFs processed at 5.5% than at 1.3% proteins, even if the activation energy of β-LG denaturation was lower in the IMFs processed at 5.5% proteins (note that below 80°C, in the unfolding limited regime, the activation energy we determined was the unfolding activation rate). This apparent contradictory result suggests that the aggregation step of the unfolded β-LG delayed the β-LG denaturation since β-LG unfolding was facilitated. Anema (2000) showed that the increase of total solid prior to heat treatment of bovine milk at 95°C led to the slowdown of the β-LG denaturation, due to the increase of lactose content, as lactose interacted with β-LG and decreased the accessibility of its free thiol group. Moreover, the decrease of the β-LG rate constants were 3-times higher in presence of LF (i.e. the LF⁺ IMF) than in absence of LF (i.e. the control IMF). We showed previously that the heat-induced denaturation of β-LG in the IMFs processed at 1.3% proteins was enhanced in presence of LF. This was explained by the unfolding of LF prior to that of β-LG, which made the exposed disulfide bonds of LF readily accessible to β-LG free thiol group for thiol/disulfide intermolecular reactions. As LF was more stable in the IMFs processed at 5.5% than at 1.3% proteins, it was assumed that less disulfide bonds of LF were exposed during the unfolding of β-LG, delaying the thiol/disulfide intermolecular reactions and the denaturation kinetics of β-LG.

A

B

C

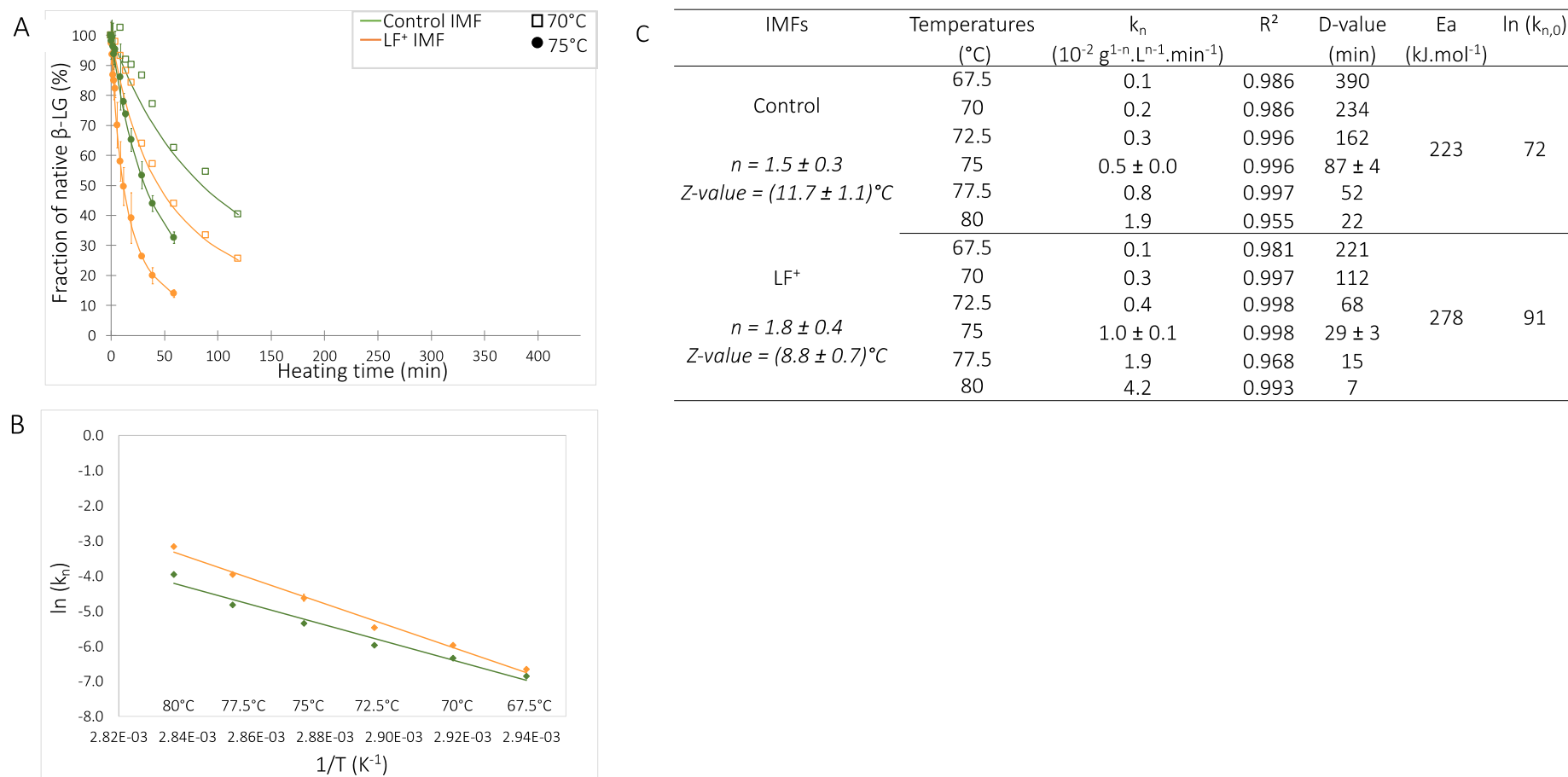| IMFs	Temperatures (°C)	k_n (10^{-2} g^{1-n}.L^{n-1}.min^{-1})	R^2	D-value (min)	Ea (kJ.mol^{-1})	ln ($k_{n,0}$)
	67.5	0.1	0.986	390		
Control	70	0.2	0.986	234		
	72.5	0.3	0.996	162		
$n = 1.5 \pm 0.3$	75	0.5 ± 0.0	0.996	87 ± 4	223	72
Z-value = (11.7 ± 1.1)°C	77.5	0.8	0.997	52		
	80	1.9	0.955	22		
	67.5	0.1	0.981	221		
LF$^+$	70	0.3	0.997	112		
	72.5	0.4	0.998	68		
$n = 1.8 \pm 0.4$	75	1.0 ± 0.1	0.998	29 ± 3	278	91
Z-value = (8.8 ± 0.7)°C	77.5	1.9	0.968	15		
	80	4.2	0.993	7		

Figure 32. (A) Heat denaturation kinetics of β-LG for temperatures 70°C and 75°C (B) Arrhenius plots and (C) kinetic parameters associated, for the IMFs processed at 5.5% proteins

(A) Residual native fractions were calculated as a C_t / C_0 ratio. Ct (g.L^{-1}) is the native protein concentration at t holding time (min) and C$_0$ is the native protein concentration of unheated IMFs or protein solutions (g.L^{-1}). The results at 75°C represent means ± SD (n = 3). (B) K_n is the unfolding reaction rate constant (g^{1-n}.L^{n-1}.min^{-1}) and 1/T the inverse of the heating temperature (K^{-1}). The point at 75°C represents means ± SD (n = 3). (C) n is the reaction order and it is expressed as the average of the reaction orders determined at each heating temperature ± SD. K_n corresponds to the unfolding reaction rate constant (g^{1-n}.L^{n-1}.min^{-1}). Ea corresponds to the activation energy (kJ.mol^{-1}) and ln ($k_{n,0}$) represents the frequency factor logarithm, as determined by Arrhenius plots.

The rate constants of LF heat-denaturation in pure solution were similar at 1.3% and 5.5% proteins, meaning that the heat-denaturation of LF is not affected by the amount of lactose and minerals in solution (Figure 29.C and Figure 33.C). For the IMFs processed at 5.5% proteins, the denaturation rate of LF was higher than in pure LF solution, in agreement with the observations made at 1.3% proteins. This was mainly explained by the interactions between LF and the casein micelles, destabilising LF native structure as indicated previously (Chapter 4 – section 3.2.1). However, the increase of LF denaturation rate constants (IMFs *vs.* pure LF solution) was less pronounced in the IMFs processed at 5.5% than at 1.3% proteins, suggesting that native LF had a more stable structure within IMFs proteins at 5.5% proteins, in agreement with a higher activation energy for LF denaturation (Figure 29.C). Protein charge screening caused by the higher mineral content in the IMFs processed at 5.5% proteins (4.2-times) could reduce the electrostatic interactions between LF and caseins. The dissociation of LF from the casein micelles would explain its higher stability.
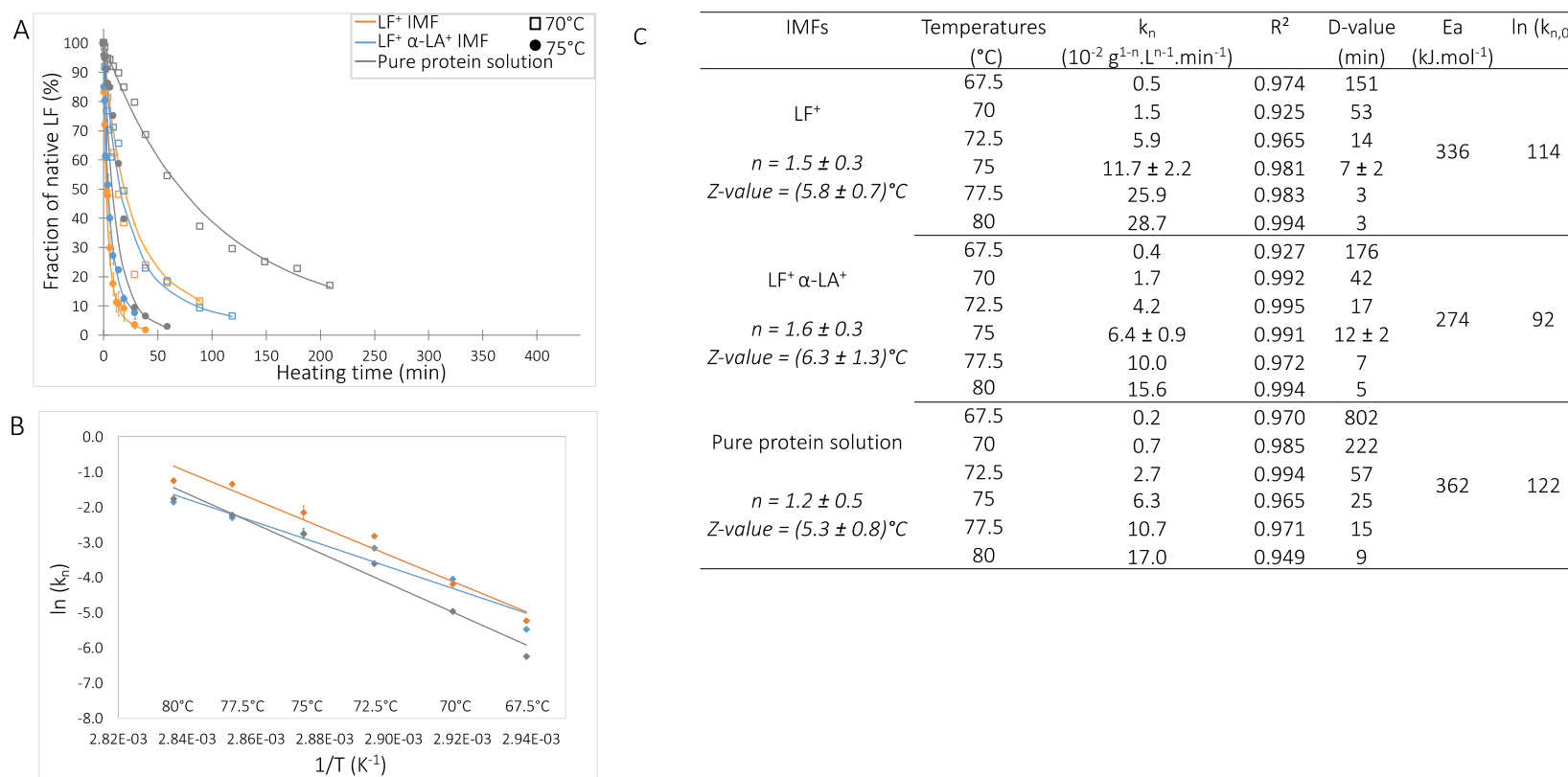
Figure 33. (A) Heat denaturation kinetics of LF for temperatures 70°C and 75°C (B) Arrhenius plots and (C) kinetic parameters associated, for the IMFs processed at 5.5% proteins and pure protein solution

(A) The pure protein solutions correspond to solution of LF at identical amount as found in the LF+ α-LA+ IMF and respecting the mineral and lactose contents of IMFs. Residual native fractions were calculated as a C_t / C_0 ratio. C_t (g.L^{-1}) is the native protein concentration at t holding time (min) and C_0 is the native protein concentration of unheated IMFs or protein solutions (g.L^{-1}). The results at 75°C represent means ± SD (n = 3). **(B)** K_n is the unfolding reaction rate constant (g^{1-n}.L^{n-1}.min^{-1}) and 1/T the inverse of the heating temperature (K^{-1}). The point at 75°C represents means ± SD (n = 3). **(C)** n is the reaction order and it is expressed as the average of the reaction orders determined at each heating temperature ± SD. K_n corresponds to the unfolding reaction rate constant (g^{1-n}.L^{n-1}.min^{-1}). Ea corresponds to the activation energy (kJ.mol^{-1}) and ln ($k_{n,0}$) represents the frequency factor logarithm, as determined by Arrhenius plots.

Overall, the denaturation kinetics of β-LG and LF were accelerated and the denaturation kinetics of α-LA were reduced in the IMFs processed at 5.5% than at 1.3% proteins. The denaturation kinetics of total whey proteins (i.e. α-LA, β-LG and/or LF) at 70°C and 75°C were determined and compared between IMFs processed at 1.3% or 5.5% proteins (Figure 34). The denaturation kinetics of the total whey proteins were reduced for the control and LF[+] IMFs processed at 5.5% proteins. The decrease of the whey protein denaturation kinetics at increasing total solid was in accordance with McKenna & O'Sullivan (1971), who showed that the whey protein denaturation after heating skimmed bovine milk at 80°C for 20 min decreased from 80% to 59% and 39% as the total solid increased from 9% to 28% and 44%, respectively. In contrast, Anema et al. (2006) and Law & Leaver (1997) showed that the whey protein denaturation was enhanced by increasing protein concentration, probably due to the increase of collision probability between protein molecules at higher protein concentration. However, the authors only modified the protein concentration using ultrafiltration method and not the total solid as done in our study, which can explain the different kinetic profiles. Interestingly, the denaturation kinetics of total whey proteins were near similar for the LF[+] α-LA[+] IMF processed at 1.3% or 5.5% proteins. This was explained by the opposite concentration-dependent heat denaturation of α-LA and LF.
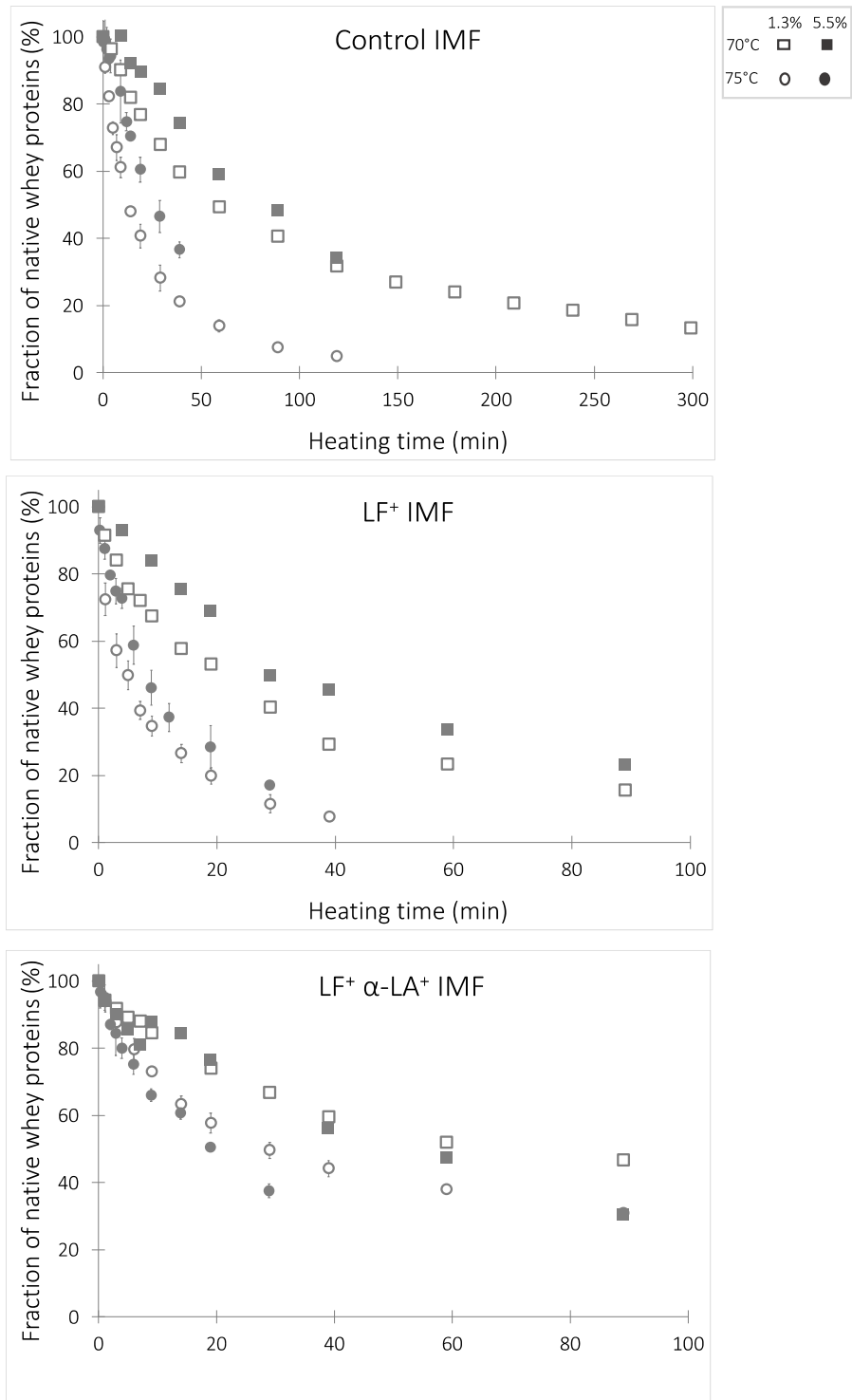
Figure 34. Heat denaturation kinetics of total whey proteins for temperatures 70°C and 75°C for the IMFs processed at 1.3% or 5.5% proteins

Fractions of native whey proteins were calculated as the ratio of the sum of native whey protein concentrations (i.e. α-LA, β-LG and/or LF) at t holding time (min) (g.L^{-1}) vs the sum of native whey protein concentrations of unheated IMFs (g.L^{-1}). The results at 75°C represent means ± SD (n = 3).

5. Conclusion

In this chapter, we demonstrated that the kinetics of heat-denaturation of α-LA, β-LG and LF were influenced by the whey protein composition of the IMFs, either for the IMFs processed at 1.3 or 5.5% proteins. The heat-denaturation of LF was not modified by the presence of α-LA or β-LG in the IMFs. As expected, the heat-denaturation of α-LA was enhanced in the presence of β-LG, but LF did not modify it. The contribution of β-LG to the heat-denaturation of α-LA was reduced in the concentrated IMFs. The presence of LF in the IMFs boosted the heat denaturation kinetics of β-LG, probably by exposing numerous disulfide bonds that are accessible to the free thiol group of β-LG. In addition, the kinetics of heat denaturation were slowed down with the increase of total solid of IMFs from 1.3% to 5.5% proteins prior to heating for the IMFs containing β-LG. This could be explained by the protection of the free thiol group of β-LG by lactose, reducing its accessibility for thiol/disulfide bond interchange reactions and the initiation of the whey protein denaturation.

The simulation of pasteurisation treatments for the IMFs processed at 1.3% proteins confirmed that the yield of total whey protein denaturation is function of both the whey protein composition of the IMFs and the heating conditions. The control IMF, formulated with WPI and SMP as protein sources, preserved a higher amount of native whey proteins after heat treatment at 62.5°C/30 min or at 75°C/15 s than IMF mimicking human milk protein profile, whereas a reverse trend was observed for heat treatments at higher temperature (90°C/15 s) or longer holding time (75°C/10 min). Finally, the formulation of IMFs containing both α-LA and LF, and so mimicking the protein profile of human milk, is a way to preserve a higher proportion of native whey proteins after heating, as long as the heat intensity applied is in the upper range of the intensity tested in the present study, conditions usually encountered at industrial scale to ensure microbial safety and to extend IMF shelf-life.

> ## Main messages
>
> - Whey protein composition of model IMFs governs the heat protein denaturation yield
> - Heat denaturation of α-LA is reduced in the absence of β-LG, as the free thiol group of β-LG is necessary for the irreversible α-LA denaturation
> - Heat denaturation of β-LG is enhanced in the presence of LF, because LF unfolds readily and exposes many disulfide bonds that react with the free thiol group of β-LG through thiol/disulfide exchange reactions
> - Heat denaturation of LF is not modified by the presence of the other whey proteins, as LF denaturation occurs at temperature lower than those of α-LA and β-LG
> - Whey protein heat denaturation is slowed down in concentrated IMFs containing β-LG

Chapter 5: Structural characterisation of heat-induced protein aggregates in model infant milk formulas

Based on the following publication for the IMFs processed at 1.3% proteins and on unpublished results for the IMFs processed at 5.5% proteins.
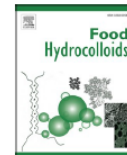
Structural characterization of heat-induced protein aggregates in model infant milk formulas

Amira Halabi [a], Amélie Deglaire [a], Marie Hennetier [b], Fréderic Violleau [b], Agnès Burel [c], Said Bouhallab [a], Didier Dupont [a], Thomas Croguennec [a,*]

[a] INRAE, Agrocampus Ouest, UMR STLO, 35042, Rennes Cedex, France
[b] Université de Toulouse, Institut National Polytechnique de Toulouse – Ecole d'Ingénieurs de Purpan, Département Sciences Agronomiques et Agroalimentaires, 31076, Toulouse Cedex 03, France
[c] Université de Rennes 1, Plateforme de microscopie MRic BIOSIT UMS 3480, 35043, Rennes, France

1. Abstract

Heat treatments induce structural modifications of bovine milk proteins. In this chapter, we aimed to investigate how these structural modifications are affected by the total solid, the whey protein profile IMFs as well as the heating conditions. Three model IMFs at 1.3% or 5.5% proteins were produced with a casein:whey protein ratio of 40:60, differing only by the whey protein profile. They were heated at 67.5°C or 80°C to reach an akin whey protein denaturation extent of 65%. Protein structures were analysed by asymmetrical flow field-flow fractionation coupled with multiangle light scattering and differential refractometer, transmission electron microscopy and electrophoresis. The unheated IMFs were used as reference. The results for the IMF processed at 1.3% proteins showed that LF addition in IMFs induced partial casein micelle disintegration before heating. In the absence of added LF, the heat-denatured whey proteins either formed soluble whey protein aggregates or casein micelle-bound whey protein aggregates. The latter were favoured at the expense of soluble aggregates in the heated IMFs with the LF content increase and the concomitant β-LG content decrease. Consequently, the casein micelle structure was strongly dependent on the β-LG and LF amounts in IMFs and on the heating temperature. In the IMFs containing β-LG and LF and at temperature greater than the β-LG denaturation temperature, the casein micelles exhibited filamentous appendages on its surface after heating. Below the denaturation temperature of β-LG and in IMFs containing trace β-LG amount, the heated casein micelles were perfectly spherical with a smooth surface. At higher total solid, denatured whey proteins, mainly α-LA and LF, preferential bound on the casein micelle surface, leading to the increase of the size of the modified casein micelle particles and the alteration of their structure.

2. Context and objectives

Once heat-denatured, whey proteins can form soluble whey protein aggregates or whey protein aggregates bound to the surface of casein micelles mainly through interactions with κ-caseins (Guyomarc'h, 2006; Nguyen, Wong, Anema, Havea, Guyomarc'h, 2012; Sawyer, 1969). Environmental conditions, as the casein:whey protein ratio (Beaulieu et al., 1999; Oldfield et al., 2005), the whey protein profile (Crowley et al., 2016), pH (Anema & Li, 2003) and the heating conditions (Qian et al., 2017) strongly affect the changes in the protein structure occurring during milk processing. These heat-induced modifications of protein structure have been extensively investigated for bovine milk (Anema & Klostermeyer, 1997; Patel et al., 2006; Sutariya et al., 2017; Vasbinder et al., 2003). Nevertheless, to our knowledge, only a few studies have focused on the IMFs (Buggy et al., 2017; Crowley et al., 2016), and even fewer have centred on the IMFs whose protein profile is based on human milk.

In this chapter, the aim was to characterise the protein structures formed during heating of IMFs as a function of the whey protein profile of IMFs and the heating conditions (i.e. the total solid of IMFs and the heating temperatures). We decided to select for the rest of the project two heating temperatures (67.5°C and 80°C) and a similar total whey protein denaturation in heated IMFs of 65%, a value within the range of that found in commercial IMFs. The thermodynamic parameters determined in chapter 4 were used to predict, for each IMF (i.e. the control, LF$^+$ and LF$^+$ α-LA$^+$ IMFs) at each total solid (i.e. IMFs processed at 1.3% or 5.5% proteins), the holding times to reach this total whey protein denaturation. Fixing the extent of whey protein denaturation in the IMFs rather than the heating time at a given temperature, which would have resulted in different extents of protein denaturation, allowed us to better describe differences between heat-induced protein entities. We hypothesised that changing the whey protein profile and the total solids prior to heating and/or the heating conditions would result in aggregates with different compositions and structures (e.g. size, shape and interactions between proteins), which could in turn affect the techno-functional properties of IMFs, as shown by Joyce et al. (2017), and its nutritional properties.

3. Results and discussion

3.1. Infant milk formulas processed at 1.3% proteins

3.1.1. Native whey protein profile in unheated and heated infant milk formulas

The whey protein profiles differed among the three unheated IMFs but the sum of α-LA, β-LG, and LF contents was similar (0.67 ± 0.02 g/100 g of liquid IMF) (Figure 35). The major whey proteins (i.e. α-LA, β-LG, and LF) represented 84% of total whey proteins, as determined by the Kjeldahl method (0.80 ± 0.04 g/100 g of liquid IMF). The difference was explained by the presence of other proteins, such as BSA, Igs or enzymes in the pH 4.6-soluble fraction that were not quantified by RP-HPLC.

The native whey protein contents (i.e. α-LA, β-LG and LF) in the heated IMFs summed to 0.24 ± 0.01 g/100 g of liquid IMF, corresponding to an extent of denaturation of total whey proteins of 64% ± 1% (Figure 35). Nonetheless, the extent of denaturation of each whey protein (α-LA, β-LG and LF) differed among IMF whey protein profiles and between heating temperatures. The percentage of native β-LG was lower, and those of native α-LA and LF higher, in the control and LF⁺ IMFs heated at 80°C than those heated at 67.5°C. This agreed with the heat sensitivity of whey proteins, since β-LG denatures at a higher temperature (78°C) than α-LA and LF (68°C and 60°C, respectively) (Bengoechea et al., 2011; Brodkorb et al., 2016; Nielsen et al., 2018). Similar percentages of native α-LA and LF were obtained in the LF⁺ α-LA⁺ IMF heated at 67.5°C and 80°C. LF, one of the most heat-sensitive proteins in milk, was the most heat-denatured whey protein at both heating temperatures (97 ± 1%), as previously observed in chapter 4.
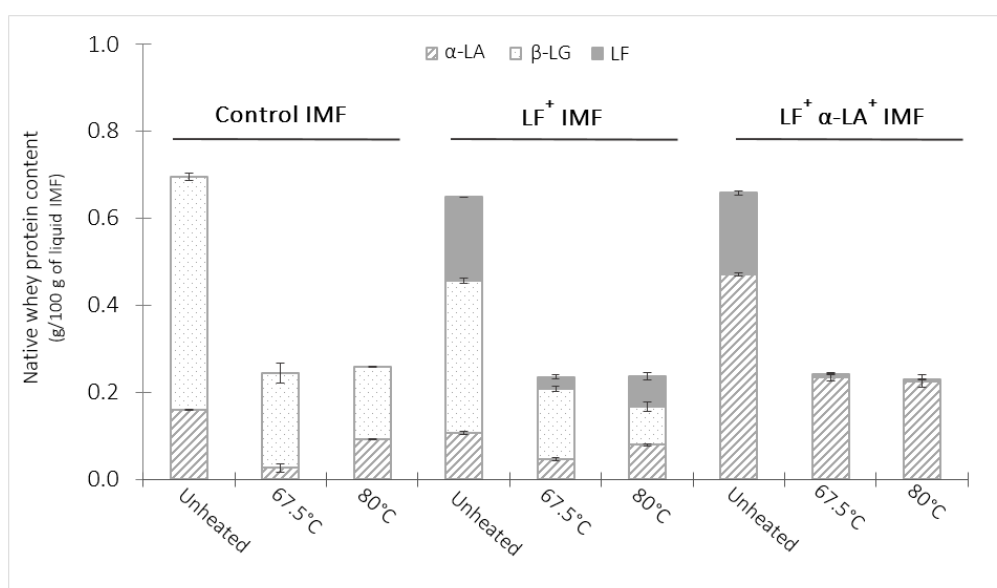
Figure 35. Whey protein composition of the pH 4.6-soluble fractions of the IMFs processed at 1.3% proteins

Data are means ± SD (n = 3). Heating times at target temperatures were selected in order to reach a whey protein denaturation rate of 65%. Value of β-LG content in the unheated LF⁺ α-LA⁺ IMF was too low to be quantified by RP-HPLC (0.06% w/w, by calculation from the amount of β-LG in SMP and the proportion of SMP in the IMF).

3.1.2. Protein entity characterisation in unheated and heated infant milk formulas

3.1.2.1. Unheated infant milk formulas

Protein fractograms of the unheated IMFs obtained by asymmetric flow field flow fractionation coupled with multiangle light scattering and differential refractometer (AF$_4$-MALS-dRi) (Figure 36.A) showed that two distinct populations were eluted and identified using elution profiles of the purified whey protein and the SMP standards. The first population, eluted from 10 to 15 min, was attributed to the native whey proteins. Native α-LA, β-LG and LF were eluted at 10.5, 11 and 12 min, respectively, with the peak areas of native whey proteins differing among the unheated IMFs, in agreement with the whey protein profile of the IMFs (Figure 35). A LF peak was observed only in the LF$^+$ and LF$^+$α-LA$^+$ IMF fractograms, but the peak area at 12.5 min was lower than expected given the LF content in these IMFs. This could have been because the low LF content naturally found in bovine milk is predominantly associated with casein micelles, and when additional LF is added to bovine milk, some of it spontaneously binds to the casein micelles (Anema & de Kruif, 2011; Croguennec, Li, Phelebon, Garnier-Lambrouin, & Gésan-Guiziou, 2012). The minor whey proteins in IMFs (i.e. BSA and Igs) could co-elute with α-LA, β-LG and LF but the amount of the minor whey proteins is low compared to the amount of α-LA, β-LG and LF. A second population, eluted from 20 to 28 min, was assigned to the casein micelles. Mean casein micelle characteristics (molecular weight $\overline{M_w}$, gyration and hydrodynamic radius $\overline{R_g}$ and $\overline{R_h}$, shape factor (i.e. $\overline{R_g}$:$\overline{R_h}$ ratio), and apparent fractal dimension df$_{app}$) are shown in Figure 36.B. For all unheated IMFs, the casein micelles had a similar shape factor (1.5 ± 0.1). However, the $\overline{M_w}$ and the df$_{app}$ of the casein micelles differed, with a $\overline{M_w}$ of 6.4 x 10^8 g.mol^{-1} and a df$_{app}$ of 3.0 for the control IMF compared to a $\overline{M_w}$ of 4.7 x 10^8 g.mol^{-1} and a df$_{app}$ of 2.5-2.6 for the IMFs with added LF (i.e. LF$^+$ and LF$^+$α-LA$^+$ IMFs). The structural change observed meant that the casein micelles lost their spherical shape and some molecular entities that initially formed part of the casein micelles were dissociated when LF was added to the LF$^+$ and LF$^+$α-LA$^+$ IMFs. A third protein population with a low peak area, eluted from 15 to 17 min, was observed for the unheated LF$^+$ and LF$^+$α-LA$^+$ IMFs.
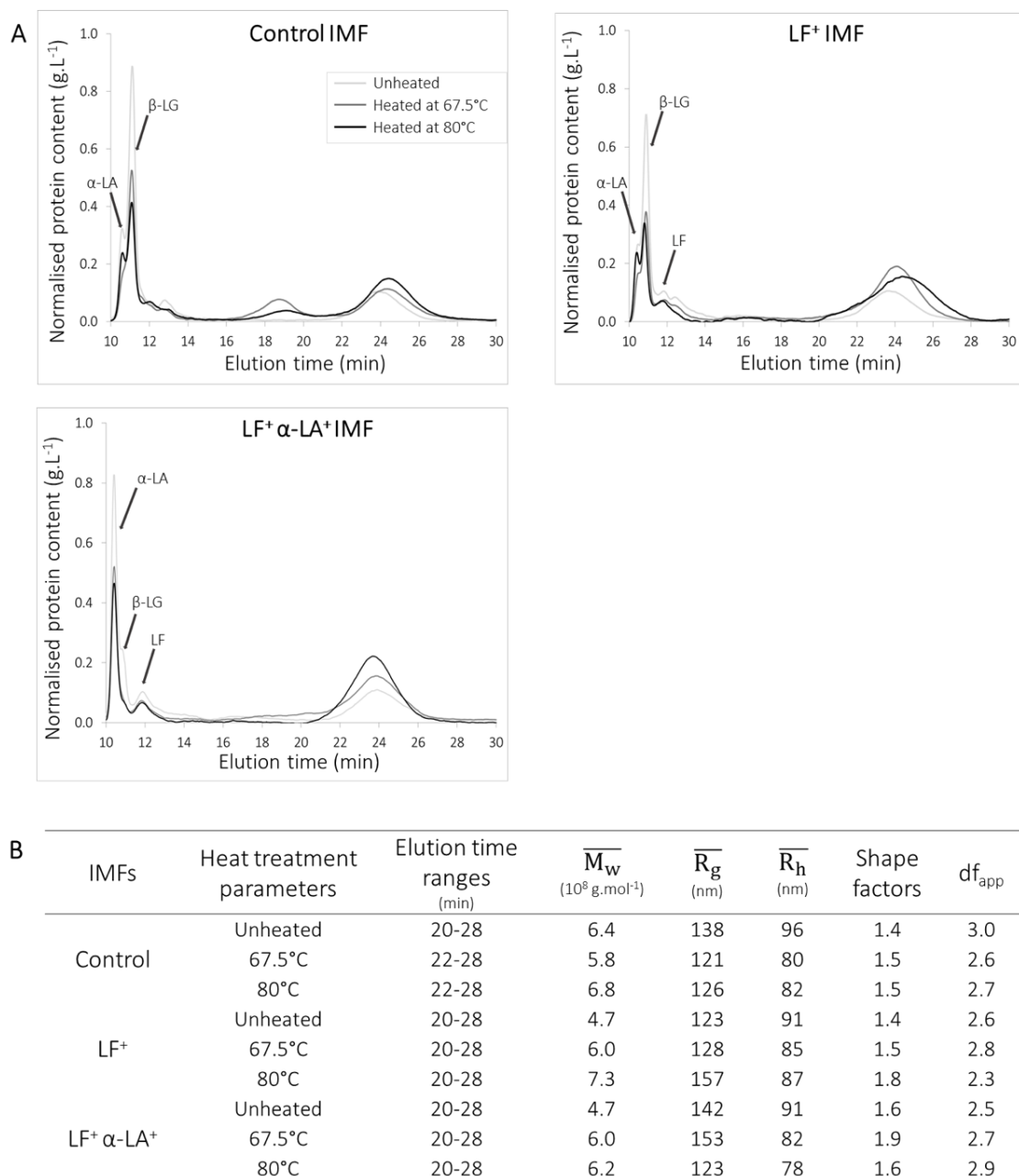
Figure 36. (A) Fractograms and (B) casein micelle characteristic parameters for the IMFs processed at 1.3% proteins

(A) The fractograms represent the protein content (g.L^{-1}), determined at 280 nm by the UV-visible detector and normalised by the mass recovery after the elution vs the elution time (min). Heating times at target temperatures were selected in order to reach a whey protein denaturation rate of 65%. (B) Data are the averaged values calculated from the whole casein micelle peaks. $\overline{M_w}$ (g.mol^{-1}) corresponds to the molecular weight. $\overline{R_g}$ and $\overline{R_h}$ (nm) correspond to the z-average radius of gyration and z-average hydrodynamic radius, respectively. The shape factor is determined from the ratio of $\overline{R_g}$ vs. $\overline{R_h}$. df$_{app}$ is the apparent fractal dimension and is determined from the slope of the log-log linear regression plot of R$_g$ vs. M$_w$. Heating times at target temperatures were selected in order to reach a whey protein denaturation rate of 65%.

The TEM images of the three unheated IMFs (Figure 37) confirmed the difference in casein micelle structure between the unheated control IMF and the unheated LF$^+$ and LF$^+$ α-LA$^+$ IMFs. The casein micelles of the unheated control IMF appeared relatively uniform in size (60-140 nm in diameter), with

a smooth surface. In contrast, the unheated LF$^+$ and LF$^+$ α-LA$^+$ IMFs showed small complexes and/or partially disintegrated casein micelles with an irregular shape, and casein micelles appearing "intact" but with an inner structure less dense than those of the casein micelles in the unheated control IMF. The partial disintegration of casein micelles in the unheated IMFs containing LF, which resulted in small LF/casein complexes in the soluble phase, agreed with results of Anema & de Kruif (2013). By forming electrostatic interactions with caseins, LF weakens interactions among caseins within casein micelles. In their study, the LF-casein micelle structures initially swelled and then disintegrated during longer storage, which increased milk transparency. In the present study, no change in IMF transparency was observed, but the LF:casein mass ratio in the LF$^+$ and LF$^+$ α-LA$^+$ IMFs (1:3) and the storage duration of the IMFs before analysis (24 h) lay within the lower range of the LF:casein mass ratio and storage durations reported by Anema & de Kruif (2013). Only small complexes released from casein micelles in the presence of LF were observed by TEM and were eluted between the whey proteins and the casein micelles by AF$_4$ analysis.
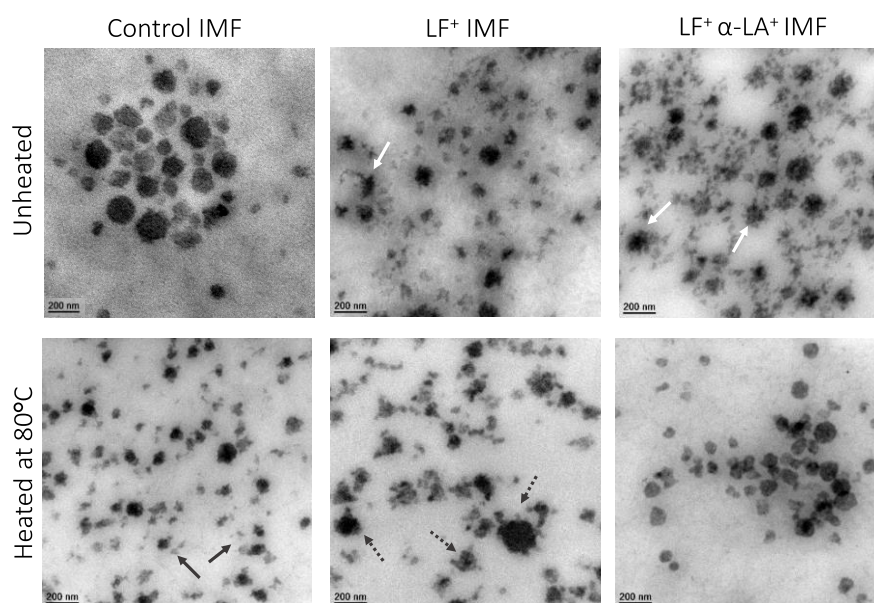
Figure 37. Transmission electron microscopy images of the supramolecular entities of the IMFs processed at 1.3% proteins

Images were captured at 50,000x magnification. The scale bar corresponds to 200 nm. Grey solid line arrows indicate small complexes, probably soluble whey protein aggregates. White arrows indicate partially disintegrated casein micelles. Grey dotted line arrows indicate casein micelle-bound whey protein aggregates with filamentous structure. Heating times at target temperatures were selected in order to reach a whey protein denaturation rate of 65%.

3.1.2.2. Heated infant milk formulas without lactoferrin

Fractograms of the control IMF heated at 67.5°C or 80°C (Figure 36.A) revealed a decrease in the peak areas of native whey proteins, with a larger decrease in the α-LA peak area at 67.5°C than at 80°C, and

vice versa for the β-LG peak area (i.e. a larger decrease at 80°C than at 67.5°C), which agreed with the RP-HPLC quantification (Figure 35). In addition, some casein micelle characteristics were modified after heating (Figure 36.B). Compared to the unheated control IMF, the $\overline{R_g}$ and $\overline{R_h}$ of the casein micelles decreased in the control IMFs heated at 67.5°C (121 and 80 nm, respectively) and 80°C (126 and 82 nm, respectively). The molecular mass of casein micelles in the control IMF decreased after heating at 67.5°C, while it increased slightly at 80°C. The shape factor (1.5) did not change, while the df$_{app}$ (2.6-2.7) decreased after heating at 67.5°C and 80°C. Interestingly, fractograms of the heated control IMFs revealed the presence of an intermediate protein population, eluted from 16.5 to 21 min, which was not observed in the other heated IMFs.

TEM images of the heated control IMF at 80°C (Figure 37) confirmed the presence of two types of protein entities. The first type had characteristics similar to those of the casein micelles observed in the unheated control IMF. The second type, assigned to the intermediate population detected by AF$_4$ analysis, were composed of smaller, more elongated and less dense aggregates (20-50 nm). Based on observations of Liyanaarachchi, Ramchandran, & Vasiljevic (2015), the second type was attributed to heat-induced soluble whey protein aggregates composed of denatured whey proteins and possibly individual caseins. These authors observed the formation of soluble aggregates 30 nm in size after heating at pH 6.7 a mixture of milk proteins and whey proteins with a casein:whey protein ratio of 30:70. Other authors have observed that heat denaturation of whey proteins in bovine milk resulted in the formation of soluble aggregates composed of α-LA and β-LG, with κ-caseins dissociated from the casein micelles (Anema, 2007; Anema & Klostermeyer, 1997; Donato, Guyomarc'h, et al., 2007; Donato & Guyomarc'h, 2009). The heat-induced κ-casein dissociation from casein micelles in bovine milk observed by Anema & Klostermeyer (1997) and Anema (2008) could explain the decrease in the $\overline{R_g}$ and $\overline{R_h}$ of the casein micelles in the heated control IMFs at both temperatures, as well as the lower $\overline{M_w}$ at 67.5°C. Moreover, adding whey proteins to bovine skimmed milk at natural pH has been observed to increase the amount of κ-casein recovered in the soluble phase after heat treatment at 80°C for 30 min (Anema, 2018).

For the same extent of whey protein denaturation, the amount of soluble aggregates obtained after heating the control IMF was higher at 67.5°C than at 80°C (Figure 36), whereas the $\overline{M_w}$ of casein micelles was lower after heating at 67.5°C (5.8 x 10^8 g.mol^{-1}) than at 80°C (6.8 x 10^8 g.mol^{-1}). This suggests that mainly heat-denatured whey proteins formed soluble aggregates at 67.5°C, while some of them interacted with casein micelles at 80°C. Qian et al. (2017) also observed heat-temperature dependence of the distribution of denatured whey proteins between soluble whey protein aggregates and casein-micelle-bound whey protein aggregates. This could be due to the lower percentage of denatured β-LG in the control IMF heated at 67.5°C than at 80°C. Casein micelle structure was not modified drastically,

as revealed by comparing TEM images of the unheated and heated control IMF at 80°C (Figure 37), suggesting even distribution of denatured whey proteins within the casein micelles. This binding could strengthen interactions between proteins within the casein micelles that had lower $\overline{R_g}$ and $\overline{R_h}$ but higher molecular mass after heating at 80°C.

3.1.2.3. Heated infant milk formulas with lactoferrin

Fractograms of the heated LF[+] IMF (Figure 36.A) indicated that the heat-induced decrease in α-LA and β-LG peak areas at 67.5°C and 80°C followed the same trend as those of the heated control IMFs, and that the LF peak area decreased more at 67.5°C than at 80°C, which agreed with the RP-HPLC quantification (Figure 35). The peak of the population eluted from 15 to 17 min was still visible in heated LF[+] IMFs. Compared to the unheated LF[+] IMF, the $\overline{M_w}$ of the casein micelle fraction of the heated LF[+] IMF increased at 67.5°C (6.0×10^8 g.mol^{-1}) and even more at 80°C (7.3×10^8 g.mol^{-1}) (Figure 36.B). This increase in $\overline{M_w}$ was accompanied by a decrease in $\overline{R_h}$ (~ 86 nm at 67.5°C and 80°C), while the $\overline{R_g}$ increased at 67.5°C (128 nm) and even more at 80°C (157 nm). Heat treatment of the LF[+] IMF at 67.5°C resulted in a slight increase in the df$_{app}$ (2.8), while at 80°C, the df$_{app}$ (2.3) decreased and the shape factor (1.8) increased compared to those of the unheated LF[+] IMF, assuming a branched structure of casein micelles. This was confirmed by TEM analysis of the LF[+] IMF heated at 80°C (Figure 37), which revealed a branched casein micelle structure with filamentous appendages on the surface. The binding of small protein aggregates on the micelle surface explained the drastic increase in the casein micelle $\overline{M_w}$ after heating (+ 55%). In addition, some features similar to those observed before heating were observed, such as the coexistence of partly disrupted and «intact casein micelles». However, all structures appeared more contracted, indicating that they were denser after heating.

Fractograms of the heated LF[+] α-LA[+] IMF (Figure 36.A) revealed a similar decrease in the α-LA and LF peak areas at both heating temperatures, which was consistent with the similar denaturation of α-LA and LF at both heating temperatures (Figure 35). The shoulder on the α-LA peak for the unheated LF[+] α-LA[+] IMF, identified as β-LG traces in the IMF, disappeared almost entirely after heating. The peak area of the population eluted from 15 to 17 min decreased for the LF[+] α-LA[+] IMF heated at 67.5°C, and even more after heating at 80°C. The lower content of partially disintegrated casein micelles after heating was confirmed by TEM images of the heated LF[+] α-LA[+] IMF at 80°C (Figure 37), with the absence of small assemblies in the soluble phase, like those identified for the unheated LF[+] α-LA[+] IMF. TEM images after heating at 80°C showed mainly spherical-shape protein entities with dimensions similar to those of the casein micelles (90-220 nm in diameter). In parallel, the $\overline{M_w}$ of casein micelles increased after heating (~ 6.1×10^8 g.mol^{-1} at 67.5°C and 80°C), while the $\overline{R_h}$ decreased (82 and 78 nm at 67.5°C and 80°C, respectively), as observed for the heated LF[+] IMF (Figure 36.B). The $\overline{R_g}$ of the casein micelles increased

at 67.5°C (153 nm) and decreased at 80°C (123 nm). The shape factor increased for the heated LF⁺ α-LA⁺ IMF at 67.5°C (1.9) compared to that of the unheated LF⁺ α-LA⁺ IMF but did not change at 80°C (1.6), while the df_{app} increased after heating at both temperatures (2.7 and 2.9 at 67.5°C and 80°C, respectively). Structural changes to casein micelles after heating LF⁺ α-LA⁺ IMF suggested that LF and perhaps α-LA could strengthen interactions among caseins within casein micelles, thus making the partially disintegrated casein micelle appeared more spherical and denser after heating.

3.1.3. Protein interactions in unheated and heated infant milk formulas

3.1.3.1. Unheated infant milk formulas

Intermolecular interactions among proteins in the unheated and heated IMFs were analysed by SDS-PAGE under non-reducing and reducing conditions before and after ultracentrifugation (Figure 38). A slight smear was observed at the top of the gel for all unheated IMFs under non-reducing conditions before ultracentrifugation; it disappeared after IMF reduction, probably due to the presence of aggregated whey proteins (α-LA and β-LG) in the SMP used to prepare the IMFs. In fact, compared to the unheated IMFs under non-reducing conditions, the intensity of electrophoretic bands after sample reduction changed more for α-LA and β-LG (at 14 and 18 kDa, respectively) than for caseins (at 29-37 kDa) and LF (at 80 kDa), which was almost unchanged. Nonetheless, the migration and intensity of the whey protein bands for the unheated IMFs corresponded to the whey protein profile expected for the IMFs (Figure 35).

After ultracentrifugation of the unheated IMFs, the supernatant electrophoretic bands that corresponded to caseins disappeared completely, indicating that the pellet contained all caseins, including partially disintegrated casein micelles and small complexes containing caseins. Intensities of the α-LA and β-LG bands were similar to those observed before ultracentrifugation, revealing that these proteins were completely recovered in the supernatant of ultracentrifugation and did not interact with casein micelles. On the contrary, the LF band was less intense in the ultracentrifugation supernatant of the unheated LF⁺ and LF⁺ α-LA⁺ IMFs under both non-reducing and reducing conditions. This suggests that some LF molecules were free and remained in the supernatant after ultracentrifugation, while the rest existed as larger entities and were pelleted with casein micelles. The interactions involving LF in these larger entities were non-covalent, since the unheated LF⁺ and LF⁺ α-LA⁺ IMFs had similar LF intensity bands under both non-reducing and reducing conditions. This observation agreed with those of Anema & de Kruif (2013), who showed that LF fixed the casein micelles mainly *via* electrostatic interactions due to the opposite charges of LF and casein micelles at natural milk pH.
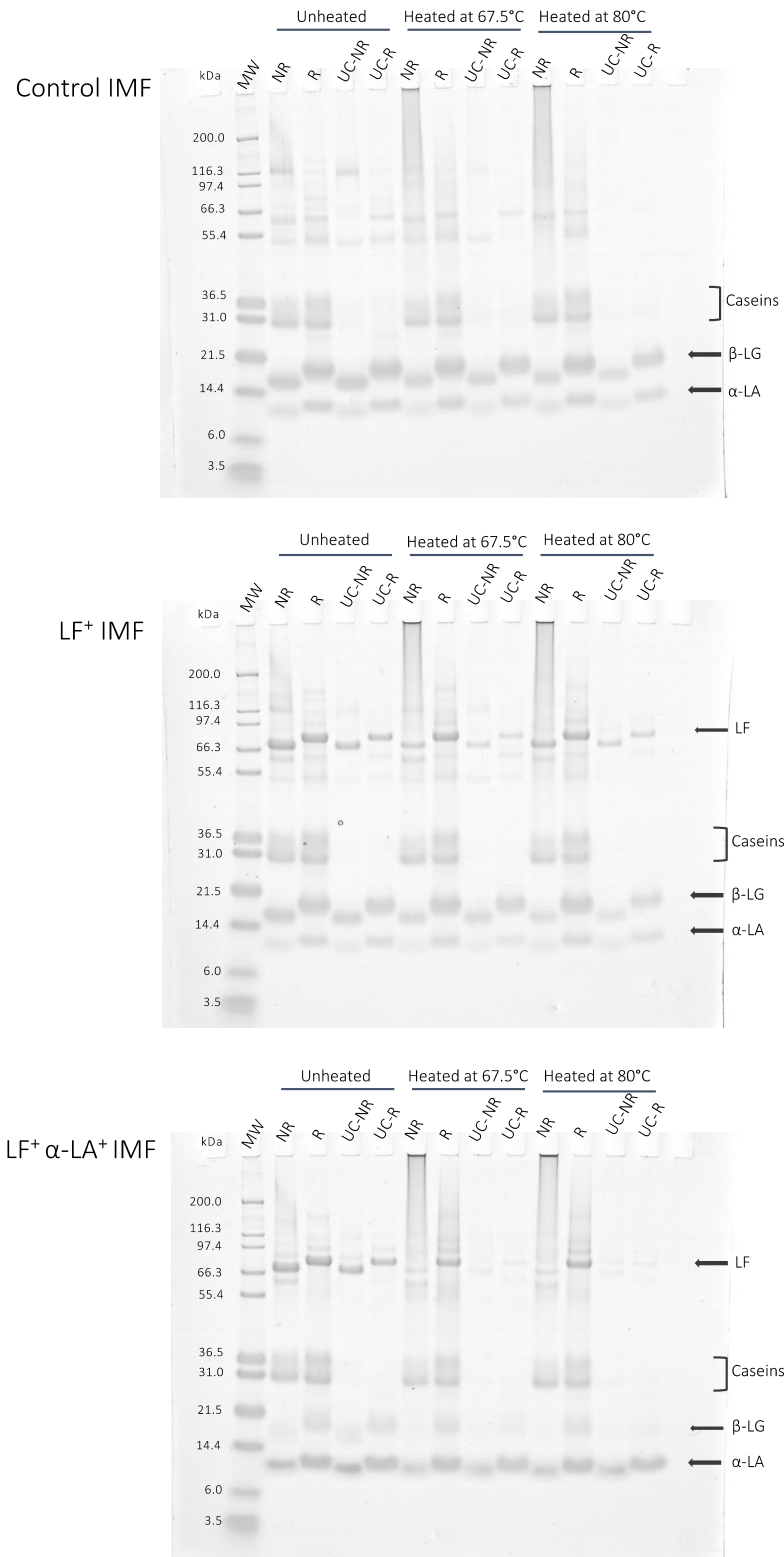
Figure 38. Gel electrophoregrams of the IMFs processed at 1.3% proteins

MW: Molecular weight marker; α-LA: α-lactalbumin; β-LG: β-lactoglobulin; LF: lactoferrin; NR: non-reduced condition; R: reduced condition; UC: ultracentrifuged condition.

Heating times at target temperatures were selected in order to reach a whey protein denaturation rate of 65%.

3.1.3.2. Heated infant milk formulas without lactoferrin

SDS-PAGE analysis of the heated control IMFs (Figure 38) revealed protein electrophoretic bands in the wells before ultracentrifugation and under non-reducing conditions; they were attributed to high-molecular-weight aggregates unable to enter the gel. Since these bands were not observed under reducing conditions, we concluded that intermolecular disulfide bonds helped stabilise the protein aggregates. The casein band intensity of the unheated and heated control IMFs increased only slightly under reducing conditions, indicating that heat-induced covalent intermolecular interactions between caseins and whey proteins or among caseins were not the most abundant. Conversely, the whey protein band intensities, particularly the β-LG band intensity, increased under reducing conditions at both heating temperatures. Hence, covalent disulfide bonds contributed mainly to whey protein cross-linking in the aggregates, in agreement with the observations of (Corredig, Dalgleish, 1999; Guyomarc'h et al., 2003; Raikos, 2010; Vasbinder et al., 2003). α-LA and β-LG band intensities did not differ before and after ultracentrifugation of the heated control IMFs under non-reducing conditions. Thus, the whey protein bands observed after ultracentrifugation corresponded to non-aggregated whey proteins and possibly soluble disulfide-bound whey protein aggregates, since α-LA and β-LG band intensities increased slightly after reduction.

3.1.3.3. Heated infant milk formulas with lactoferrin

SDS-PAGE analysis of IMFs containing LF before ultracentrifugation indicated that disulfide-bound high-molecular-weight aggregates composed of α-LA, β-LG, LF and caseins were formed during heating, since all band intensities increased after reduction (Figure 38). Moreover, in the heated LF⁺ IMFs, LF band intensity decreased, while α-LA and β-LG band intensities did not change after ultracentrifugation under non-reducing conditions, indicating that some LF molecules were also bound to the casein micelles by non-covalent interactions. The β-LG band intensity under non-reducing conditions was higher at 67.5°C than at 80°C, and *vice versa* for LF. The greater contribution of β-LG to forming covalent aggregates at 80°C than at 67.5°C could be explained by the greater β-LG denaturation at 80°C than at 67.5°C (Figure 35). As observed in bovine milk (Dalgleish et al., 1997; Nielsen et al., 2018; Wehbi et al., 2005) and the control IMF (Chapter 5 - section 3.1.3.2), the exposed thiol group of the denatured β-LG could have had a major influence on the formation of covalent aggregates in the heated LF⁺ IMFs. β-LG promoted the formation of intermolecular bonds with heat-unfolded LF (Li & Zhao, 2018), α-LA and, to a lesser extent, caseins. These reactions occurred on the surface and inside the casein micelles, since most LF were interacting electrostatically with casein micelles before heating as discussed previously (Anema & de Kruif, 2011; Croguennec, Li, Phelebon, Garnier-Lambrouin, & Gésan-Guiziou, 2012). They caused the

profound changes in characteristics of the casein micelles, particularly the $\overline{M_w}$ (+ 55% after heating at 80°C) and surface roughness (Figure 37).

SDS-PAGE analysis of the heated LF$^+$ α-LA$^+$ IMFs before and after reduction showed that almost all LF were involved in disulfide-bound high-molecular-weight aggregates (Figure 38). The small fraction of LF observed before ultracentrifugation under non-reducing conditions was recovered in the pellet after ultracentrifugation, indicating that the heated LF$^+$ α-LA$^+$ IMFs contain no free LF. The fact that more LF molecules interacted with casein micelles in the heated LF$^+$ α-LA$^+$ IMFs than in the heated LF$^+$ IMFs also suggests competition between LF and β-LG for binding sites on the casein micelles. From these observations, we hypothesised that LF molecules unfolded during heating and exposed hydrophobic residues, disulfide bonds and/or reactive thiol groups due to the cleavage of some disulfide bonds, as shown by Brisson, Britten, & Pouliot (2007) and de Figueiredo Furtado, Pereira, Vicente, & Cunha (2018). The denatured LF formed intermolecular disulfide bonds, mainly *via* thiol/disulfide exchange reactions, and interacted with caseins and probably the denatured α-LA that formed the spherical protein entities observed by TEM (Figure 37).

3.2. Infant milk formulas processed at 5.5% proteins

3.2.1. Native whey protein profile in unheated and heated infant milk formulas

The native whey protein contents (i.e. α-LA, β-LG and LF) in the unheated and heated IMFs summed to 3.53 ± 0.09 and 1.37 ± 0.08 g/100 g of liquid IMFs processed at 5.5% proteins, respectively, corresponding to an extent of denaturation of total whey proteins of 61% ± 2% (Figure 39). As for the IMFs processed at 1.3% proteins, the extent of denaturation of each whey protein (α-LA, β-LG and LF) in the IMFs processed at 5.5% proteins differed in function of the whey protein profiles and the heating temperatures (Figure 39). Overall, the extent of denaturation of each whey protein was almost similar between the heated IMFs processed at 5.5% and at 1.3% proteins. The main difference was that the lower proportion of native α-LA and the higher proportions of native β-LG and native LF in the heated IMFs processed at 5.5% proteins. On the other side, the ratio between native β-LG and native LF was identical in the IMFs processed at 5.5% and 1.3% proteins. These observations are in agreement with the results on the kinetics of denaturation of the whey proteins in the IMFs processed at 5.5% proteins, showing that the increase of the IMF dry matter slowed down the kinetics of denaturation of β-LG and LF and accelerated the kinetics of denaturation of α-LA (Chapter 4-section 4).
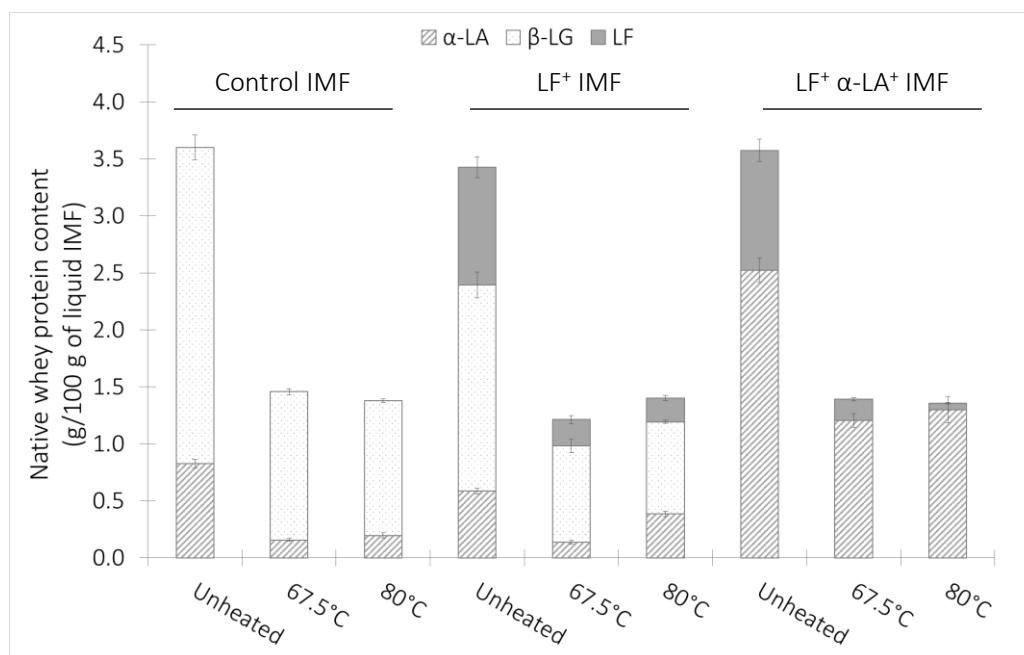
Figure 39. Whey protein composition of the pH 4.6-soluble fractions of IMFs processed at 5.5% proteins

Data are means ± SD (n = 3). Heating times at target temperatures were selected in order to reach a whey protein denaturation rate of 65%. Value of β-LG content in the unheated LF⁺ α-LA⁺ IMF was too low to be quantified by RP-HPLC (0.25% w/w, by calculation from the amount of β-LG in SMP and the proportion of SMP in the IMF).

3.2.2. Protein entity characterisation in unheated and heated infant milk formulas

3.2.2.1. Unheated infant milk formulas

As observed for the unheated IMFs processed at 1.3% proteins, protein fractograms of the unheated IMFs obtained by AF_4-MALS-dRi (Figure 40.A) showed two distinct eluted populations, the first population (10-15 min) corresponding to the native whey proteins and the second population (20-28 min) corresponding to the casein micelles. Mean characteristics of the casein micelles in the IMFs processed at 5.5% proteins (molecular weight $\overline{M_w}$, gyration and hydrodynamic radius $\overline{R_g}$ and $\overline{R_h}$, shape factor (i.e. $\overline{R_g}$:$\overline{R_h}$ ratio), and apparent fractal dimension df_{app}) are shown in Figure 40.B.

For all unheated IMFs, the main characteristics of casein micelles were similar than those determined for the unheated IMFs processed at 1.3% proteins. The main difference concerns the df_{app}, lower in the IMFs processed at 5.5% proteins (2.0 − 2.3) than at 1.3% proteins (2.5 - 3.0). The third protein population, eluted from 15 to 17 min and assigned to particles dissociated from caseins due to LF fixation (Chapter 5 - section 3.1.2.1), was observed for the unheated LF^+ and LF^+ α-LA^+ IMFs.

3.2.2.2. Heated infant milk formulas

The fractograms of the heated IMFs processed at 5.5% proteins indicated that the casein micelles were systematically larger after than before heating, the increase of their Mw being larger after heating the IMFs processed at 5.5% than at 1.3% proteins. This can be interpreted by the binding of a larger amount of whey proteins to the casein micelles or the cross-linking of different casein micelles by heat-denatured whey proteins. Fractograms of the control IMF heated at 67.5°C or 80°C (Figure 40.A) revealed that the peak area of the intermediate protein population eluted from 15 to 20 min, previously assigned to heat-induced soluble whey protein aggregates (Chapter 5 - section 3.1.2.2), was reduced compared to the IMFs processed at 1.3% proteins. This was opposite to the observations of Dumpler et al. (2017), who showed that after heat treatment of skimmed bovine milk, the extent of dissociation of κ-caseins and/or k-casein/β-LG complexes from casein micelle surface increased with total solid content (from 18% to 25% of total solid). This difference could be explained by the different experimental conditions, especially the heating temperature, as Dumpler et al. (2017) worked in the temperature range 90-150°C vs 67.5-80°C for our study. Indeed, Anema (1998) showed that the content of heat-induced dissociated caseins was dependent on the heating temperature. It is also possible that the whey protein-casein complexes were larger due to the higher protein content in the heated IMFs processed at 5.5% proteins and they were co-eluted with the casein micelles. In addition, the $\overline{R_g}$ and shape factor of the (modified) casein micelles were higher in the IMFs processed at 5.5% than at 1.3% proteins, and the opposite was observed for df_{app}. This suggested that the denatured whey proteins preferably fixed

the casein micelle surface leading to irregular particles in the heated IMFs processed at 5.5% proteins, while they formed small casein micelle-bound whey protein aggregates and/or soluble aggregates in the heated IMFs processed at 1.3% proteins.

IMFs	Heat treatment parameters	Elution time ranges (min)	$\overline{M_w}$ (10^8 g.mol^{-1})	$\overline{R_g}$ (nm)	$\overline{R_h}$ (nm)	Shape factors	df$_{app}$
Control	Unheated	20-28	5.7	150	89	1.7	2.0
	67.5°C	20-28	7.6	138	83	1.7	1.5
	80°C	20-30	13.8	207	105	2.0	1.6
LF$^+$	Unheated	20-28	5.2	147	93	1.6	2.0
	67.5°C	20-30	9.8	172	84	2.0	1.8
	80°C	20-30	8.1	185	84	2.2	1.8
LF$^+$ α-LA$^+$	Unheated	20-28	3.9	108	75	1.4	2.3
	67.5°C	20-30	6.3	135	74	1.8	1.5
	80°C	20-30	11.6	189	83	2.3	1.6
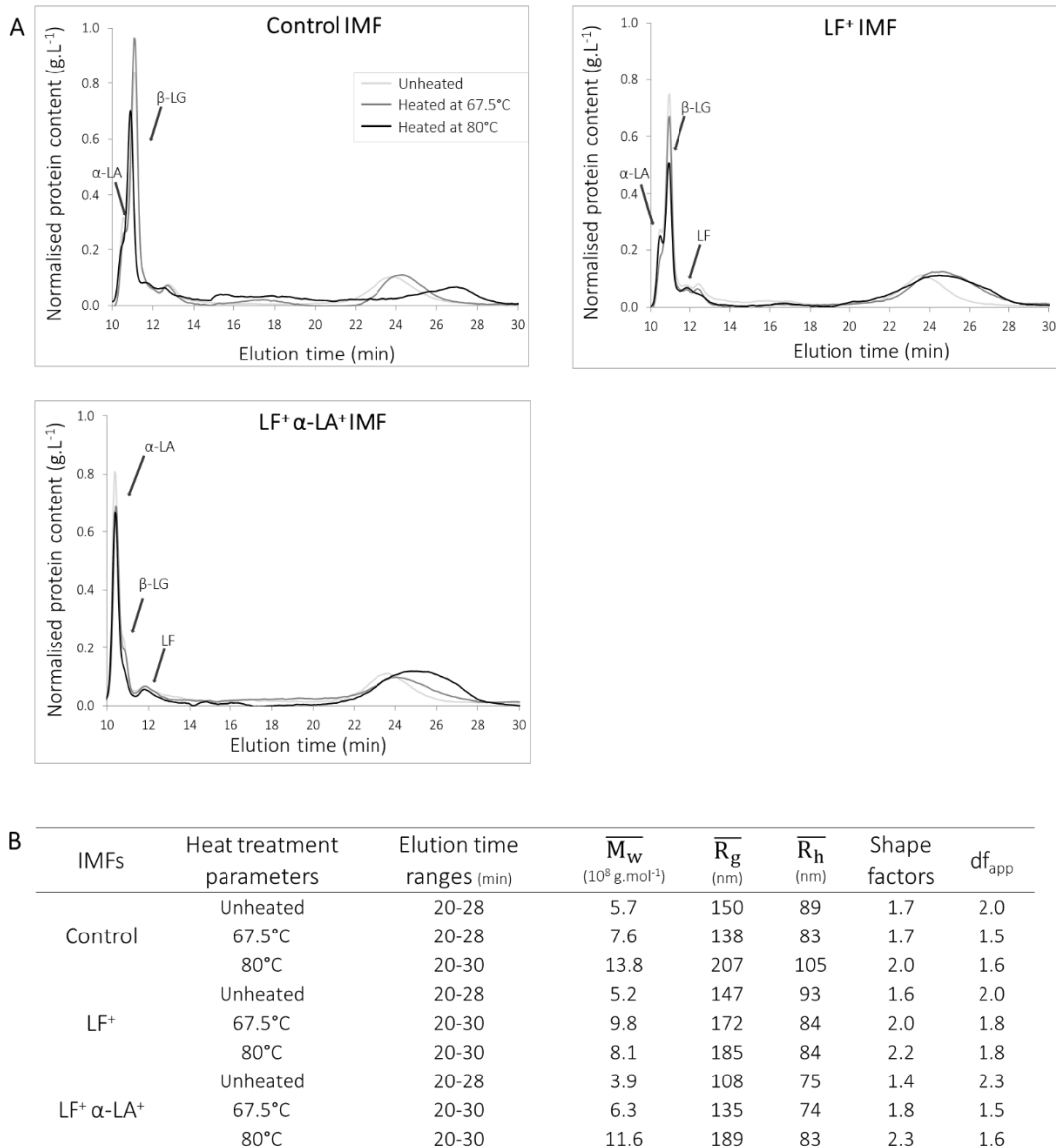
Figure 40. (A) Fractograms and (B) casein micelle characteristic parameters for the IMFs processed at 5.5% proteins

(A) The fractograms represent the protein content (g.L^{-1}), determined at 280 nm by the UV-visible detector and normalised by the mass recovery after the elution vs the elution time (min). Heating times at target temperatures were selected in order to reach a whey protein denaturation rate of 65%. (B) Data are the averaged values calculated from the whole casein micelle peaks. $\overline{M_w}$ (g.mol^{-1}) corresponds to the molecular weight. $\overline{R_g}$ and $\overline{R_h}$ (nm) correspond to the z-average radius of gyration and z-average hydrodynamic radius, respectively. The shape factor is determined from the ratio of $\overline{R_g}$ vs. $\overline{R_h}$. df$_{app}$ is the apparent fractal dimension and is determined from the slope of the log-log linear regression plot of R$_g$ vs. M$_w$. Heating times at target temperatures were selected in order to reach a whey protein denaturation rate of 65%.

3.2.3. Protein interactions in unheated and heated infant milk formulas

The participation of intermolecular disulfide bonds to the stabilisation of the heat-induced protein aggregates in the IMFs processed at 5.5% proteins were analysed by SDS-PAGE under non-reducing (Figure 41.A) and reducing (Figure 41.B) conditions.

The IMFs heating at 67.5°C and 80°C led to the formation of large aggregates recovered in the wells of the SDS-PAGE under non-reducing conditions and the concomitant decrease of electrophoretic band intensities of mainly α-LA for the control and LF[+] IMFs and LF for the LF[+] and LF[+] α-LA[+] IMFs. In contrast, the band intensity of caseins and β-LG barely changed after heating. Protein bands at ~ 55 kDa and ~ 116 kDa, observed on the tracks of the unheated control and LF[+] IMFs under non-reducing conditions, disappeared after heat treatments of these IMFs, especially at 80°C. The electrophoretic band observed at ~ 55 kDa was assigned to the heavy chain of IgG (Costa et al., 2014; G. Liu et al., 2020). The aggregates recovered in the wells of the SDS-PAGE under non-reducing conditions disappeared under reducing conditions (Figure 41.A and Figure 41.B). Thus, it was deduced that these high-molecular-weight aggregates were composed of mainly denatured α-LA and LF, and some caseins and denatured β-LG. They were stabilised by intermolecular disulfide bonds, as observed for the IMFs processed at 1.3% proteins (Chapter 5 – section 3.1.3).
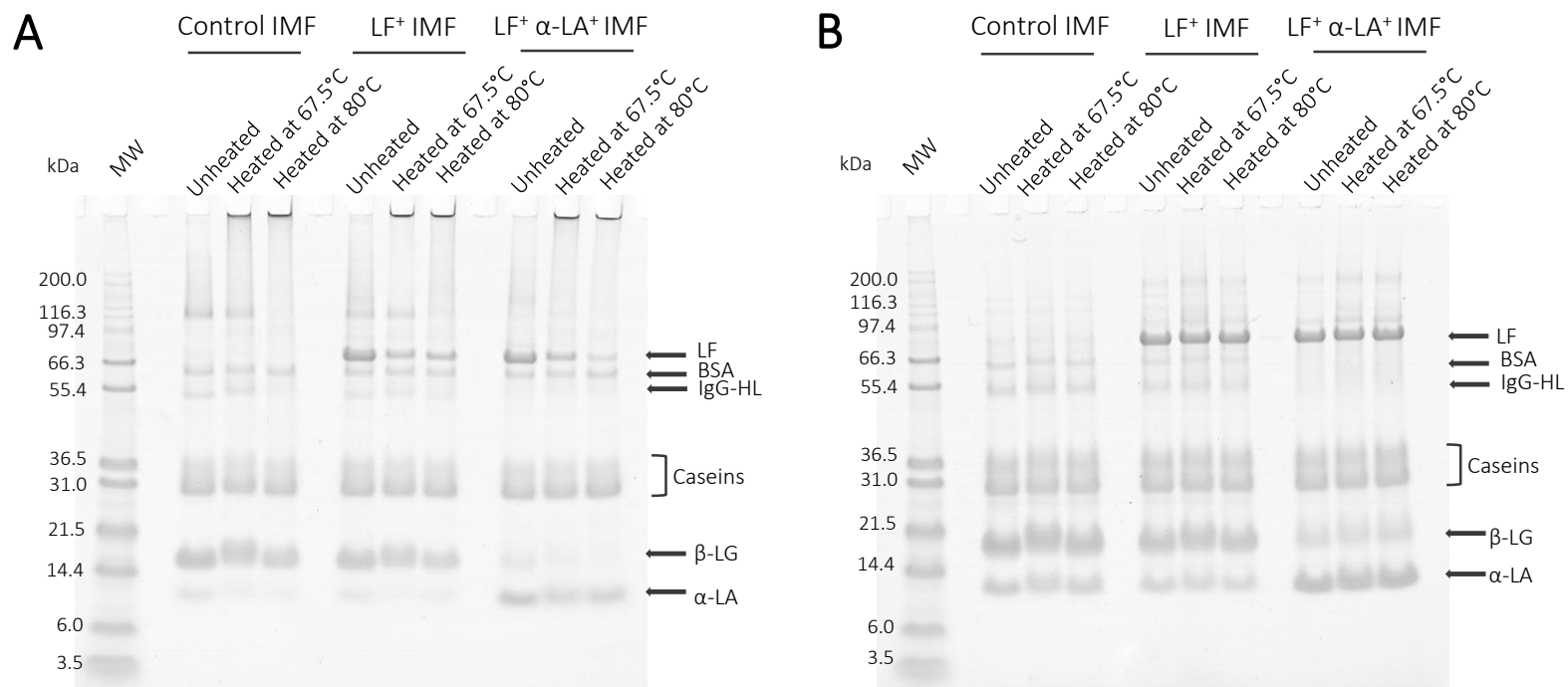
Figure 41. Gel electrophoregrams of the IMFs processed at 5.5% proteins under non-reducing (A) and reducing (B) conditions

MW: Molecular weight marker; α-LA: α-lactalbumin; β-LG: β-lactoglobulin; IgG-HL: high chain of IgG; BSA: bovine serum albumin; LF: lactoferrin.

Heating times at target temperatures were selected in order to reach a whey protein denaturation rate of 65%

4. Conclusion

In this chapter, we demonstrated that protein structure was influenced by the total solid and whey protein profile of IMFs, as well as the heating conditions. For the IMFs processed at 1.3% proteins, modifying the whey protein profile changed the structure of casein micelles even before heating, since the casein micelles were partially disintegrated in LF-enriched IMFs. Above the β-LG denaturation temperature and for the IMFs with a high β-LG content (i.e. the control and LF+ IMFs), most of the heat-induced changes in protein structure were attributed to the influence of β-LG. Under these conditions, heat-induced denaturation of whey proteins resulted in the formation of soluble whey protein aggregates and/or casein-micelle-bound whey protein aggregates; the proportion of the latter depended on the heating temperature and LF content in the IMFs. Increasing the heating temperature and the LF content in the IMFs, and thus decreasing the β-LG content, promoted the formation of casein-micelle-bound whey protein aggregates. Increasing the total solid of IMFs prior to heating led to the preferential binding of denatured whey proteins, mainly α-LA and LF on the casein micelle surface, which increased the size of the modified casein micelle particles and notably their structure.

Heat-induced protein entities with different protein compositions, sizes, shapes and distributions of covalent and non-covalent interactions could differ in their influence on processing and storage of IMFs (e.g. viscosity changes, emulsifying capacity, sedimentation stability), as well as in enzymatic susceptibility, thus yielding different nutritional benefits for infants.

Main messages

- Heat-induced protein structures depend on total solid, whey protein profile, as well as the heating conditions
- Before heating, LF induces partial casein micelle disintegration
- In the heated LF-free IMFs, denatured whey proteins mainly formed soluble aggregates at low total solid content, especially at 80°C, and formed casein micelle-bound whey protein aggregates at high total solid content
- In the heated IMFs containing LF, denatured whey proteins cover casein micelles, and the casein micelle shape depends on the β-LG content
- The Mw of the modified casein micelles increases and their shape changes with increasing total solid of IMFs

---

Chapter 6: modification of protein structures by altering the whey protein profile and heat treatment affects digestion of model infant milk formulas – an *in vitro* static study

Based on the following publication for the IMFs processed at 1.3% proteins and on unpublished results for the IMFs processed at 5.5% proteins.

Modification of protein structures by altering the whey protein profile and heat treatment affects *in vitro* static digestion of model infant milk formulas†

Amira Halabi, [ID] Thomas Croguennec, Said Bouhallab, Didier Dupont and Amélie Deglaire [ID] *

1. Abstract

Heat treatments induce changes in the protein structure in IMFs. The present study aims to investigate whether these structural modifications affect protein digestion. Model IMFs with a bovine or a human whey protein profile, were unheated or heated at 67.5°C or 80°C to reach 65% of denaturation and processed at 1.3% or 5.5% proteins. This resulted in different protein structures. IMFs were submitted to *in vitro* static gastrointestinal digestion simulating infant conditions. During digestion, laser light scattering was performed to analyse IMF destabilisation and SDS-PAGE, OPA assay and cation exchange chromatography were used to monitor proteolysis.

Results showed that, during gastric digestion, α-LA and β-LG were resistant to hydrolysis in a similar manner for the IMFs processed at 1.3% proteins ($p > 0.05$), while β-LG hydrolysis was enhanced for the heated IMFs processed at 5.5% proteins, probably due to the high susceptibility to pepsin hydrolysis when β-LG is bound on the casein micelle surface. In addition, the heat-induced denaturation of LF significantly increased its susceptibility to hydrolysis, this increase depending on the extent of LF denaturation. Casein hydrolysis was enhanced when the native casein micelle structure was modified, i.e. partially disintegrated in the presence of LF or covered by heat-denatured whey proteins. The IMF destabilisation at the end of the gastric digestion varied with protein structures, with larger particle size for IMF containing native casein micelles. During intestinal digestion, the kinetics of protein hydrolysis varied with the protein structures within IMFs, particularly for IMFs containing denatured LF, and denatured α-LA and β-LG for the IMFs processed at 5.5% proteins. Overall, the protein structures, generated by modulating the protein profile of IMFs and the heating conditions (i.e. total solid of IMFs and heating temperatures), impacted the IMF destabilisation during the gastric phase and the proteolysis during the entire simulated infant digestion.

2. Context and objectives

Up to now, little is known on the relationship between size, shape and structure of milk proteins and their behaviour during gastrointestinal digestion, especially in IMF environment. In chapter 5, the protein structures formed by varying the protein profile of IMFs and the heating conditions (i.e. total solid of IMFs and heating temperatures) have been characterised. The aim of this chapter was to investigate the impact of these protein structures on proteolysis kinetics using an *in vitro* static model simulating infant digestion. The control and LF$^+$ α-LA$^+$ IMFs were selected for this study, as the control IMF had a whey protein profile close to that of the majority of commercialised IMFs, while the whey protein profile of the LF$^+$ α-LA$^+$ IMF was close to that of human milk. The IMFs processed at 1.3% or 5.5% proteins were unheated or heated at 67.5°C or 80°C to reach the same extent of whey protein denaturation fixed at 65%, such as in chapter 5. IMFs were submitted to *in vitro* static gastrointestinal digestion simulating infant conditions. During digestion, IMF destabilisation was monitored by laser light scattering. Protein digestion kinetics were followed by determination of the proportion of residual intact milk proteins by SDS-PAGE under reducing condition, the degree of hydrolysis by OPA (*o*-phthalaldehyde) assay and the amino acid bioaccessibility by cation exchange chromatography.

3. Results and discussion

3.1. Infant milk formulas processed at 1.3% proteins

3.1.1. Particle size distribution

Figure 42 shows the particle size distributions of the unheated and heated control and LF[+] α-LA[+] IMFs. At this scale of observation, the particle size distributions of the undigested IMFs were similar with an almost unimodal distribution (Figure 42). The main peak with an average mode of 0.14 µm was assigned to the casein micelles as this peak was significantly reduced in the presence of ethylenediaminetetraacetic acid (EDTA), a calcium-chelator which induced casein micelle dissociation (Lin et al., 1972). A wide peak of small intensity in the region of 10-100 µm, probably corresponding to heat-induced protein entities formed by heating and/or insoluble particles resulting from IMF preparation, was also observed.

3.1.1.1.   At the end of the gastric digestion

After 60 min of gastric digestion, the particle size of the digesta was increased for the control and LF[+] α-LA[+] IMFs compared to the corresponding undigested IMFs (Figure 42), but in a different manner depending on the IMF (whey protein profile and/or heating temperature).

3.1.1.1.1. The unheated control IMF

The particle size for the unheated control IMF (mode of 82.4 ± 0.7 µm) was larger than that for the heated control IMFs (mode of 10.3 ± 1.7 µm). This was in accordance with the previous observations of a larger casein coagulum size of raw skimmed bovine milk compared to that of heated skimmed milk during gastric digestion (Ye et al., 2016). The large increase of particle size at the end of the gastric digestion for the unheated control IMF was a consequence of the pepsin action and not of the acidification, as demonstrated after pH adjustment of the undigested IMF at 5.3 without pepsin (Figure 42). This was expected as the gastric pH (pH 5.3) was superior to the pH at which the aggregation of native casein micelles occurs (pH 4.9) (Donato, Alexander, et al., 2007). The casein micelles of the unheated control IMF were in a spherical form with κ-caseins covering its surface at pH between 6.7 and 5.2 (Martin et al., 2007). Pepsin action on k-caseins must have conducted to the destabilisation of the casein micelles and to the formation of large particles at pH 5.3 (Plowman & Creamer, 1995).

3.1.1.1.2. The unheated LF[+] α-LA[+] IMF

Contrary to the control IMFs, the particle size for the unheated LF[+] α-LA[+] IMF (mode of 1.2 ± 0.4 µm) was lower than that for the heated LF[+] α-LA[+] IMFs (mode of 11.1 ± 2.4 µm). Opposite observations were made by de Oliveira et al. (2016) on human milk, having a protein profile close to that of the LF[+] α-LA[+] IMF, where the particle size during dynamic *in vitro* gastric digestion was larger for raw human milk than

for pasteurised human milk at ~ pH 5.4. The apparent contrast between our results and the conclusions of de Oliveira et al. (2016) may be explained by the different composition and/or structure between the LF$^+$ α-LA$^+$ IMF and human milk and the different *in vitro* digestion conditions. For the unheated LF$^+$ α-LA$^+$ IMF, the particle size at 60 min of gastric digestion was moderately increased, presenting a bimodal distribution with a major peak centred at 1.2 ± 0.4 μm and a minor peak at 0.15 ± 0.03 μm (Figure 42). Similar size increase was also observed for the undigested IMF at pH 5.3 without pepsin. Before digestion of the unheated LF$^+$ α-LA$^+$ IMF, LF binding to casein micelles partially disintegrated the latter, leading to open casein micelle structure (Chapter 5 - section 3.1.2.1) (Anema & de Kruif, 2013). The acidification of LF$^+$ α-LA$^+$ IMF at pH 5.3 induced a reduction of the electrostatic interactions between LF and the casein micelles, due to the decrease of casein micelle net charge (Anema, 2019). In the same time, the partially disintegrated casein micelles seemed to be able to interact in the form of small particles (mainly lower than 10 μm). Such entities were not observed with the native casein micelles.

3.1.1.1.3. The heated IMFs

All the heated IMFs presented a near similar particle size distribution at the end of the gastric digestion, independently of the heating temperature (67.5°C or 80°C) or of the whey protein profile of IMFs (Figure 42). The particle size increase at the end of the gastric digestion of the heated IMFs compared to that for the undigested IMFs was due to the acid coagulation of whey protein-coated casein micelles as similar size increase was also observed for the undigested heated IMF at pH 5.3 without pepsin. This increase in particle size at pH 5.3 was in agreement with the observations made on heated bovine milk (Donato et al., 2007; Guyomarc'h et al., 2003).

3.1.1.2.   At the end of the intestinal digestion

After 60 min of intestinal digestion (Figure 42), the bimodal particle size distributions for all IMFs were alike. The wide peak between 1 and 1000 μm was assigned to pancreatin contained in the intestinal digesta (Supplementary Figure 3). The global decrease of particle sizes (with an approximately mode of 0.1 μm) compared to those at the end of gastric digestion was due to protein hydrolysis by intestinal enzymes and/or to residual protein structures within undigested IMFs.
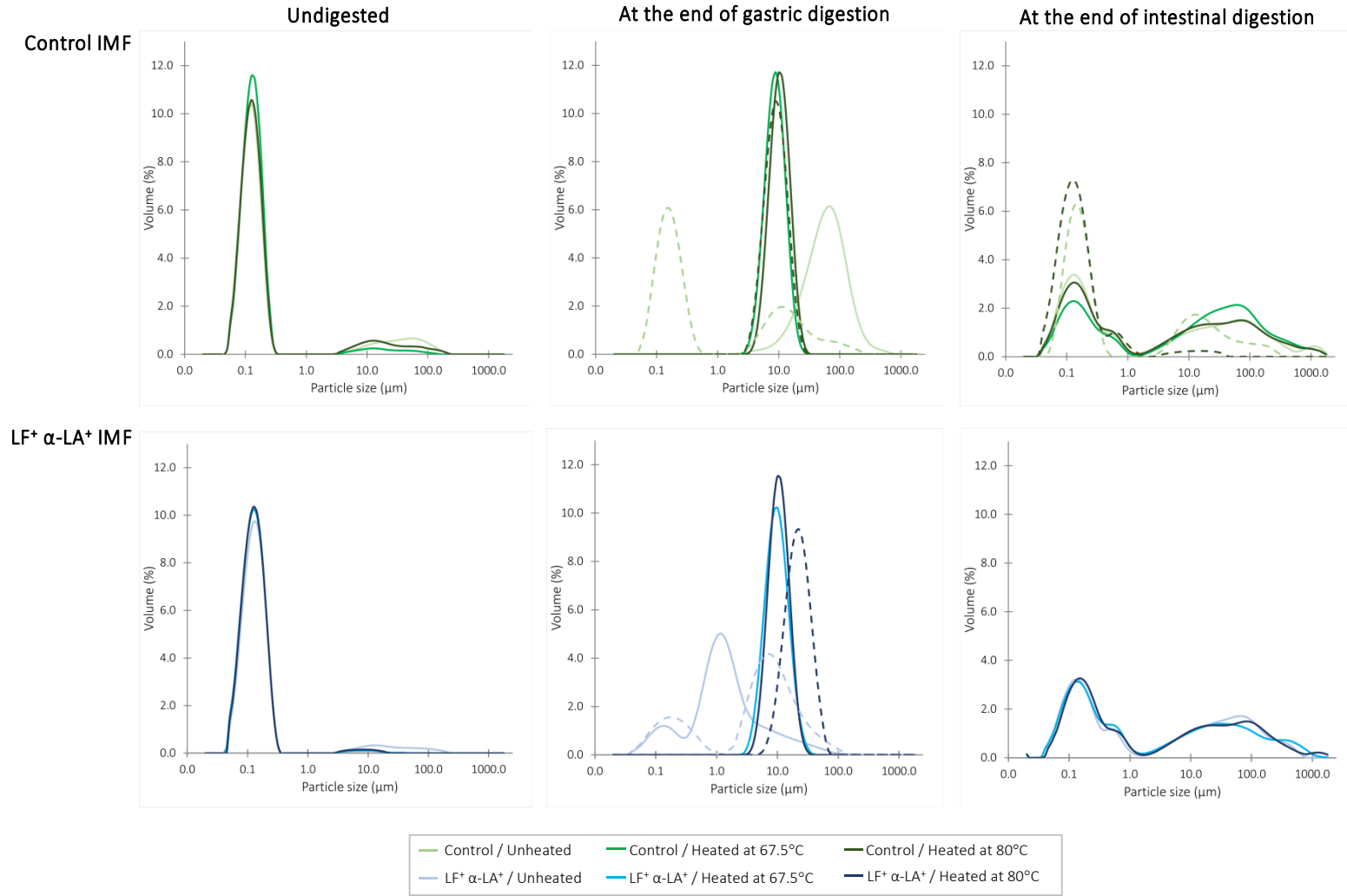
Figure 42. Particle size distributions of the IMFs processed at 1.3% proteins before digestion and at the end of the *in vitro* static gastric and intestinal digestions

The pH of the IMFs was 6.8 before digestion, 5.3 at the end of the gastric digestion and 6.6 at the end of the intestinal digestion. The dotted lines correspond to the particle size distribution of the IMFs after pH adjustment at 5.3 or 6.6 in absence of digestive enzymes. Data represent means of three independent digestion experiments (n = 3), with each measurement performed in triplicate.

3.1.2. Protein hydrolysis kinetics

Proteolysis kinetics of caseins, α-LA, β-LG and LF, as quantified from SDS-PAGE analysis under reducing conditions (Figure 43), are presented in Figure 44. During the gastrointestinal digestion of the unheated control IMF and the heated control IMF at 67.5°C, BSA resisted to enzymatic hydrolysis, as observed previously during gastric digestion of human milk (de Oliveira et al., 2016) or IMFs (Nguyen, 2017). However, it was progressively hydrolysed during the gastric digestion of the heated control IMF at 80°C until total band disappearance at 60 min of gastric digestion. This could be explained by different conformation of BSA in IMF heated at 80°C *vs.* in unheated IMF or IMF heated at 67.5°C. The heat denaturation of BSA in IMF heated at 80°C enhanced its susceptibility to pepsin hydrolysis. BSA content in IMFs was too low to be quantified.

3.1.2.1. Caseins

During the gastric digestion, the kinetics of casein hydrolysis were slower for the unheated control IMF than for the other IMFs (Figure 44.A), particularly at 30 min of gastric digestion where it reached statistical significance with 17 ± 4% *vs.* 6 ± 1% of residual intact caseins for the unheated control IMF vs the other IMFs, respectively. The resistance of the native casein micelles (unheated control IMF) to pepsin hydrolysis could be explained by the larger size of particles formed during gastric digestion compared to those formed from the dissociated casein micelles by LF (unheated LF[+] α-LA[+] IMF) or the casein micelles bound to denatured whey proteins (heated IMFs) (Figure 44.B), thus limiting the pepsin access to cleavage sites. Concomitantly to the casein hydrolysis, bands ranging from 3.5 to 6 kDa, assigned to products of casein proteolysis amongst other, such as reported previously (Ménard et al., 2018), were less intense for the unheated IMFs compared to the heated IMFs (Figure 44.A).

3.1.2.2. α-lactalbumin and β-lactoglobulin

The SDS-PAGE analysis of the control and LF[+] α-LA[+] IMFs (Figure 44.A) showed a resistance to pepsin hydrolysis for β-LG and α-LA, particularly compared to caseins. β-LG was totally resistant to pepsin hydrolysis over the gastric digestion with no significant difference between the unheated and heated control IMFs (Figure 44.B). α-LA was hydrolysed during gastric digestion in a similar manner for all IMFs (p > 0.05), down to 71 ± 10% of residual intact α-LA at 60 min (Figure 44.C).

The similar kinetics of β-LG or α-LA hydrolysis between the unheated and heated IMFs were in agreement with a previous study investigating the pasteurisation effects on *in vitro* digestion of IMFs, where, in addition, a lower pepsin resistance of α-LA compared to that of β-LG was also observed (Bourlieu et al., 2015). However, other authors have reported an enhancement of whey protein hydrolysis with heat treatment due to whey protein unfolding and thus an increased accessibility of

protein cleavage sites (Kitabatake & Kinekawa, 1998; Mulet-Cabero et al., 2019; Wada & Lönnerdal, 2014), or at the opposite a slowing down of their hydrolysis (Stender et al., 2018) during gastric digestion. The apparent discrepancy among studies are likely due to different heat-induced protein structures that can vary depending on the heating parameters, such as reported by Peram et al. (2013). In the present study, denatured α-LA and β-LG within the heated IMFs were bound on the casein micelle surface and/or formed soluble aggregates (Chapter 5 - Section 3.1.2.2). The similar β-LG or α-LA gastric hydrolysis between the unheated and heated IMFs could be explained by the limited access of pepsin cleavage sites on the heat-induced protein structures due to steric hindrance (Harjinder Singh & Creamer, 1993). In addition, the disulfide interactions involved in the heat-induced protein structures within the heated IMFs could limit the pepsin hydrolysis, in contrary to the non-covalent interactions (Zhang & Vardhanabhuti, 2014).

Regarding the intestinal digestion, β-LG and α-LA were rapidly hydrolysed during the first minutes as no intact protein was detected after 5 min of digestion (Figure 43).

3.1.2.3.   Lactoferrin

The band intensity of the LF for the unheated and heated LF[+] α-LA[+] IMFs was similar before digestion (Figure 43), while 97% of LF was in non-native form for the heated IMFs (Chapter 5 - Section 3.1.1). This was in accordance with the previous chapter showing that LF formed, with α-LA and caseins, heat-induced aggregates linked by disulfide interactions, which were thus reversible after reducing SDS-PAGE (Figure 38).

The kinetics of LF hydrolysis during gastric digestion (Figure 44.D) showed that LF in its native form (unheated LF[+] α-LA[+] IMF) was resistant to pepsin hydrolysis with 94 ± 9% of residual intact LF at 60 min. The resistance of native LF to pepsin hydrolysis was explained by its globular structure (Britton & Koldovsky, 1989). On the contrary, its hydrolysis was drastically enhanced in the denatured form (heated LF[+] α-LA[+] IMFs) since the very first minutes of digestion, with only 19 ± 4 % of residual intact LF remaining at 5 min of gastric digestion. The same increase of LF hydrolysis was noticed after holder pasteurisation of human milk (de Oliveira et al., 2016). It was supposed that the heat-induced LF denaturation led to better accessibility of hidden pepsin cleavage sites (Stǎnciuc et al., 2013). The LF hydrolysis by pepsin during the gastric digestion of the heated LF[+] α-LA[+] IMFs generated a peptide of ~ 50 kDa (Figure 43), such as previously observed during the *in vitro* infant gastric digestion of LF solution (Moscovici et al., 2014). This 50 kDa-peptide, identified as the C-terminal fragment of the protein (Sharma et al., 2013), was resistant to pepsin hydrolysis as its band intensity was unchanged during the gastric digestion.

Regarding the intestinal digestion, and as observed for β-LG and α-LA, the LF hydrolysis occurred since the first minutes of digestion of the unheated LF[+] α-LA[+] IMF, with a total LF band disappearance at 60 min of intestinal digestion (Figure 43). Concomitantly to LF hydrolysis, an electrophoretic band

corresponding to the C-terminal fragment of LF was observed in the early stages of intestinal digestion of the unheated LF⁺ α-LA⁺ IMF. The C-terminal fragment of LF was resistant to intestinal hydrolysis for all IMFs, such as previously reported (Rastogi et al., 2014). In addition to the 50 kDa electrophoretic band, another band at ~ 37 kDa was observed from 5 min of intestinal digestion for the unheated and heated LF⁺ α-LA⁺ IMFs, with a higher intensity for the unheated IMF. This polypeptide, resistant to intestinal digestion, was attributed to a product of LF hydrolysis by intestinal enzymes.

The resistance of the C-terminal fragment of LF to hydrolysis throughout the gastrointestinal digestion for the unheated and heated LF⁺ α-LA⁺ IMFs could have nutritional benefits for infants as this peptide has been reported to keep some bioactive properties of native LF such as the ability to bind one iron ion (Rastogi, Singh, et al., 2014; Sharma et al., 2013), the antimicrobial and antifungal activities (Rastogi et al., 2014). However, it does not cover the diverse range of physiological functions of native LF, such as the cell growth promoting and differentiation activities or the anti-inflammatory properties (Lönnerdal, 2016). Previous works showed that the osteogenic activity of LF (Fan et al., 2019) and the antibacterial activity of LF on *Cronobacter sakazakii* (Harouna et al., 2015) were decreased when the heat treatment intensity increased. Overall, the physiological impact of the unheated vs heated LF⁺ α-LA⁺ IMFs remains to be evaluated *in vivo.*
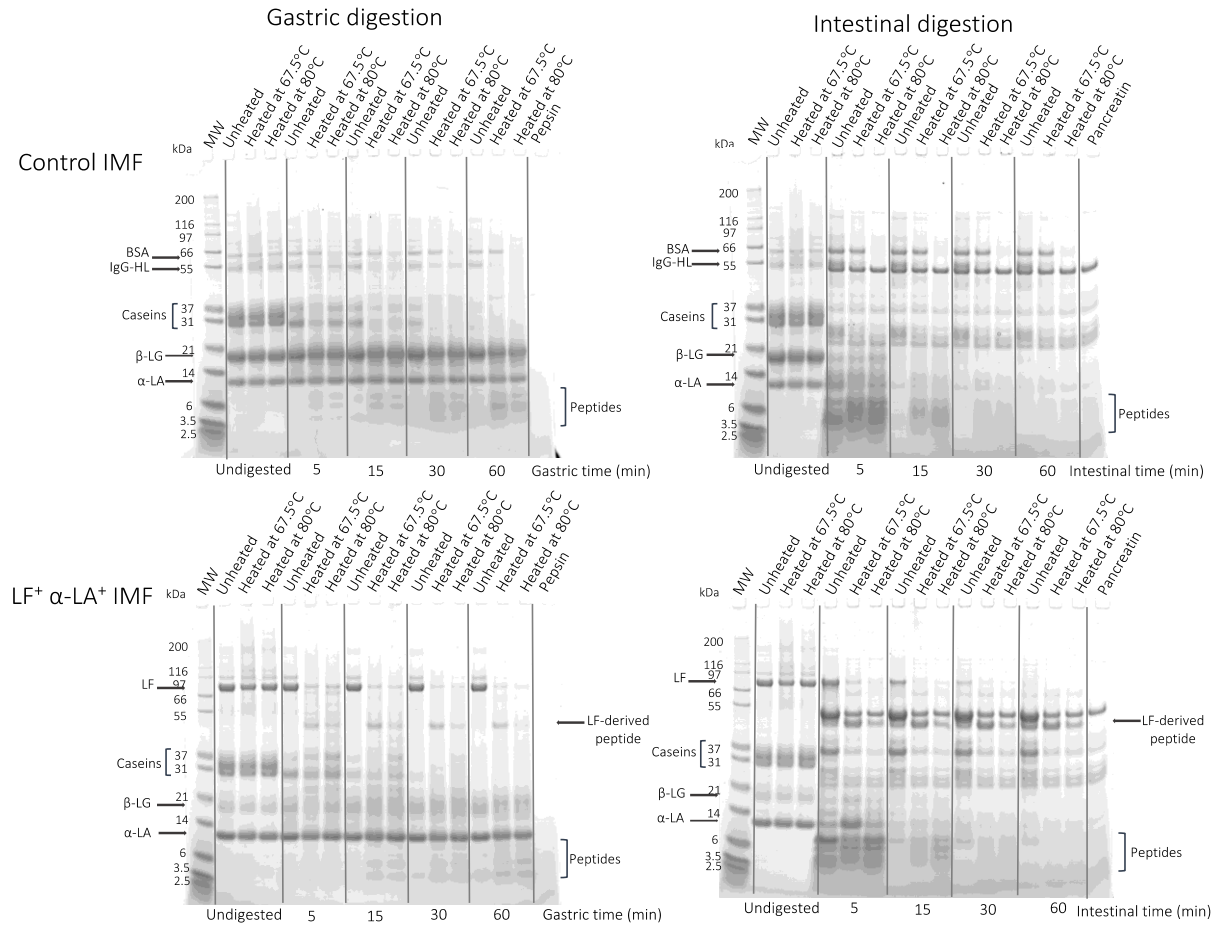
Figure 43. Electrophoretic patterns of the IMFs processed at 1.3% proteins during the *in vitro* static gastric and intestinal digestions

MW: Molecular weight marker; α-LA: α-lactalbumin; β-LG: β-lactoglobulin; IgG-HL: high chain of IgG; BSA: bovine serum albumin; LF: lactoferrin.

MW was deposited as protein elution reference, as well as pepsin or pancreatin solutions in the same amounts than those of the gastric or intestinal samples, respectively. 5 μg of proteins per well were deposited for the undigested IMFs and gastric samples and 30 μg of proteins per well were deposited for the intestinal samples. SDS-PAGE analysis was realised once for each *in vitro* digestion experiments (n = 3).
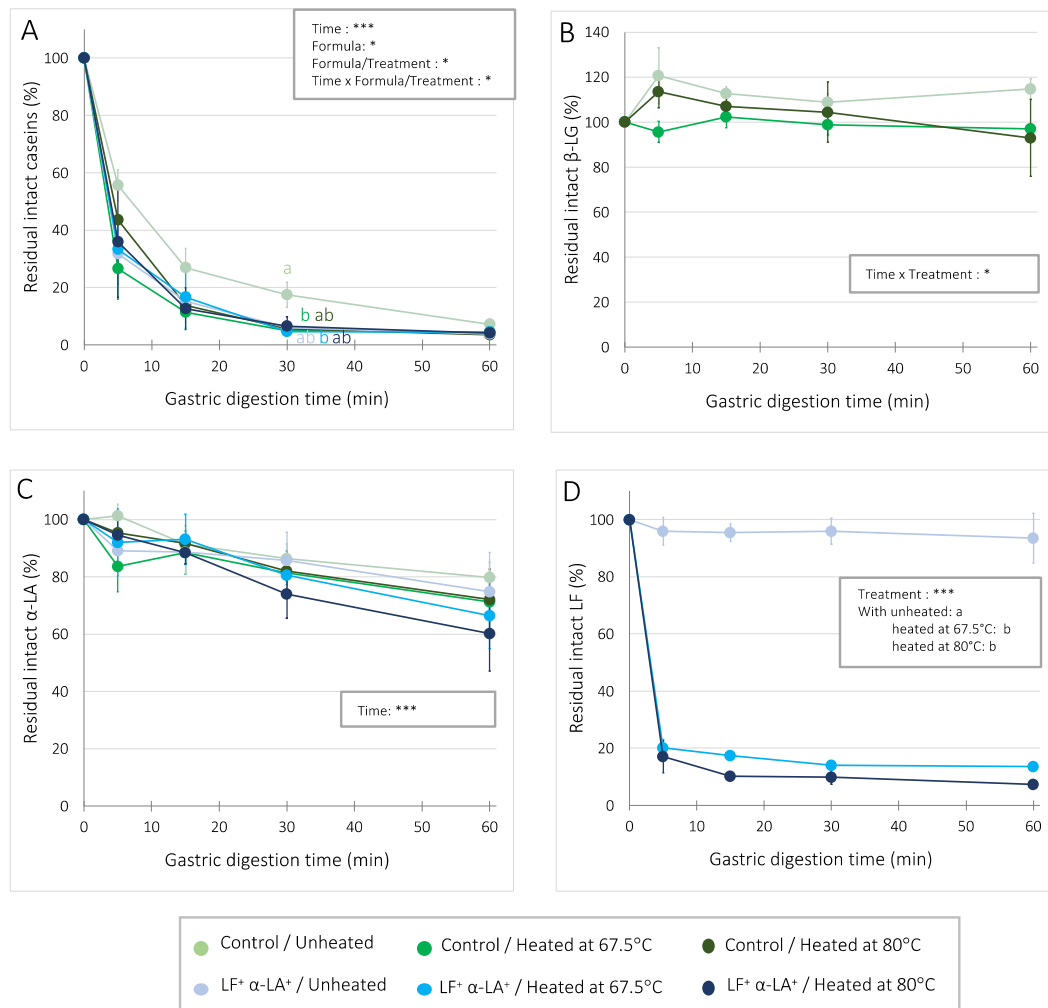
Figure 44. Proportions of residual intact caseins (A), β-lactoglobulin (B), α-lactalbumin (C), and lactoferrin (D) during the *in vitro* static gastric digestion of the IMFs processed at 1.3% proteins

Data are means ± SD (n = 3). Statistically significant factors were referenced with $p < 0.001$ (***), $p < 0.01$ (**), $p < 0.05$ (*) and $p > 0.05$ (NS). Different superscript letters for a given digestion time represent significant difference among treatments nested within formulas ($p < 0.05$). Data from undigested IMFs were not included in the statistical analysis. Data for residual intact caseins were log-transformed to respect residual normality and variance homogeneity (BoxCox transformation).

3.1.3. Degree of hydrolysis and amino acid bioaccessibility

Figure 45 shows the evolution of DH during the *in vitro* intestinal digestion of the IMFs. Regarding the gastric digestion, the hydrolysis was very limited for all IMFs, with a DH of 2 ± 1% at 60 min (data not shown). This low DH value was due to the large peptides formed during gastric digestion of IMFs, as observed at 60 min of gastric digestion by SDS-PAGE analysis (Figure 44.A). For all IMFs, DH increased sharply in the first 5 min of the intestinal digestion but to a different extent depending on the IMF, with a DH reaching 14 ± 2% (heated control IMFs), 24 ± 2% (unheated IMFs) or 44 ± 1% (heated LF⁺ α-LA⁺ IMFs). From 5 min to 60 min of intestinal digestion, the DH increase slowed down, but again with a

kinetics depending on the IMF. The DH increase was only of 1.5-times for the unheated IMFs and the heated LF$^+$ α-LA$^+$ IMFs, and of more than 2-times for the heated control IMFs.

Within the control IMFs, the only significant difference between the unheated and heated IMFs were found in the early phase of intestinal digestion (5 min), with a lower DH for the heated control IMFs (14 ± 2%) compared to the unheated control IMF (24 ± 2%). Similar kinetics of proteolysis was observed after 15 min of intestinal digestion for the unheated and heated control IMFs, which reached a final DH of 35 ± 2%, value in accordance with Le Roux et al. (2020), who reported a DH of ~ 40% at 60 min of *in vitro* static intestinal digestion of bovine milk-based IMF.

During the whole intestinal digestion period, DH values were significantly higher for the heated LF$^+$ α-LA$^+$ IMFs compared to all the other IMFs (p < 0.001). The final DH reached 61 ± 1% for the heated LF$^+$ α-LA$^+$ IMFs vs 40 ± 1% for the unheated LF$^+$ α-LA$^+$ IMF, which was a consequence of the greater extent of LF hydrolysis during the gastric digestion for the denatured LF compared to the native LF (Figure 44.D). These final DH were significantly higher than that for the unheated control IMF, which reached a value of 32 ± 1%. The different kinetics of proteolysis among the heated LF$^+$ α-LA$^+$ or control IMFs and unheated IMFs is likely to impact the *in vivo* kinetics of amino acid absorption, which in turn could modulate the postprandial regional metabolism of nitrogen, at least as demonstrated in adult (Deglaire, Fromentin, et al., 2009).
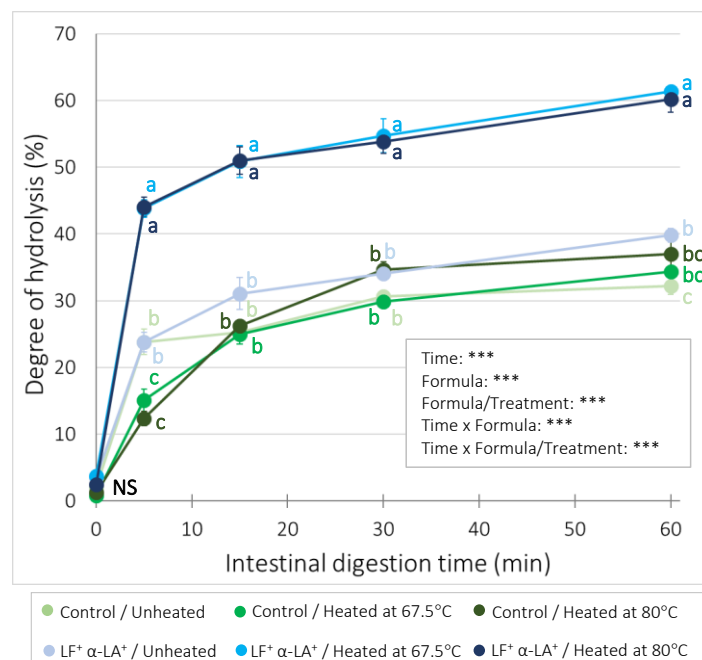

Figure 45. Evolution of the degree of hydrolysis during the *in vitro* static intestinal digestion of the IMFs processed at 1.3% proteins

Data are means ± SD (n = 3), with each measurement performed in triplicate. Statistically significant factors were referenced with $p < 0.001$ (***), $p < 0.01$ (**), $p < 0.05$ (*) and $p > 0.05$ (NS). Different superscript letters for a given digestion time represent significant difference among treatments nested within formulas ($p < 0.05$). Data at time 0 min correspond to those obtained at 60 min of the gastric digestion. Data were square root-transformed to respect residual normality and variance homogeneity (BoxCox transformation).

Figure 46 shows the bioaccessibility of essential and non-essential amino acids at the end of *in vitro* digestion of the unheated and heated control and LF⁺ α-LA⁺ IMFs. At 60 min of intestinal digestion, similar bioaccessibility of α-amino nitrogen (24 ± 2%) was observed among all the IMFs ($p > 0.05$), while the DH varied among IMFs (from 35 to 61%) (Figure 45). This means that most of the peptide bond cleavages resulted in the release of amino acids for the unheated IMFs and the heated control IMFs (DH = 35-40%). In contrast, the heated LF⁺ α-LA⁺ IMFs after digestion also contains a significant amount of small peptides (DH = 61%). The higher proportion of peptides generated for the heated LF⁺ α-LA⁺ IMFs could be due to the products of LF hydrolysis during the gastric digestion, resistant to intestinal digestion (Figure 43).

The bioaccessibility of the essential amino acids was approximatively 3-times higher than that of the non-essential amino acids (36 ± 2% and 11 ± 1%, respectively). These values were much lower than the true amino acid digestibility (superior to 85%) of bovine milk-based IMFs as determined in animal models (Rutherfurd et al., 2006; Sarwar et al., 1989). This can be explained by the lack of brush borders enzymes (exopeptidases) in the present *in vitro* digestion model, enzymes which drive the final stages of hydrolysis into amino acids (Picariello et al., 2015; Tobey et al., 1985). The bioaccessibility of lysine, phenylalanine, tyrosine, leucine (59 ± 3%; 57 ± 3%; 59 ± 5%; 40 ± 2%, respectively) and arginine (81 ± 10%) were higher than those of the other amino acids at the end of *in vitro* digestion for all IMFs (Figure 46.B). These results agreed with the cleavage specificities for pepsin (phenylalanine, tyrosine, leucine and tryptophan residues) (Inouye & Fruton, 1967) and trypsin (arginine and lysine residues) (Keil, 1992) endopeptidases, in addition to the action of the carboxypeptidase contained in pancreatin (exopeptidase). For all IMFs, a very low amount of proline was released at the end of intestinal digestion, mostly due to the absence of aminopeptidases in the present *in vitro* digestion model (Huërou-Luron, 2002).

	Bioaccessibility (%)						Effect of	
Amino acid category	Control Unheated	Control Heated at 67.5°C	Control Heated at 80°C	LF⁺ α-LA⁺ Unheated	LF⁺ α-LA⁺ Heated at 67.5°C	LF⁺ α-LA⁺ Heated at 80°C	Formula	Formula/Treatment
Essential	34.1 ± 1.5^{ab}	36.2 ± 3.1^{ab}	35.5 ± 1.2^{ab}	32.6 ± 0.9^{b}	37.7 ± 2.0^{a}	36.9 ± 0.8^{ab}	NS	*
Non-essential	10.2 ± 0.7	10.8 ± 2.0	10.3 ± 0.6	11.0 ± 1.8	13.2 ± 0.8	12.6 ± 0.6	**	NS
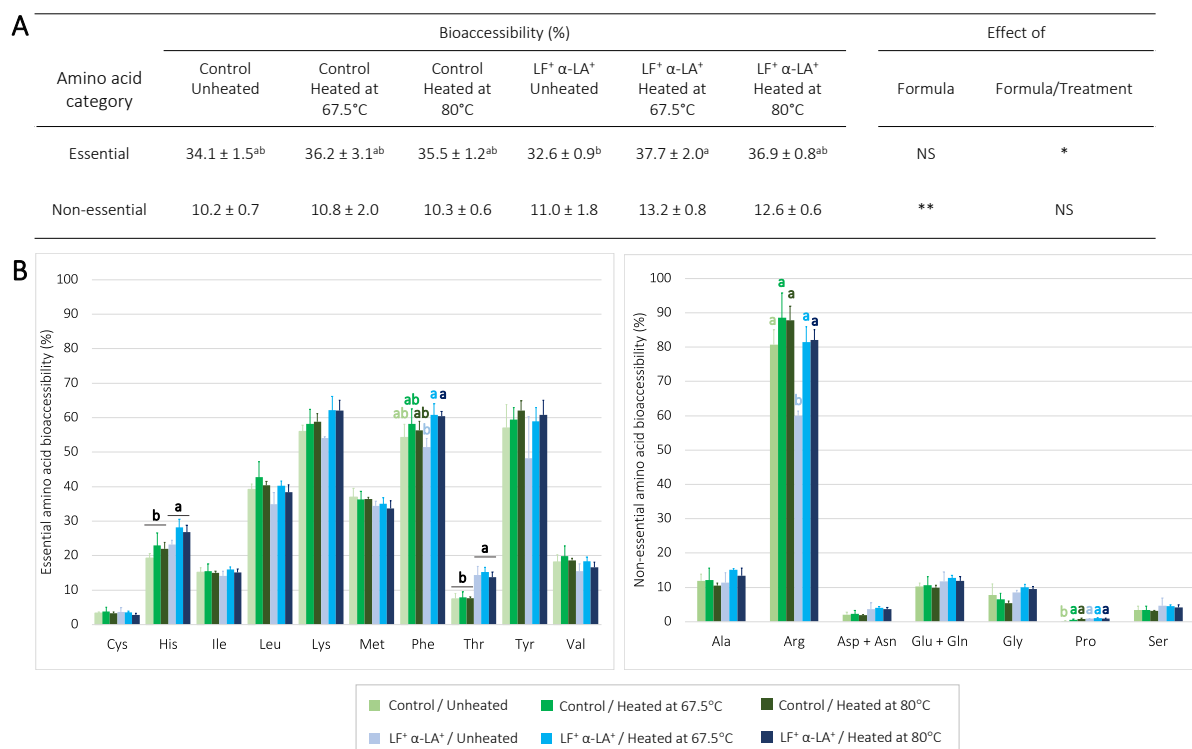
Figure 46. Bioaccessibility of total (A) and individual (B) essential and non-essential amino acids released at the end of the *in vitro* static intestinal digestion of the IMFs processed at 1.3% proteins.

(A) The (non-) essential amino acid bioaccessibility was expressed as the ratio of the sum of free (non-)essential amino acid contents in digesta (g/kg of IMF) related to the sum of total (non-) essential amino acid contents within IMFs (g/kg of IMF). The essential amino acids were cysteine, histidine, isoleucine, leucine, lysine, methionine, phenylalanine, threonine, tyrosine and valine. The non-essential amino acids were alanine, arginine, aspartic acid, asparagine, glutamic acid, glutamine, glycine, proline and serine. Statistically significant factors were referenced with p < 0.001 (***), p < 0.01 (**), p < 0.05 (*) and p > 0.05 (NS). (B) Data represent means ± SD (n = 3). Different superscript letters for a given amino acid represent significant difference (p < 0.05).

3.2. Infant milk formulas processed at 5.5% proteins

3.2.1. Particle size distribution

Figure 47 shows the particle size distributions of the unheated and heated IMFs before and during digestion, which were near similar to those observed for the corresponding IMFs processed at 1.3% proteins (Figure 42).

For both types of IMFs, the particle size distributions of the undigested IMFs (Figure 47) were characterised by a main peak at 0.13 µm assigned to the casein micelles, and a second peak in the region of 10-100 µm, present only in the heated IMFs. The latter peak, related to high-molecular weight complexes, were more present in IMFs treated at higher temperature. The large entities were more abundant in the heated IMFs processed at 5.5% (Figure 47) than at 1.3% proteins (Figure 42).

After 60 min of gastric digestion, the particle size of the digesta was increased for all IMFs compared to the corresponding undigested IMFs, in a similar manner to that observed for the IMFs processed at 1.3% proteins (Figure 42). The particle size for the unheated control IMF (mode of 82.4 ± 0.7 µm) was 5-times higher than that for the heated control IMFs (mode of 16.0 ± 2.8 µm). On the contrary, the particle size for the unheated LF$^+$ α-LA$^+$ IMF (mode of 1.2 ± 0.4 µm) was 15-times lower than that for the heated LF$^+$ α-LA$^+$ IMFs (mode of 17.8 ± 5.7 µm). All the heated IMFs presented a near similar particle size distribution at the end of the gastric digestion, independently of the heating temperature (67.5°C or 80°C) or of the whey protein profile of IMFs (control or LF$^+$ α-LA$^+$ IMFs).

After 60 min of intestinal digestion, the particle size distributions for all IMFs were alike and bimodal. The wide peak between 1 and 1000 µm was assigned to the pancreatin contained in the intestinal digesta. The global decrease of particle sizes (with a mode close to 0.1 µm) compared to those at the end of gastric digestion was due to protein hydrolysis by intestinal enzymes and/or to residual protein structures within undigested IMFs.

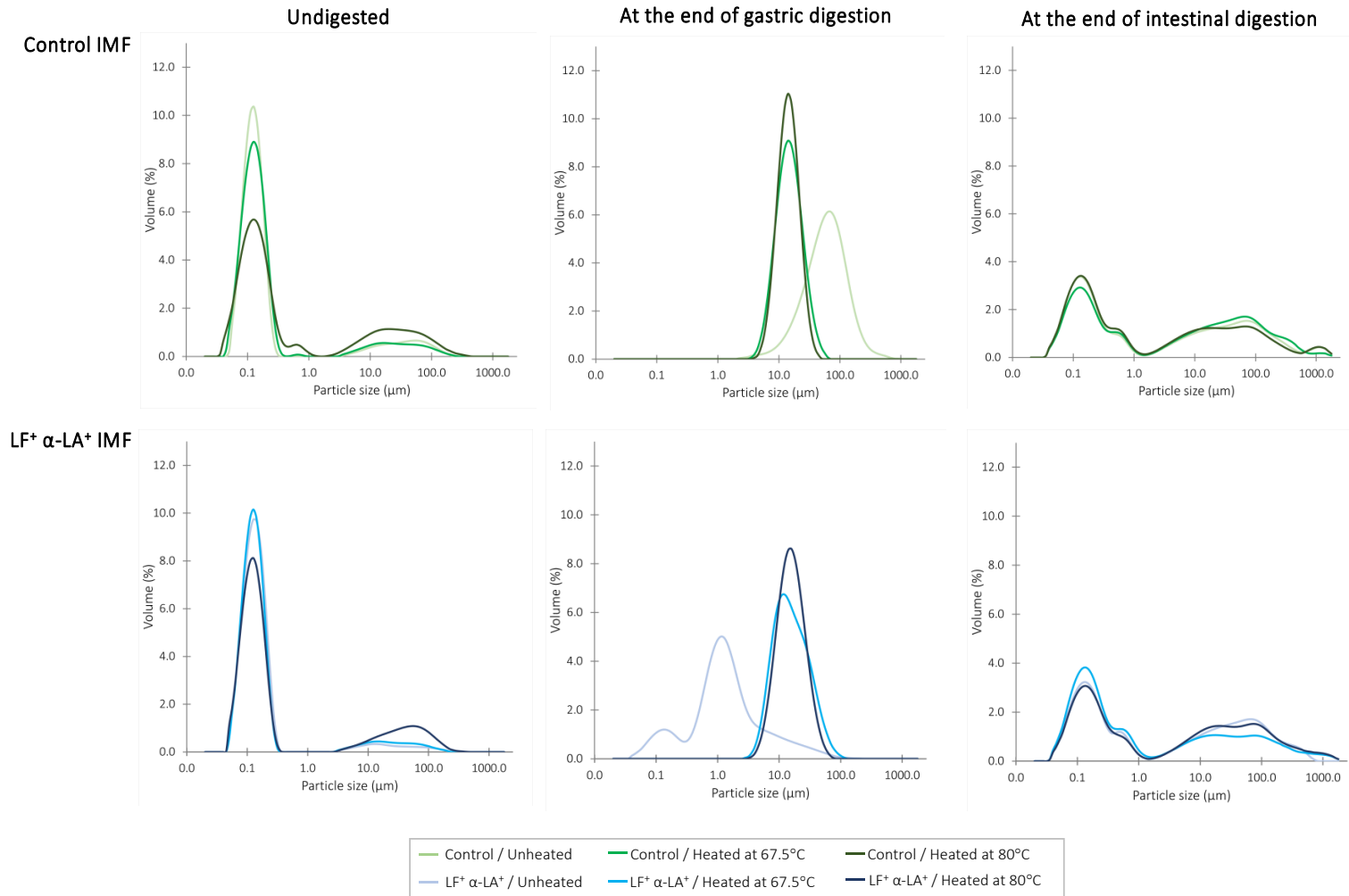Figure 47. Particle size distributions of the IMFs processed at 5.5% proteins before digestion and at the end of the *in vitro* static gastric and intestinal digestions

The pH of the IMFs was 6.8 before digestion, 5.3 at the end of the gastric digestion and 6.6 at the end of the intestinal digestion. Data represent means of three independent digestion experiments (n=3), with each measurement performed in triplicate.

3.2.2. Protein hydrolysis kinetics

Proteolysis kinetics of caseins, α-LA, β-LG and LF, as quantified from SDS-PAGE analysis under reducing conditions (Figure 48), are presented in Figure 49. During the gastrointestinal digestion, BSA resisted to enzymatic hydrolysis for the unheated and heated control IMF at 67.5°C, while it was progressively hydrolysed during the gastric digestion of the heated control IMF at 80°C until total band disappearance at 60 min of gastric digestion, as observed for the corresponding IMFs processed at 1.3% proteins (Figure 43).

During the gastric digestion, the kinetics of casein hydrolysis were significantly slower for the control IMFs than for the LF$^+$ α-LA$^+$ IMFs (Figure 49.A), which was less evident for the IMFs processed at 1.3% proteins (Figure 44.A). Nevertheless, for the IMFs processed at 1.3% and 5.5% proteins, the caseins tended to be more resistant to pepsin hydrolysis for the unheated control IMFs. Concomitantly to the casein hydrolysis, bands ranging from 3.5 to 6 kDa, assigned to casein-derived products amongst others, appeared less intense for the unheated IMFs compared to the heated IMFs, as observed for the IMFs processed at 1.3% of proteins (Figure 44.A).

The SDS-PAGE analysis for the control and LF$^+$ α-LA$^+$ IMFs (Figure 48) showed a resistance to pepsin hydrolysis for β-LG and α-LA as compared to caseins. A significant heat treatment effect was observed for β-LG hydrolysis in the control IMFs, with a slight level of hydrolysis evidenced in the heated IMFs only (88 ± 14% of residual intact β-LG at the end of the gastric phase) but not for the corresponding unheated IMF. In contrast, the kinetics of β-LG proteolysis were similar for the unheated and heated control IMFs processed at 1.3% proteins (Figure 44.B). The higher susceptibility of β-LG to proteolysis for IMFs processed at 5.5% than at 1.3% proteins was not explained by the difference of extent of β-LG denaturation. Indeed, the extent of β-LG denaturation was higher for IMFs processed at 1.3% proteins (59 ± 5% at 67.5°C or 69 ± 0% at 80°C) than at 5.5% proteins (53 ± 1% at 67.5°C or 57 ± 1% at 80°C) while the β-LG proteolysis was slowed down for the IMFs processed at 1.3% than at 5.5% proteins. As discussed previously (Chapter 5 - section 3.2.2.2), the denatured whey proteins are preferentially bound on the casein micelle surface in the IMFs processed at 5.5% proteins. Particularly, the fixation of β-LG onto the casein micelle surface may have favour its hydrolysis because the proteins are denatured and exposed to the solvent whereas in the soluble aggregates they are covered at least partially by some k-casein released from the casein micelle during IMF heating. In addition, the fixation of denatured β-LG on casein micelle surface had probably facilitated the action of pepsin due to the concentration of β-LG in a limited area surface, in contrary to denatured β-LG forming k-caseins/whey protein aggregates, dispersed on the soluble phase.

The kinetics of hydrolysis for α-LA (Figure 49.C) showed the progressive decrease of residual intact α-LA for all IMFs, reaching 72 ± 14% of residual intact α-LA at 60 min of gastric digestion. Formula effect was

observed only at 5 min of gastric digestion, with higher residual intact α-LA for the control IMFs (106 ± 11%) than for the LF[+] α-LA[+] IMFs (91 ± 4%) (Figure 49.C).This could be attributed to the values higher than 100% determined for the control IMF heated at 80°C. The kinetics of α-LA hydrolysis were near similar to those for the corresponding IMFs processed at 1.3% proteins, except for the heated control IMF at 80°C, for which the pepsin resistance of α-LA seemed to be higher for the IMF processed at 5.5% than at 1.3% proteins during the entire gastric digestion.

As observed previously, the hydrolysis of LF was drastically enhanced for the denatured form (heated LF[+] α-LA[+] IMFs) since the very first minutes of digestion, with 44 ± 2% and 25 ± 4% of residual intact LF remaining at 5 min of gastric digestion for the IMFs heated at 67.5°C and 80°C, respectively (Figure 49.D). In contrast to the IMFs processed at 1.3% proteins, the kinetics of LF hydrolysis were significantly slower at 67.5°C than at 80°C during the whole gastric digestion. This could be explained by the lower denaturation extent of LF at 67.5°C (82 ± 1%) than at 80°C (95 ± 1%) for the LF[+] α-LA[+] IMFs processed at 5.5% proteins (Figure 39), while the extent of LF denaturation was akin at both heating temperatures for the IMFs processed at 1.3% proteins (97 ± 1%) (Figure 35). Nevertheless, LF at different extent of denaturation (33 or 75%) did not result in different level of gastric hydrolysis for human milk processed with different pasteurisation techniques, using a dynamic digestion model (Nebbia et al., 2020).

For the heated LF[+] α-LA[+] IMFs, the gastric hydrolysis of LF generated the C-terminal fragment of the protein, resistant to enzymatic hydrolysis during the entire gastrointestinal digestion such as previously observed (Figure 48 and Figure 43).
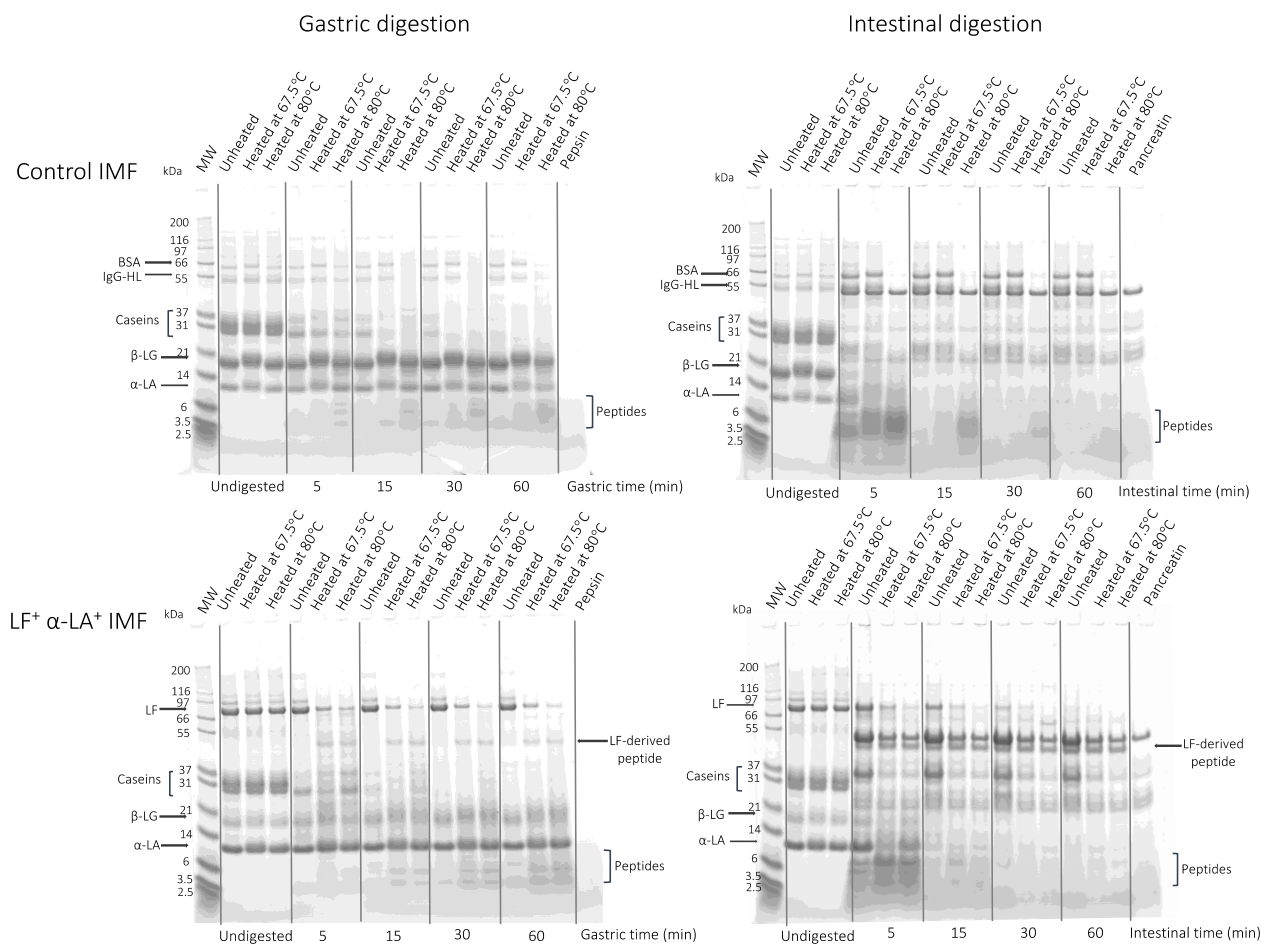
Figure 48. Electrophoretic patterns of the IMFs processed at 5.5% proteins during the *in vitro* static gastric and intestinal digestions

MW: Molecular weight marker; α-LA: α-lactalbumin; β-LG: β-lactoglobulin; IgG-HL: high chain of IgG; BSA: bovine serum albumin; LF: lactoferrin.

MW was loaded as protein elution reference, as well as pepsin or pancreatin solutions in the same amounts than those of the gastric or intestinal samples, respectively. 5 μg of proteins per well were deposited for the undigested IMFs and gastric samples and 30 μg of proteins per well were deposited for the intestinal samples. SDS-PAGE analysis was realized once for each *in vitro* digestion experiments (n=3).
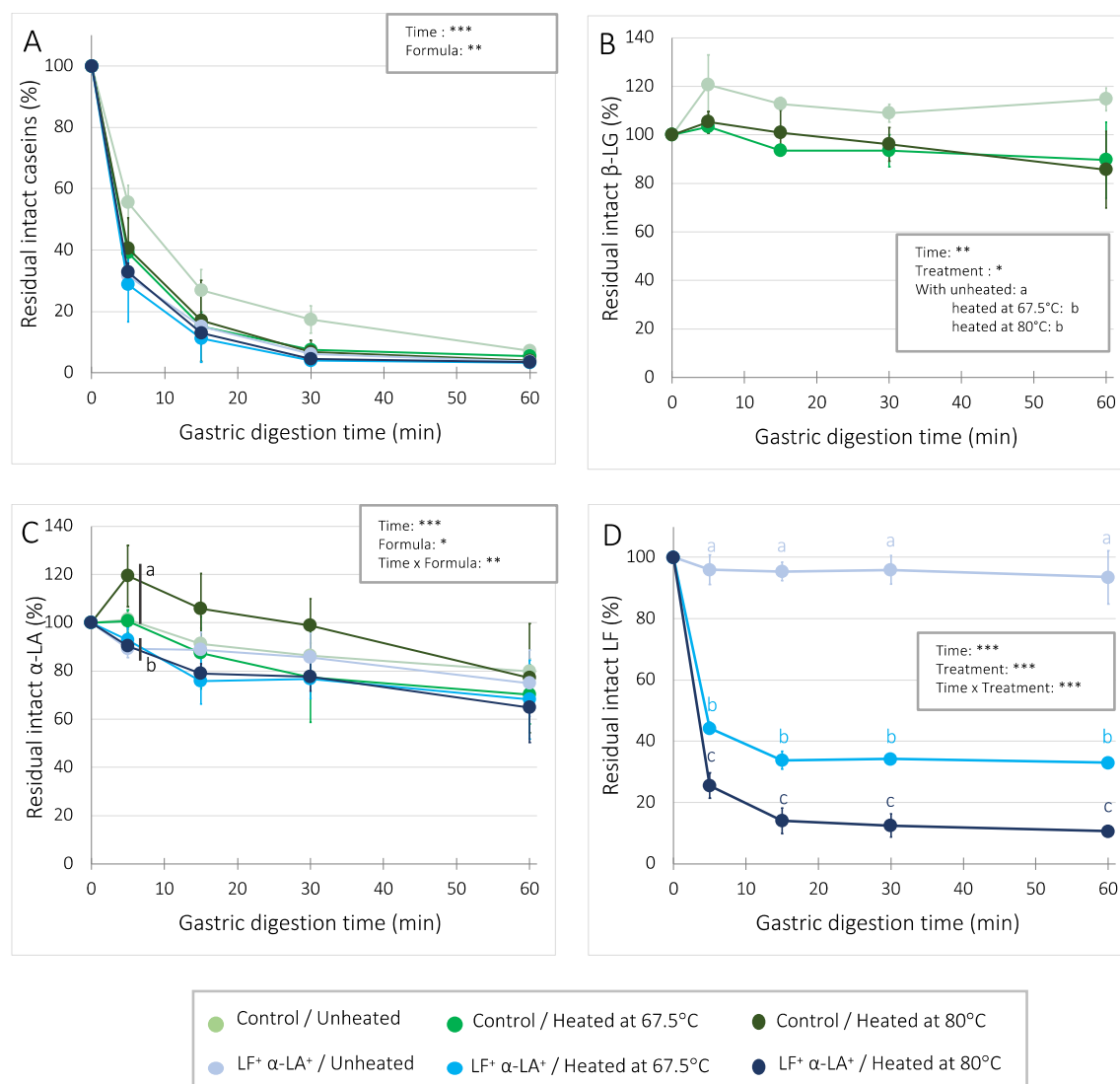
Figure 49. Proportions of residual intact caseins (A), β-lactoglobulin (B), α-lactalbumin (C), and lactoferrin (D) during the *in vitro* static gastric digestion of the IMFs processed at 5.5% proteins

Data are means ± SD (n = 3). Statistically significant factors were referenced with p < 0.001 (***), p < 0.01 (**), p < 0.05 (*) and p > 0.05 (NS). Different superscript letters for a given digestion time represent significant difference among treatments nested within formulas (p < 0.05) and asterisks represent significant differences among formulas for a given digestion time. Data from undigested IMFs were not included in the statistical analysis. Data for residual intact caseins were log-transformed and data for residual intact α-LA were transformed square-transformed to respect residual normality and variance homogeneity (BoxCox transformation).

3.2.3. Degree of hydrolysis and amino acid bioaccessibility

Figure 50 shows the evolution of DH during the *in vitro* intestinal digestion of the IMFs. For all IMFs, DH increased sharply in the first 5 min of the intestinal digestion but to a different extent depending solely on the heat treatment, with a DH reaching 24 ± 0% for the unheated IMFs and 41 ± 1% for the heated IMFs. From 5 min to 60 min of intestinal digestion, the DH values of the unheated IMFs were lower than those for the heated IMFs, with DH at the end of intestinal digestion of 32 ± 1%, 40 ± 1% and 56 ± 1% for the unheated control IMF, the unheated LF+ α-LA+ IMF and the heated IMFs, respectively. While a

similar evolution of DH was observed for the unheated LF⁺ α-LA⁺ IMFs and the control IMFs processed at 1.3% proteins, this was not true for the heated control IMFs, which presented a higher DH value during the entire intestinal digestion for the IMFs processed at 5.5% than at 1.3% proteins (Figure 50 and Figure 45). This could be linked to the higher enzyme susceptibility of β-LG, as observed in the gastric phase.
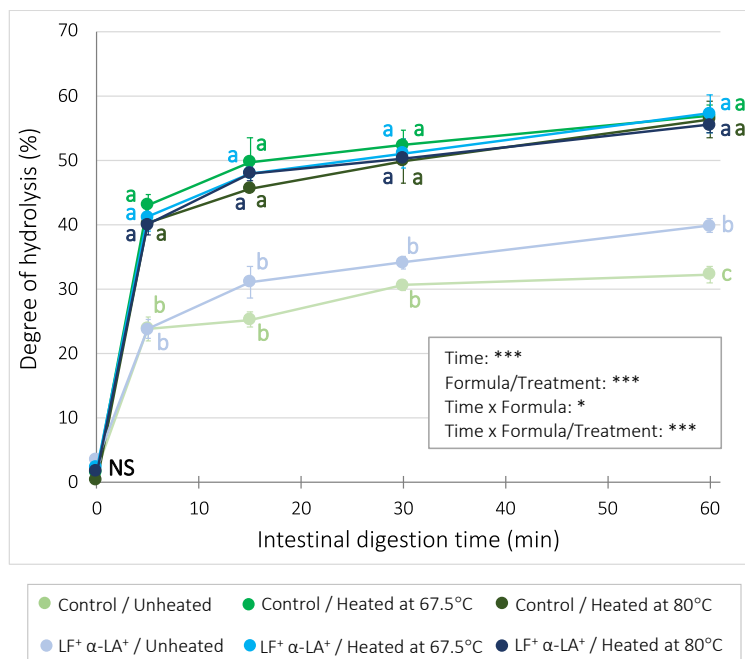
Figure 50. Evolution of the degree of hydrolysis during the *in vitro* static intestinal digestion of the IMFs processed at 5.5% proteins

Data are means ± SD (n = 3), with each measurement performed in triplicate. Statistically significant factors were referenced with $p < 0.001$ (***), $p < 0.01$ (**), $p < 0.05$ (*) and $p > 0.05$ (NS). Different superscript letters for a given digestion time represent significant difference among treatments nested within formulas ($p < 0.05$). Data at time 0 min correspond to those obtained at 60 min of the gastric digestion.

Figure 51 shows the bioaccessibility of essential and non-essential amino acids at the end of *in vitro* digestion of the unheated and heated control and LF⁺ α-LA⁺ IMFs. At 60 min of intestinal digestion, similar bioaccessibility of α-amino nitrogen (23 ± 1%) was observed among all the IMFs ($p > 0.05$), while the DH varied among IMFs (from 32 to 57%) (Figure 50). This means that most of the peptide bond cleavages resulted in the release of amino acids for the unheated IMFs (DH = 32-40%). In contrast, the heated IMFs after digestion contained a greater amount of small peptides (DH = 56%). Similar conclusions were made for the IMFs processed at 1.3% proteins, except for the heated control IMFs, for which the products of hydrolysis were mainly free amino acids (Chapter 6 - section 3.1.3).

The bioaccessibility of the essential and non-essential amino acids were relatively close to those determined for IMFs processed at 1.3% proteins (Figure 46). As observed previously, the bioaccessibility of lysine, phenylalanine, tyrosine, leucine (56 ± 3%; 57 ± 3%; 60 ± 6%; 38 ± 3%, respectively) and arginine

(79 ± 10%) were higher than that for the other amino acids at the end of *in vitro* digestion for all IMFs, due to the cleavage specificities for pepsin (phenylalanine, tyrosine, leucine and tryptophan residues) (Inouye & Fruton, 1967) and trypsin (arginine and lysine residues) (Keil, 1992) endopeptidases.
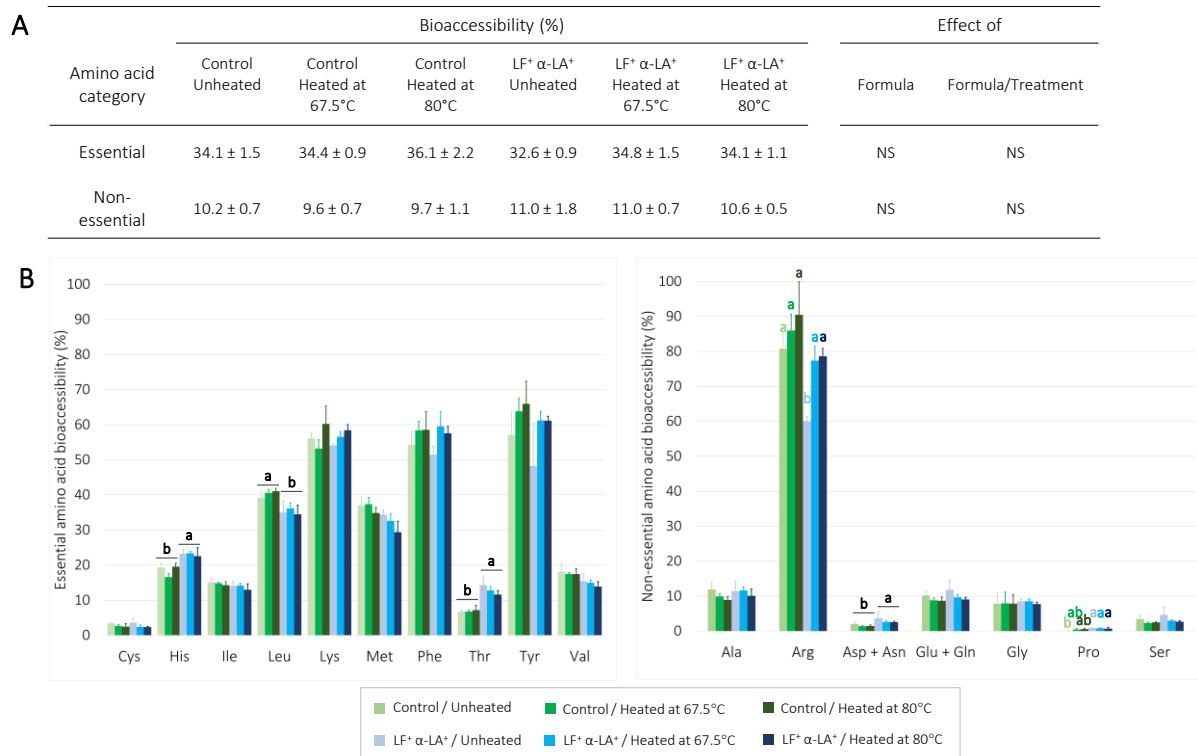
Figure 51. Bioaccessibility of total (A) and individual (B) essential and non-essential amino acids released at the end of the *in vitro* static intestinal digestion of the IMFs processed at 5.5% proteins.

(A) The (non-) essential amino acid bioaccessibility was expressed as the ratio of the sum of free (non-)essential amino acid contents in digesta (g/kg of IMF) related to the sum of total (non-) essential amino acid contents within IMFs (g/kg of IMF). The essential amino acids were cysteine, histidine, isoleucine, leucine, lysine, methionine, phenylalanine, threonine, tyrosine and valine. The non-essential amino acids were alanine, arginine, aspartic acid, asparagine, glutamic acid, glutamine, glycine, proline and serine. Statistically significant factors were referenced with $p < 0.001$ (***), $p < 0.01$ (**), $p < 0.05$ (*) and $p > 0.05$ (NS). (B) Data represent means ± SD (n = 3). Different superscript letters for a given amino acid represent significant difference ($p < 0.05$).

4. Conclusion

The present study underlined the impacts of protein structures within IMFs, resulting from variation of total solid and whey protein profile of IMFs, as well as the heating conditions, on the protein digestion kinetics under simulated *in vitro* static term infant digestion.

Gastric aggregation of caseins was strongly influenced by the casein micelle structures within IMFs. The casein micelles within the unheated control IMF (i.e. native micelles) led to the formation of larger curd particles (~ 100 μm) compared to those contained in the heated IMFs (i.e. micelles covered by denatured whey proteins) (~ 10 μm) or in the unheated LF$^+$ α-LA$^+$ IMF (i.e. dissociated micelles) (~ 1 μm) for both processing protein concentration. As a consequence, caseins in the larger curd particles were found to be less susceptible to pepsin hydrolysis due to the limited access to cleavage sites.

During the gastric digestion, the resistance of α-LA and β-LG to pepsin hydrolysis was unchanged by the heating of IMFs for the IMFs processed at 1.3% proteins, while β-LG was less resistant to hydrolysis for the heated IMFs processed at 5.5% proteins, which may be linked to a preferential fixation onto the casein micelle surface rather than the formation of soluble aggregates. On the contrary, the heating of IMFs drastically decreased the resistance of LF to pepsin hydrolysis compared to the compact globular native form and this appeared to be dependent of the LF denaturation extent, as shown for the heated LF$^+$ α-LA$^+$ IMFs processed at 5.5% proteins. During the intestinal digestion, the kinetics of hydrolysis were enhanced for the IMFs either processed at 1.3% or 5.5% proteins and containing denatured LF, as well as for the heated control IMFs processed at 5.5% proteins.

The hydrolysis of denatured LF could be balanced by some remaining bioactive properties (iron-binding properties, antimicrobial and antifungal activities) of generated peptides. However, other functionalities of native LF are likely to be altered (e.g. anti-inflammatory activity), which remains to be explored *in vivo*. Meanwhile, alternative treatments to intense heating, such as low-heat or non-thermal treatments, could be considered to guarantee the nutritional benefits of the IMF supplemented with LF. Finally, the dynamic aspect of the digestion could modulate the present results and this aspect will be considered by using an *in vitro* dynamic digestion model in the next chapter.

Main messages

- Gastric protein destabilisation depends on the protein structures within IMFs

- The denatured form of LF is susceptible to pepsin hydrolysis, its susceptibility increasing with the extent of LF denaturation

- LF-derived peptides are resistant to gastrointestinal digestion

- Intestinal hydrolysis is increased for IMFs containing denatured LF, independently to the total solid of IMFs, due to the gastric hydrolysis of LF in its denatured form

- Intestinal hydrolysis increases with increasing total solid of IMFs for IMFs containing β-LG, likely due to its higher susceptibility to enzymatic hydrolysis when fixed on the surface of casein micelles than as soluble aggregates

Chapter 7: The protein structure impacts the proteolysis kinetics during digestion of model infant milk formulas – an *in vitro* dynamic study

The results of this chapter are in preparation for submission to Food Chemistry journal. For this chapter, only IMFs processed at 1.3% proteins were studied.

1. Abstract

As previously demonstrated, the protein behaviour during *in vitro* static digestion was function of the protein structure within IMFs. The present study aims to complete our previous investigations by taking into account some more physiological digestion parameters such as continuous pH monitoring, fluid secretion and compartment emptying. Model IMFs at 1.3% proteins, with a bovine (control IMF) or a human-like (LF$^+$ α-LA$^+$ IMF) whey protein profile, were unheated or heated at 80°C to reach 65% of denaturation, resulting in four protein structures. IMFs were submitted to *in vitro* dynamic digestion simulating infant conditions. During digestion, laser light scattering, and confocal scanning laser microscopy were performed to analyse IMF destabilisation. The kinetics of proteolysis were monitored by SDS-PAGE (residual intact protein), OPA assay (degree of hydrolysis), cation exchange chromatography (amino acids) and tandem mass spectrometry (peptides). I*n vitro* digestibility was determined at the end of intestinal digestion using the Kjeldhal method.

During gastric digestion, the protein destabilisation varied with the protein structures within IMFs. High-size protein particles were formed after 40 min for the unheated control IMF containing native casein micelles, while protein destabilisation occurred after 80 min for the heated IMFs and after 120 min for the unheated LF$^+$ α-LA$^+$ IMF containing LF-binding casein micelles. The casein hydrolysis during the gastric digestion was not significantly different among IMFs at the early and late gastric digestion times (p > 0.05). However, at 80 min, it tended to be lower for the unheated than for the heated control IMF (p-value = 0.0503) and, at 120 min, it was significantly higher for the unheated than for the heated LF$^+$ α-LA$^+$ IMF. α-LA and β-LG in their native and denatured forms were resistant to pepsin hydrolysis, while the heat-induced denaturation of LF significantly increased its susceptibility to hydrolysis. During the whole intestinal digestion, the degree of protein hydrolysis did not significantly differ, except at 120 min where it was lower for the unheated control IMF containing native casein micelles.

Most identified peptides (6 to 50 amino acid residues) released during digestion originated from β-casein (61%). The peptide mapping onto the parent proteins showed a different digestion pattern depending on the protein structures within IMFs. During intestinal digestion, the bioactive peptides were more numerous for the LF$^+$ α-LA$^+$ IMFs than for the control IMFs, and more resistant for the unheated than for the heated LF$^+$ α-LA$^+$ IMF. Further physiological studies should be conducted to investigate the impact of the differential release of bioactive peptides on infant health.

2. Context and objectives

As discussed in chapter 6, the proteolysis kinetics during *in vitro* gastrointestinal digestion using a static model was affected by the protein structures within IMFs, obtained by varying the protein profile of IMFs and the heating conditions (i.e. total solid of IMFs and heating temperatures). The static model is a simple technique to investigate *in vitro* protein digestion, however it does not simulate the dynamic physiological conditions of the human gastrointestinal digestion such as the continuous pH monitoring, the digestive fluid secretion and the gastric and intestinal emptying, in contrary to the dynamic digestion model.

The aim of the present chapter was to further investigate the protein digestion kinetics of the protein structures within IMFs using an *in vitro* dynamic digestion model, with a focus on the kinetics of peptide release during gastrointestinal digestion. This study was conducted on the unheated and heated control and $LF^+\alpha\text{-}LA^+$ IMFs processed at 1.3% proteins. Heat treatment was performed at 80°C and the heating times was defined in order to reach an extent of whey protein denaturation of 65% in both IMFs. Digestion was simulated using an *in vitro* dynamic model at the infant stage, where digestive enzymes, pH and digestive compartment emptying were continuously controlled. During the gastric digestion, IMF destabilisation was monitored by laser light scattering and confocal scanning laser microscopy. The kinetics of protein hydrolysis was followed using SDS-PAGE under reducing conditions (residual intact proteins), OPA assay (degree of hydrolysis), cation exchange chromatography (amino acids) and tandem mass spectrometry (peptides). In addition, *in vitro* digestibility was determined using the Kjeldhal method.

3. Results and discussion

3.1. Structural changes during *in vitro* gastric digestion

Figure 52 shows the particle size distributions (Figure 52.A) and the microstructure (Figure 52.B) of the unheated and heated control and LF[+] α-LA[+] IMFs before and during the *in vitro* gastric digestion.

3.1.1. Prior to digestion

Before digestion, the particle size distributions were akin among IMFs, all presenting a main peak at an average mode of 0.15 ± 0.01 µm, assigned to the casein micelles. A wide peak of small intensity was observed in the region of 10-100 µm, probably corresponding to heat-induced protein entities formed by heating and/or to insoluble particles resulting from IMF preparation. Confocal microscopy images of all undigested IMFs showed homogeneous and small particles of protein particles, with similar protein particle morphology among IMFs at this scale of observation (Figure 52.B).

3.1.2. After 40 min of gastric digestion

After 40 min of gastric digestion (gastric pH at 6.2), the protein particle size only changed for the unheated control IMF with large aggregated protein structures (Figure 52.B) having a 408 ± 66 µm modal diameter (Figure 52.A). These protein particles were visible to the naked eye in the gastric compartment as soon as ~ 20 min of gastric digestion (~ pH 6.5) (Supplementary Figure 4). This increase of protein size must be the result of the pepsin-induced hydrolysis of κ-casein, inducing the aggregation of para-casein micelles (Tam & Whitaker, 1972), as observed by Wang et al. (2018) and Ye et al. (2019) for bovine milk at gastric pH ~ 6.3 and by Huppertz & Lambers (2020) for IMFs at gastric pH 6.0.

3.1.3. After 80 min of gastric digestion

After 80 min of gastric digestion (pH at 5.6), the protein particle size for the unheated control and LF[+] α-LA[+] IMFs were almost unchanged compared to those at 40 min of gastric digestion, with large protein aggregates for the unheated control IMF (mode of 526 ± 51 µm) and small protein particles for the unheated LF[+] α-LA[+] IMF (mode of 0.14 µm), as shown in Figure 52.B. In contrast, the protein particle size for the heated IMFs greatly increased, with an increase of x 98 for the heated control IMF (mode of 13.7 ± 1.2 µm) and of x 165 for the heated LF[+] α-LA[+] IMF (mode of 21.5 ± 1.0 µm). The confocal microscopy analysis showed a dense and compact protein network for the heated control IMF while linear strands of proteins were observed for the heated LF[+] α-LA[+] IMF (Figure 52.B). This increase of protein particle size for the heated IMFs was probably more the result of acid casein coagulation than of enzymatic coagulation. After heat treatment, denatured whey proteins formed soluble aggregates and/or fixed the casein micelle surface, mainly *via* k-caseins (Chapter 5 – section 3.1.2.2), decreasing k-casein accessibility to pepsin due to steric hindrance, as observed for the rennet-induced gelation of

heated milk (Ferron-Baumy et al., 1991). Casein micelle coating by denatured whey proteins increased the pH at which proteins coagulate from 4.9 (i.e. pI of native casein micelles) to 5.6 (Lucey et al., 1997; Vasbinder, Van Mil, Bot, de Kruif, 2001). The present protein particle profile supported what was previously obtained at the end of the gastric static digestion of the same IMFs, for which the pH was initially fixed at 5.3 (Figure 42).

3.1.4. After 120 min of gastric pH

After 120 min of gastric digestion, the protein particle size for the unheated control IMF was too low to be quantified by laser light scattering or observed by confocal microscopy. The protein particle size for the heated IMFs was slightly higher than those at 80 min of gastric digestion, with mode of 21.6 ± 1.1 μm or 32.4 ± 3.0 μm for the heated control or LF$^+$ α-LA$^+$ IMF, respectively. The protein particle size for the unheated LF$^+$ α-LA$^+$ IMF (mode of 12.9 ± 0.9 μm) greatly increased compared to that at 80 min of gastric digestion and get closer to that for the heated IMFs. For all IMFs (except the unheated control IMF), linear strands of proteins were observed (Figure 52.B).

The addition of LF to IMFs seemed to hinder pepsin action on k-casein, probably due to the LF fixation on casein micelle surface (Anema & de Kruif, 2013), as previously discussed in Chapter 5 – section 3.1.2.3. This could explain the low particle size observed during the first times of gastric digestion. At lower gastric pH (4.9), the increase of protein particle size for IMF containing native LF was explained by the decrease of casein micelle net charge and so the reduction of the electrostatic interactions between LF and the casein micelles, leading to casein coagulation (Anema, 2019).
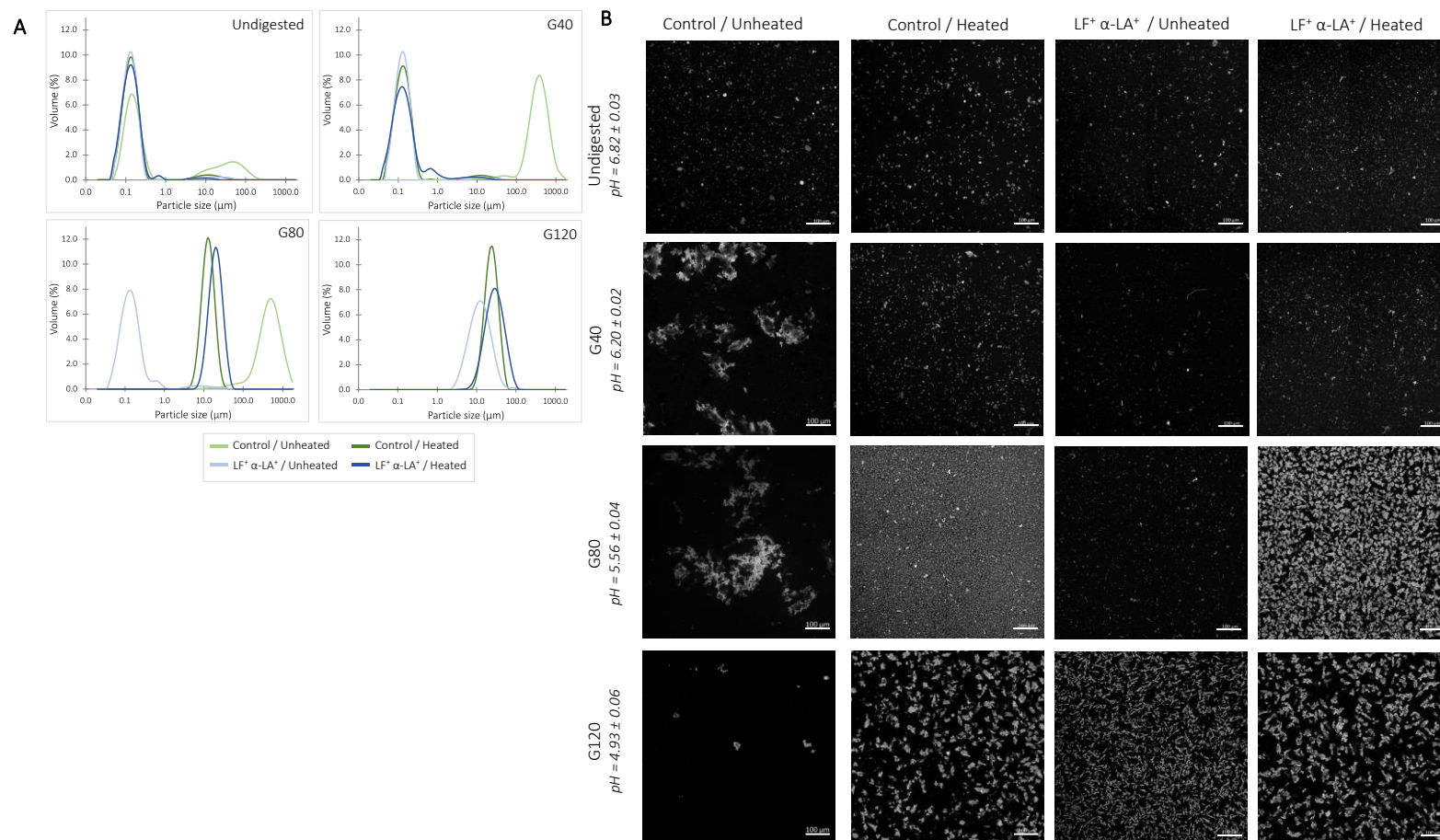
Figure 52. (A) Particle size distribution profiles and (B) confocal laser scanning microscopy images during the *in vitro* dynamic gastric digestion of IMFs processed at 1.3% proteins

(A) Data represent means of three independent digestion experiments (n = 3), with each measurement performed in triplicate. At G120, the protein particle size for the unheated control IMF was too low to be quantified. **(B)** Confocal images were observed at a magnification of x 20. Proteins are coloured in white (FastGreen®). Scale bar: 100 μm

3.2. Protein hydrolysis during *in vitro* gastrointestinal digestion

Proteolysis kinetics of caseins, α-LA, β-LG and LF, as quantified from SDS-PAGE analysis under reducing conditions (Figure 53.A), are presented in Figure 53.B. The proportion of the meal remaining in the total digesta volume (meal + secretions), set up to be the same for all IMFs, indicated whether the protein disappearance was only due to dilution by secretions and emptying or was additionally due to hydrolysis.

The electrophoretic band intensity of BSA, a minor protein observed only on the gels of both unheated and heated control IMFs (Figure 53.A), visually decreased progressively during the gastric digestion until total disappearance at the end of the gastric digestion. Some intact BSA was still observed during intestinal digestion only for the unheated control IMFs. The BSA content in the control IMFs was too low to be quantified by densitometry.

3.2.1. Caseins

The caseins were rapidly hydrolysed as observed in Figure 53.B. The kinetics of casein hydrolysis were not significantly different among the IMFs at the early and late gastric digestion times (p > 0.05). At 80 min of gastric digestion, the casein hydrolysis tended to be slower for the unheated control IMF than for the heated control IMF (p-value = 0.0503), which can be explained by the large protein aggregates observed at this time (figure 1.A) thus reducing the surface area accessible for pepsin action. For the same reason, a high sampling heterogeneity was observed at this time and only two out of three samples could be considered for SDS-PAGE analysis for the unheated control IMF (Figure 53.B and Supplementary Figure 4). Nevertheless, the present result is in agreement with what was observed during the static digestion of the same IMFs. Previous studies also showed that the protein coagulation occurring in rat stomach (Miranda & Pelissier, 1981) or in human gastric simulator (Ye et al., 2016) slowed down the casein hydrolysis during digestion of raw bovine milk, due to the limited diffusion of pepsin into the clot. At 120 min of gastric digestion, a treatment effect was observed only within the LF$^+$ α-LA$^+$ IMFs with 2 ± 0% vs. 9 ± 5% of residual intact caseins for the unheated or heated LF$^+$ α-LA$^+$ IMFs, respectively, which could be linked to the slightly higher size (x 2.5) of the protein aggregates in the heated LF$^+$ α-LA$^+$ IMF (Figure 52.A) . No more intact caseins were present during the intestinal digestion.

3.2.2. β-lactoglobulin and α-lactalbumin

During the gastric digestion, β-LG was resistant to pepsin hydrolysis in a similar manner in both unheated and heated control IMFs. α-LA also exhibited some resistance to pepsin hydrolysis. However, the kinetics of the α-LA band disappearance was significantly enhanced for the control IMFs compared to the LF$^+$ α-LA$^+$ IMFs. This was probably an artefact due to the co-elution at this band of LF-derived peptides for the LF$^+$ α-LA$^+$ IMFs, as shown after trypsinolysis and mass spectrometry analysis of the excised α-LA band

(data not shown). Similar resistance to pepsin hydrolysis was observed for the unheated and heated IMFs using *in vitro* static digestion model (Figure 44.C), as well as for raw and pasteurised human milk (de Oliveira et al., 2016; Nebbia et al., 2020). No more intact β-LG or α-LA were present during the intestinal digestion.

3.2.3. Lactoferrin

In the unheated LF[+] α-LA[+] IMF, LF was resistant to pepsin hydrolysis during the entire gastric phase, while in the heated LF[+] α-LA[+] IMF, LF hydrolysis was faster (Figure 53.B). This was in agreement with the results obtained for raw *vs.* pasteurised human milk digested using the same dynamic model (Nebbia et al., 2020). This was also in accordance with the results obtained for the same IMFs but digested using an *in vitro* static model (Figure 44.C), except that the kinetics of hydrolysis was much faster using the static model, with only 5 min needed to reach 19 ± 4 % of remaining intact LF *vs.* an estimated time of 106 min to reach the same proportion of remaining intact LF with the dynamic model. This was probably due to the progressive pH decrease and pepsin secretion for the latter. The resistance of native LF to pepsinolysis can be explained by its closed conformation (García-Montoya et al., 2012). In contrast, denatured LF, for which the extent of denaturation was 97% in the present study (Chapter 5 – section 3.1.1), was prone to pepsin hydrolysis due to a better accessibility of its cleavage sites following its unfolding (Stănciuc et al., 2013). Interestingly, the kinetics of LF disappearance in the heated LF[+] α-LA[+] IMF was very similar to that of caseins in the same IMF, suggesting that pepsin hydrolysed similarly both proteins within the LF-caseins aggregates.

In contrast to the heated LF[+] α-LA[+] IMF, a slight electrophoretic band at ~ 50 kDa was observed at 120 min and 180 min of gastric digestion for the unheated LF[+] α-LA[+] IMF. This protein band, assimilated to the C-terminal fragment of LF (Sharma et al., 2013), was still present during the intestinal digestion and appeared to be resistant to intestinal enzymes, as previously reported (Rastogi et al., 2014). In addition, a protein band at ~ 37 kDa was observed from 40 min of intestinal digestion for the unheated LF[+] α-LA[+] IMF. This polypeptide was assimilated to a product of LF hydrolysis by intestinal enzymes. Besides, some intact LF was observed in the early intestinal digestion time solely in the unheated LF[+] α-LA[+] IMF.
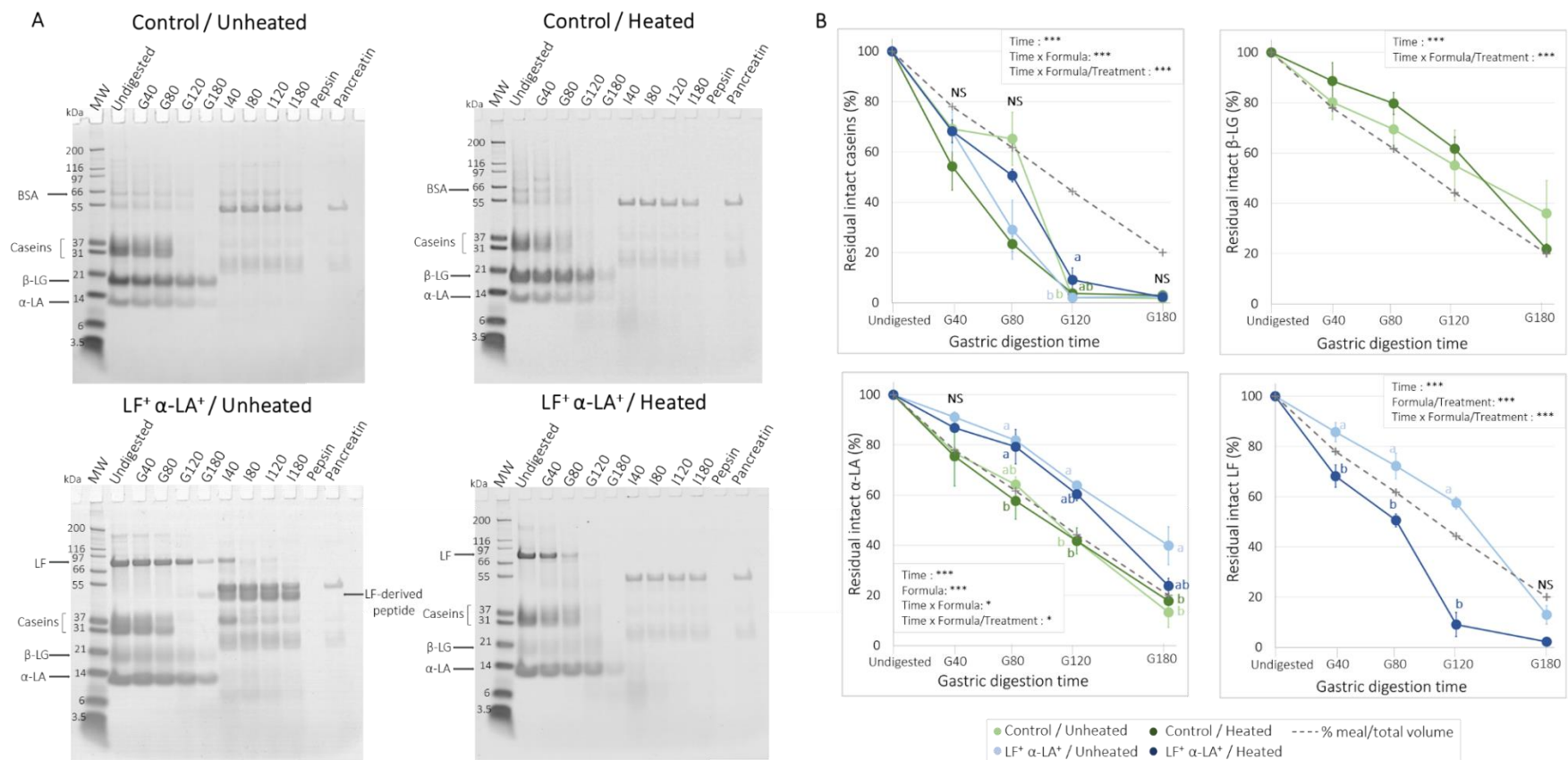
Figure 53. (A) Electrophoretic patterns and (B) proportions of residual intact caseins and major whey proteins during the *in vitro* dynamic gastrointestinal digestion of IMFs processed at 1.3% proteins

(A) Molecular weight marker (MW) was loaded in the first lane and pepsin or pancreatin solutions in the last lanes in the same amounts than those in the gastric or intestinal samples, respectively. SDS-PAGE analysis was conducted once for each *in vitro* digestion experiments (n = 3). **(B)** Data are means ± SD (n = 3), except for remained intact casein data after 80 min of gastric digestion, where n = 2 due to one non-representative sampling. Statistically significant factors were referenced with p < 0.001 (***), p < 0.01 (**), p < 0.05 (*) and p > 0.05 (NS). Different superscript letters for a given digestion time represent significant difference among treatments nested within formulas (p < 0.05). Asterisks for a given digestion time represent significant differences among formulas. Data from undigested IMFs were not included in the statistical analysis. Data for residual intact caseins were log-transformed to respect the hypotheses of residual normality and variance homogeneity (BoxCox transformation) required for the analysis of variance.

3.2.4. Degree of hydrolysis and *in vitro* digestibility of proteins

Figure 54.A shows the evolution of the degree of hydrolysis (DH) of all the IMFs during *in vitro* gastrointestinal digestion. During the gastric digestion, the DH barely increased for all IMFs to reach at 180 min of gastric digestion a DH of 5 ± 1% for the control IMFs and 6 ± 1% for the LF⁺ α-LA⁺ IMFs. These values were in line with Le Roux et al. (2020b) at the same digestion time for a bovine milk-based IMF (4 ± 1%) using the same dynamic model, and about 3-times higher than that determined at the end of static gastric digestion of IMFs (Chapter 6 – section 3.1.3).

In the intestinal compartment, proteolysis drastically increased for all IMFs to reach an average DH of 30 ± 2% after 40 min of intestinal digestion. From 80 min to 180 min of intestinal digestion, the DH progressively increased for all IMFs (p < 0.05), but in a different manner depending on the IMFs. From 80 min of intestinal digestion, DH tended to be lower for the unheated control IMF than for the other IMFs, which became significantly lower only at 120 min. Finally, DH did not significantly differed among IMFs at 180 min of intestinal digestion and reached 46 ± 4% for all IMFs, value in line with Le Roux et al. (2020b) for a bovine milk-based IMF at similar digestion time using the same dynamic model (49 ± 4%). The final DH values were higher under dynamic than static conditions for the control IMFs (45 ± 5% *vs.* 35 ± 3%, respectively) and the unheated LF⁺ α-LA⁺ IMF (46 ± 3% *vs.* 40 ± 1%, respectively) and *vice versa* for the heated LF⁺ α-LA⁺ IMF (49 ± 1% *vs.* 60 ± 2%, respectively) (Figure 45). This difference was due to the almost complete hydrolysis of the denatured LF during the static gastric digestion, reaching afterwards the intestinal compartment, while in the dynamic model, the LF hydrolysis was progressive and concomitantly delivered to the intestinal phase (Figure 53.D).

In vitro protein digestibility was calculated taking into account all the intestinal digestible nitrogen (nitrogen < 10 kDa) related to either the total nitrogen content of the meal (overall digestibility) or the total nitrogen content of the same intestinal phase (instantaneous digestibility). At the end of intestinal digestion, the overall protein digestibility for the unheated control IMF (73.4 ± 2.3%) was significantly lower than that for the other IMFs (86.6 ± 3.9%), while the instantaneous digestibility was not significantly different among IMFs, with a mean value of 91.5 ± 4.8%. For all IMFs, the overall protein digestibility was lower than the instantaneous one, likely due to a small fraction of dietary nitrogen remaining in the gastric compartment. However, the difference was greater for the unheated control IMF (-18 points), which was likely due to the high-size protein particles formed during the gastric digestion of this IMF (Figure 52.B), and from which the dietary nitrogen did not reach the intestinal compartment. This suggests that proteins from the unheated control IMF are slower to be digested, which impacts not only the kinetics of digestion and absorption, but also modulates the postprandial regional metabolism of nitrogen, at least as demonstrated in adults (Dangin et al., 2002, 2003; Deglaire,

Bos, et al., 2009). Nevertheless, the overall in vitro digestibility of all IMFs except for the unheated control (86.6 ± 3.9%) corroborated with the *in vitro* protein digestibility reported by Le Roux et al. (2020b) (89.2 ± 3.9%) and Nguyen et al. (2015) (81.5 ± 0.0%) for bovine milk-based IMFs, while the overall protein digestibility for the unheated control IMF remained in the range of that reported by Maathuis et al. (2017) for bovine milk-based IMF (73.4 ± 2.7%).
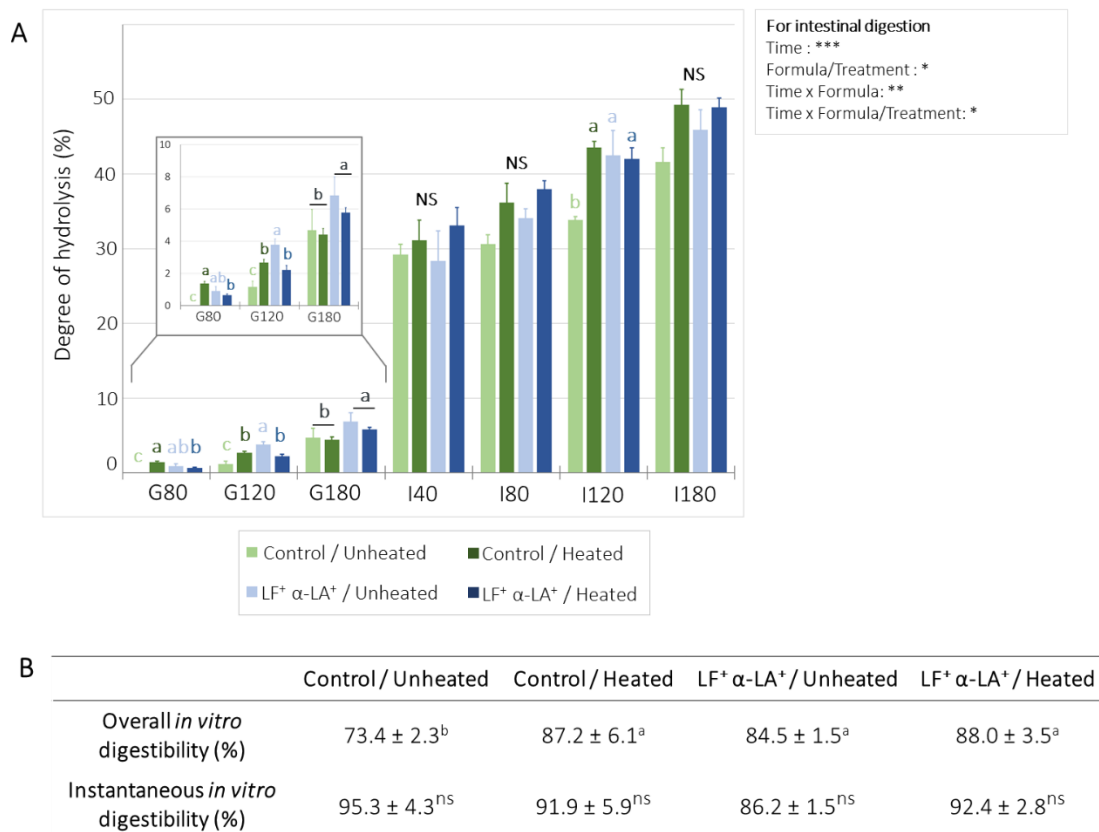
Figure 54. (A) Evolution of the degree of hydrolysis during the *in vitro* dynamic gastrointestinal digestion and (B) overall or instantaneous *in vitro* digestibility at the end of intestinal digestion of IMFs processed at 1.3% proteins

(A) Data are means ± SD (n = 3), with each measurement performed in triplicate. Statistically significant factors were referenced with $p < 0.001$ (***), $p < 0.01$ (**), $p < 0.05$ (*) and $p > 0.05$ (NS). Different superscript letters for a given digestion time represent significant difference among treatments nested within formulas ($p < 0.05$). Statistical analysis was conducted time per time for gastric samples as boxcox transformation was not sufficient to respect the residual normality and the variance homogeneity. (B) Data are means ± SD (n = 3), with each measurement performed in duplicate. Instantaneous *in vitro* digestibility data were transformed as the inverse of the square data to respect the hypotheses of residual normality and variance homogeneity (BoxCox transformation) required for the analysis of variance. Different superscript letters for a given digestibility category represent significant difference among treatments nested within formulas ($p < 0.05$). ns: $p > 0.05$.

3.3. Protein hydrolysis products released during *in vitro* gastrointestinal digestion

3.3.1. Amino acid bioaccessibility during *in vitro* intestinal digestion

The bioaccessibility of the essential and non-essential amino acids during the intestinal digestion of IMFs is presented in Figure 55. During the course of the intestinal digestion, the bioaccessibility of essential and non-essential amino acids increased significantly ($p < 0.001$) and was in overall 3-times higher for the essential amino acids than for the non-essential amino acids, which was linked to the cleavage specificity of the proteases. At 40 min of intestinal digestion, a significant treatment effect was observed for the control IMFs with a higher bioaccessibility of essential amino acids for the unheated control IMF compared to the heated control IMF ($p < 0.05$). This was not anymore true for the latter intestinal digestion times, where the bioaccessibility of essential and non-essential amino acids did not significantly differed between the unheated and heated control IMFs, such as between the unheated and heated LF$^+$ α-LA$^+$ IMFs. However, some significant differences were observed between the unheated control IMF and the heated LF$^+$ α-LA$^+$ IMF. The bioaccessibility of (non-) essential amino acids at the end of the intestinal dynamic digestion was in the same range as those determined at the end of the static digestion of the corresponding IMFs (Figure 46.A); however, the latter was reached much more rapidly (60 min) than in the present dynamic model (180 min). At the end of the dynamic digestion, the bioaccessibility of α-amino nitrogen was similar among IMFs (22 ± 2%; p-value > 0.05) and was in accordance with that determined at the end of the static digestion of the IMFs (24 ± 2%) (Chapter 6 – section 3.1.3).
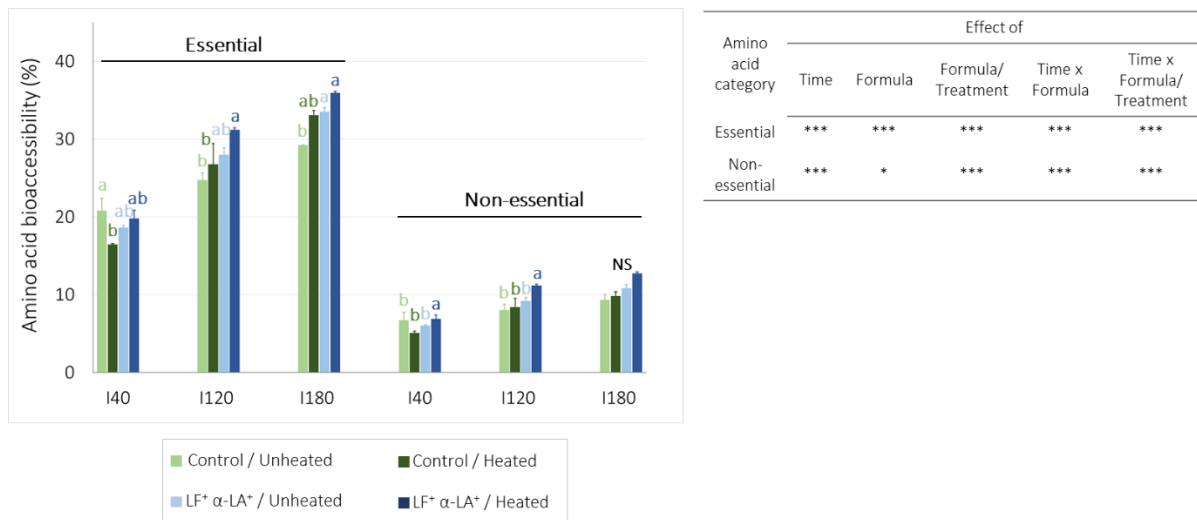
Figure 55. Bioaccessibility of (non-) essential amino acids during the *in vitro* dynamic intestinal digestion of IMFs processed at 1.3% proteins

Data are means ± SD (n = 3). Statistically significant factors were referenced with $p < 0.001$ (***), $p < 0.01$ (**), $p < 0.05$ (*) and $p > 0.05$ (NS). For each amino acid category, different superscript letters for a given digestion time represent significant difference among treatments nested within formulas ($p < 0.05$).

The bioaccessibility of the individual amino acids is provided in Supplementary Table 3. Briefly, the bioaccessibility of cysteine, proline and serine remained low during the intestinal digestion and not significantly different among IMFs ($p > 0.05$). There were some significant differences among IMFs, particularly for the unheated control IMF, which showed significantly lower bioaccessibility values for lysine, phenylalanine, tyrosine, arginine, threonine, lysine, valine, asparagine and glutamic acid. At the end of the intestinal digestion, the bioaccessibility of lysine (46.7-56.3%), methionine (41.7-46.7%), phenylalanine (42.6-57.9%), tyrosine (44.3-62.0%) and arginine (48.8-68.1%) were higher than that for the other amino acids, as previously reported under the static condition, except for methionine (Figure 46.B). This was in accordance with the specific cleavage sites of the endopeptidases that were pepsin (phenylalanine, tyrosine, leucine and tryptophan residues; Inouye & Fruton, 1967), trypsin (arginine and lysine residues; Keil, 1992), chymotrypsin (phenylalanine, tyrosine and tryptophan residues; Appel, 1986), and elastase (adjacent bonds of neutral amino acid residues; Keil, 1992), in addition to the action of the carboxypeptidase, an exopeptidase having a large cleavage site affinity. At the end of intestinal digestion, the bioaccessibility of individual essential amino acids were somewhat lower than those determined by Le Roux et al. (2020b), except for methionine and histidine.

3.3.2. Peptidomic profile of digesta during *in vitro* gastrointestinal digestion

3.3.2.1. Identification and quantification of peptides

Figure 56.A shows the number of unique peptides for all the IMFs during the *in vitro* gastrointestinal digestion. The peptide sequence length ranged from 6 to 50 amino acids, which corresponded to a mass range from 0.6 to 6.0 kDa.

Prior to digestion, the number of unique peptides was 488 and 434, or 451 and 410 for the unheated and heated control IMFs, or for the unheated and heated LF[+] α-LA[+] IMFs, respectively. Only 192 peptides were common among all IMFs prior to digestion. Peptides were equally distributed in the ranges 0.6-2.5 kDa and 2.5-4.5 kDa, and in a minor part in the range 4.5-6.0 kDa (13%) for all IMFs. For the undigested IMFs, the majority of the identified peptides derived from caseins (76%), while the major whey proteins (i.e. α-LA, β-LG and LF) minimally contributed to peptide formation (14%) (data not shown), as previously reported for bovine milk (Dallas, Guerrero, Parker, et al., 2014; Meltretter et al., 2008) or human milk (Dallas et al., 2013; Deglaire et al., 2019). These peptides could be the result of the action of some endogenous bovine milk proteases including plasmin system, neutrophil elastase, as well as several amino- and carboxy-peptidases that can act either within the bovine mammary gland or after milk expression (Bastian & Brown, 1996; Dallas et al., 2015; Kelly et al., 2006; Li et al., 2014).

During the gastric digestion, the peptide number sharply increased to reach 1869 and 2021, or 2015 and 2120 peptides at 180 min of gastric digestion of the unheated and heated control IMFs, or of the unheated and heated LF[+] α-LA[+] IMFs, respectively (Figure 56.A). This increase was mainly due to the release of peptides between 0.6 and 2.5 kDa (~ 70% of the total peptides at the end of gastric digestion for all IMFs). At the same time of digestion, the peptide number was much lower for the intestinal samples with most peptides (> 85%) belonging to the 0.6-2.5 kDa class. The peptide number decreased linearly and similarly for all IMFs, except for the unheated control IMF, where the decrease was observed only at the end of the intestinal digestion. A total of 450 and 493, or 604 and 515 peptides were identified at this last digestion time for the unheated and heated control IMFs, or the unheated and heated LF[+] α-LA[+] IMFs, respectively. The intestinal evolution of the peptide number was concomitant to the extent of hydrolysis, which was much greater in the intestinal than in the gastric phase and which tended to increase faster for the heated control IMF and the LF[+] α-LA[+] IMFs than for the unheated control IMF (Figure 54.A). This likely resulted in the production of peptides with less than 6 amino acids, not identified here, as well as in the release of free amino acids (Figure 55).

Prior to and during the *in vitro* gastrointestinal digestion of the IMFs, a total of 3169 unique peptides were identified, with 2148 peptides common among the IMFs (Figure 56.B). The majority of the identified peptides derived from caseins (61%) and to a minor extent from the major whey proteins

(21%), as previously reported for IMFs (Hodgkinson et al., 2019) or human milk (Deglaire et al., 2016, 2019). More precisely, the majority of the identified peptides originated from β-casein (29% of the total unique peptides), as previously reported for IMFs (Wada et al., 2017) or human milk (Deglaire et al., 2016, 2019; Nielsen et al., 2018). In addition, 17% of the total unique peptides derived from α_{S1}-casein and 10% from α_{S2}-casein. Compared to the other caseins, k-casein released the lowest number of identified peptides (6% of total peptides), as previously reported for dairy products during infant digestion (Dupont et al., 2010). Concerning the whey proteins, 10% of total unique peptides derived from β-LG, 9% from LF and 2% from α-LA (Figure 56.C). The low number of peptides originating from whey proteins could reflect the resistance of whey proteins to pepsin hydrolysis during the gastric digestion, as observed by SDS-PAGE analysis (Figure 53.B, Figure 53.C and Figure 53.D), but also probably the limited detection due to the presence of disulfide bonds within these peptides, making difficult their identification by LC-MS/MS. Finally, 18% of the common peptides derived from minor proteins such as GLCM1, OSTP, ALBU, BT1A1 and PIGR.

Venn diagram (Figure 56.B) showed that 55 and 34, or 72 and 33 peptides were specific for the unheated and heated control IMFs, or for the unheated and heated LF[+] α-LA[+] IMFs, respectively. Specific peptides for the control IMFs mainly derived from the minor proteins (47%), with a greater proportion of peptides originating from polymeric immunoglobulin receptor for the unheated control IMF than the heated control IMF. In the latter, a greater proportion of specific peptides were deriving from β-LG and α_{S1}-casein. In the LF[+] α-LA[+] IMFs, the specific peptides mainly derived from LF (57% and 45% for the unheated and heated LF[+] α-LA[+] IMFs, respectively).
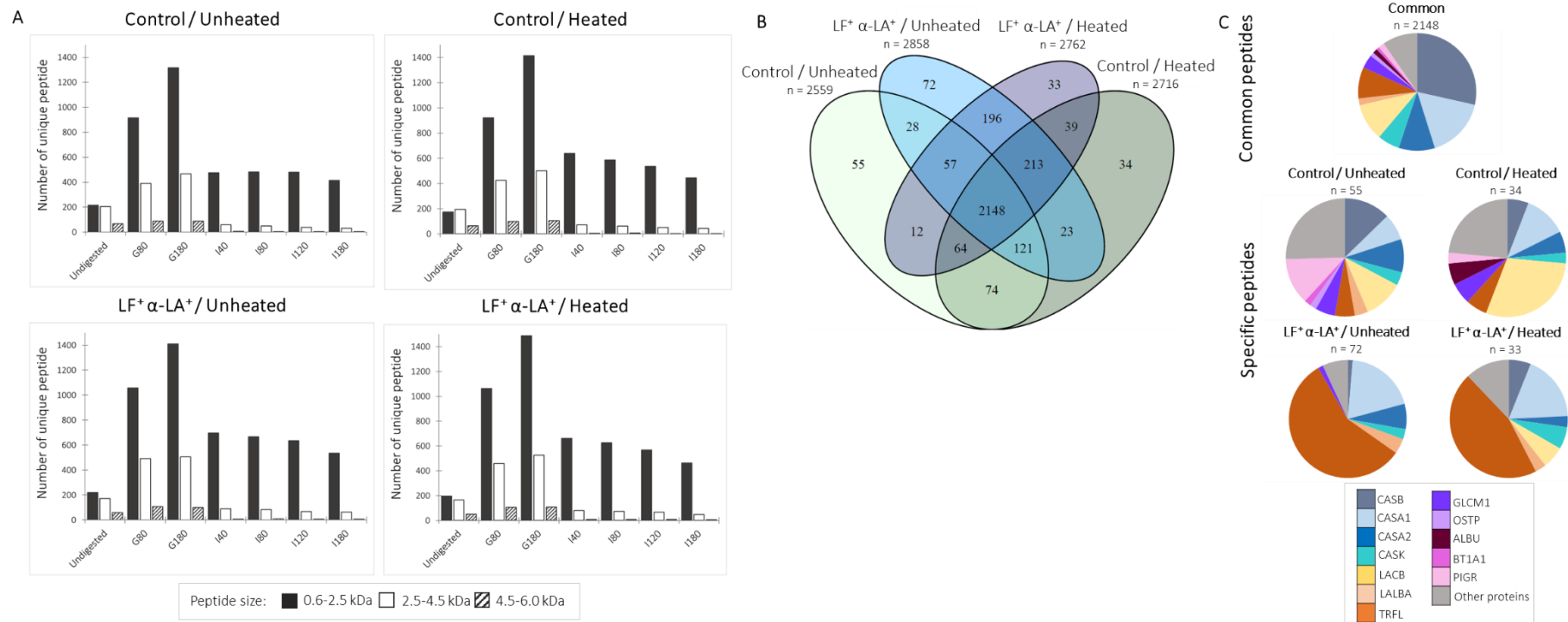
Figure 56. (A) Peptide size distribution, (B) Venn diagram of peptides and (C) parent protein of the common and specific peptides during the *in vitro* dynamic gastrointestinal digestion of IMFs processed at 1.3% proteins

(A) The peptides were regrouped in three classes: 0.6-2.5 kDa, 2.5-4.5 kDa and 4.5-6.0 kDa, corresponding to peptide lengths of approximatively 6-20, 20-35 and 35-50 amino acids, respectively. **(B)** n values correspond to the peptide amounts. Venn diagram was created with all the identified peptides before digestion and released during the *in vitro* dynamic gastrointestinal digestion of the IMFs. **(C)** Abbreviations are CASA1: α_{s1}-casein, CASA2: α_{s2}-casein, CASB: β-casein, CASK: κ-casein, LACB: β-lactoglobulin, LALBA: α-lactalbumin, TRFL: lactoferrin, GLCM1: glycosylation-dependent cell adhesion molecule 1, OSTP: osteopontin, ALBU: albumin, BT1A1: Butyrophilin Subfamily 1 Member A1, PIGR: Polymeric immunoglobulin receptor. Peptides were identified against the « Bos Taurus » protein database (6 905 proteins; source: https://uniprot.org).

3.3.2.2. Peptide clustering and kinetics of release during the gastrointestinal digestion

The cluster analysis grouped the 3169 unique peptides into six clusters (Figure 57). Parent protein and number of essential amino acids were the variables the most significantly associated to the clustering (Table 17).

Clusters 4, 5 and 6 included peptides mainly released during the gastric digestion (Figure 57.B). Cluster 4 included peptides originating mostly from caseins (78% of cluster peptides), which were present before digestion and further released during the gastric digestion in a near similar manner for all IMFs. Cluster 5, which showed a progressive increase and similar peptide abundance through the gastric digestion, contained the same proportion of casein-derived peptides as in overall (i.e. the entire dataset) but significantly less LF-derived peptides than in overall. Cluster 6 showed a higher peptide abundance in the LF$^+$ α-LA$^+$ IMFs than in the control IMFs at 80 min of gastric digestion, which was due to the higher proportion of LF-derived peptides in this cluster and the higher LF amount in the LF$^+$ α-LA$^+$ IMFs than in the control IMFs. At 180 min of digestion, the abundance in the heated LF$^+$ α-LA$^+$ IMF was higher than that in the unheated LF$^+$ α-LA$^+$ IMF, which can be linked to the extensive proteolysis of the denatured LF (Figure 53.D). Leucine (cleavage specificity for pepsin) in position P1' was significantly represented in clusters 4 and 5, as well as tryptophan (cleavage specificity for pepsin) in positions P1 and P1' for cluster 4 (Table 17).

In contrast, clusters 2 and 3 (11% and 7% of the total peptides, respectively) gathered peptides mostly released during the intestinal digestion of IMFs (Figure 57.B). Cluster 2 contained the same proportion of caseins-derived peptides as in overall and was significantly associated to α-LA but to a minor extent (6% of cluster peptides). A constantly lower abundance of peptides from the unheated control IMF was observed, which could result from the slower dietary nitrogen transfer for this IMF due to the formation of high-size particles in the gastric compartment. In cluster 3, peptides were mainly originating from LF (33% of cluster peptides) and β-LG (22% of cluster peptides) (Table 17). As observed for cluster 2, the abundance was lower for the unheated control IMF but the difference was greater during the first 2 hours before reaching a similar abundance as compared to the heated IMFs. This could be linked to a slower release of β-LG peptides in the unheated control IMF compared to the heated control IMF, as Nicoleta et al. (2008) showed that heat treatment of β-LG solution resulted in the increase of the extent of β-LG hydrolysis by trypsin. On the contrary, the abundance was higher for the unheated LF$^+$ α-LA$^+$ IMF, likely due to the resistance of LF-derived peptides to intestinal digestion, as shown by SDS-PAGE (Figure 53.D).

Finally, cluster 1 (9% of the total peptides) included peptides released during the gastric phase and progressively hydrolysed during the intestinal phase; a few peptides were initially present in the undigested IMFs. Cluster 1 was significantly associated to LF and β-LG and negatively correlated to α-LA, α_{s2}-casein and k-casein (Table 17). During the gastric digestion, the peptide abundances for cluster 1 were lower for the control IMFs than for the LF$^+$ α-LA$^+$ IMFs, which was likely due to the high proportion of peptides deriving from LF, being in higher concentration in the LF$^+$ α-LA$^+$ IMFs. During the intestinal digestion, different kinetics of peptide release were observed across all the IMFs and a similar trend to that for cluster 3 was observed, especially regarding the abundance for the unheated LF$^+$ α-LA$^+$ and control IMFs. The lower abundance of peptides for the unheated control IMF could be either the result of a faster peptide hydrolysis at the early intestinal digestion time (40 min), corroborating the higher amino acid bioaccessibility observed at this time, or could result from the slower nitrogen transfer into the intestinal compartment due to the coagulum formed in the gastric phase at this digestion time (Figure 52). Nevertheless, at the end of intestinal digestion, the abundance of peptides for this IMF was similar to that for the heated control and LF$^+$ α-LA$^+$ IMFs.
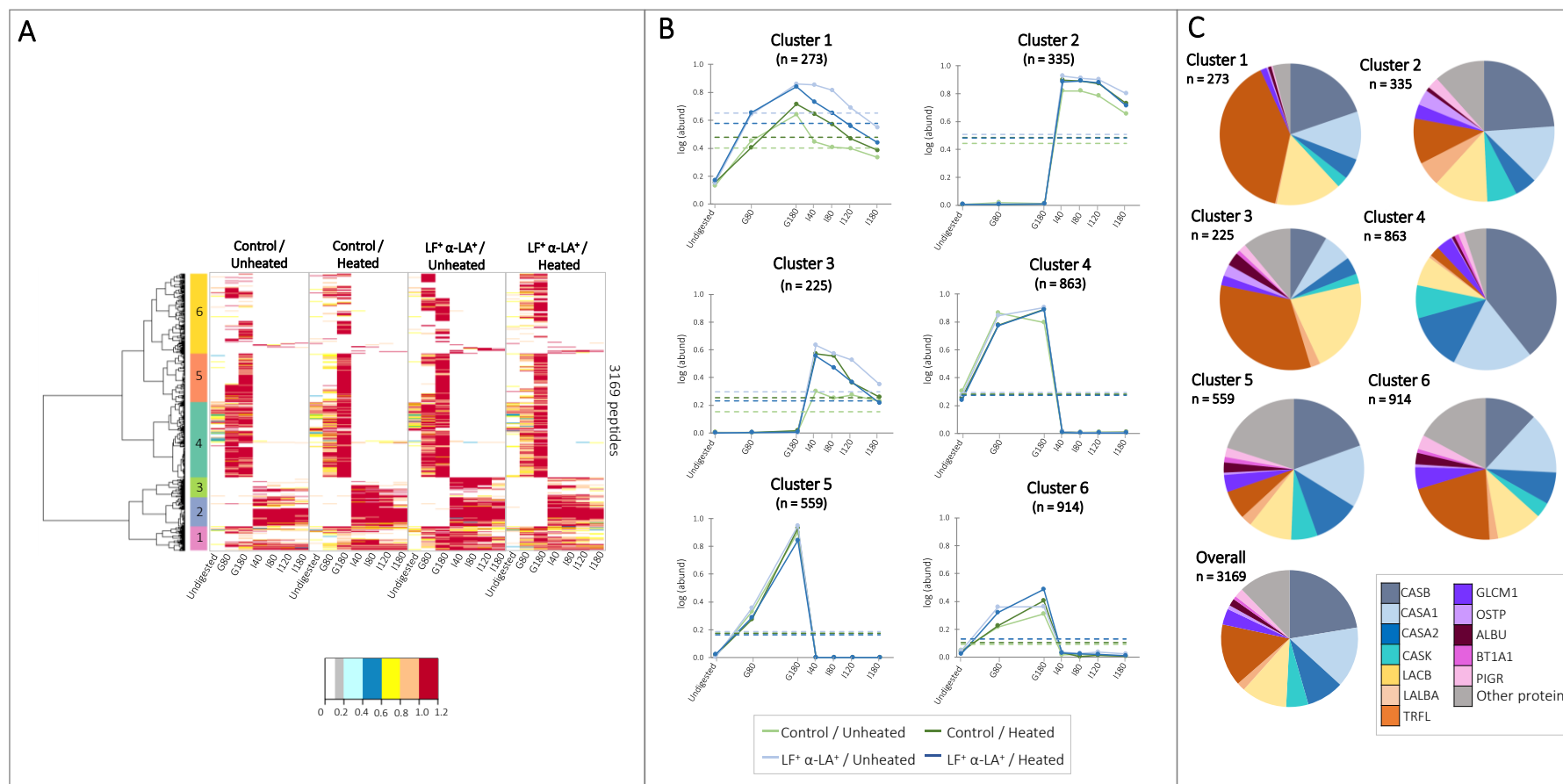
Figure 57. (A) Heatmap abundances as classified by hierarchical classification and (B) average abundances of the peptides by cluster during the *in vitro* dynamic gastrointestinal digestion of IMFs processed at 1.3% proteins - (C) parent proteins of the peptides by cluster

Peptide abundances were log10-transformed followed by setting the maximum abundance to 1

(A) White stretches indicate regions where no peptides were identified. Blue colour indicates low abundance graduating to red colour for high abundance of peptide identified. **(B)** the dashed-pointed curves represent the mean kinetics for each IMFs. **(C)** Abbreviations are CASA1: α_{s1}-casein, CASA2: α_{s2}-casein, CASB: β-casein, CASK: κ-casein, LACB: β-lactoglobulin, LALBA: α-lactalbumin, TRFL: lactoferrin, GLCM1: glycosylation-dependent cell adhesion molecule 1, OSTP: osteopontin, ALBU: albumin, BT1A1: Butyrophilin Subfamily 1 Member A1, PIGR: Polymeric immunoglobulin receptor. Overall peptides correspond to peptides within the entire dataset.

Table 17. Peptide biochemical characteristics significantly associated (p < 0.05) with clusters

	Qualitative modalities						Quantitative modalities				
	Modality[1]	Cla/Mod[2]	Mod/Cla[3]	Overall[4]	v.test	p.value	Modality[5]	Mean ± SD in category	Mean ± SD in overall	v.test	p.value
				(n = 3169)					(n = 3169)		
Cluster 1	prot = TRFL	23.08	39.27	14.70	10.57	< 0.0001	pI	6.32 ± 2.04	6.67 ± 2.25	-2.68	0.0073
	P1'=E	14.16	11.64	7.10	2.86	0.0042	EAA	7.49 ± 3.70	8.44 ± 4.68	-3.53	0.0004
	P1'=A	13.55	10.55	6.72	2.49	0.0128	length	15.95 ± 6.93	18.10 ± 9.25	-4.04	< 0.0001
	prot = LACB	11.95	14.91	10.77	2.22	0.0261					
	P1=Y	13.13	7.64	5.03	1.96	0.0496					
	P1=K	5.22	4.73	7.82	-2.08	0.0372					
	P1'=K	5.30	5.45	8.89	-2.18	0.0291					
	prot = LALBA	1.61	0.36	1.95	-2.20	0.0279					
	prot = CASK	4.22	2.55	5.21	-2.21	0.0271					
	prot = GLCM1	3.33	1.45	3.77	-2.27	0.0229					
	prot = PIGR	1.47	0.36	2.14	-2.38	0.0172					
	prot = CASA2	4.66	4.73	8.76	-2.62	0.0087					
	P1'=Q	3.14	1.82	4.99	-2.77	0.0056					
	P1=Q	2.22	1.09	4.24	-3.05	0.0023					
Cluster 2	P1=Q	27.41	11.01	4.24	5.61	< 0.0001	length	12.97 ± 5.33	18.10 ± 9.25	-10.75	< 0.0001
	P1'=N	26.42	8.33	3.33	4.68	< 0.0001	EAA	5.40 ± 2.70	8.44 ± 4.68	-12.62	< 0.0001
	P1'=H	30.88	6.25	2.14	4.63	< 0.0001	pI	5.13 ± 1.61	6.67 ± 2.25	-13.19	< 0.0001
	P1'=I	30.43	6.25	2.17	4.57	< 0.0001					
	prot = LALBA	30.65	5.65	1.95	4.37	< 0.0001					
	prot = OSTP	40.00	3.57	0.94	4.20	< 0.0001					
	P1'=V	21.47	10.42	5.12	4.19	< 0.0001					
	P1=N	27.27	6.25	2.42	4.15	< 0.0001					
	P1=T	22.73	8.93	4.15	4.14	< 0.0001					
	P1'=P	25.93	4.17	1.70	3.21	0.0013					
	P1=Y	5.63	2.68	5.03	-2.19	0.0282					
	P1=R	4.96	2.08	4.43	-2.36	0.0185					
	prot = TRFL	7.48	10.42	14.70	-2.41	0.0158					
	prot = CASA2	6.09	5.06	8.76	-2.67	0.0075					
	P1'=F	5.42	4.46	8.70	-3.11	0.0019					
	P1=P	2.54	0.89	3.71	-3.27	0.0011					
	P1=L	5.96	7.14	12.66	-3.40	0.0007					
	P1=F	3.88	2.38	6.47	-3.55	0.0004					
	P1'=L	2.93	6.25	22.52	-8.45	< 0.0001					
Cluster 3	prot = TRFL	15.81	32.74	14.70	7.13	< 0.0001	length	15.29 ± 7.41	18.10 ± 9.25	-4.73	< 0.0001
	prot = LACB	14.29	21.68	10.77	4.96	< 0.0001	pI	5.93 ± 2.05	6.67 ± 2.25	-5.06	< 0.0001
	P1'=K	15.19	19.03	8.89	4.95	< 0.0001	EAA	6.89 ± 4.04	8.44 ± 4.68	-5.18	< 0.0001
	P1=T	13.64	7.96	4.15	2.70	0.0069					
	P1=G	14.44	5.75	2.83	2.46	0.0138					
	prot = OSTP	20.00	2.65	0.94	2.31	0.0209					
	P1=A	11.16	11.06	7.04	2.31	0.0210					
	P1=Q	2.96	1.77	4.24	-2.04	0.0413					
	P1=W	0.00	0.00	1.57	-2.25	0.0245					
	prot = CASK	3.01	2.21	5.21	-2.26	0.0238					
	P1=Y	2.50	1.77	5.03	-2.54	0.0110					
	P1=F	2.91	2.65	6.47	-2.62	0.0087					
	prot = CASA2	3.23	3.98	8.76	-2.84	0.0045					
	prot = CASA1	3.30	6.64	14.29	-3.68	0.0002					
	P1'=F	1.08	1.33	8.70	-4.83	< 0.0001					
	prot = CASB	2.68	8.41	22.30	-5.69	< 0.0001					
	P1'=L	2.51	7.96	22.52	-5.97	< 0.0001					

	Qualitative modalities						Quantitative modalities				
	Modality[1]	Cla/Mod[2]	Mod/Cla[3]	Overall[4] (n = 3169)	v.test	p.value	Modality[5]	Mean ± SD in category	Mean ± SD in overall (n = 3169)	v.test	p.value
Cluster 4	prot = CASB	47.75	39.15	22.30	13.45	< 0.0001	EAA	10.62 ± 5.24	8.44 ± 4.68	16.08	< 0.0001
	P1=P	49.15	6.70	3.71	5.15	< 0.0001	length	22.35 ± 10.60	18.10 ± 9.25	15.86	< 0.0001
	prot = CASA2	40.50	13.05	8.76	5.04	< 0.0001	pI	7.04 ± 2.21	6.67 ± 2.25	5.61	< 0.0001
	prot = CASA1	34.73	18.24	14.29	3.82	0.0001					
	prot = CASK	39.16	7.51	5.21	3.43	0.0006					
	P1'=L	32.08	26.56	22.52	3.30	0.0010					
	P1'=W	46.67	3.23	1.88	3.23	0.0012					
	P1'=Q	35.85	6.58	4.99	2.45	0.0143					
	P1=H	37.78	3.93	2.83	2.22	0.0268					
	P1=W	40.00	2.31	1.57	1.97	0.0488					
	P1=A	20.54	5.31	7.04	-2.37	0.0179					
	P1'=N	16.98	2.08	3.33	-2.48	0.0130					
	P1'=G	13.56	0.92	1.85	-2.48	0.0130					
	prot = OSTP	6.67	0.23	0.94	-2.75	0.0060					
	P1'=A	19.16	4.73	6.72	-2.81	0.0050					
	prot = ALBU	10.91	0.69	1.73	-2.91	0.0036					
	P1'=D	11.76	0.92	2.14	-3.07	0.0021					
	prot = LALBA	8.06	0.58	1.95	-3.74	0.0002					
	P1'=E	15.49	4.04	7.10	-4.30	< 0.0001					
	prot = LACB	17.20	6.81	10.77	-4.57	< 0.0001					
	prot = TRFL	4.27	2.31	14.70	-13.81	< 0.0001					
Cluster 5	P1'=L	23.43	29.89	22.52	4.49	< 0.0001	pI	6.97 ± 2.18	6.67 ± 2.25	3.48	0.0005
	P1=T	11.36	2.67	4.15	-2.00	0.0458	EAA	7.66 ± 3.64	8.44 ± 4.68	-4.38	< 0.0001
	P1'=W	8.33	0.89	1.88	-2.00	0.0451	length	16.01 ± 7.51	18.10 ± 9.25	-5.90	< 0.0001
	P1=S	11.22	3.91	6.16	-2.53	0.0113					
	P1'=R	9.60	2.14	3.93	-2.54	0.0112					
	P1'=V	9.82	2.85	5.12	-2.84	0.0045					
	P1'=P	3.70	0.36	1.70	-3.04	0.0024					
	P1'=K	8.13	4.09	8.89	-4.75	< 0.0001					
	prot = TRFL	7.91	6.58	14.70	-6.46	< 0.0001					
Cluster 6	prot = TRFL	41.45	21.11	14.70	6.32	< 0.0001	pI	6.98 ± 2.36	6.67 ± 2.25	5.03	< 0.0001
	P1=K	41.37	11.21	7.82	4.39	< 0.0001					
	prot = PIGR	44.12	3.26	2.14	2.69	0.0071					
	prot = ALBU	43.64	2.61	1.73	2.34	0.0192					
	prot = GLCM1	38.33	5.01	3.77	2.27	0.0230					
	P1=Q	21.48	3.16	4.24	-1.96	0.0494					
	P1'=V	22.09	3.92	5.12	-1.99	0.0467					
	P1'=P	16.67	0.98	1.70	-2.05	0.0404					
	P1'=H	17.65	1.31	2.14	-2.12	0.0341					
	P1'=I	17.39	1.31	2.17	-2.19	0.0288					
	prot = CASK	19.28	3.48	5.21	-2.88	0.0040					
	prot = CASB	15.35	11.86	22.30	-9.42	< 0.0001					

Grey lines correspond to modalities that are negatively associated to a cluster.

[1] Minor proteins were not considered. P1 and P1′ correspond to the cleavage site of digestive enzymes.

[2] Cla/Mod: occurrence of the modality category in the cluster divided by its occurrence in the entire dataset.

[3] Mod/Cla: proportion of the modality category within the cluster.

[4] Overall proportion of this modality category within the entire dataset.

[5] EAA: essential amino acids; length: number of amino acid residue in peptides.

3.3.2.3. Mapping on the parent protein sequence of peptides released during the gastrointestinal digestion of IMFs

Figure 58 shows the cumulative abundance of the peptides mapped onto the parent protein sequence during the gastrointestinal digestion of the major proteins.

3.3.2.3.1. The casein-derived peptides

Compared to α_{S2}-casein and κ-casein, the peptides released from β-casein and α_{S1}-casein hydrolysis covered almost the whole sequence of these proteins, as previously shown during *in vivo* intestinal digestion of IMFs in rats (Wada et al., 2017) or casein solution in adults (Sanchón et al., 2018).

For β-casein, in all IMFs, the regions 57-93, 142-163 and 192-209 were well represented during the gastrointestinal digestion, while peptides in the regions 1-32, 93-142 and 163-191 were less abundant during the intestinal digestion. At 80 min of gastric digestion, peptides in the region 28-128 for the heated control IMF and 28-142 for the heated LF[+] α-LA[+] IMF were less abundant than those for the unheated IMFs. During the intestinal digestion, peptides from the region 30-56 seemed to be more resistant to intestinal digestion for the unheated LF[+] α-LA[+] IMF compared to the other IMFs. Peptides in the region 106-113 and in the bioactive region 133-139 were less abundant during the intestinal digestion for the unheated control IMF compared to the other IMFs. In addition, peptides from the bioactive region 170-176 were more abundant during the whole intestinal digestion for the unheated LF[+] α-LA[+] IMF compared to the other IMFs. The relatively high abundance of β-casein-derived peptides during the gastrointestinal digestion of IMFs may reflect some resistance of β-casein to enzymatic hydrolysis, as previously reported for the region 57-96 during *in vitro* gastrointestinal digestion of skimmed bovine milk (Sánchez-Rivera et al., 2015) and in jejunal aspirates of healthy adults after casein ingestion (Boutrou et al., 2013). In addition, the high abundance of peptides in the region 76-93 was explained by the resistance to enzymatic hydrolysis, as previously reported after static gastrointestinal digestion of raw or heated bovine milk using infant digestion model (Dupont et al., 2010). Many peptides from this region were also identified in the digesta from IMF-fed piglets (Bouzerzour et al., 2012). In addition, other regions of the protein (i.e. 67–90, 128–140, and 190–209) have been found to be resistant to enzymatic hydrolysis during adult digestion regardless of the heat treatment applied prior to digestion (Boutrou et al., 2013; Svedberg et al., 1985). This resistance to enzymatic hydrolysis could be explained by the high proportion of proline residues in β-casein sequence (35 out of 209 residues) (McSweeney & O'Mahony, 2016). The higher abundance for peptides in the region 30-56 for the unheated IMFs than the heated IMFs was in accordance with Sánchez-Rivera et al. (2015), who showed higher abundance for peptides in the region 45-58 for raw bovine milk than heated bovine milk during gastrointestinal digestion.

For α_{s1}-casein, after 80 min of gastric digestion, peptides from the regions 24-40 and 99-142 were more abundant for the unheated IMFs compared to the heated IMFs. At the end of gastric digestion, peptides identified in the regions 1-40, 99-142 and 165-199 were the most abundant for all IMFs. During the intestinal digestion, these peptides seemed to be less resistant to intestinal enzymes for the unheated control IMF compared to the other IMFs. In addition, the abundance of the peptides from the region 80-89 increased after 40 min of intestinal digestion, and they were less resistant to intestinal digestion for the unheated control IMF compared to the other IMFs. For the bioactive region 110-121, peptides from the unheated LF^+ α-LA^+ IMF were more resistant to hydrolysis compared to the other IMFs, as observed for raw human milk compared to pasteurised human milk during in $vitro$ dynamic intestinal digestion (Deglaire et al., 2019).

For α_{s2}-casein, the sequence coverage during the gastrointestinal digestion of IMFs was low. After 80 min of gastric digestion, peptides from the regions 89-114 and 151-183 were more abundant for the unheated LF^+ α-LA^+ IMF compared to the other IMFs. At the end of gastric digestion, the main peptides released were originated from the region 69-207, especially for the heated control IMF and the unheated LF^+ α-LA^+ IMF. During the intestinal digestion of IMFs, the α_{s2}-casein regions 1–24, 36-65 (except for the heated control IMF), 81-98, 125-149 and 163-182 had no sequence coverage.

For κ-casein, peptides were mainly identified in the regions 18-75 and in the region 96-124 at the end of gastric digestion. Then, during the intestinal digestion, only few peptides were identified along the amino acid sequence, except for the region 52-59 for the heated control IMF and unheated LF^+ α-LA^+ IMF, the region 113-124 particularly for the unheated LF^+ α-LA^+ IMF, and the region 154-161 especially for the unheated control IMF. In addition, there were no (or only few) identified peptides in the N-terminal region 1-30, in the region 60-95 and in the C-terminal region 163-169 during the intestinal digestion.

3.3.2.3.2.   The whey protein-derived peptides

As stated previously, the individual whey proteins differed between the control and LF^+ α-LA^+ IMFs (Table 13), especially the β-LG and LF amount, which impacted the abundance of the whey protein-derived peptides. Consequently, only the heat treatment effect was investigated for the peptides derived from whey proteins.

For α-LA, prior to digestion, peptides in the region 41-110 were identified for both unheated control and LF^+ α-LA^+ IMFs but not in both heated control and LF^+ α-LA^+ IMFs. Peptides identified at 180 min of gastric digestion were more abundant in the region 41-52 for all IMFs. Intestinal peptides were more

abundant in the bioactive region 17-27 for the LF$^+$ α-LA$^+$ IMFs than for the control IMFs, such as in the region 96-102.

For β-LG, at the end of gastric digestion, peptide abundance in the regions 1-32, 74-104 and 123-156 was higher for the heated than for the unheated control IMF, which was still true during the intestinal digestion solely for the region 1-32, which included a bioactive area. This could be explained by the heat-induced unfolding of β-LG, favouring the accessibility for intestinal enzymes. For the LF$^+$ α-LA$^+$ IMFs, some difference of peptide abundance occurred in the bioactive region 127-138, being higher for the unheated IMF. Overall, the central region seemed more resistant to hydrolysis due to its numerous β-sheets (Cheison et al., 2011; Fernández & Riera, 2013).

Peptides derived from LF barely covered the LF sequence during the gastrointestinal digestion of IMFs, with many regions (i.e. 1-51, 153-208, 336-383, 399-440, 450-559 and 641-650) without peptides, as previously shown for *in vitro* (Deglaire et al., 2019) or *in vivo* intestinal digestion of human milk (Wada et al., 2017). This could be explained by the presence of 17 disulfide bonds stabilising bovine LF structure, making the peptide detection by LC-MS/MS difficult. The pattern was quite similar during the gastric digestion of both unheated and heated LF$^+$ α-LA$^+$ IMFs, unlike the different LF hydrolysis extent (Figure 53.B). This was due to the small size of peptides that can be detected, corresponding at the maximum to 7% of the LF size. During intestinal digestion, the cumulative peptide release was more abundant for the unheated LF$^+$ α-LA$^+$ IMF than for the heated one in the regions 52-96, 209-222, 283-327 and 572-640, which reflected the higher resistance of the native LF to gastrointestinal digestion (Figure 53.B).
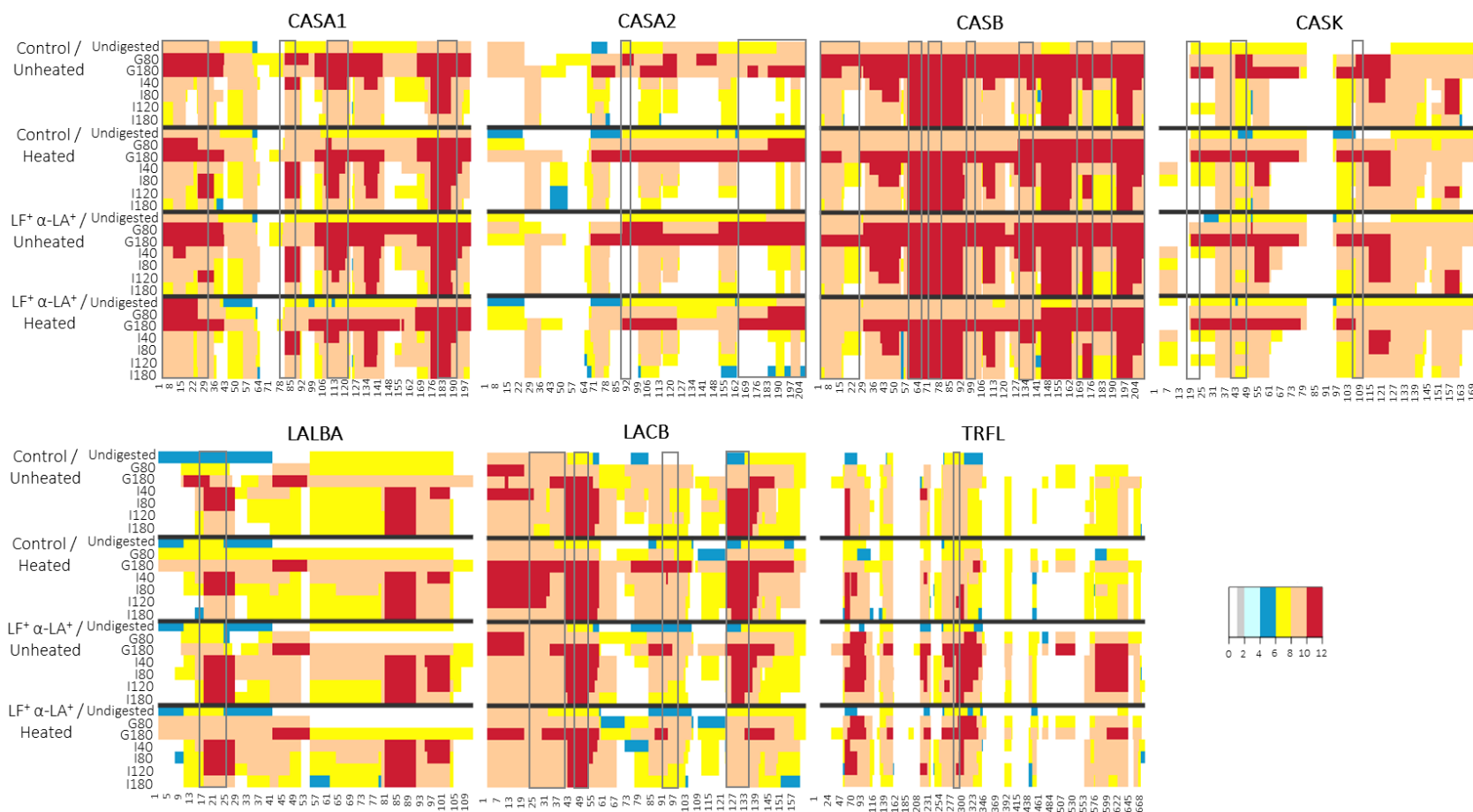
Figure 58. Mapping on the sequence of the major parent proteins of the peptides released during the *in vitro* dynamic gastrointestinal digestion of IMFs processed at 1.3% proteins

Abbreviations are CASA1: αs1-casein, CASA2: αs2-casein, CASB: β-casein, CASK: κ-casein, LACB: β-lactoglobulin, LALBA: α-lactalbumin, TRFL: lactoferrin. Peptide abundances, summed at each amino acid, were log10-transformed. The x-axis represents the amino acid sequence of parent protein and the y-axis represents the digestion time for each IMFs. White stretches indicate regions where no peptides were identified. Blue colour indicates low abundance graduating to red colour for high abundance of amino acid identification within the protein sequence. The boxed areas correspond to areas where bioactive peptides have been identified using BIOPEP and MBPDB databases.

3.3.2.4. Bioactive peptides release during the *in vitro* intestinal digestion

All the peptides were submitted to bioactivity search for exact matching using the databases BIOPEP, and, for LF-derived peptides, using the MBPDB database. A focus was made on the bioactive peptides released during the intestinal digestion (Table 18) as intestines are the main site for exerting the peptide bioactivity if any and as peptide absorption is likely to occur only across intestinal epithelium cells.

Bioactive peptides released during the gastric digestion are presented in Supplementary Table 4. Briefly, 37 bioactive peptides were identified during the gastric digestion, with about half of them originating from α_{s2}-casein (16), and a minor part from β-casein (8) and α_{s1}-casein (7). The majority of these peptides had antimicrobial and ACE inhibitor properties, as observed by Hodgkinson et al. (2019) during the infant *in vitro* gastric digestion of bovine milk. In contrast, no bioactive peptides derived from α-LA or LF were identified.

During the intestinal digestion, 18 and 19, or 25 and 24 bioactive peptides were identified for the unheated and heated control IMFs, or the unheated and heated LF⁺ α-LA⁺ IMFs, respectively, with 16 of them being common among IMFs. The lower number of bioactive peptides in the control IMFs was due to a lower number of casein-derived bioactive peptides in these IMFS as compared to that in the LF⁺ α-LA⁺ IMFs. Among the identified bioactive peptides, 9 of them, mainly originating from caseins, were generated during the gastric digestion and were still present during the intestinal digestion (Table 18). These casein-derived peptides had at least one proline residue in their sequence, which could explain their resistance to enzymatic hydrolysis (Sanchón et al., 2018). However, it should be noted that brush border peptidases, including proline-specific peptidases, were not included in our digestion model (Picariello et al., 2015).

The kinetics of bioactive peptide release during the intestinal digestion differed from one peptide to another and among IMFs. Bioactive peptides from α_{s1}-casein as well as CASB (170-176) were more abundant and more resistant in the unheated LF⁺ α-LA⁺ IMF than in the other IMFs. In addition, the sole bioactive peptide from α_{s2}-casein (i.e. CASA2 183-207) was only present in the LF⁺ α-LA⁺ IMFs, and was still present at the end of the digestion only for this heated IMF (Table 18).

CASB (134-139) was abundantly released since the early intestinal digestion time for the unheated control IMF, and then progressively hydrolysed, while the opposite was true for the heated control IMF (Table 18). CASB (191-209) was identified only in the LF⁺ α-LA⁺ IMFs and was more resistant in the corresponding heated IMF. CASK (51-60) was more resistant in the unheated LF⁺ α-LA⁺ IMF than in the heated control and LF⁺ α-LA⁺ IMFs.

LACB (92-100) was more abundant and more resistant in the heated control IMF compared to the other IMFs, such as for LACB (125-135), in accordance with Picariello et al. (2010) for bovine milk who suggested that this peptide had high allergenic potential due to its high resistance to hydrolysis during digestion. On the contrary, LACB (142-148) was more resistant in the heated LF$^+$ α-LA$^+$ IMF than in the corresponding unheated IMF and the heated control IMF.

LALBA (61-68) was identified earlier but was hydrolysed sooner for the unheated LF$^+$ α-LA$^+$ IMF as compared to the unheated control IMF. This peptide was not identified in the heated IMFs, except at the last intestinal time for the heated LF$^+$ α-LA$^+$ IMF.

Only one bioactive peptide deriving from LF (fragment 325-340) was identified for the unheated LF$^+$ α-LA$^+$ IMF during the first times of intestinal digestion. The low number of bioactive peptides originating from LF, in line with Beverly et al., (2019) and Deglaire et al. (2019) for human milk digestion, could be linked to the low number of such peptides yet identified in the literature (65 identified peptides in the MBPDB database) (Nielsen et al., 2017), and the presence of disulfide bonds in LF sequence.

Table 18. Bioactive peptides identified during the *in vitro* dynamic intestinal digestion of IMFs processed at 1.3% proteins

Parent protein [1]	Peptide position [2]	Peptide sequence [3,4]	Activity	Abundance [5] Control / Unheated (I40 I80 I120 I180)	Control / Heated (I40 I80 I120 I180)	LF+ α-LA+ / Unheated (I40 I80 I120 I180)	LF+ α-LA+ / Heated (I40 I80 I120 I180)
CASA1	1-23	RPKHPIKHQGLPQEVLNENLLRF	Immunomodulating; Antibacterial; Antiviral				
	80-90	HIQKEDVPSER	Antioxidative				
	110-121	EIVPNSAEERLH	ACE inhibitor				
	180-193	SDIPNPIGSENSEK	Antibacterial				
CASA2	183-207	VYQHQKAMKPWIQPKTKVIPYVRYL	Haemolytic; Antibacterial; Campde inhibitor				
CASB	60-68	YPFPGPIPN	ACE inhibitor				
	73-82	NIPPLTQTPV	ACE inhibitor				
	98-105	VKEAMAPK	Antioxidative				
	133-139	LHLPLPL	ACE inhibitor				
	134-139	HLPLPL	Antiamnestic				
	170-176	VLPVPQK	Antioxidative				
	191-209	LLYQEPVLGPVRGPFPIIV	Immunomodulating				
	194-206	QEPVLGPVRGPFP	ACE inhibitor				
	202-209	RGPFPIIV	ACE inhibitor				
CASK	31-37	VLSRYPS	Antioxidative				
	42-49	YYQQKPVA	Antibacterial				
	51-60	INNQFLPYPY	Dipeptidyl peptidase IV inhibitor				
	106-111	MAIPPK	Antithrombotic				
LACB	33-42	DAQSAPLRVY	ACE inhibitor				
	92-100	VLVLDTDYK	Antibacterial; Dipeptidyl peptidase IV inhibitor				
	125-135	TPEVDDEALEK	Dipeptidyl peptidase IV inhibitor				
	142-148	ALPMHIR	ACE inhibitor				
LALBA	17-26	GYGGVSLPEW	Dipeptidyl peptidase IV inhibitor				
	61-68	CKDDQNPH	Antibacterial				
TRFL	325-340	DLIWKLLSKAQEKFGK	Antibacterial				

Abundance scale: 4 6 8 10 12

[1] Abbreviations are CASA1: α$_{s1}$-casein, CASA2: α$_{s2}$-casein, CASB: β-casein, CASK: κ-casein, LACB: β-lactoglobulin, LALBA: α-lactalbumin, TRFL: lactoferrin

[2] Peptide position on the parent protein without taking into account the signal peptide.

[3] Bioactive peptides identified using an exact matching search within the BIOPEP database (dated on March 2020; 3897 peptides) for all peptides and the MBPDB database (dated on July 2020; 65 peptides) for LF-derived peptides.

[4] Bold sequences are common peptides between gastric and intestinal phases

[5] Peptide abundances were log10-transformed for each IMF at each digestion time.

4. Conclusion

The present study confirmed that the protein structures within IMFs generated by varying the protein profile of IMFs and the heating conditions impacted the digestive kinetics of proteolysis, such as demonstrated under static conditions. However, the present model highlighted the importance of the dynamic parameters, particularly the continuous pH control and enzyme secretion and the concomitant gastric and intestinal digestion, on the kinetics of proteolysis, which was thus more progressive particularly regarding the gastric LF hydrolysis.

The gastric protein coagulation was markedly dependent of the casein micelle structure within IMFs, with high-size protein particles formed in the early period of gastric digestion for IMF mostly containing native casein micelles. As a result, the resistance of caseins upon gastric digestion tended to increase and the nutrient delivery to the intestinal compartment was supposed to be delayed leading to lower degree of hydrolysis and overall apparent protein digestibility. In contrast, linear protein strands were formed for IMFs containing casein micelle-bound whey proteins in the middle of gastric digestion and low-size protein particles were observed for IMF containing partial disintegrated casein micelles in the latter period of gastric digestion. While α-LA and β-LG were resistant to gastric hydrolysis in their native and denatured forms, the susceptibility of LF to pepsin was significantly enhanced for its denatured form.

The impact of the protein structures within IMF on the peptidome release was evidenced, particularly on the peptide clusters significantly associated to LF and β-LG. A slower release of peptides from the IMF containing native casein micelles was observed, on the contrary to the greater peptide resistance of the IMF containing native LF. Bioactive peptides were more abundant for the IMFs having a whey protein profile close to that of human milk, due to a greater number of casein-derived bioactive peptides. This may have physiological relevance for the infants. Further *in vivo* study is warranted to evaluate whether these peptides would survive the action of brush border enzymes and be further absorbed.

Main messages

- Protein coagulation during gastric digestion depends on the casein micelle structure in IMFs

- Native and denatured whey proteins, except denatured LF, are resistant to pepsinolysis

- Digestive dynamic conditions impact the protein behaviour during gastric digestion and consequently during intestinal digestion

- Protein structures within IMFs impact the peptide release during the gastrointestinal digestion of IMFs.

- The nature and abundance of bioactive peptides are function of the IMF whey protein profile as well as of the heating conditions.

Chapter 8: general discussion

Des traitements thermiques (pasteurisation, stérilisation) sont appliqués pendant la fabrication des PPNs afin d'assurer la sécurité sanitaire et la stabilité du produit. Néanmoins, ces traitements sont susceptibles d'altérer les constituants natifs du lait bovin et notamment les protéines. Ces altérations peuvent avoir des conséquences nutritionnelles chez le nourrisson car potentiellement impactant les cinétiques de protéolyse, et par conséquent, le métabolisme protéique (Lacroix et al., 2008). L'objectif de cette étude était alors de mieux comprendre le comportement lors du traitement thermique des protéines dans des PPNs modèles (cinétique de dénaturation, structure et propriétés physico-chimiques des agrégats thermo-induits) et leur devenir lors de la digestion gastro-intestinale simulée *in vitro*.

Trois PPNs modèles ont été développées et se différenciaient uniquement par leur profil en protéines du lactosérum. La PPN Contrôle avait un profil en protéines du lactosérum identique à celui du lait bovin. Les PPNs LF[+] ou LF[+] α-LA[+] étaient supplémentées en LF ou LF et α-LA, respectivement, dans les mêmes quantités que celles du lait maternel mature. Les trois PPNs ont été formulées et traités thermiquement à 5.5% protéines ou à 1.3% protéines, correspondant aux concentrations protéiques auxquelles sont appliqués les traitements thermiques au cours de la fabrication des PPNs en poudre ou liquides. Pour une teneur protéique équivalente (13 g/L), la quantité estimée de tryptophane, l'acide aminé limitant pour les PPNs, était au niveau de la teneur réglementaire (0.19 g/L; European Union, 2016) pour la PPN contrôle (0.19 g/L) ou juste en dessous pour la PPN supplémentée en LF (0.16 g/L), contrairement à la PPN supplémentée en α-LA et LF (0.30 g/L). Ainsi, la supplémentation en α-LA et LF des PPNs permettrait de diminuer la teneur en protéine à la teneur minimale réglementaire (11 g/L) tout en respectant l'aminogramme réglementaire. Il serait nécessaire de le confirmer en quantifiant le tryptophane en HPLC après hydrolyse alcaline (Draher & White, 2019; European Union, 2000), la méthode de quantification étant en cours de développement au laboratoire.

Dans la première partie de la thèse, les cinétiques de dénaturation des protéines majeures du lactosérum (α-LA, β-LG et LF) ont été étudiées à des températures comprises entre 67.5°C et 80°C, selon le profil protéique des PPNs et leur teneur en matière sèche (Chapitre 4). Les cinétiques de dénaturation thermique des protéines laitières ont largement été étudiées pour des solutions protéiques (Loveday et al., 2014; Wolz & Kulozik, 2015) ou pour le lait bovin (Dannenberg & Kessler, 1988; Liu et al., 2020; Oldfield et al., 1998), mais très peu pour les PPNs (Wazed et al., 2020). Nous avons ainsi montré que, tel qu'observé pour le lait bovin, la vitesse de dénaturation de l'α-LA était augmentée en présence de β-LG (Dalgleish et al., 1997; Schokker et al., 2000; Wehbi et al., 2005). En présence de LF, la cinétique de l'α-LA n'était pas modifiée, tandis que celle de la β-LG était augmentée. A notre connaissance, cette étude est la première qui met en évidence l'implication de la LF sur les cinétiques de dénaturation de l'α-LA et la β-LG. La cinétique de dénaturation de la LF était indépendante de l'α-LA et la β-LG.

L'augmentation de la teneur en matière sèche des PPNs avant traitement thermique ralentissait la cinétique de dénaturation protéique uniquement pour les PPNs contenant de la β-LG. Au contraire, les cinétiques de dénaturation protéique étaient indépendantes de la teneur en matière sèche pour la PPN supplémentée en α-LA et LF. De plus, la PPN supplémentée en α-LA et LF présentait un taux estimé de protéines natives supérieur aux hautes températures et/ou pour de longues durées de traitement en comparaison aux autres PPNs. Ainsi, la supplémentation en α-LA et LF des PPNs permettrait pour un traitement thermique équivalent d'obtenir une teneur en protéines natives supérieure aux PPNs actuellement commercialisées. Néanmoins, des études supplémentaires sur l'impact de la supplémentation en α-LA et LF sur les propriétés techno-fonctionnelles (évolution de viscosité, stabilité au stockage, etc.) des PPNs sont nécessaires pour optimiser les paramètres de production pour une telle PPN.

Dans une seconde partie de thèse, les PPNs ont été traitées à 67.5°C ou 80°C pour un taux de dénaturation global des protéines de lactosérum de 65%, taux moyen déterminé dans des PPNs commerciales (65 ± 11%, n = 4). En variant le profil protéique et la teneur en matière sèche des PPNs ainsi que la température et la durée du traitement, 18 structures protéiques ont été générées et caractérisées (Figure 59) (Chapitre 5). Ces structures ont été analysées par AF$_4$ et confirmé par microscopie électronique à transmission uniquement pour les PPNs traitées à 1.3% protéines. Avant traitement thermique, l'ajout de LF dans les PPNs a conduit à la désintégration partielle des micelles de caséines. Après traitement thermique et en présence d'α-LA et de β-LG, les protéines dénaturées formaient principalement des agrégats solubles pour les PPNs traitées à 1.3% protéines tandis qu'elles se fixaient à la surface des micelles de caséines après traitement à 5.5% protéines. En présence de LF, les protéines dénaturées se fixaient exclusivement à la surface des micelles de caséines, soit sous forme d'agrégats filamenteux en présence d'α-LA et de β-LG, soit plus uniformément sur les micelles de caséines en présence d'α-LA et en quasi-absence de β-LG.
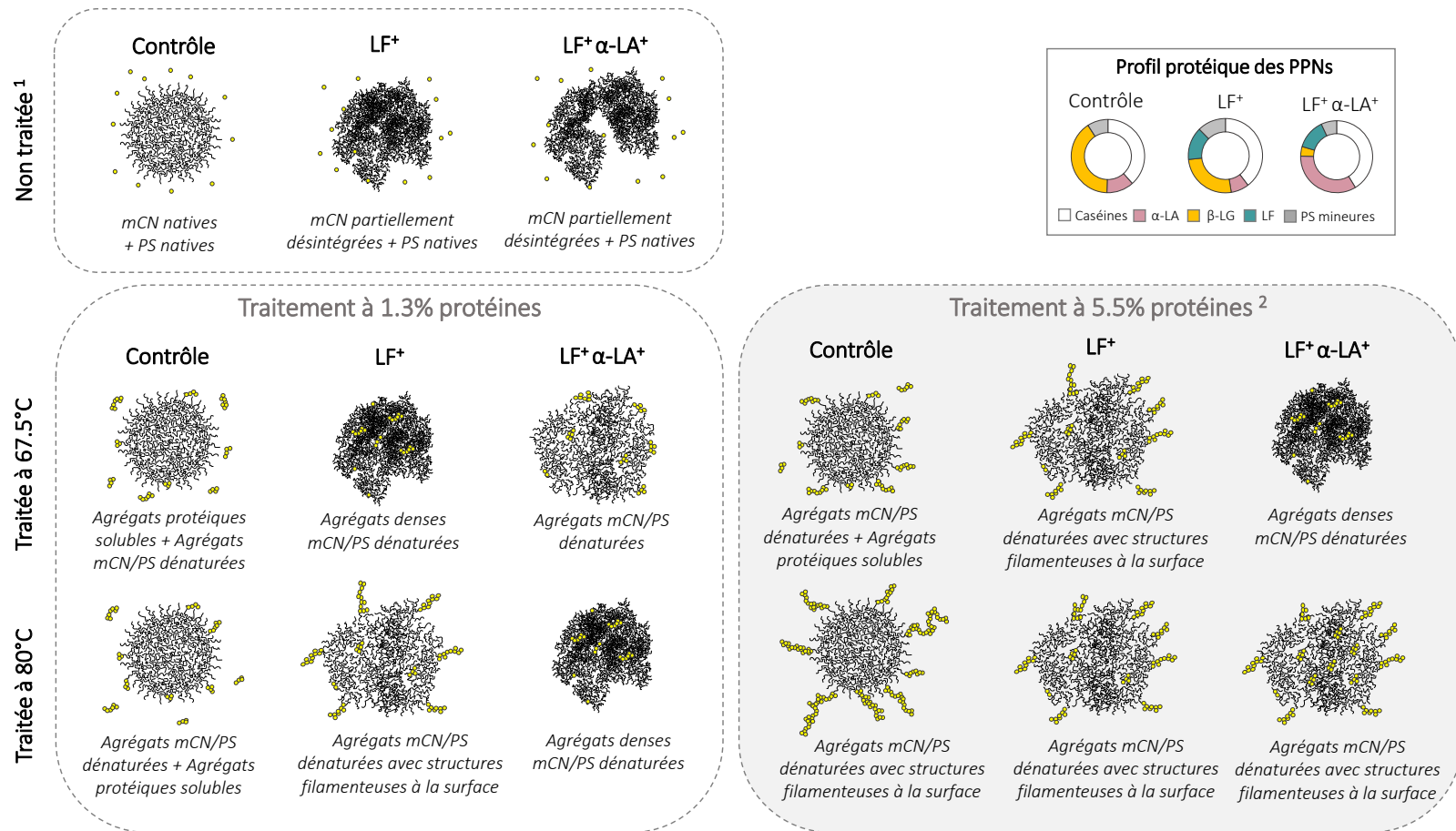
Figure 59. Schéma récapitulatif des structures protéiques des PPNs générées en variant le profil protéique et le taux en matière sèche des PPNs avant traitement thermique ainsi que la température de traitement

[1] Les structures protéiques des PPNs non chauffées sont considérées identiques aux deux teneurs en matière sèche des PPNs (1.3% ou 5.5% protéines)

[2] Les structures protéiques des PPNs traitées à 5.5% protéines ont été uniquement caractérisées par AF4, contrairement à celles des PPNs à 1.3% protéines, caractérisées par AF4 et microscopie électronique à transmission

mCN : micelles de caséines; PS : protéines du lactosérum

Enfin, en dernière partie de thèse, le devenir de ces structures protéiques au cours de la digestion a été étudié *in vitro*. Un modèle de digestion mimant la digestion chez le nourrisson a été utilisé en conditions statiques dans un premier temps (Chapitre 6) puis dynamiques dans un second temps (Chapitre 7).

Pour l'étude en conditions statiques, seules les PPNs contrôle ou supplémentée en α-LA et LF ont été étudiées, les profils en protéines du lactosérum de ces PPNs étant proches de ceux des PPNs commerciales ou du lait maternel, respectivement. Cette étude a montré que les structures protéiques des PPNs avaient un impact sur le devenir des protéines au cours de la digestion (Tableau 19). Tout d'abord, la taille du coagulum en fin de digestion gastrique variait fortement en fonction de la structure protéique des IMFs. Le coagulum formé était de plus grande taille pour la PPN dont les micelles de caséines et les protéines de lactosérum étaient sous forme native, un coagulum de taille intermédiaire était observé pour les PPNs dont les micelles de caséines étaient en interaction à leur surface avec des protéines du lactosérum dénaturées, et un coagulum de plus petite taille se formait pour la PPN dont les micelles de caséines étaient partiellement désintégrées. Le coagulum de plus grande taille semblait alors limiter l'accès de la pepsine, résultant en une hydrolyse des caséines ayant tendance à être ralentie. Ainsi, l'ajout d'α-LA et LF dans les PPNs pourrait être une voie intéressante pour réduire la taille du coagulum formé au cours de la digestion gastrique des PPNs chez le nourrisson, qui pourrait être responsable du temps de vidange gastrique plus élevé pour les PPNs que pour le lait maternel, avec des temps de demi-vidange de 78 et 54 min, respectivement (Bourlieu et al., 2014). D'autres méthodes ont été proposées afin de réduire la taille du coagulum gastrique après ingestion de PPNs telles que la déphosphorylation de la β-caséine bovine (Li-Chan & Nakai, 1989), la réduction de la teneur en calcium (Huppertz & Lambers, 2020; Wang et al., 2018), ou la substitution du lait bovin par du lait de chèvre (Ye, Cui, et al., 2019). Au cours de notre étude, il est à noter que la taille de particules n'a été observée qu'en fin de digestion gastrique. Un suivi en cours de digestion est nécessaire et a été réalisée au cours de la digestion dynamique, couplé à une observation microscopique. De plus, des études supplémentaires sont nécessaires en conditions *in vivo* afin de prendre en considération les mouvements physiques (mouvements péristaltiques) et leurs effets sur la formation du coagulum. En effet, De oliveira (2016) a montré que la taille du coagulum formé chez le prématuré pendant la digestion gastrique de lait maternel était supérieure en condition *in vivo* qu'en condition *in vitro* dynamique. La composition plus complexe du chyme *in vivo* pourrait partiellement expliquer ces différences (e.g. mucines).
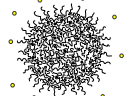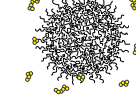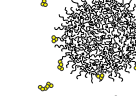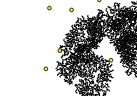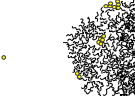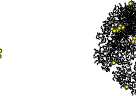
Par ailleurs, l'α-LA, aussi bien native ou dénaturée sous la forme d'agrégats solubles ou fixée à la surface des micelles de caséines, était résistante à l'hydrolyse par la pepsine. La β-LG était également résistante à l'hydrolyse par la pepsine sous sa forme native, tandis que sa résistance sous la forme dénaturée dépendait de la structure protéique. La β-LG dénaturée était plus résistante à la protéolyse sous la forme d'agrégats solubles (i.e. PPN contrôle traitée à 1.3% protéines) que d'agrégats fixés à la surface des
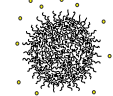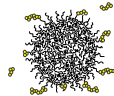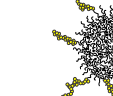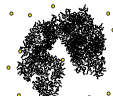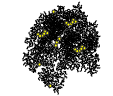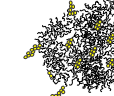
micelles de caséines (i.e. PPN contrôle traitée à 5.5% protéines). A notre connaissance, aucune étude n'a mis en évidence cette différence de sensibilité à la pepsine de la β-LG dénaturée selon sa localisation en solution (i.e. sous forme d'agrégats solubles ou fixée à la surface des micelles de caséines). Seule une étude a montré que la susceptibilité de la β-LG à la pepsine était supérieure lorsque la protéine était à la surface des gouttelettes lipidiques qu'en solution (Macierzanka et al., 2009). Des expérimentations complémentaires pourraient être menées pour confirmer cette différence de susceptibilité à l'hydrolyse de la β-LG dénaturée selon sa localisation en solution, notamment en fixant ou non les agrégats sur un support inerte et en suivant son hydrolyse biochimiquement et visuellement, sous microscope.

Enfin, la LF sous sa forme native était résistante à la protéolyse, contrairement à sa forme dénaturée, quasiment totalement hydrolysée en fin de digestion gastrique. La cinétique d'hydrolyse de la LF dénaturée dépendait alors du degré de dénaturation de celle-ci. La LF dénaturée à 97 ± 1% (PPN traitée à 1.3% protéines) ou à 95 ± 1% (PPN traitée à 5.5% protéines à 80°C) était plus sensible à la pepsine que la LF dénaturée à 82 ± 1% (PPN traitée à 5.5% à 67.5°C). Cette observation nous a conduits à nous poser la question de l'intérêt de la supplémentation des PPNs en LF, dans la mesure où les PPNs sont systématiquement traités thermiquement et que le traitement thermique induisait une dénaturation quasi-totale de la LF. En effet, pour que la LF assure ses propriétés physiologiques chez le nourrisson, elle doit résister à la digestion gastro-intestinale afin de se fixer sur des récepteurs situés sur la paroi intestinale. Néanmoins, on peut supposer que les peptides libérés par la pepsinolyse de la LF dénaturée aient un intérêt nutritionnel pour le nourrisson (Tomita et al., 1991). Parmi ces peptides, nous avons mis en évidence le fragment 50 kDa, dont les propriétés antimicrobiennes et antifongiques sont équivalentes à celles de la LF native (Rastogi, Nagpal, et al., 2014; Rastogi, Singh, et al., 2014; Sharma et al., 2013). Cependant, il est apparu en condition dynamique que celui-ci n'était pas résistant à l'hydrolyse intestinale dans la PPN traitée thermiquement, contrairement à la PPN non traitée. Des études supplémentaires en conditions *in vivo* sont donc nécessaires pour confirmer ces propriétés pour la PPN chauffée supplémentée en α-LA et LF. De plus, afin de s'assurer de l'avantage nutritionnel de la supplémentation des PPNs en LF, une protection de la LF à la dénaturation thermique par son encapsulation pourrait être envisagée (Darmawan et al., 2020; Jiang et al., 2020). Par ailleurs, la LF pourrait également être ajoutée aux dernières étapes du procédé de fabrication, sous réserve de sa bonne qualité microbiologique. Enfin, les traitements thermiques classiquement utilisés pour garantir la qualité sanitaire pourraient être remplacés par des technologies de décontamination moins dénaturantes, telles que la microfiltration ou le traitement par hautes pressions. En effet, la microfiltration améliore la qualité bactérienne du lait bovin tout en limitant les modifications de structure des protéines (Ceja-Medina et al., 2020; Fagnani et al., 2016; Griep et al., 2018; Verruck et al., 2019). De plus, le traitement par hautes pressions semble également être une alternative intéressante,

du fait de la diminution de la dénaturation des protéines en comparaison à des traitements thermiques type pasteurisation (Mayayo et al., 2014; Wazed & Farid, 2019).

Tableau 19. Tableau récapitulatif de la relation entre la structure protéique des PPNs traitées à 1.3% protéines (A) ou 5.5% protéines (B) et le devenir des protéines au cours de la digestion *in vitro* en condition statique

A

PPN		Contrôle			LF+α-LA+		
Condition thermique		Non traitée	Traitée à 67.5°C	Traitée à 80°C	Non traitée	Traitée à 67.5°C	Traitée à 80°C
Structure protéique des PPNs		*mCN natives + PS natives*	*Agrégats protéiques solubles + Agrégats mCN/PS dénaturées*	*Agrégats mCN/PS dénaturées + Agrégats protéiques solubles*	*mCN partiellement désintégrées + PS natives*	*Agrégats mCN/PS dénaturées*	*Agrégats denses mCN/PS dénaturées*
En fin de phase gastrique	Diamètre des particules (µm)	82.4 ± 0.7	9.2 ± 0.4	11.2 ± 2.0	1.2 ± 0.4	11.4 ± 2.9	11.5 ± 2.4
	Protéines résiduelles intactes (%)						
	Caséines	7 ± 2	4 ± 1	3 ± 1	4 ± 0	4 ± 0	4 ± 0
	α-LA	80 ± 5	71 ± 8	72 ± 3	75 ± 14	67 ± 12	60 ± 13
	β-LG	> 100 [1]	97 ± 2	> 100 [1]		n.d.	
	LF		n.d.		94 ± 14 [a]	14 ± 2 [b]	7 ± 1 [c]
	Degré d'hydrolyse (%)	2 ± 0	1 ± 0	1 ± 0	3 ± 0	4 ± 0	2 ± 1
En fin de phase intestinale	Degré d'hydrolyse (%)	32 ± 2 [c]	34 ± 1 [bc]	37 ± 2 [bc]	40 ± 1 [b]	61 ± 0 [a]	60 ± 2 [a]
	Bioaccessibilité des acides aminés (%)						
	Essentiel	34 ± 2 [ab]	36 ± 3 [ab]	36 ± 1 [ab]	33 ± 1 [b]	38 ± 1 [a]	37 ± 1 [ab]
	Non essentiel	10 ± 1	11 ± 2	10 ± 1	11 ± 2	13 ± 1	13 ± 1

B	PPN	Contrôle			LF⁺ α-LA⁺		
	Condition thermique	Non traitée	Traitée à 67.5°C	Traitée à 80°C	Non traitée	Traitée à 67.5°C	Traitée à 80°C
	Structure protéique des PPNs [2]	*mCN natives + PS natives*	*Agrégats mCN/PS dénaturées + Agrégats protéiques solubles*	*Agrégats mCN/PS dénaturées avec structures filamenteuses à la surface*	*mCN partiellement désintégrées + PS natives*	*Agrégats denses mCN/PS dénaturées*	*Agrégats mCN/PS dénaturées avec structures filamenteuses à la surface*
En fin de phase gastrique	Diamètre des particules (µm)	82.4 ± 0.7	16.4 ± 3.9	15.6 ± 2.0	1.2 ± 0.4	18.7 ± 8.2	16.9 ± 3.5
	Protéines résiduelles intactes (%)						
	Caséines	7 ± 2	5 ± 0	4 ± 1	4 ± 0	3 ± 1	3 ± 1
	α-LA	80 ± 5	70 ± 12	77 ± 23	75 ± 14	68 ± 16	65 ± 14
	β-LG	> 100 [1]	90 ± 16	86 ± 16		n.d.	
	LF		n.d.		94 ± 14 [a]	33 ± 1 [b]	11 ± 2 [b]
	Degré d'hydrolyse (%)	2 ± 0 [b]	2 ± 0 [bc]	0 ± 1 [c]	3 ± 0 [a]	2 ± 0 [ab]	2 ± 1 [b]
En fin de phase intestinale	Degré d'hydrolyse (%)	32 ± 2 [c]	57 ± 2 [a]	56 ± 3 [a]	40 ± 1 [b]	57 ± 3 [a]	55 ± 1 [a]
	Bioaccessibilité des acides aminés (%)						
	Essentiel	34 ± 2	34 ± 1	36 ± 2	33 ± 1	35 ± 2	34 ± 1
	Non essential	10 ± 1	10 ± 1	10 ± 1	11 ± 2	11 ± 1	11 ± 0

[1] La proportion en β-LG native résiduelle supérieure à 100% peut être expliquée par un élargissement de la bande de la β-LG lors de l'analyse de l'électrophorégramme et/ou par une co-élution des produits d'hydrolyse des protéines ayant un poids moléculaire supérieur à celui de la β-LG (les caséines par exemple)

[2] Les structures protéiques des PPNs traitées à 5.5% protéines sont à considérer avec précautions, les limites de l'AF₄ ayant été probablement atteintes.

mCN : micelle de caséines; PS : protéine du lactosérum ; n.d: non déterminé. Les différentes lettres en exposant représentent une différence significative entre colonnes, c'est-à-dire entre traitements imbriqués dans les PPNs (p < 0.05). L'analyse statique a été réalisée en utilisant un modèle linéaire mixte pour mesures répétées avec le temps de digestion, la PPN et le traitement imbriqué dans la PPN comme facteurs fixes, et les réplicas de digestion comme facteurs aléatoires

En comparaison au modèle de digestion statique, le modèle dynamique est plus proche physiologiquement de la digestion chez l'Homme car l'évolution de l'acidification en phase gastrique, les flux d'enzymes et de secrétions et les vidanges gastro-intestinales sont régulées. Ainsi, la même étude a été réalisé en condition dynamique en utilisant le système DIDGI® pour les PPNs traités à 1.3% protéines, non chauffée ou chauffée à 80°C, l'étude statique ayant montré que les cinétiques de digestion étaient similaires pour les PPNs traitées à 67.5°C ou 80°C.

Les résultats de l'étude de l'impact de la structure protéique des PPNs sur la digestion en conditions dynamiques sont synthétisés au Tableau 21, et comparés aux résultats obtenus en conditions statiques. Il est important de rappeler qu'un scale-up du traitement thermique a été nécessaire, le volume requis pour la digestion en condition statique (20 mL) étant inférieur à celui en condition dynamique (150 mL). Le traitement thermique a donc été optimisé afin de maintenir les combinaisons température/temps, notamment par un pré-traitement à 53.5°C pour les plus grands volumes. Les taux de dénaturation thermique avant et après scale-up ont été jugés équivalents (Tableau 20) et il a été supposé que les structures protéiques après le scale-up du traitement thermique étaient identiques à celles précédemment caractérisées.

Tableau 20. Taux de dénaturation protéique des PPNs traitées à 1.3% protéines et à 80°C pour les études de digestion *in vitro* en conditions statique ou dynamique

Taux de dénaturation (%)	Contrôle		LF⁺α-LA⁺	
	Condition statique	Condition dynamique	Condition statique	Condition dynamique
PS totales	63 ± 0	69 ± 0	68 ± 2	68 ± 0
α-LA	42 ± 1	44 ± 1	52 ± 3	56 ± 0
β-LG	69 ± 0	76 ± 1	/	/
LF	/	/	98 ± 0	98 ± 0

PS : protéines du lactosérum.
Un scale-up du traitement thermique des PPNs a été nécessaire pour l'étude de la digestion *in vitro* en condition dynamique en raison du volume de PPN plus élevé requis pour le modèle de digestion dynamique (150 ml) que pour le modèle de digestion statique (20 ml). Le protocole du scale-up est détaillé au chapitre 3 - section 4.2.

Comme pour la digestion statique, la déstabilisation des protéines en phase gastrique dépendait de la structure des micelles de caséines dans les PPNs. A pH gastrique quasi-équivalent (pH 5.3 en condition statique et pH 5.6 en condition dynamique), la taille du coagulum était du même ordre de grandeur pour les PPNs contenant des micelles de caséines en interaction avec des protéines du lactosérum dénaturées en conditions statique et dynamique. Au contraire, la taille du coagulum pour la PPN contrôle non chauffée était environ 6 fois plus importante en condition dynamique que statique. Des observations similaires ont été rapportées par Egger et al. (2019) au cours de la digestion du lait bovin

en conditions statique ou dynamique. En revanche, la taille des particules protéiques pour la PPN contenant des micelles de caséines partiellement désintégrées était presque 10 fois inférieure en condition dynamique que statique. Cette différence de coagulation en conditions statique et dynamique pourrait être expliquée par le pH constant en condition statique vs une acidification progressive en condition dynamique, ainsi que par l'ajout simple vs continu des enzymes en conditions statique vs dynamique. De plus, l'α-LA et la β-LG sous leur forme native et dénaturée étaient résistante à la protéolyse. Néanmoins, la quantité en α-LA et β-LG résiduelle intacte était supérieure en fin de phase gastrique en condition dynamique qu'en condition statique, excepté pour l'α-LA pour la PPN contrôle non chauffée. La LF sous sa forme native était également résistante à la pepsinolyse, tandis que sous sa forme dénaturée, la LF était hydrolysée par la pepsine. Au contraire, la quantité de protéine résiduelle intacte était inférieure en fin de phase intestinale pour la LF native.

En fin de phase intestinale, les degrés d'hydrolyse étaient identiques entre PPNs (46 ± 4%) et supérieurs à ceux déterminés en conditions statiques, excepté pour la PPN LF$^+$ α-LA$^+$ chauffée. La même différence sur le degré d'hydrolyse en phase intestinale entre conditions statique et dynamique a été observée par Le Roux, (2019). Ceci pourrait être expliqué par le mode d'ajout des enzymes digestives, en une fois et au début de la réaction en condition statique et en continu en condition dynamique. L'ajout des enzymes en continu pourrait limiter la diminution de l'activité enzymatique suite à l'autolyse enzymatique. De plus, l'absence de vidange gastrique en condition statique pourrait conduire à une inhibition des enzymes digestives par certains produits de protéolyse (Egger et al., 2019). Ce phénomène a également été démontré par Gauthier et al. (1982) qui ont suggéré que le remplacement des tampons et l'augmentation du taux de vidange pourraient réduire l'inhibition de l'activité enzymatique par les produits de la digestion. En fin de phase intestinale, la digestibilité protéique instantanée (92 ± 5%) était identique entre PPNs tandis que la digestibilité protéique globale était inférieure pour la PPN formant un coagulum de plus grande taille en phase gastrique par rapport à celle des autres PPNs (73 ± 2% vs 87 ± 4%, respectivement), probablement due à un ralentissement de la vidange gastrique du coagulum.

L'analyse peptidique des digesta a montré que la majorité des peptides libérés était issue de l'hydrolyse de la β-caséine. La nature et l'abondance des peptides libérés variaient en fonction du profil protéique et du traitement thermique des PPNs. Par ailleurs, les peptides bioactifs libérés en phase intestinale étaient plus nombreux et plus résistants à l'hydrolyse intestinale pour la PPN LF$^+$ α-LA$^+$ (profil α-LA et LF) en comparaison à la PPN Contrôle (profil α-LA et β-LG). Les cinétiques de libération des peptides bioactifs variaient également en fonction des conditions thermiques, pour chacune des PPNs.

Tableau 21. Tableau récapitulatif de la relation entre la structure protéique des PPNs traitées à 1.3% protéines et le devenir des protéines au cours de la digestion *in vitro* en condition dynamique – comparaison avec la digestion *in vitro* en condition statique

PPN		Contrôle				LF⁺α-LA⁺			
Condition thermique		Non traitée		Traitée à 80°C		Non traitée		Traitée à 80°C	
Modèle *in vitro* de digestion		Statique	Dynamique	Statique	Dynamique	Statique	Dynamique	Statique	Dynamique
Phase gastrique [1]	Diamètre des particules (µm)	82.4 ± 0.7	526.3 ± 51.1	11.2 ± 2.0	13.7 ± 1.2	1.2 ± 0.4	0.1 ± 0.0	11.5 ± 2.4	21.5 ± 1.0
	Protéines résiduelles intactes (%)								
	Caséines	7 ± 2	9 ± 2	3 ± 1	15 ± 1	4 ± 0	13 ± 4	4 ± 0	11 ± 2
	α-LA	80 ± 5	66 ± 30	72 ± 3	89 ± 6	75 ± 14	> 100	60 ± 13	> 100
	β-LG	68 ± 17	> 100	65 ± 9	> 100		n.d.		
	LF		n.d.			94 ± 14	65 ± 18	7 ± 1	10 ± 3
	Degré d'hydrolyse (%)	2 ± 0	5 ± 1	1 ± 0	4 ± 0	3 ± 0	7 ± 1	2 ± 1	6 ± 0
Phase intestinale [1]	Degré d'hydrolyse (%)	32 ± 2	42 ± 2	37 ± 2	49 ± 2	40 ± 1	46 ± 3	60 ± 2	49 ± 1
	Bioaccessibilité des acides aminés (%)								
	Essentiel	34 ± 2	29 ± 0	36 ± 1	33 ± 1	33 ± 1	34 ± 1	37 ± 1	36 ± 0
	Non essentiel	10 ± 1	9 ± 1	10 ± 1	10 ± 1	11 ± 2	11 ± 0	13 ± 1	13 ± 0
	Digestibilité (%)								
	Globale	n.d.	73 ± 2	n.d.	87 ± 6	n.d.	85 ± 2	n.d.	88 ± 4
	Instantanée	n.d.	95 ± 4	n.d.	92 ± 6	n.d.	86 ± 2	n.d.	92 ± 3

n.d: non déterminé

[1] Les données ont été déterminées en fin de chacune des phases digestives en conditions statique (60 min) ou dynamique (180 min), excepté pour le diamètre des particules, comparé à pH ± équivalent en condition statique (pH 5.3 ; 60 min de digestion) ou dynamique (pH 5.6 ; 80 min de digestion)

Nous nous sommes heurtés à plusieurs contraintes au cours de ce travail de thèse. La première difficulté a été la solubilisation des ingrédients pour les PPNs à 5.5% protéines. La première étape de la préparation des PPNs consistait en la préparation d'une solution de lactose dans l'eau MilliQ à 30% (w/w). Or, à température ambiante, la solubilisation du lactose dans l'eau est d'environ 20% (w/w) (Fox et al., 2015). Pour pallier cela, nous avons choisi d'optimiser la solubilisation du lactose en chauffant la solution lactosée à environ 50°C, température optimale pour la solubilisation du lactose dans l'eau à une concentration 40%. De plus, le choix des ingrédients s'est fait selon la réglementation européenne (European Commission, 2006), qui autorise l'ajout de calcium sous la forme de sels de calcium de l'acide orthophosphorique ou de chlorure de calcium (parmi d'autres sources). Notre premier choix de source de calcium était alors le tri-calcium di-orthophosphorique. Néanmoins, sa solubilisation est très faible dans l'eau (1.2 mg/L à 20°C), ce qui s'est manifesté par un dépôt blanc lors de la fabrication des PPNs. Le choix de la source de calcium des PPNs s'est alors tourné vers le chlorure de calcium, dont la solubilisation est supérieure (745 g/L dans l'eau à 20°C). Cela nous a donc amené à nous questionner sur la solubilisation des ingrédients lors de la fabrication des PPNs, celle-ci pouvant altérer la qualité nutritionnelle du produit fini mais également modifier les propriétés techno-fonctionnelles des PPNs au cours du procédé technologique.

De plus, les cinétiques de dénaturation protéique ont été étudiées par RP-HPLC après précipitation à pH 4.6 des formes protéiques dénaturées et des caséines. Néanmoins, cette procédure ne permet pas d'isoler les protéines uniquement sous la forme native car certaines formes non-natives restent solubles à pH 4.6 (par exemple, les formes glycosylées). Ceci s'est alors manifesté par une modification de la forme des pics des chromatogrammes des PPNs traitées à 5.5% protéines et/ou traitées à haute température et/ou traitées pendant une longue durée. Pour pallier cela, la gamme de températures (67.5°C-80°C) ainsi que les temps de traitement ont été définis afin de s'affranchir au mieux de l'apparition de ces formes modifiées. De plus, seuls les pics correspondant aux formes natives non-modifiées ont été considéré pour l'analyse des chromatogrammes.

L'étude de la digestion *in vitro* a été réalisé selon les protocoles mis en place dans notre laboratoire, en particulier par Ménard et al. (2018) pour le modèle statique et de Oliveira et al. (2016) pour le modèle dynamique, et ce afin de mimer la digestion des nourrissons. Ces auteurs proposent l'ajout de la lipase pancréatique et de la trypsine en phase intestinale *via* la pancréatine porcine. En effet, la pancréatine permet d'apporter l'ensemble des enzymes pancréatiques digestives en un seul ajout et est une solution économiquement avantageuse. La quantité de pancréatine à ajouter a été déterminée pour une activité lipase de 90 U/mL de contenu intestinal (Norman et al., 1972), correspondant alors dans les lots utilisés à une activité trypsine de 16 U/mL de contenu intestinal. Concernant l'activité de la trypsine dans le contenu intestinal du nourrisson à terme pendant la période postprandiale, quelques données sont

disponibles. En moyenne, entre 20 et 120 minutes après l'ingestion du repas, des valeurs de 30 μg/mL de contenu intestinal ont été déterminées chez 5 nourrissons à terme âgés de 10 jours (poids corporel de 3.5 kg) (Borgström et al., 1960) jusqu'à 81 μg/mL chez 3 nourrissons à terme âgés de 3 à 5 mois (poids corporel de 6.3 kg) (Borgström et al., 1960) ou 94 μg/mL chez 8 nourrissons à 8 jours (poids corporel de 3.8 kg) (Norman et al., 1972). Si nous supposons que toute la trypsine était active, cela correspond à des valeurs comprises entre 7 et 22 U de TAME/mL. Dans notre étude, la quantité de pancréatine apportant une activité lipasique de 90 U/mL correspondait à une activité trypsine de 7.1 U/mL, limite basse des activités reportées précédemment. Néanmoins, le degré d'hydrolyse pour la PPN contrôle chauffée à 80°C était proche de celui déterminé pour une PPN à base de lait bovin et pour une activité trypsique de 16 U/mL de contenu intestinal en fin de digestion intestinale en condition dynamique (49 ± 2% *vs* 50 ± 4%), mais inférieur en condition statique (37 ± 2% *vs* 47 ± 4%). Afin d'optimiser le protocole de digestion des nourrissons à terme en conditions *in vitro*, l'ajout de trypsine purifiée permettrait de respecter l'activité des enzymes individuelles chez le nourrisson à terme. De plus, il est important de rappeler que les modèles de digestion *in vitro* utilisés dans notre étude ne prennent pas en compte les enzymes de la bordure en brosse, du fait du peu de connaissance sur l'activité de celles-ci chez le nourrisson, de leur commercialisation limitée et de l'absence d'un consensus pour les conditions expérimentales à mettre en place (pH, tampons, rapport substrat :enzyme, temps d'incubation, etc) (Picariello et al., 2016). Une fois ces paramètres établis, les modèles de digestion *in vitro* utilisés dans notre étude pourraient être optimisés par l'ajout des enzymes de la bordure en brosse sous la forme de vésicules purifiées à partir de la muqueuse intestinale de l'intestin grêle porcin (Picariello et al., 2015).

D'autre part, comme discuté dans les chapitres 6 et 7, la déstabilisation des protéines au cours de la phase gastrique conduit à la formation de particules protéiques de plus ou moins grande taille selon la PPN considérée. Plus particulièrement, la PPN contrôle non traitée thermiquement formait les particules de plus grande taille (de l'ordre de la centaine de μm). Ainsi, l'hétérogénéité du bol gastrique rendait l'échantillonnage représentatif de la phase gastrique complexe. Afin de remédier à cela, le bol gastrique a été mélangé tout au long de la digestion *in vitro* et la verrerie adéquate a été utilisée pour l'échantillonnage. Cependant, certains résultats en conditions dynamiques, notamment les mesures de digestibilités globale ou instantanée, nous amènent à penser que cet échantillonnage n'était pas optimisé. Une autre méthode d'échantillonnage serait alors à réfléchir.

De plus, l'étude de la cinétique d'hydrolyse des protéines au cours de la phase gastrique par SDS-PAGE suivie d'une analyse densitométrique a montré une proportion de protéines résiduelles intactes supérieure à 100%. Ceci était notamment observé pour l'α-LA et la β-LG, résistantes à la pepsinolyse, probablement en raison de la co-élution de peptides provenant de la protéolyse de protéines de masse

moléculaire plus élevée telles que les caséines ou la LF. Ceci constitue une limite de l'analyse SDS-PAGE, technique d'analyse qui permet l'observation visuelle de l'hydrolyse protéique au cours de la digestion mais qui reste semi-quantitative. Outre la SDS-PAGE, qui reste une des méthodes les plus employées pour suivre l'hydrolyse protéique au cours de la digestion de protéines laitières, la méthode de RP-HPLC peut également être choisie mais reste elle aussi une méthode semi-quantitative du fait de la co-élution des protéines résiduelles natives et de leur produit d'hydrolyse enzymatique (Singh et al., 2014).

Enfin, il est important de rappeler que les PPNs développées dans notre étude étaient dépourvues de lipides, ce qui a permis de caractériser les structures protéiques par la méthode AF$_4$, la méthode n'étant pas optimisée à ce jour pour la caractérisation des structures protéiques en présence de lipides. Or, les lipides et les protéines interagissent lors du traitement thermique du lait de vache (Ye et al., 2004) ou des PPNs (Rowley & Richardson, 1985), ce qui peut altérer la digestion des protéines (Tunick et al., 2016). Au cours d'un projet concomitant au STLO (Nativif), une PPN ayant un profil protéique proche de celui de la PPN contrôle, traitée thermiquement à 5.5% protéines et contenant des lipides, a été développée. Au cours de sa digestion *in vitro* gastrique en condition dynamique, l'impact du traitement thermique sur la taille des particules était similaire à celui observé dans notre étude. De plus, les cinétiques de protéolyse des caséines et de l'α-LA n'étaient pas impactées par le traitement thermique, contrairement à la β-LG, tel qu'observé pour la PPN contrôle traitée à 5.5% protéines en condition statique. Enfin, le degré d'hydrolyse ainsi que la lipolyse n'étaient pas influencés par le traitement thermique.

General conclusion and perspectives

In the present study, we sought to understand the impact of whey protein formulation and heating on the protein structure generated within IMFs and its effects on protein digestion. The main results of the study are summarised in Table 22. IMFs were formulated by varying the whey protein profile to be close to that of mature human milk and the total solid content was chosen to mimic the manufacturing process of powdered or liquid IMFs. The study of the kinetics of protein denaturation for a temperature range of 67.5-80°C showed that the supplementation of IMFs with α-LA and LF had the advantages to slow down protein denaturation, either for diluted or concentrated phases.

Protein structures within IMFs were generated by varying several parameters: the protein profile of IMFs, the total solid of IMFs, and the heating temperatures. The characterisation of the protein entities in the IMFs showed that the supramolecular structures varied in term of protein composition, size, shape and the distribution of covalent and non-covalent interactions. The stability of proteins under the digestion conditions and the protein digestive behaviour, i.e. kinetics of protein hydrolysis and kinetics of release of proteolysis products, were function of the protein supramolecular structure. More precisely, we showed that, in absence of heat treatment, LF was resistant to hydrolysis during gastric digestion and in the first times of intestinal digestion, which could have nutritional benefits for infants. Moreover, in its native form, LF exerts some iron-binding properties, which could limit the oxidative damages, especially within IMFs enriched with DHA, an essential poly-unsaturated fatty acid prone to oxidation. Nevertheless, after heat treatment, the almost total denaturation of LF induced a greater pepsinolysis and probably altered the iron-binding properties of native LF. Further studies on the bioactive properties of peptides released during LF hydrolysis should be conducted to justify the nutritional interest of LF supplementation. Another possibility is the use of alternative technology to heat treatment, as microfiltration, to guarantee the microbiological safety of IMFs while preserving LF native protein structure. Despite the larger size of protein particles formed for all IMFs heated at higher total solid content (5.5% of proteins), the size of gastric coagulum, the protein digestion kinetics and the amino acid bioaccessibility were similar. Only the gastric hydrolysis of β-LG was enhanced for IMFs heated at 5.5% proteins, which impacted the intestinal hydrolysis.

This work has unravelled the complex relationships between protein structure and digestion behaviour in the context of IMFs. It has highlighted the importance of considering not only protein composition, but also the effect of the protein structure when talking about digestion. The present IMFs formulated in this study were not fully in accordance with the European regulation as they were free of lipids or added vitamins. It is well-known that lipids and proteins interact during heat treatment of bovine milk (Ye et al., 2004) or IMFs (Rowley & Richardson, 1985). However, it has been shown in a concomitant project studying complete IMFs with different levels of heat treatment that similar results to the present ones were obtained. Moreover, the heat treatment of IMFs was conducted at laboratory scale. Even if

the heating conditions were targeted to be in the range of protein denaturation extent of current commercialised IMFs, they did not correspond to heating conditions at industrial scale. The denaturation extent of individual whey protein and the whey protein/casein interactions are function of the heating temperature and the holding time (Qian et al., 2017). In addition, the manufacture of IMFs can generate shear stresses notably during the flow through pipes, pumps and heat exchangers, or during stirring, homogenisation and spraying (Rao, 2010). Flow induced-shear stress can alter the denaturation and aggregation of proteins (Bogahawaththa & Vasiljevic, 2020; Mediwaththe et al., 2018). Thus, it could be interesting to produce IMFs at an industrial scale that includes shear stresses to highlight their effects on the structure of the generated aggregates and the protein digestion behaviour, but also on performance of the production steps. Finally, even if the protein digestion pattern is comparable under *in vitro* or *in vivo* conditions (Egger et al., 2017, 2019), some physiological digestive specificities are missing from the current *in vitro* digestion models. *In vitro* static and dynamic digestion models do not reproduce the complex digestion mechanism, as the regulatory processes, particularly hormonal and nervous control allowing a feedback mechanism, the complexity of the peristaltic movements or the absorption process through the mucosal barrier. *In vivo* study with piglet models should be conducted to investigate the physiological consequences of the supplementation of IMFs with α-LA and LF. Other *in vitro* models could be considered to further investigate the intestinal absorption by using Caco-2 cells (Andersson et al., 2011; Goulart et al., 2014) or the Ussing chamber technique (He et al., 2013). This method could be particularly interesting to study the intestinal transport of the bioactive peptides that were released in this study and to bring some information on the impact of the supplementation of IMFs with α-LA and LF on their nutritional properties (Picariello et al., 2013).

Table 22. Highlights of the main results of the PhD project

Research steps			Main messages
Kinetics of heat-induced denaturation of whey proteins			• Heat denaturation of α-LA is reduced in the absence of β-LG • Heat denaturation of β-LG is enhanced in the presence of LF • Heat denaturation of LF is not modified by the presence of the other whey proteins • Whey protein heat denaturation is slowed down in concentrated IMFs containing β-LG
Characterisation of protein structures			• Before heating, LF induces partial casein micelle disintegration • In the heated LF-free IMFs, denatured whey proteins form either soluble aggregates at low total solid content or fix casein micelle surface at high total solid content • In the heated IMFs containing LF, denatured whey proteins cover casein micelles homogeneously in absence of β-LG or in the form of appendages in presence of β-LG • The molecular weight of the modified casein micelles increases and their shape changes with increasing total solid of IMFs
Kinetics of protein digestion	Gastric digestion	Protein particle	• Particles are larger for IMF containing native casein micelles • Particle size is intermediate for IMF containing denatured whey proteins as soluble aggregates or fixed on the casein micelle surface • Particles are smaller for IMF containing partial disintegrated casein micelles and native whey proteins
		Protein hydrolysis	• The casein proteolysis (tends to) slow for IMF containing native casein micelles • The α-LA proteolysis is similar in its native and denatured forms • The β-LG proteolysis is enhanced when the denatured protein is fixed on the casein micelle surface • The LF proteolysis is enhanced in its denatured form, depending on the extent of LF denaturation
	Intestinal digestion	Protein hydrolysis	• Under static conditions: protein hydrolysis is enhanced for IMFs containing denatured LF or denatured β-LG fixed on the casein micelle surface • Under dynamic conditions: similar protein hydrolysis among IMFs, except at 120 min of digestion with a slowdown of protein hydrolysis for IMF containing native casein micelles
		Essential amino acid bioaccessibility (at the end of digestion)	• Under static conditions, the bioaccessibility is higher for IMFs containing denatured LF at higher extent of denaturation • Under dynamic conditions, the bioaccessibility is lower for IMF containing native casein micelles
		Protein digestibility (at the end of digestion, under dynamic conditions)	• Overall protein digestibility is lower for IMF containing native casein micelles • Instantaneous protein digestibility is similar among IMFs
		Release of bioactive peptides (under dynamic conditions)	• Higher number of bioactive peptides released for IMFs containing LF • In overall, the resistance to intestinal digestion of bioactive peptides is higher for IMF containing LF in its native form than in its denatured form

Supplementary material

Supplementary Table 1. Composition of the infant milk formulas at 5.5% proteins

Elements		Control IMF	LF[+] IMF	LF[+] α-LA[+] IMF
Total proteins		5.66 ± 0.06	5.71 ± 0.05	5.54 ± 0.05
Whey proteins		3.52 ± 0.15	3.45 ± 0.01	3.18 ± 0.01
α-LA	*g / 100 g liquid meal*	6.82 ± 0.20	4.62 ± 0.22	19.77 ± 0.74
β-LG		24.32 ± 1.41	15.60 ± 0.79	0.26 [1]
LF		n.d.	8.17 ± 0.16	7.89 ± 0.39
Caseins		2.13 ± 0.11	2.26 ± 0.04	2.35 ± 0.03
Lactose		23.9 ± 1.8	24.3 ± 1.5	23.8 ± 0.7
Calcium		174.9 ± 3.1	173.7 ± 5.8	178.4 ± 3.1
Chloride		278.2 ± 7.1	294.4 ± 3.9	285.9 ± 1.8
Iron	*mg / 100 g liquid IMF*	1.8 ± 0.1	1.7 ± 0.1	1.8 ± 0.0
Inorganic phosphorus		89.4 ± 2.6	87.0 ± 5.4	88.0 ± 1.6
Potassium		254.5 ± 26.6	268.4 ± 5.4	264.1 ± 1.6
Sodium		91.1 ± 6.5	88.3 ± 5.1	105.8 ± 3.1
Ash	*%, w/w*	0.75 ± 0.2	± 0.2	0.68 ± 0.1

[1] Value of β-LG content in the LF[+] α-LA[+] IMF was estimated by calculation from the amount of β-LG in SMP and the proportion of SMP in the IMF
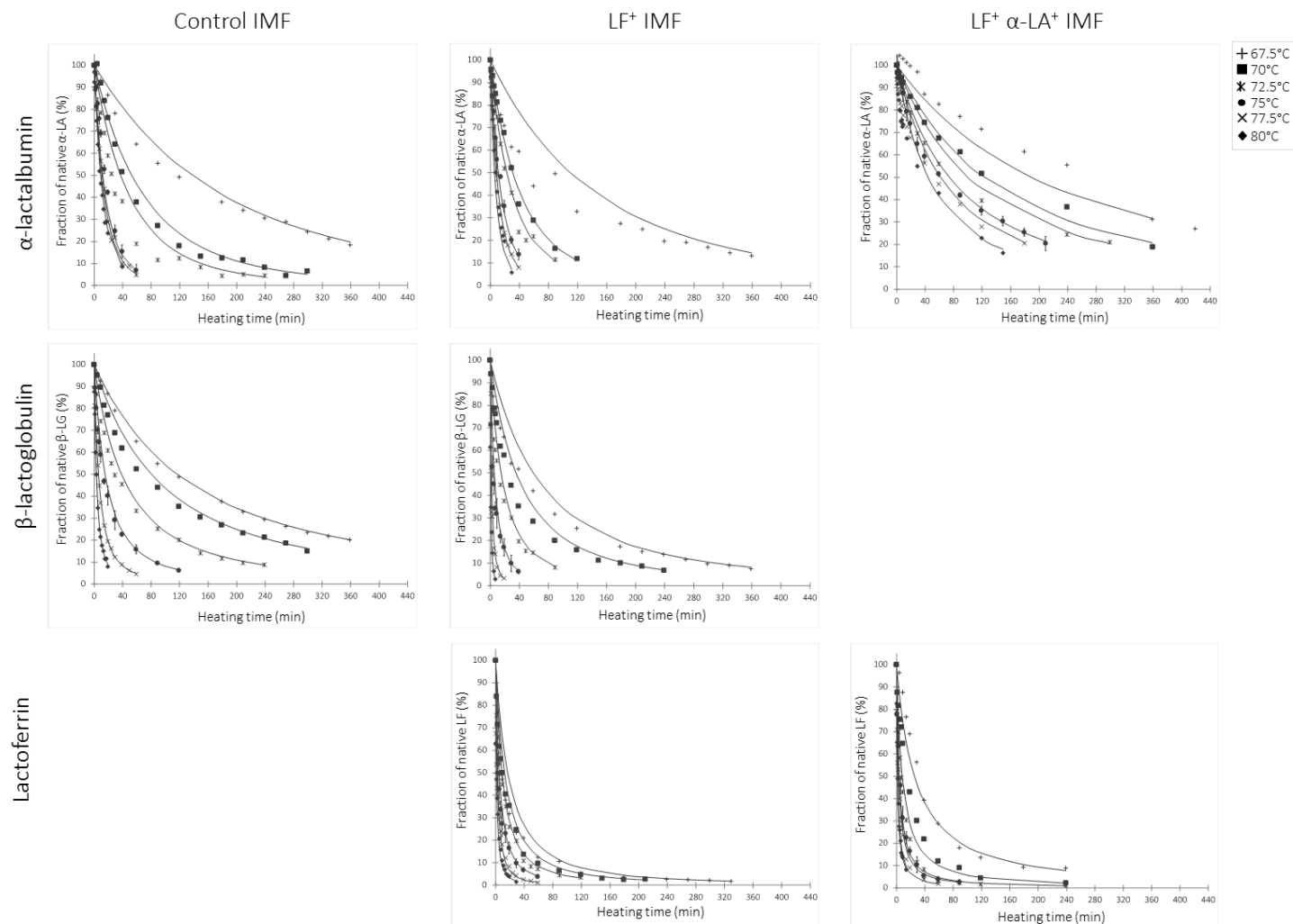
Supplementary Figure 1. Kinetics of heat denaturation of α-LA, β-LG and LF for the IMFs processed at 1.3% proteins at temperatures 67.5°C-80°C

Residual native fractions were calculated as a C_t/C_0 ratio. C_t (g.L^{-1}) is the native protein concentration at t holding time (min) and C_0 is the native protein concentration of unheated IMFs or protein solutions (g.L^{-1}). The results at 75°C represent means ± SD (n = 3).

Supplementary Table 2. Equations for the estimations of the native whey proteins fractions for the IMFs processed at 1.3% proteins

IMFs	Whey proteins		
	α-LA	β-LG	LF
Control	$\sqrt[-0.2]{1 + 0.2 \times e^{-27.35 \times \frac{1}{T+273}} \times e^{75.32} \times 1.36^{0.2} \times t}$	$\sqrt[-0.6]{1 + 0.6 \times e^{-36.67 \times \frac{1}{T+273}} \times e^{101.63} \times 5.07^{0.6} \times t}$	n.d.
LF$^+$	$\sqrt[-0.2]{1 + 0.2 \times e^{-26.51 \times \frac{1}{T+273}} \times e^{73.25} \times 1.02^{0.2} \times t}$	$\sqrt[-0.5]{1 + 0.5 \times e^{-44.92 \times \frac{1}{T+273}} \times e^{126.81} \times 3.35^{0.5} \times t}$	$\sqrt[-0.6]{1 + 0.6 \times e^{-24.36 \times \frac{1}{T+273}} \times e^{68.08} \times 1.72^{0.6} \times t}$
LF$^+$ α-LA$^+$	$\sqrt[-0.5]{1 + 0.5 \times e^{-13.27 \times \frac{1}{T+273}} \times e^{32.91} \times 3.87^{0.5} \times t}$	n.d.	$\sqrt[-0.8]{1 + 0.8 \times e^{-25.87 \times \frac{1}{T+273}} \times e^{72.75} \times 1.50^{0.8} \times t}$

The relations are determined from the equation $\frac{C_t}{C_0} = \sqrt[1-n]{\left(1 + (n-1) \times e^{\left(-\frac{E_a}{R} \times \frac{1}{T+273}\right)} \times k_{n,0} \times C_0^{n-1} \times t\right)}$. C_t (g.L^{-1}) corresponds to the protein content at holding time t (min), C_0 is the protein content in the unheated IMFs (g.L^{-1}). T corresponds to the heating temperature (°C). n.d. Non determined
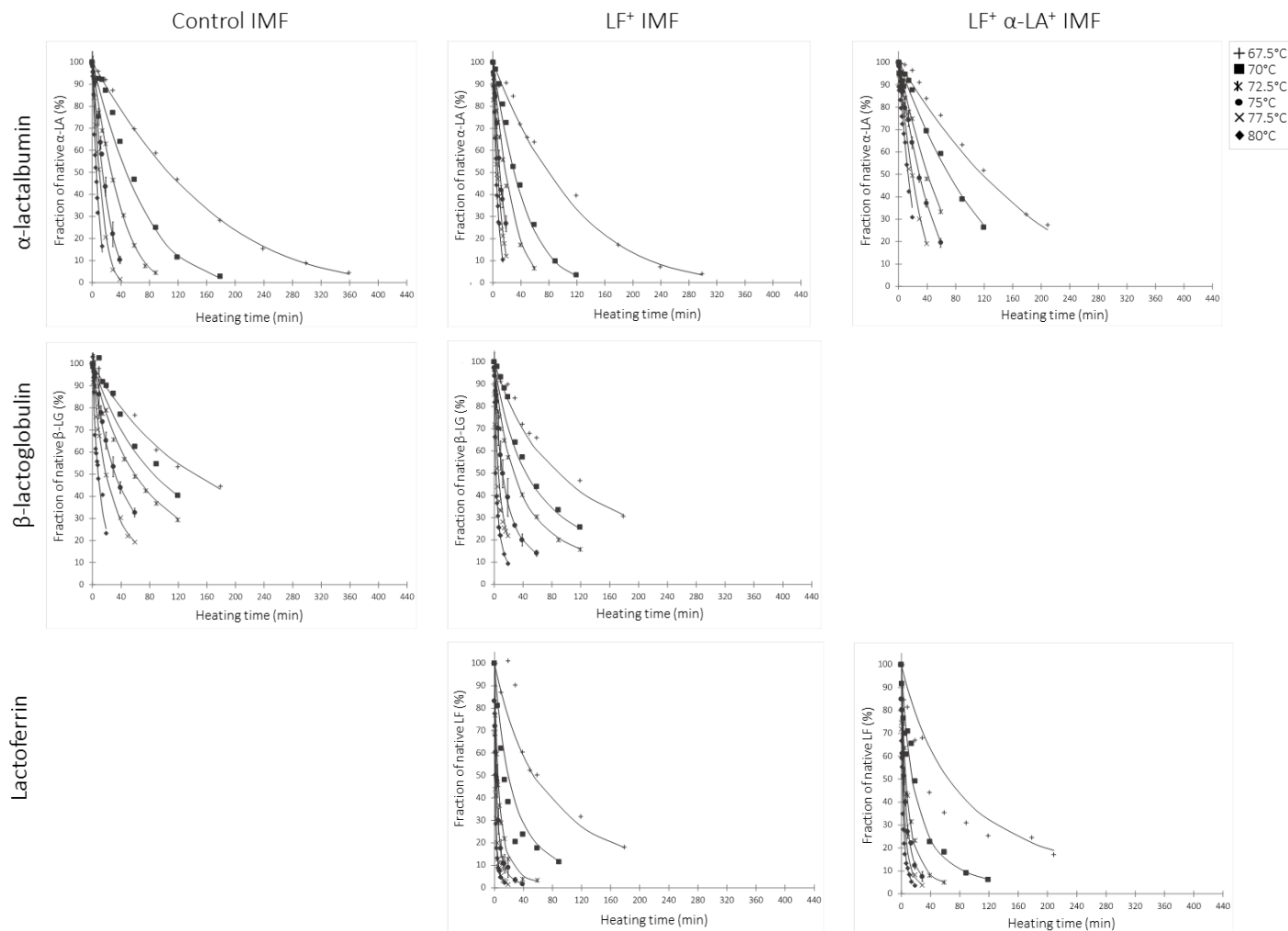
Supplementary Figure 2. Kinetics of heat denaturation of α-LA, β-LG and LF for the IMFs processed at 5.5% proteins at temperatures 67.5°C-80°C

Residual native fractions were calculated as a C_t/C_0 ratio. C_t (g.L^{-1}) is the native protein concentration at t holding time (min) and C_0 is the native protein concentration of unheated IMFs or protein solutions (g.L^{-1}). The results at 75°C represent means ± SD (n = 3).
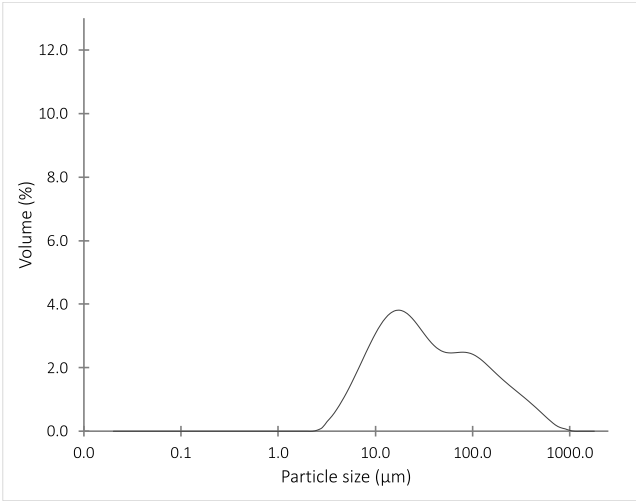
Supplementary Figure 3. Particle size distribution of pancreatin

The pancreatin solution was prepared to a same amount than that of the intestinal samples.
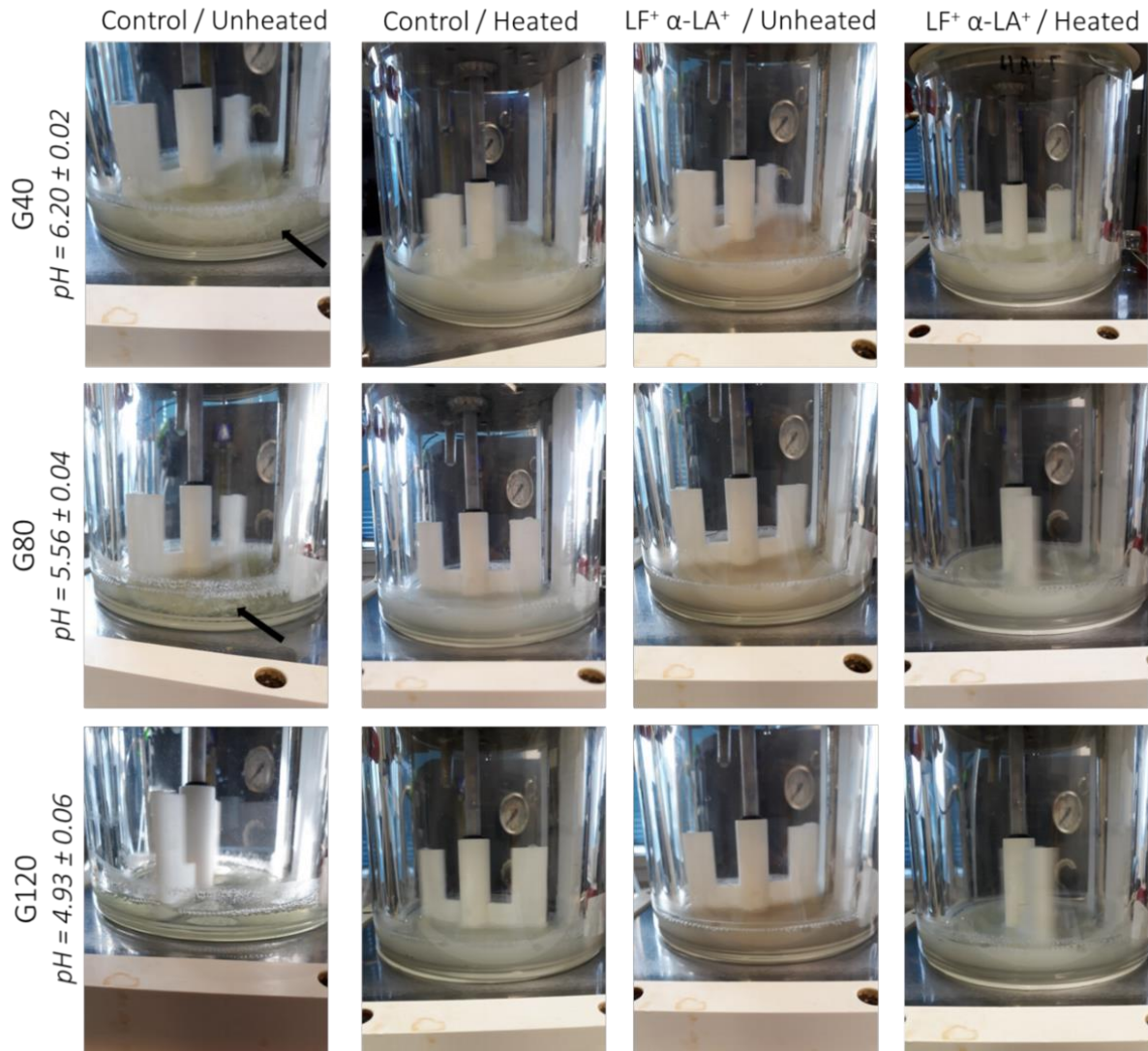
Supplementary Figure 4. Photographic images of the gastric behaviour during the *in vitro* dynamic gastric digestion of IMFs processed at 1.3% proteins

The images correspond to the chyme into the gastric compartment immediately before sampling. Black arrows point the protein particles due to coagulation at 40 min and 80 min of gastric digestion for the unheated control IMF.

Supplementary Table 3. Bioaccessibility of individual essential (A) and non-essential (B) amino acids during the *in vitro* dynamic intestinal digestion of the IMFs processed at 1.3% proteins

A

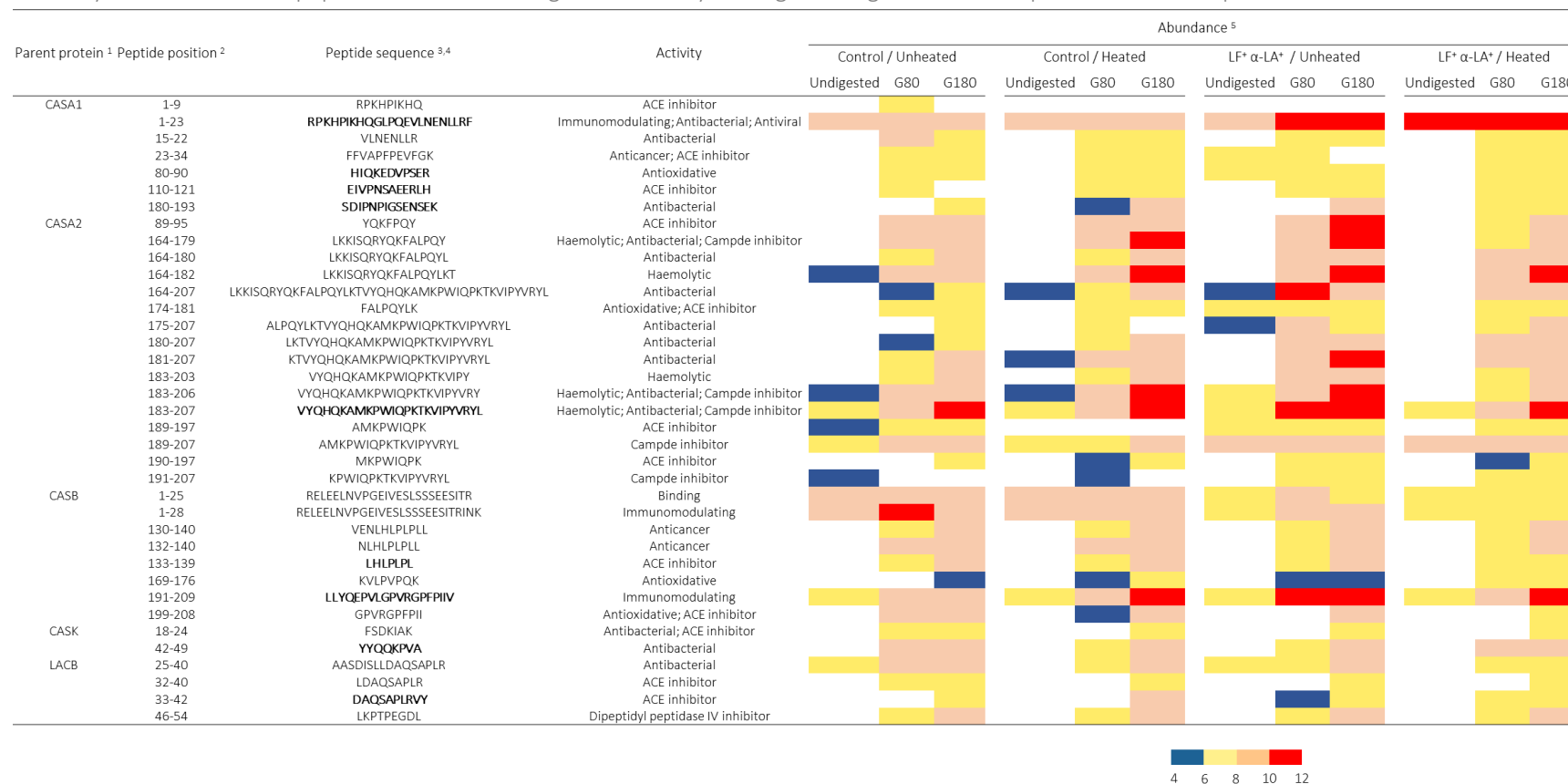|		Bioaccessibility (%)			Effect of				
		Intestinal digestion time							
		I40	I120	I180	Time	Formula	Formula/Treatment	Time x Formula	Time x Formula/Treatment
Cys	Control - Unheated	6.8 ± 2.8	6.3 ± 6.0	7.7 ± 6.6	NS	NS	NS	NS	NS
	Control - Heated	0.7 ± 2.5	5.8 ± 6.0	5.0 ± 10.2					
	LF$^+$ α-LA$^+$ - Unheated	4.1 ± 2.1	2.8 ± 6.1	3.8 ± 5.0					
	LF$^+$ α-LA$^+$ - Heated	2.0 ± 2.8	4.4 ± 4.7	6.1 ± 4.0					
His	Control - Unheated	10.4 ± 1.1^{ab}	14.2 ± 0.3	17.4 ± 0.4	***	**	NS	NS	**
	Control - Heated	7.7 ± 0.6^b	13.8 ± 2.5	18.0 ± 1.8					
	LF$^+$ α-LA$^+$ - Unheated	11.8 ± 0.7^a	16.7 ± 0.5	20.3 ± 0.7					
	LF$^+$ α-LA$^+$ - Heated	10.2 ± 0.7^{ab}	16.9 ± 0.5	19.9 ± 1.1					
Ile	Control - Unheated	6.8 ± 1.4	10.6 ± 0.7	13.7 ± 0.2	***	NS	**	***	*
	Control - Heated	3.5 ± 0.4	8.4 ± 2.2	13.4 ± 0.6					
	LF$^+$ α-LA$^+$ - Unheated	3.8 ± 0.3	9.1 ± 0.2	14.2 ± 1.6					
	LF$^+$ α-LA$^+$ - Heated	4.3 ± 0.4	10.3 ± 0.3	15.5 ± 1.0					
Leu	Control - Unheated	22.8 ± 1.7^a	27.1 ± 0.9	33.7 ± 0.4	***	NS	*	***	***
	Control - Heated	15.7 ± 0.3^b	27.9 ± 3.7	36.6 ± 0.8					
	LF$^+$ α-LA$^+$ - Unheated	16.7 ± 0.6^b	27.0 ± 0.9	34.5 ± 0.8					
	LF$^+$ α-LA$^+$ - Heated	17.2 ± 1.4^b	30.6 ± 0.5	37.4 ± 1.7					
Lys	Control - Unheated	35.2 ± 2.7	42.7 ± 1.8^{ab}	46.7 ± 0.5^b	***	***	***	*** (I120; I180)	***
	Control - Heated	29.7 ± 0.4	47.2 ± 3.4^b	53.7 ± 0.1^a					
	LF$^+$ α-LA$^+$ - Unheated	31.8 ± 0.2	48.0 ± 2.1^{ab}	53.7 ± 1.9^a					
	LF$^+$ α-LA$^+$ - Heated	33.0 ± 1.6	51.9 ± 0.7^a	56.3 ± 1.0^a					
Met	Control - Unheated	30.5 ± 1.7^a	37.8 ± 1.8	42.4 ± 2.1	***	NS	*	***	***
	Control - Heated	18.2 ± 1.1^b	33.8 ± 5.6	41.7 ± 1.1					
	LF$^+$ α-LA$^+$ - Unheated	22.2 ± 1.1^a	36.9 ± 0.7	46.7 ± 2.0					
	LF$^+$ α-LA$^+$ - Heated	19.5 ± 1.2^a	33.9 ± 1.4	43.1 ± 3.2					
Phe	Control - Unheated	35.7 ± 2.6^{ab}	37.6 ± 1.0^c	42.6 ± 0.9^c	***	***	***	*** (I120; I180)	***
	Control - Heated	31.3 ± 0.3^b	45.6 ± 3.0^b	52.2 ± 0.5^b					
	LF$^+$ α-LA$^+$ - Unheated	34.5 ± 0.4^{ab}	47.1 ± 1.6^b	53.1 ± 0.8^b					
	LF$^+$ α-LA$^+$ - Heated	39.0 ± 1.5^a	54.6 ± 0.8^a	57.9 ± 0.5^a					
Thr	Control - Unheated	3.7 ± 0.8^{ab}	5.8 ± 0.7^b	7.6 ± 0.3^b	***	***	**	*** (I40; I120; I180)	*
	Control - Heated	2.4 ± 0.1^b	4.7 ± 1.0^b	7.5 ± 0.7^b					
	LF$^+$ α-LA$^+$ - Unheated	5.0 ± 0.1^a	8.6 ± 0.4^a	11.2 ± 0.5^a					
	LF$^+$ α-LA$^+$ - Heated	5.0 ± 0.7^a	9.6 ± 0.3^a	12.7 ± 0.5^a					
Tyr	Control - Unheated	36.7 ± 4.1^b	40.3 ± 1.2^c	44.3 ± 0.3^c	***	***	***	*** (I40; I120; I180)	***
	Control - Heated	37.9 ± 0.4^b	54.7 ± 1.9^b	59.6 ± 1.7^{ab}					
	LF$^+$ α-LA$^+$ - Unheated	39.1 ± 1.4^b	51.8 ± 1.5^b	54.9 ± 0.8^b					
	LF$^+$ α-LA$^+$ - Heated	45.5 ± 1.7^a	60.7 ± 0.3^a	62.0 ± 1.2^a					
Val	Control - Unheated	8.2 ± 1.4	11.2 ± 0.9	14.5 ± 0.3^b	***	NS	*	***	***
	Control - Heated	4.7 ± 0.1	10.5 ± 2.3	16.0 ± 0.7^{ab}					
	LF$^+$ α-LA$^+$ - Unheated	4.5 ± 0.1	10.7 ± 0.5	15.1 ± 0.3^{ab}					
	LF$^+$ α-LA$^+$ - Heated	4.7 ± 0.4	12.2 ± 0.5	16.7 ± 0.6^a					

B		Bioaccessibility (%)			Effect of				
		Intestinal digestion time							
		I40	I120	I180	Time	Formula	Formula/Treatment	Time x Formula	Time x Formula/Treatment
Ala	Control - Unheated	8.7 ± 1.5[a]	11.5 ± 1.4	15.1 ± 0.4	***	NS	***	NS	***
	Control - Heated	4.1 ± 0.3[b]	8.4 ± 2.0	13.4 ± 0.5					
	LF[+] α-LA[+] - Unheated	5.7 ± 0.6[ab]	9.9 ± 0.9	14.1 ± 1.6					
	LF[+] α-LA[+] - Heated	5.4 ± 0.7[ab]	11.6 ± 0.7	16.5 ± 0.8					
Arg	Control - Unheated	45.8 ± 4.8[ab]	43.3 ± 2.6[c]	48.8 ± 2.0[c]	**	***	***	*** (I120; I180)	***
	Control - Heated	49.1 ± 1.1[ab]	66.2 ± 2.0[a]	65.0 ± 3.6[ab]					
	LF[+] α-LA[+] - Unheated	40.8 ± 1.0[b]	54.0 ± 2.9[b]	58.9 ± 2.4[b]					
	LF[+] α-LA[+] - Heated	53.9 ± 2.0[a]	68.5 ± 0.8[a]	68.1 ± 1.6[a]					
Asp + Asn	Control - Unheated	1.1 ± 0.8	1.7 ± 0.6[ab]	2.1 ± 0.7[b]	**	NS	**	NS	**
	Control - Heated	0.3 ± 0.1	1.0 ± 0.6[b]	1.6 ± 0.3[b]					
	LF[+] α-LA[+] - Unheated	1.2 ± 0.2	2.3 ± 0.3[a]	3.0 ± 0.8[ab]					
	LF[+] α-LA[+] - Heated	1.5 ± 0.2	3.4 ± 0.1[ab]	4.5 ± 0.3[a]					
Glu + Gln	Control - Unheated	6.16 ± 1.2	8.5 ± 0.6	10.4 ± 0.1[b]	***	NS	*	*** (I180)	*
	Control - Heated	3.2 ± 0.4	6.9 ± 1.7	10.6 ± 1.1[b]					
	LF[+] α-LA[+] - Unheated	4.7 ± 0.3	8.8 ± 0.5	12.2 ± 0.4[ab]					
	LF[+] α-LA[+] - Heated	4.4 ± 0.6	9.4 ± 0.3	13.2 ± 0.5[a]					
Gly	Control - Unheated[ab]	7.1 ± 1.5	8.97 ± 0.7	9.7 ± 1.3	**	NS	*	NS	NS
	Control - Heated[b]	5.5 ± 1.3	7.8 ± 1.3	7.4 ± 0.8					
	LF[+] α-LA[+] - Unheated[ab]	6.9 ± 0.2	8.9 ± 0.4	10.3 ± 0.6					
	LF[+] α-LA[+] - Heated[a]	7.4 ± 0.7	10.7 ± 1.1	11.2 ± 1.1					
Pro	Control - Unheated	0.2 ± 0.3	0.1 ± 0.1	0.2 ± 0.7	NS	NS	NS	NS	NS
	Control - Heated	0.2 ± 0.2	0.0 ± 0.5	0.0 ± 0.1					
	LF[+] α-LA[+] - Unheated	0.2 ± 0.6	0.1 ± 0.6	0.2 ± 0.8					
	LF[+] α-LA[+] - Heated	0.1 ± 0.3	0.3 ± 0.3	0.6 ± 0.4					
Ser	Control - Unheated	4.6 ± 1.2	5.8 ± 2.1	4.2 ± 4.4	NS	NS	NS	NS	NS
	Control - Heated	3.4 ± 0.1	6.8 ± 1.4	2.6 ± 2.9					
	LF[+] α-LA[+] - Unheated	4.0 ± 0.1	5.7 ± 1.3	1.7 ± 0.4					
	LF[+] α-LA[+] - Heated	3.9 ± 0.2	7.8 ± 1.0	4.2 ± 3.2					

Data are means ± SD (n = 3). Statistically significant factors were referenced with $p < 0.001$ (***), $p < 0.01$ (**), $p < 0.05$ (*) and $p > 0.05$ (NS). For each amino acid, different superscript letters for a given digestion time represent significant difference among treatments nested within formulas ($p < 0.05$). Data for Phe, Val, Glu + Gln, Gly, and Ser were square-transformed, data for His were square root-transformed and data for Leu were log-transformed to respect residual normality and variance homogeneity (BoxCox transformation).

Supplementary Table 4. Bioactive peptides identified during the *in vitro* dynamic gastric digestion of IMFs processed at 1.3% proteins

Parent protein [1]	Peptide position [2]	Peptide sequence [3,4]	Activity	Abundance [5]											
				Control / Unheated			Control / Heated			LF⁺ α-LA⁺ / Unheated			LF⁺ α-LA⁺ / Heated		
				Undigested	G80	G180	Undigested	G80	G180	Undigested	G80	G180	Undigested	G80	G180
CASA1	1-9	RPKHPIKHQ	ACE inhibitor												
	1-23	**RPKHPIKHQGLPQEVLNENLLRF**	Immunomodulating; Antibacterial; Antiviral												
	15-22	VLNENLLR	Antibacterial												
	23-34	FFVAPFPEVFGK	Anticancer; ACE inhibitor												
	80-90	**HIQKEDVPSER**	Antioxidative												
	110-121	**EIVPNSAEERLH**	ACE inhibitor												
	180-193	**SDIPNPIGSENSEK**	Antibacterial												
CASA2	89-95	YQKFPQY	ACE inhibitor												
	164-179	LKKISQRYQKFALPQY	Haemolytic; Antibacterial; Campde inhibitor												
	164-180	LKKISQRYQKFALPQYL	Antibacterial												
	164-182	LKKISQRYQKFALPQYLKT	Haemolytic												
	164-207	LKKISQRYQKFALPQYLKTVYQHQKAMKPWIQPKTKVIPYVRYL	Antibacterial												
	174-181	FALPQYLK	Antioxidative; ACE inhibitor												
	175-207	ALPQYLKTVYQHQKAMKPWIQPKTKVIPYVRYL	Antibacterial												
	180-207	LKTVYQHQKAMKPWIQPKTKVIPYVRYL	Antibacterial												
	181-207	KTVYQHQKAMKPWIQPKTKVIPYVRYL	Antibacterial												
	183-203	VYQHQKAMKPWIQPKTKVIPY	Haemolytic												
	183-206	VYQHQKAMKPWIQPKTKVIPYVRY	Haemolytic; Antibacterial; Campde inhibitor												
	183-207	**VYQHQKAMKPWIQPKTKVIPYVRYL**	Haemolytic; Antibacterial; Campde inhibitor												
	189-197	AMKPWIQPK	ACE inhibitor												
	189-207	AMKPWIQPKTKVIPYVRYL	Campde inhibitor												
	190-197	MKPWIQPK	ACE inhibitor												
	191-207	KPWIQPKTKVIPYVRYL	Campde inhibitor												
CASB	1-25	RELEELNVPGEIVESLSSSEESITR	Binding												
	1-28	RELEELNVPGEIVESLSSSEESITRINK	Immunomodulating												
	130-140	VENLHLPLPLL	Anticancer												
	132-140	NLHLPLPLL	Anticancer												
	133-139	**LHLPLPL**	ACE inhibitor												
	169-176	KVLPVPQK	Antioxidative												
	191-209	**LLYQEPVLGPVRGPFPIIV**	Immunomodulating												
	199-208	GPVRGPFPII	Antioxidative; ACE inhibitor												
CASK	18-24	FSDKIAK	Antibacterial; ACE inhibitor												
	42-49	**YYQQKPVA**	Antibacterial												
LACB	25-40	AASDISLLDAQSAPLR	Antibacterial												
	32-40	LDAQSAPLR	ACE inhibitor												
	33-42	**DAQSAPLRVY**	ACE inhibitor												
	46-54	LKPTPEGDL	Dipeptidyl peptidase IV inhibitor												

Abundance scale (log10): 4 — 6 — 8 — 10 — 12

[1] Abbreviations are CASA1: α_{s1}-casein, CASA2: α_{s2}-casein, CASB: β-casein, CASK: κ-casein, LACB: β-lactoglobulin, LALBA: α-lactalbumin, TRFL: lactoferrin

[2] Peptide position on the parent protein without taking into account the signal peptide.

[3] Bioactive peptides identified using an exact matching search within the BIOPEP database (dated on March 2020; 3897 peptides) for all peptides and the MBPDB database (dated on July 2020; 65 peptides) for LF-derived peptides.

[4] Bold sequences are common peptides between gastric and intestinal digestions.

[5] Peptide abundances were log10-transformed for each IMF at each digestion time.

Thesis outputs

1. Research papers

1.1. In peer-reviewed journal

Halabi, A., Deglaire, A., Hamon, P., Bouhallab, S., Dupont, D., Croguennec, T. (2020). Kinetics of heat-induced denaturation of proteins in model infant milk T formulas as a function of whey protein composition. *Food Chemistry*, 302, 125296. https://doi.org/10.1016/j.foodchem.2019.125296

Halabi, A., Deglaire, A., Hennetier, M., Violleau, F., Burel, A., Bouhallab, S., Dupont, D., Croguennec, T. (2020). Structural characterization of heat-induced protein aggregates in model infant milk formulas. *Food Hydrocolloids*, 107, 105928. https://doi.org/10.1016/j.foodhyd.2020.105928

Halabi, A., Croguennec, T., Bouhallab, S., Dupont, D., Deglaire, A. (2020). Modification of protein structures by altering the whey protein profile and heat treatment affects *in vitro* static digestion of model infant milk formulas. *Food & function*, https://doi.org/10.1039/D0FO01362E

1.2. In preparation to submission

Halabi, A., Croguennec, T., Ménard, O., Le-Gouar, Y., Bouhallab, S., Dupont, D., Deglaire, A. Impact of protein structure on the digestion kinetics during *in vitro* dynamic digestion of model infant milk formulas.

2. Communications

2.1. Oral

8th International Symposium on Food Rheology and Structure. June 2019. Zurich, Switzerland

Kinetics of heat-induced denaturation of whey proteins and characterization of protein aggregates in model infant formulas

Amira Halabi[1], Amélie Deglaire[1], Marie Hennetier[2], Frédéric Violleau[2], Said Bouhallab[1], Didier Dupont[1], Thomas Croguennec[1]

[1] UMR STLO, Agrocampus Ouest, INRA, 35000 Rennes, France
[2] Université de Toulouse, Ecole d'Ingénieurs de Purpan, 31076 Toulouse, France

In 2018, about 60% of world's newborns received cow milk-based infant formulas (IF) instead of human milk (UNICEF). The process of manufacturing IF involves heat treatments altering the physicochemical properties of milk components, especially whey proteins (WP), and so the rheological properties of IF. The objective of the study was to investigate the impacts of thermal treatments on the denaturation of WP of IF, particularly for those mimicking the protein profile of human milk, and to characterize the heat-induced protein structures.

Three model IF were produced with a caseins:WP ratio of 40:60 at 1.3% and 5.5% of total proteins, i.e. the protein contents at which are applied heat treatments during the manufacture of liquid or powder IF, respectively. Skimmed milk was mixed with a WP isolate, a mix of WP isolate and purified lactoferrin or a mix of both purified lactoferrin and α-lactalbumin in proportion similar to that in human milk. The kinetic of heat-induced denaturation of each WP was investigated between 67.5°C and 80°C by RP-HPLC. The heat-induced protein structures were studied by dynamic light scattering, electrophoresis and asymmetric flow field flow fractionation coupled with MALLS.

The results revealed that the extent of denaturation of WP depended on the protein content and the nature of the WP within the IF. IF at 5.5% of proteins and containing β-lactoglobulin gelled for longer heating time at 80°C. At similar rate of total WP denaturation at 67.5°C and 80°C, the protein composition of the heat-induced aggregates changed between formulas, protein concentrations and heating temperatures but disulfide bonds were the main intermolecular links. The aggregates were larger and of fractal shape (df$_{app}$=2.1) in formulas at 5.5% proteins whereas they were of spherical shape (df$_{app}$=2.9) in formulas at 1.3% proteins.

These results will give to industrials reliable data on the protein structures formed during the heat treatments of IF. The impact on digestibility will be subsequently investigated.

Kinetics of heat-induced denaturation of whey proteins and characterization of protein aggregates in model infant formulas

Amira Halabi[1], Amélie Deglaire[1], Marie Hennetier[2], Frédéric Violleau[2], Said Bouhallab[1], Didier Dupont[1], Thomas Croguennec[1]

[1] UMR STLO, Agrocampus Ouest, INRA, 35000 Rennes, France
[2] Université de Toulouse, Ecole d'Ingénieurs de Purpan, 31076 Toulouse, France

Introduction: In 2018, about 60% of world's newborns received cow milk-based infant formulas (IF) instead of human milk (UNICEF). The process of manufacturing IF involves heat treatments altering the physicochemical properties of milk components, especially whey proteins (WP). The objective of the study was to investigate the impacts of thermal treatments on the denaturation of WP of IF, particularly for those mimicking the protein profile of human milk, and to characterize the heat-induced protein structures.

Methods: Three model IF were produced with a caseins:WP ratio of 40:60 at 1.3% and 5.5% of total proteins, differing in the quality of WP. The kinetic of heat-induced denaturation of each WP was investigated between 67.5°C and 80°C by quantification of the residual native proteins by RP-HPLC. The heat-induced protein structures were studied by dynamic light scattering, electrophoresis and asymmetric flow field flow fractionation coupled with MALLS.

Results: The quantification of native WP fractions revealed an enhanced denaturation of α-lactalbumin in presence of both β-lactoglobulin and lactoferrin, an increased denaturation of β-lactoglobulin in presence of lactoferrin, and an increased denaturation lactoferrin in presence of β-lactoglobulin. At similar rate of total WP denaturation at 67.5°C and 80°C, the protein composition of the heat-induced aggregates changed between formulas, protein concentrations and heating temperatures but disulfide bonds were the main intermolecular links. The aggregates were larger and of fractal shape (apparent fractal dimension df_{app} = 2.1) in formulas at 5.5% proteins whereas they were of spherical shape (df_{app} = 2.9) in formulas at 1.3% proteins.

Discussion: Effects of heat treatment on the denaturation of α-lactalbumin, β-lactoglobulin and lactoferrin and the protein structure are influenced by the WP quality of IF. These results will give to industrials reliable data on the protein structures formed during the heat treatments of IF. The impact on digestibility will be subsequently investigated.

20th International Symposium on Field- and Flow-Based Separations. February 2020. Vienne, Austria

Field-flow fractionation techniques for milk protein characterization

Marie Hennetier[1], Amira Halabi[3], Agnès Burel[5], Amélie Deglaire[3], Thomas Croguennec[3], Audrey Romelard[4], Alain Baniel[4], Frédéric Violleau[1,2]

[1] Toulouse FFF Center, Université de Toulouse, INP-PURPAN, Toulouse, France
[2] Laboratoire de chimie agro-industrielle, LCA, Université de Toulouse, INRA, Toulouse
[3] Agrocampus Ouest-INRA science & technologie du lait et de l'œuf (STLO), Rennes, France
[4] Ingredia, Arras, France
[5] Plateforme Mric, microscopy - Rennes imaging center, Rennes, France

Milk contains two types of proteins: Caseins and whey proteins. There are four caseins: α/β/γ/κ caseins that formed micelles in milk. Whey proteins are globular proteins between 12 and 200 kDa: α-lactalbumin; β-lactoglobulin; Serum albumin; Immunoglobulin and Lactoferrin. Industrials fractionate milk to produce whey protein and casein isolate to make ingredients for the formulation of dairy products. Whey protein isolate can be heated to functionalize or pasteurize them. The objective of these three studies are to characterize the isolates of whey proteins and the impact of heating treatment on whey protein fractions and formulations using different FFF techniques: Asymmetrical-FFF; 2D AsFlFFF-RPLC and Centrifugal-FFF Whey protein isolate heated at high temperature were studied by Centrifugal-FFF coupled with MALS and RI. Aggregates with the lowest density and size elute in the void peak and represent 51% of the mass fraction. For the bigger one, there are two populations: one smaller than 1 micrometer and one higher, up to 4.5 micrometers. For size determination, the biggest population fractionated has been collected and analyzed by DLS in batch. Infant milk formulation without fat was investigated by Asymmetrical Flow FFF coupled with MALS; QELS and RI. The formulation contains bovine milk and isolate whey protein fractions. The technique separates the non-aggregated whey protein to the casein micelles. The addition of lactoferrin partially disintegrated the casein micelles. The formulations are heated at 67.5°C or 80°C. Native whey protein content decreases with the heat treatment, leading to their aggregation on with the casein micelles. The phenomena depend on the temperature and protein composition. At 80°C, shape ratio Rg/Rh of casein micelles increase with the temperature when the formulation is enriched in lactoferrin. The Rg and Rh decrease when the formulation is enriched in α-lactalbumin and lactoferrin. Transmission Electronic Microscopy are correlated with these results. At 80°C, whey protein aggregates are fixed outside the micelle for the first formulation and they are fixed inside the micelles for the second formulation. Whey protein isolate contains few quantities of caseins. The second objective of this study is to identify the presence of trace of caseins in whey protein isolate using 2D AsFlFFF-RP-HPLC. This technique allows to separate proteins by their size and by their polarity. A whey protein standard mix is studied: α-lactalbumin, β-lactoglobulin A and B, BSA, and 3 caseins. A 2D map is obtained with all separated proteins.

2.2. Posters

STLOpen Days. March 2019. Rennes, France

Infant milk formulas: effect of heat treatments on the protein physicochemical properties and the nutritional quality

Amira Halabi[1], Amélie Deglaire[1], Said Bouhallab[1], Didier Dupont[1], Thomas Croguennec[1]

[1] UMR STLO, Agrocampus Ouest, INRA, 35000 Rennes, France

Journées Francophones de la Nutrition. Novembre 2019. Rennes, France

Effets de la composition et des structures protéiques thermo-induites sur les cinétiques de protéolyse des préparations pour nourrissons

Amira Halabi[1], Amélie Deglaire[1], Marie Hennetier[2], Frédéric Violleau[2], Agnès Burel[3], Said Bouhallab[1], Didier Dupont[1], Thomas Croguennec[1]

[1] UMR STLO, Agrocampus Ouest, INRA, 35000 Rennes, France
[2] Université de Toulouse, Ecole d'Ingénieurs de Purpan, 31076 Toulouse, France
[3] Université de Rennes 1, Plateforme de microscopie MRic BIOSIT, Rennes, France

Introduction et but de l'étude : Le processus de fabrication des préparations pour nourrissons (PPNs) implique des traitements thermiques, modifiant les propriétés physico-chimiques des protéines et éventuellement leur cinétique de protéolyse. L'objectif de l'étude consiste en l'analyse des effets de la composition et des structures protéiques thermo-induites des PPNs sur la cinétique de protéolyse.

Matériel et méthodes : Deux PPNs modèles ont été formulées à 1,3% de protéines. Elles se distinguent par la qualité des protéines du lactosérum (α-lactalbumine, β-lactoglobuline et lactoferrine) : la PPN « standard » mime la composition protéique de la majorité des PPNs 1er âge commercialisées et la PPN « LF+ ALA+ » celle du lait maternel. Les PPNs ont été traitées thermiquement à 67,5°C ou 80°C avec un taux de dénaturation des protéines du lactosérum identique de 65%. Les PPNs sans traitement thermique ont servies de référence. Les structures protéiques thermo-induites ont été caractérisées par électrophorèse, fractionnement d'écoulement de champ couplé à la diffusion de lumière multi-angle et microscopie électronique. D'autre part, les PPNs ont été soumises à la digestion gastro-intestinale en condition statique in vitro au stade nouveau-né à terme (n = 3). Le degré d'hydrolyse a été mesuré par dosage des amines primaires, la cinétique de protéolyse suivie par électrophorèse et l'évolution de la structure au cours de la digestion par granulométrie à diffraction laser.

Résultats et analyse statistique : A taux de dénaturation protéique équivalent, les caractéristiques morphologiques des structures protéiques thermo-induites différent selon la composition protéique des PPNs et la température de traitement thermique. La formation d'agrégats solubles a été observée uniquement pour la PPN « standard », tandis que la fixation de protéines dénaturées sur les micelles de caséines a été constatée pour les deux PPNs. Les agrégats formés à 67,5°C ont une plus petite masse pour la PPN « standard » et un plus petit diamètre pour la PPN « LF+ ALA+ » que ceux formés à 80°C. Au cours de la phase gastrique, le traitement thermique accélère la cinétique de protéolyse des caséines de la PPN « standard » contrairement à la PPN « LF+ ALA+ ». La cinétique de protéolyse de l'α-lactalbumine dépend de la composition protéique des PPNs et de la température de chauffage de la PPN « LF+ ALA+ ». La protéolyse de la lactoferrine est fortement affectée par le traitement thermique.

Les entités protéiques formées par agrégation en fin de phase gastrique sont affectées par la composition protéique des PPNs et le traitement thermique.

Conclusion : Notre étude a permis de mettre en évidence les effets de la composition protéique des PPNs et des structures protéiques thermo-induites sur les cinétiques de protéolyse. Ces deux paramètres sont donc à prendre en compte pour l'optimisation des PPNs en termes de stratégie nutritionnelle.

Effets de la composition et des structures protéiques thermo-induites sur les cinétiques de protéolyse des préparations pour nourrissons
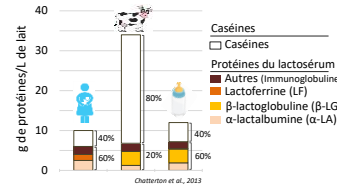
INRA SCIENCE & IMPACT

AGRO CAMPUS OUEST

Amira Halabi[1], Amélie Deglaire[1], Marie Hennetier[2], Frédéric Violleau[2], Agnès Burel[3], Saïd Bouhallab[1], Didier Dupont[1], Thomas Croguennec[1]
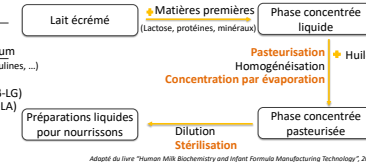
Contexte

1 Nutrition des nourrissons âgés de 0-5 mois dans le monde en 2018

Lait maternel 41%
Préparation pour nourrissons 59%

UNICEF global databases, 2018
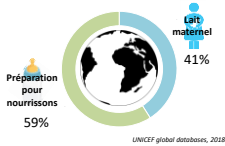
2 **Préparations pour nourrissons** majoritairement à base **de lait bovin**
→ **Variation de la composition protéique** entre le lait bovin et le lait maternel

g de protéines/L de lait

Caséines
□ Caséines
Protéines du lactosérum
■ Autres (Immunoglobulines, ...)
■ Lactoferrine (LF)
■ β-lactoglobuline (β-LG)
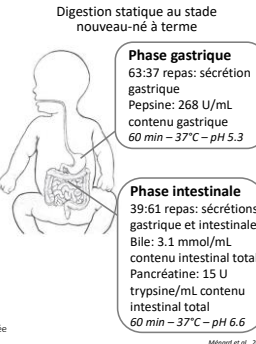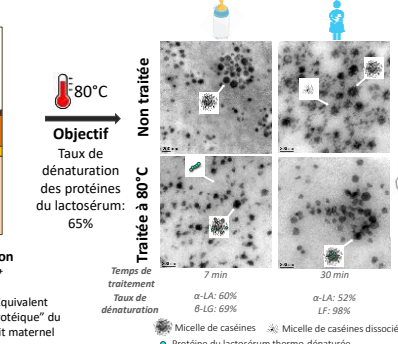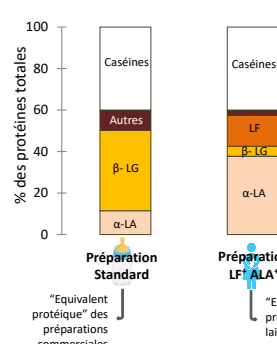■ α-lactalbumine (α-LA)

Chatterton et al., 2013

3 **Traitements thermiques** appliqués pendant **le processus de fabrication** des préparations pour nourrissons
→ Avantages: **Qualité sanitaire-durée de conservation**
→ Inconvénients: **Altération des propriétés physicochimiques**

Lait écrémé → Matières premières (Lactose, protéines, minéraux) → Phase concentrée liquide
Pasteurisation + Huiles
Homogénéisation
Concentration par évaporation
Préparations liquides pour nourrissons ← Dilution / **Stérilisation** ← Phase concentrée pasteurisée

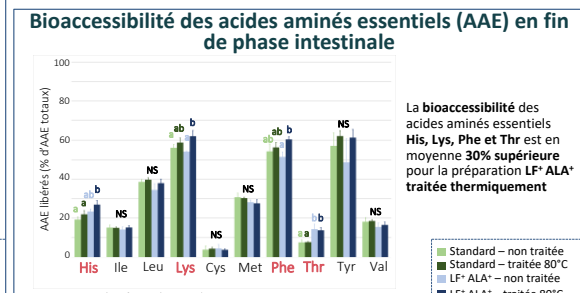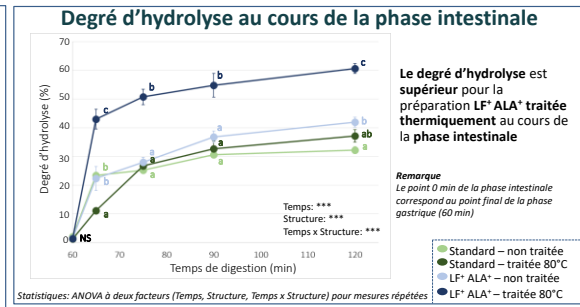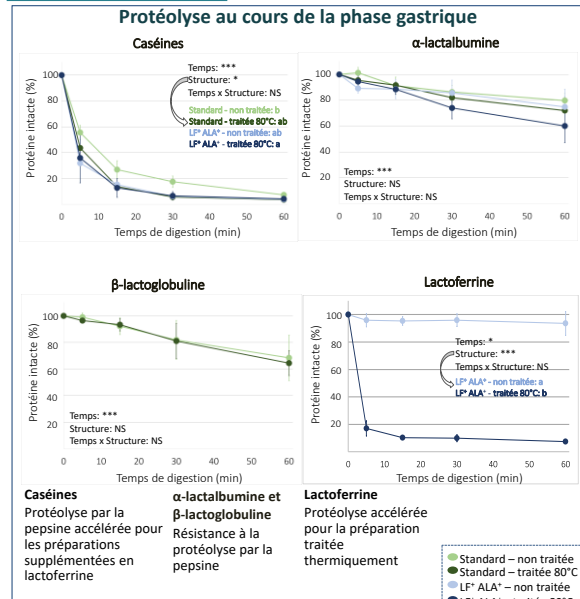*Adapté du livre "Human Milk Biochemistry and Infant Formula Manufacturing Technology", 2014*

Objectif

Etude des effets de la **composition protéique** des préparations pour nourrissons 1er âge et du **traitement thermique** sur la **protéolyse** au cours de la **digestion** en condition *in vitro*

Méthodes

Deux compositions

% des protéines totales

Caséines / Autres / β-LG / α-LA
Préparation Standard
"Equivalent protéique" des préparations commerciales

Caséines / LF / β-LG / α-LA
Préparation LF⁺ ALA⁺
"Equivalent protéique" du lait maternel

Deux conditions thermiques

🌡 **80°C**
Objectif
Taux de dénaturation des protéines du lactosérum: 65%

Non traitée / Traitée à 80°C

Temps de traitement
Taux de dénaturation

7 min — α-LA: 60%, β-LG: 69%
30 min — α-LA: 52%, LF: 98%

● Micelle de caséines
✳ Micelle de caséines dissociée
● Protéine du lactosérum thermo-dénaturée

→ **4 structures protéiques différentes**

Digestion *in vitro*

Digestion statique au stade nouveau-né à terme

Phase gastrique
63:37 repas: sécrétion gastrique
Pepsine: 268 U/mL contenu gastrique
60 min – 37°C – pH 5.3

Phase intestinale
39:61 repas: sécrétions gastrique et intestinale
Bile: 3.1 mmol/mL contenu intestinal total
Pancréatine: 15 U trypsine/mL contenu intestinal total
60 min – 37°C – pH 6.6

Ménard et al., 2018

Analyses

1 **SDS-PAGE réductrice** et **densitométrie** des gels
→ Protéolyse au cours de la phase gastrique

2 **Dosage OPA** (orthophtaldialdéhyde)
→ Degré d'hydrolyse protéique au cours de la phase intestinale
(Rapport de la quantité d'amines primaires libérés à un temps t et de celle de la préparation après hydrolyse totale avec HCl 6 N)

3 **Chromatographie échangeuse de cations**
→ Bioaccessibilité des acides aminés essentiels (AAE) en fin de phase intestinale
(Rapport de la quantité d'AAE libérés à un temps t et celle de la préparation après hydrolyse totale avec HCl 6 N)

Résultats

Protéolyse au cours de la phase gastrique

Caséines
Temps: ***
Structure: *
Temps x Structure: NS
Standard – non traitée: b
Standard - traitée 80°C: ab
LF⁺ ALA⁺ - non traitée: ab
LF⁺ ALA⁺ - traitée 80°C: a

α-lactalbumine
Temps: ***
Structure: NS
Temps x Structure: NS

β-lactoglobuline
Temps: ***
Structure: NS
Temps x Structure: NS

Lactoferrine
Temps: *
Structure: ***
Temps x Structure: NS
LF⁺ ALA⁺- non traitée: a
LF⁺ ALA⁺ - traitée 80°C: b

Caséines
Protéolyse par la pepsine accélérée pour les préparations supplémentées en lactoferrine

α-lactalbumine et β-lactoglobuline
Résistance à la protéolyse par la pepsine

Lactoferrine
Protéolyse accélérée pour la préparation traitée thermiquement

Standard – non traitée
Standard – traitée 80°C
LF⁺ ALA⁺ – non traitée
LF⁺ ALA⁺ – traitée 80°C

Statistiques: ANOVA à deux facteurs (Temps, Structure, Temps x Structure) pour mesures répétées

Degré d'hydrolyse au cours de la phase intestinale

Temps: ***
Structure: ***
Temps x Structure: ***

Le degré d'hydrolyse est **supérieur** pour la préparation **LF⁺ ALA⁺** traitée **thermiquement** au cours de la **phase intestinale**

Remarque
Le point 0 min de la phase intestinale correspond au point final de la phase gastrique (60 min)

Standard – non traitée
Standard – traitée 80°C
LF⁺ ALA⁺ – non traitée
LF⁺ ALA⁺ – traitée 80°C

Statistiques: ANOVA à deux facteurs (Temps, Structure, Temps x Structure) pour mesures répétées

Bioaccessibilité des acides aminés essentiels (AAE) en fin de phase intestinale

His / Ile / Leu / Lys / Cys / Met / Phe / Thr / Tyr / Val

La **bioaccessibilité** des acides aminés essentiels **His, Lys, Phe et Thr** est en moyenne **30% supérieure** pour la préparation **LF⁺ ALA⁺** traitée thermiquement

Standard – non traitée
Standard – traitée 80°C
LF⁺ ALA⁺ – non traitée
LF⁺ ALA⁺ – traitée 80°C

Statistiques: ANOVA à un facteur (Structure)

Conclusion

- La **composition protéique** impacte la **protéolyse gastrique des caséines**: la lactoferrine dissociant les micelles de caséines augmente leur accessibilité enzymatique.
- **Le traitement thermique** accélère la **protéolyse gastrique de la lactoferrine**, ce qui s'explique par la dénaturation quasi-totale de la lactoferrine.
- Le **degré d'hydrolyse** au cours de la **phase intestinale**, ainsi que la **bioaccessibilité** de **certains acides aminés essentiels** en fin de digestion, sont significativement **supérieurs** pour la préparation **LF⁺ ALA⁺** traitée à **80°C/30 min**. Ceci pourrait s'expliquer par une protéolyse accélérée de la lactoferrine et des caséines par la pepsine en phase gastrique

→ Le traitement thermique des préparations pour nourrissons supplémentées en lactoferrine entraînant la quasi-totale dénaturation de la lactoferrine ainsi qu'une protéolyse de la protéine dès le début de la phase gastrique, existe-t-il un intérêt physiologique à cette supplémentation?

Advanced Analytical Technologies for Proteins. October 2019. Paris, France

Performance of Filed-Flow Fractionation technique for milk protein characterization

Marie Hennetier[1], Audrey Ric[1], Estelle N'tsiba[1], Mireille Gaucher[1], Amira Halabi[3], Thomas Croguennec[3], Audrey Romelard[4], Alain Baniel[4], Frédéric Violleau[1,2]

[1] Toulouse FFF Center, Université de Toulouse, INP-PURPAN, Toulouse, France
[2] Laboratoire de Chimie Agro-industrielle, LCA, Université de Toulouse, INRA, Toulouse, France
[3] AGROCAMPUS OUEST-INRA Science & Technologie du Lait et de l'Oeuf (STLO), Rennes, France
[4] Ingredia, Arras, France

The Toulouse FFF Center (TFFFC) project aim is the development of a shared research platform for characterization of complex samples using Field-Flow Fractionation technologies. The project is built around collaborative projects with partners from various fields of activities such as agrifood, polymer chemistry, renewable carbon valorization and analytical equipment. The financial support of the Region Occitanie, European funds and industrial partners make possible the creation of an analytical platform dedicated to FFF technologies unique in Europe and to develop innovative approaches and tools allowing the characterization of complex samples by these Field-Flow Fractionation technologies. The performance of these techniques will be evaluated for the characterization various nano and micro-structures like proteins. We will also develop analytical methodologies using different FFF techniques to better characterize complex milk protein samples used as agro-food texturing agents and lignocellulosic materials, a product of interest in renewable carbon chemistry. These projects will be carried out in collaboration with industrial partners.

Toulouse FFF Center (TFFFC):
Performance of Field-Flow Fractionation techniques for milk protein characterization

Marie Hennetier[1], Audrey Ric[1], Estelle N'tsiba[1], Mireille Gaucher[1], Amira Halabi[3], Thomas Croguennec[3], Audrey Romelard[4], Alain Baniel[4], Frédéric Violleau[1,2]

[1]Toulouse FFF Center, Université de Toulouse, INP-PURPAN, Toulouse, France
[2]Laboratoire de Chimie Agro-industrielle, LCA, Université de Toulouse, INRA, Toulouse, France
[3] AGROCAMPUS OUEST-INRA Science & Technologie du Lait et de l'Oeuf (STLO), Rennes, France
[4] Ingredia, Arras, France

Aims of the project: The Toulouse FFF Center (TFFFC) project aim is the development of a shared research platform for characterization of complex samples using Field-Flow Fractionation technologies. The project is built around collaborative projects with partners from various fields of activities such as agrifood, polymer chemistry, renewable carbon valorization and analytical equipment. The financial support of the Region Occitanie, European funds and industrial partners make possible the creation of an analytical platform dedicated to FFF technologies unique in Europe and to develop innovative approaches and tools allowing the characterization of complex samples by these Field-Flow Fractionation technologies. The performance of these techniques will be evaluated for the characterization various nano and micro-structures like proteins. We will also develop analytical methodologies using different FFF techniques to better characterize complex milk protein samples used as agro-food texturing agents and lignocellulosic materials, a product of interest in renewable carbon chemistry. These projects will be carried out in collaboration with industrial partners.

FFF techniques available: The platform is equipped with all existing FFF technologies today (FlFFF, EAF4, SdFFF, ThFFF). The coupling of these fractionation tools with different detection tools (UV, RI, Static scattering and light dynamics, particle analyzer) will make it possible to determine essential criteria (Molecular weight distribution, Size distribution, Conformation / form, State aggregation ...) to control the quality and performance of different type of products. The platform is opened to all industrial and academic partners wishing to evaluate the performance of these technologies in fields as varied as pharmacy, cosmetics, nanotechnologies, agri-food, biotechnologies, materials ...

(1) AsFlFFF & EAF4-UV-MALS-RI *(2) 2D-AsFlFFF×LC-UV-MALS-RI* *(3) ThermalFFF- UV-MALS-RI* *(4) CentrifugalFFF-UV*


Results:

Milk Proteins standards analysis by Full comprehensive 2D – AsFlFFF × LC - UV

2D AsFlFFF-RP-HPLC was investigated to separate whey proteins and caseins. This technique allows to separate proteins by their size and by their polarity. A whey protein standard mix is studied: α-lactalbumine, β-lactoglobuline A and B, BSA, and 3 caseins. A 2D map is obtained with all separated proteins.
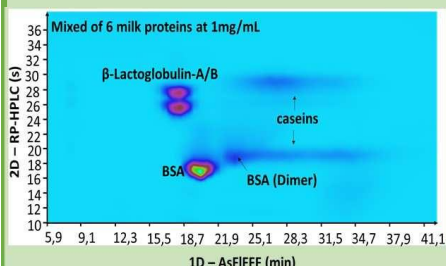
Conditions: 1D-AsFlFFF: spacer 350µm ; V$_{out}$=0,5mL/min ; eluant: PBS
2D-HPLC : Poroshell 300 C8 ; A: water 0.1% TFA; B: ACN 0.07% TFA

Infant milk formulation analysis by AsFlFFF-MALS-RI

Pasteurized Infant milk formulation without fat was investigated by AsFlFFF-MALS-RI. The technique separates the non-aggregated whey proteins to the casein micelles. Native whey proteins content decreases with the pasteurization to make aggregates which fixed to the casein micelles. Shape ratio Rg/Rh of casein micelles + aggregates increases with the temperature. At 67.5°C, aggregates are fixed inside the micelle, at 80°C they are fixed outside the micelles (+TEM results).
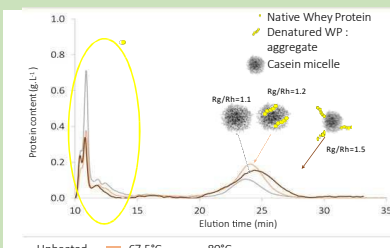
Conditions: Spacer 250µm ; V$_{out}$=1ml/min Vx = 4 to 0,1mL/min ; Eluant: NaCl 50mM + CaCl$_2$ 5mM

Milk protein aggregates characterization by CentrifugalFFF-MALS-RI

Milk proteins after heat treatment were studied by Centrifugal FFF coupled with MALS and RI. Aggregates with the lowest density and size elute in the void peak and represent 54% of the mass fraction. For the bigger one, there are two populations: one smaller than 1µm and one higher, up to 4.5µm (collect + DLS batch because MALS can't calculate size after 1µm).
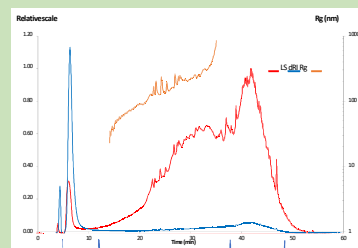
Conditions: Flow rate: 1,2 ml/min ; Speed rotation: from 4500 to 50 rpm ; Eluant: Water + FL70 0,1%

Summary: These works highlight the potentiality of FFF techniques to fractionate and characterize proteins and protein aggregates. Toulouse FFF Center is opened to all partners wishing to evaluate the performance of these technologies in fields as pharmacy, cosmetics, nanotechnologies, agri-food, biotechnologies...

3. Formations

3.1. Disciplinaires

- Planification expérimentale. Mai 2018. ONIRIS. Nantes, France
- Analyse exploratoire des données multidimentionnelles. Juin 2018. ONIRIS. Nantes, France
- Asymmetric flow field flow fractionation. Janvier 2019. Toulouse University, INP Purpan. Toulouse, France
- Statistiques de base avec le logiciel R. Mars 2019. Rennes, France
- Excel Gestion Base de Données – Perfectionnement. Mars 2019. Rennes, France
- Journées Scientifiques de l'ED EGAAL. Juillet 2019. Rennes, France
- Statistiques avancées – Les modèles linéaires. Octobre 2019. Rennes, France

3.2. Transversales

- Mettre en place une stratégie de publication scientifique. Février 2018. Rennes, France
- Anglais en immersion. Août 2018. St Brelade's College. Jersey, Channel Islands
- Introduction à l'éthique de la recherche. Novembre 2018. Rennes, France
- Genre et carrière professionnelle. Mars 2019. Rennes, France

List of references

Abbate, R. A., Raak, N., Boye, S., Janke, A., Rohm, H., Jaros, D., & Lederer, A. (2019). Asymmetric flow field flow fractionation for the investigation of caseins cross-linked by microbial transglutaminase. *Food Hydrocolloids*, *92*, 117–124. https://doi.org/10.1016/j.foodhyd.2019.01.043

Abrahamse, E., Minekus, M., van Aken, G. A., van de Heijning, B., Knol, J., Bartke, N., Oozeer, R., van der Beek, E. M., & Ludwig, T. (2012). Development of the Digestive System-Experimental Challenges and Approaches of Infant Lipid Digestion. *Food Digestion*, *3*(1–3), 63–77. PubMed. https://doi.org/10.1007/s13228-012-0025-x

Abriata, L. A., Spiga, E., & Peraro, M. D. (2016). Molecular Effects of Concentrated Solutes on Protein Hydration, Dynamics, and Electrostatics. *Biophysical Journal*, *111*(4), 743–755. https://doi.org/10.1016/j.bpj.2016.07.011

Aburjaile, F. F., Rohmer, M., Parrinello, H., Maillard, M.-B., Beaucher, E., Henry, G., Nicolas, A., Madec, M.-N., Thierry, A., Parayre, S., Deutsch, S.-M., Cocaign-Bousquet, M., Miyoshi, A., Azevedo, V., Le Loir, Y., & Falentin, H. (2016). Adaptation of Propionibacterium freudenreichii to long-term survival under gradual nutritional shortage. *BMC Genomics*, *17*(1). https://doi.org/10.1186/s12864-016-3367-x

Adolphi, U., & Kulicke, W.-M. (1997). Coil dimensions and conformation of macromolecules in aqueous media from flow field-flow fractionation/multi-angle laser light scattering illustrated by studies on pullulan. *Polymer*, *38*(7), 1513–1519. https://doi.org/10.1016/S0032-3861(96)00675-1

Agostoni, C., Braegger, C., Decsi, T., Kolacek, S., Koletzko, B., Michaelsen, K. F., Mihatsch, W., Moreno, L. A., Puntis, J., Shamir, R., Szajewska, H., Turck, D., van Goudoever, J., & ESPGHAN Committee on Nutrition: (2009). Breast-feeding: A Commentary by the ESPGHAN Committee on Nutrition. *Journal of Pediatric Gastroenterology and Nutrition*, *49*(1). https://journals.lww.com/jpgn/Fulltext/2009/07000/Breast_feeding__A_Commentary_by_the_ESPGHAN.18.aspx

Ahern, G. J., Hennessy, A. A., Ryan, C. A., Ross, R. P., & Stanton, C. (2019). Advances in Infant Formula Science. *Annual Review of Food Science and Technology*, *10*(1), 75–102. https://doi.org/10.1146/annurev-food-081318-104308

Aiqian Ye, Harjinder Singh, Michael W. Taylor, & Skelte Anema. (2004). Interactions of whey proteins with milk fat globule membrane proteins during heat treatment of whole milk. *Lait*, *84*(3), 269–283. https://doi.org/10.1051/lait:2004004

Al-Attabi, Z., D'Arcy, B. R., & Deeth, H. C. (2014). Volatile sulfur compounds in pasteurised and UHT milk during storage. *Dairy Science & Technology*, *94*(3), 241–253. https://doi.org/10.1007/s13594-013-0157-y

Alegría, A., Garcia-Llatas, G., & Cilla, A. (2015). Static Digestion Models: General Introduction. In K. Verhoeckx, P. Cotter, I. López-Expósito, C. Kleiveland, T. Lea, A. Mackie, T. Requena, D. Swiatecka, & H. Wichers (Eds.), *The Impact of Food Bioactives on Health: In vitro and ex vivo models* (pp. 3–12). Springer International Publishing. https://doi.org/10.1007/978-3-319-16104-4_1

Alexander, M., & Dalgleish, D. G. (2005). Interactions between Denatured Milk Serum Proteins and Casein Micelles Studied by Diffusing Wave Spectroscopy. *Langmuir*, *21*(24), 11380–11386. https://doi.org/10.1021/la0519958

ALjahdali, N., & Carbonero, F. (2019). Impact of Maillard reaction products on nutrition and health: Current knowledge and need to understand their fate in the human digestive system. *Critical Reviews in Food Science and Nutrition*, *59*(3), 474–487. https://doi.org/10.1080/10408398.2017.1378865

Alles, M. S., Scholtens, P. A. M. J., & Bindels, J. G. (2004). Current trends in the composition of infant milk formulas. *Current Paediatrics*, *14*(1), 51–63. https://doi.org/10.1016/j.cupe.2003.09.007

Alliet, P., Puccio, G., Janssens, E., Cajozzo, C., Corsello, G., Berger, B., Sperisen, P., Martin, F.-P., Sprenger, N., & Steenhout, P. (2016). Term infant formula supplemented with human milk oligosaccharides (2'fucosyllactose and lacto-neotetraose) shifts stool microbiota and metabolic signatures closer to

that of breastfed infants. *Journal of Pediatric Gastroenterology and Nutrition*, *63*, S55. https://doi.org/10.1097/01.mpg.0000489632.17881.57

Altomonte, I., Salari, F., Licitra, R., & Martini, M. (2019). Donkey and human milk: Insights into their compositional similarities. *International Dairy Journal*, *89*, 111–118. https://doi.org/10.1016/j.idairyj.2018.09.005

Amara, S., Patin, A., Giuffrida, F., Wooster, T. J., Thakkar, S. K., Bénarouche, A., Poncin, I., Robert, S., Point, V., Molinari, S., Gaussier, H., Diomande, S., Destaillats, F., Cruz-Hernandez, C., & Carrière, F. (2014). In vitro digestion of citric acid esters of mono- and diglycerides (CITREM) and CITREM-containing infant formula/emulsions. *Food & Function*, *5*(7), 1409–1421. https://doi.org/10.1039/C4FO00045E

Andersson, E.-L., Hernell, O., Bläckberg, L., Fält, H., & Lindquist, S. (2011). BSSL and PLRP2: Key enzymes for lipid digestion in the newborn examined using the Caco-2 cell line. *Journal of Lipid Research*, *52*(11), 1949–1956. PubMed. https://doi.org/10.1194/jlr.M015685

Andersson, Y., Sävman, K., Bläckberg, L., & Hernell, O. (2007). Pasteurization of mother's own milk reduces fat absorption and growth in preterm infants. *Acta Paediatrica (Oslo, Norway : 1992)*, *96*(10), 1445–1449. PubMed. https://doi.org/10.1111/j.1651-2227.2007.00450.x

Anema, S. (2019). Acidification of lactoferrin-casein micelle complexes in skim milk. *International Dairy Journal*, *99*, 104550. https://doi.org/10.1016/j.idairyj.2019.104550

Anema, S.G. (2000). Effect of milk concentration on the irreversible thermal denaturation and disulfide aggregation of β-lactoglobulin. *Journal of Agricultural and Food Chemistry*, *48*(9), 4168–4175. Scopus. https://doi.org/10.1021/jf991173e

Anema, S.G. (2001). Kinetics of the Irreversible Thermal Denaturation and Disulfide Aggregation of α-Lactalbumin in Milk Samples of Various Concentrations. *Journal of Food Science*, *66*(1), 2–9. https://doi.org/10.1111/j.1365-2621.2001.tb15573.x

Anema, S.G., & Li, Y. (2003). Association of denatured whey proteins with casein micelles in heated reconstituted skim milk and its effect on casein micelle size. *Journal of Dairy Research*, *70*(1), 73–83. Scopus. https://doi.org/10.1017/S0022029902005903

Anema, Skelte G. (1998). Effect of Milk Concentration on Heat-Induced, pH-Dependent Dissociation of Casein from Micelles in Reconstituted Skim Milk at Temperatures between 20 and 120 °C. *Journal of Agricultural and Food Chemistry*, *46*(6), 2299–2305. https://doi.org/10.1021/jf970909+

Anema, Skelte G. (2007). Role of κ-Casein in the Association of Denatured Whey Proteins with Casein Micelles in Heated Reconstituted Skim Milk. *Journal of Agricultural and Food Chemistry*, *55*(9), 3635–3642. https://doi.org/10.1021/jf062734m

Anema, Skelte G. (2008). Chapter 8—The whey proteins in milk: Thermal denaturation, physical interactions and effects on the functional properties of milk. In A. Thompson, M. Boland, & H. Singh (Eds.), *Milk Proteins* (pp. 239–281). Academic Press. https://doi.org/10.1016/B978-0-12-374039-7.00008-8

Anema, Skelte G. (2008). On heating milk, the dissociation of κ-casein from the casein micelles can precede interactions with the denatured whey proteins. *Journal of Dairy Research*, *75*(4), 415–421. https://doi.org/10.1017/S0022029908003555

Anema, Skelte G. (2018). Effect of whey protein addition and pH on the acid gelation of heated skim milk. *International Dairy Journal*, *79*, 5–14. https://doi.org/10.1016/j.idairyj.2017.11.008

Anema, Skelte G. (2019). Acidification of lactoferrin-casein micelle complexes in skim milk. *International Dairy Journal*, *99*, 104550. https://doi.org/10.1016/j.idairyj.2019.104550

Anema, Skelte G., & de Kruif, C. G. (Kees). (2011). Interaction of Lactoferrin and Lysozyme with Casein Micelles. *Biomacromolecules*, *12*(11), 3970–3976. https://doi.org/10.1021/bm200978k

Anema, Skelte G., & de Kruif, C. G. (Kees). (2012). Lactoferrin binding to transglutaminase cross-linked casein micelles. *International Dairy Journal*, *26*(1), 83–87. https://doi.org/10.1016/j.idairyj.2011.12.004

Anema, Skelte G., & de Kruif, C. G. (Kees). (2013). Protein Composition of Different Sized Casein Micelles in Milk after the Binding of Lactoferrin or Lysozyme. *Journal of Agricultural and Food Chemistry*, *61*(29), 7142–7149. https://doi.org/10.1021/jf401270h

Anema, Skelte G., & Klostermeyer, H. (1997). Heat-Induced, pH-Dependent Dissociation of Casein Micelles on Heating Reconstituted Skim Milk at Temperatures below 100 °C. *Journal of Agricultural and Food Chemistry*, *45*(4), 1108–1115. https://doi.org/10.1021/jf960507m

Anema, Skelte G., Lee, S. K., & Klostermeyer, H. (2006). Effect of protein, nonprotein-soluble components, and lactose concentrations on the irreversible thermal denaturation of β-lactoglobulin and α-lactalbumin in skim milk. *Journal of Agricultural and Food Chemistry*, *54*(19), 7339–7348.

Anema, Skelte G., & Li, Y. (2003). Effect of pH on the Association of Denatured Whey Proteins with Casein Micelles in Heated Reconstituted Skim Milk. *Journal of Agricultural and Food Chemistry*, *51*(6), 1640–1646. https://doi.org/10.1021/jf025673a

Anema, Skelte G., & McKenna, A. B. (1996). Reaction kinetics of thermal denaturation of whey proteins in heated reconstituted whole milk. *Journal of Agricultural and Food Chemistry*, *44*(2), 422–428.

Appel, W. (1986). Chymotrypsin: Molecular and catalytic properties. *Clinical Biochemistry*, *19*(6), 317–322. https://doi.org/10.1016/S0009-9120(86)80002-9

Apple, R. D. (1988). *Mothers and medicine. A social history of infant feeding, 1890–1950* (University of Wisconsin Press, Vol. 34).

Armand, M., Hamosh, M., Mehta, N. R., Angelus, P. A., Philpott, J. R., Henderson, T. R., Dwyer, N. K., Lairon, D., & Hamosh, P. (1996). Effect of Human Milk or Formula on Gastric Function and Fat Digestion in the Premature Infant. *Pediatric Research*, *40*(3), 429–437. https://doi.org/10.1203/00006450-199609000-00011

Atkinson, S. A., & Lönnerdal, B. (1995). Nonprotein Nitrogen Fractions of Human Milk. In R. G. Jensen (Ed.), *Handbook of Milk Composition* (pp. 369–387). Academic Press. https://doi.org/10.1016/B978-012384430-9/50017-2

Aumeistere, L., Ciprovica, I., Zavadska, D., & Bavrins, K. (2017). *A preliminary study on essential minerals in human milk: Association with dietary habits*. 230–236. https://doi.org/10.22616/rrd.23.2017.034

Aunsholt, L., Jeppesen, P. B., Lund, P., Sangild, P. T., Ifaoui, I. B. R., Qvist, N., & Husby, S. (2014). Bovine Colostrum to Children With Short Bowel Syndrome. *Journal of Parenteral and Enteral Nutrition*, *38*(1), 99–106. https://doi.org/10.1177/0148607112469630

Auricchio, S., Stellato, A., & Vizia, B. D. (1981). Development of Brush Border Peptidases in Human and Rat Small Intestine during Fetal and Neonatal Life. *Pediatric Research*, *15*(7), 991–995. https://doi.org/10.1203/00006450-198107000-00003

Baer, A., Oroz, M., & Blanc, B. (1976). Serological studies on heat-induced interactions of α-lactalbumin and milk proteins. *Journal of Dairy Research*, *43*(3), 419–432. Cambridge Core. https://doi.org/10.1017/S0022029900016009

Baker, E. N., & Baker, H. M. (2005). Lactoferrin. *Cellular and Molecular Life Sciences*, *62*(22), 2531. https://doi.org/10.1007/s00018-005-5368-9

Baker, Edward N, Baker, H. M., & Kidd, R. D. (2002). Lactoferrin and transferrin: Functional variations on a common structural framework. *Biochemistry and Cell Biology*, *80*(1), 27–34. https://doi.org/10.1139/o01-153

Baker, E.N. (1994). Structure and Reactivity of Transferrins. In A. G. Sykes (Ed.), *Advances in Inorganic Chemistry* (Vol. 41, pp. 389–463). Academic Press. https://doi.org/10.1016/S0898-8838(08)60176-2

Ballard, O., & Morrow, A. L. (2013). Human milk composition: Nutrients and bioactive factors. *Pediatric Clinics of North America*, *60*(1), 49–74. PubMed. https://doi.org/10.1016/j.pcl.2012.10.002

Bansal, B., & Chen, X. D. (2006). A Critical Review of Milk Fouling in Heat Exchangers. *Comprehensive Reviews in Food Science and Food Safety*, *5*(2), 27–33. https://doi.org/10.1111/j.1541-4337.2006.tb00080.x

Bastian, E. D., & Brown, R. J. (1996). Plasmin in milk and dairy products: An update. *International Dairy Journal*, *6*(5), 435–457. https://doi.org/10.1016/0958-6946(95)00021-6

Beaulieu, M., Pouliot, Y., & Pouliot, M. (1999). Thermal Aggregation of Whey Proteins in Model Solutions as Affected by Casein/Whey Protein Ratios. *Journal of Food Science*, *64*(5), 776–780. https://doi.org/10.1111/j.1365-2621.1999.tb15910.x

Ben, X.-M. (2008). Nutritional management of newborn infants: Practical guidelines. *World Journal of Gastroenterology*, *14*(40), 6133. https://doi.org/10.3748/wjg.14.6133

Bengoechea, C., Peinado, I., & McClements, D. J. (2011). Formation of protein nanoparticles by controlled heat treatment of lactoferrin: Factors affecting particle characteristics. *Food Hydrocolloids*, *25*(5), 1354–1360. https://doi.org/10.1016/j.foodhyd.2010.12.014

Berdagué, J. L., Grappin, R., & Duboz, G. (1987). Affinage et qualité du Gruyère de Comté. II. Influence de l'affinage sur l'évolution des caractéristiques physico-chimiques des fromages. *Le Lait*, *67*(2), 237–247.

Berger, A., Fleith, M., & Crozier, G. (2000). Nutritional Implications of Replacing Bovine Milk Fat With Vegetable Oil in Infant Formulas. *Journal of Pediatric Gastroenterology and Nutrition*, *30*(2). https://journals.lww.com/jpgn/Fulltext/2000/02000/Nutritional_Implications_of_Replacing_Bovine_Milk.6.aspx

Berry, G.C. (1966). Thermodynamic and Conformational Properties of Polystyrene. I. Light-Scattering Studies on Dilute Solutions of Linear Polystyrenes. *The Journal of Chemical Physics*, *44*(12), 4550–4564. https://doi.org/10.1063/1.1726673

Berseth, C. L. (2006). Development and physiology of the gastrointestinal tract. In P. J. Thureen & W. W. Hay (Eds.), *Neonatal Nutrition and Metabolism* (2nd ed., pp. 67–75). Cambridge University Press; Cambridge Core. https://doi.org/10.1017/CBO9780511544712.007

Beverly, R. L., Underwood, M. A., & Dallas, D. C. (2019). Peptidomics Analysis of Milk Protein-Derived Peptides Released over Time in the Preterm Infant Stomach. *Journal of Proteome Research*, *18*(3), 912–922. https://doi.org/10.1021/acs.jproteome.8b00604

Bindels, J. G. (1992). Artificial feeds for infants—Human milk substitutes: Current composition and future trends. *Current Paediatrics*, *2*(3), 163–167. https://doi.org/10.1016/0957-5839(92)90257-R

Blanchard, E., Zhu, P., & Schuck, P. (2013). Infant formula powders. In *Handbook of Food Powders* (pp. 465–483). Elsevier. https://doi.org/10.1533/9780857098672.3.465

Blanquet, S., Zeijdner, E., Beyssac, E., Meunier, J.-P., Denis, S., Havenaar, R., & Alric, M. (2004). A Dynamic Artificial Gastrointestinal System for Studying the Behavior of Orally Administered Drug Dosage Forms Under Various Physiological Conditions. *Pharmaceutical Research*, *21*(4), 585–591. https://doi.org/10.1023/B:PHAM.0000022404.70478.4b

Bocquet, A., Turck, D., Briend, A., Chouraqui, J. P., Darmaun, D., Dupont, C., Feillet, F., Frelut, M. L., Girardet, J. P., Hankard, R., Goulet, O., Rieu, D., Rozé, J. C., Simeoni, U., & Vidailhet, M. (2015). Les préparations pour nourrissons dénommées « en relais de l'allaitement maternel » sont-elles utiles ? *Archives de Pédiatrie*, *22*(12), 1213–1216. https://doi.org/10.1016/j.arcped.2015.09.020

Bode, L. (2012). Human milk oligosaccharides: Every baby needs a sugar mama. *Glycobiology*, *22*(9), 1147–1162. https://doi.org/10.1093/glycob/cws074

Bogahawaththa, D., Chandrapala, J., & Vasiljevic, T. (2017). Thermal denaturation of bovine immunoglobulin G and its association with other whey proteins. *Food Hydrocolloids*, *72*, 350–357. https://doi.org/10.1016/j.foodhyd.2017.06.017

Bogahawaththa, D., & Vasiljevic, T. (2020). Shearing accelerates denaturation of β-lactoglobulin and α-lactalbumin in skim milk during heating. *International Dairy Journal*, *105*, 104674. https://doi.org/10.1016/j.idairyj.2020.104674

Bohn, T., Carriere, F., Day, L., Deglaire, A., Egger, L., Freitas, D., Golding, M., Le Feunteun, S., Macierzanka, A., Menard, O., Miralles, B., Moscovici, A., Portmann, R., Recio, I., Rémond, D., Santé-Lhoutelier, V., Wooster, T. J., Lesmes, U., Mackie, A. R., & Dupont, D. (2018). Correlation between in vitro and in vivo data on food digestion. What can we predict with static in vitro digestion models? *Critical Reviews in Food Science and Nutrition*, *58*(13), 2239–2261. https://doi.org/10.1080/10408398.2017.1315362

Borgström, B., Lindquist, B., & Lundh, G. (1960). Enzyme Concentration and Absorption of Protein and Glucose in Duodenum of Premature Infants. *A.M.A. Journal of Diseases of Children*, *99*(3), 338–343. https://doi.org/10.1001/archpedi.1960.02070030340010

Bosscher, D., Van Caillie-Bertrand, M., Van Dyck, K., Robberecht, H., Van Cauwenbergh, R., & Deelstra, H. (2000). Thickening Infant Formula With Digestible and Indigestible Carbohydrate: Availability of Calcium, Iron, and Zinc In Vitro. *Journal of Pediatric Gastroenterology and Nutrition*, *30*(4). https://journals.lww.com/jpgn/Fulltext/2000/04000/Thickening_Infant_Formula_With_Digestible_and.5.aspx

Boudry, G., David, E. S., Douard, V., Monteiro, I. M., Le Huërou-Luron, I., & Ferraris, R. P. (2010). Role of Intestinal Transporters in Neonatal Nutrition: Carbohydrates, Proteins, Lipids, Minerals, and Vitamins. *Journal of Pediatric Gastroenterology and Nutrition*, *51*(4). https://journals.lww.com/jpgn/Fulltext/2010/10000/Role_of_Intestinal_Transporters_in_Neonatal.3.aspx

Bourlieu, C., Deglaire, A., de Oliveira, S. C., Ménard, O., Le Gouar, Y., Carrière, F., & Dupont, D. (2017). Towards infant formula biomimetic of human milk structure and digestive behaviour. *OCL*, *24*(2), D206. https://doi.org/10.1051/ocl/2017010

Bourlieu, C., Ménard, O., Bouzerzour, K., Mandalari, G., Macierzanka, A., Mackie, A. R., & Dupont, D. (2014). Specificity of Infant Digestive Conditions: Some Clues for Developing Relevant In Vitro Models. *Critical Reviews in Food Science and Nutrition*, *54*(11), 1427–1457. https://doi.org/10.1080/10408398.2011.640757

Bourlieu, C., Ménard, O., De La Chevasnerie, A., Sams, L., Rousseau, F., Madec, M.-N., Robert, B., Deglaire, A., Pezennec, S., Bouhallab, S., Carrière, F., & Dupont, D. (2015). The structure of infant formulas impacts their lipolysis, proteolysis and disintegration during in vitro gastric digestion. *Food Chemistry*, *182*, 224–235. https://doi.org/10.1016/j.foodchem.2015.03.001

Boutrou, R., Gaudichon, C., Dupont, D., Jardin, J., Airinei, G., Marsset-Baglieri, A., Benamouzig, R., Tomé, D., & Leonil, J. (2013). Sequential release of milk protein–derived bioactive peptides in the jejunum in healthy humans. *The American Journal of Clinical Nutrition*, *97*(6), 1314–1323. https://doi.org/10.3945/ajcn.112.055202

Bouzerzour, K., Morgan, F., Cuinet, I., Bonhomme, C., Jardin, J., Le Huërou-Luron, I., & Dupont, D. (2012). In vivo digestion of infant formula in piglets: Protein digestion kinetics and release of bioactive peptides. *British Journal of Nutrition*, *108*(12), 2105–2114. Cambridge Core. https://doi.org/10.1017/S000711451200027X

Boye, J. I., & Alli, I. (2000). Thermal denaturation of mixtures of α-lactalbumin and β-lactoglobulin: A differential scanning calorimetric study. *Food Research International*, *33*(8), 673–682. https://doi.org/10.1016/S0963-9969(00)00112-5

Boye, J. I., Ma, C. Y., & Ismail, A. (2004). Thermal stability of β-lactoglobulins A and B: Effect of SDS, urea, cysteine and N-ethylmaleimide. *Journal of Dairy Research*, *71*(2), 207–215. Scopus. https://doi.org/10.1017/S0022029904000184

Brenna, J. T., Varamini, B., Jensen, R. G., Diersen-Schade, D. A., Boettcher, J. A., & Arterburn, L. M. (2007). Docosahexaenoic and arachidonic acid concentrations in human breast milk worldwide. *The American Journal of Clinical Nutrition*, *85*(6), 1457–1464. https://doi.org/10.1093/ajcn/85.6.1457

Brew, K. (2011). Milk Proteins | α-Lactalbumin. In J. W. Fuquay (Ed.), *Encyclopedia of Dairy Sciences (Second Edition)* (pp. 780–786). Academic Press. https://doi.org/10.1016/B978-0-12-374407-4.00432-5

Brew, K. (2013). α-Lactalbumin. In Paul L. H. McSweeney & P. F. Fox (Eds.), *Advanced Dairy Chemistry: Volume 1A: Proteins: Basic Aspects, 4th Edition* (pp. 261–273). Springer US. https://doi.org/10.1007/978-1-4614-4714-6_8

Brew, Keith, & Grobler, J. (1992). α-Lactalbumin. *Advanced Dairy Chemistry*, *1*, 191–229.

Brisson, G., Britten, M., & Pouliot, Y. (2007). Effect of Iron Saturation on the Recovery of Lactoferrin in Rennet Whey Coming from Heat-Treated Skim Milk. *Journal of Dairy Science*, *90*(6), 2655–2664. https://doi.org/10.3168/jds.2006-725

Britten, M., Green, M. L., Boulet, M., & Paquin, P. (1988). Deposit formation on heated surfaces: Effect of interface energetics. *Journal of Dairy Research*, *55*(4), 551–562. Cambridge Core. https://doi.org/10.1017/S0022029900033331

Britton, J. R., & Koldovsky, O. (1989). Gastric luminal digestion of lactoferrin and transferrin by preterm infants. *Early Human Development*, *19*(2), 127–135. https://doi.org/10.1016/0378-3782(89)90123-0

Brock, J. H. (2002). The physiology of lactoferrin. *Biochemistry and Cell Biology*, *80*(1), 1–6. https://doi.org/10.1139/o01-212

Brodkorb, A., Croguennec, T., Bouhallab, S., & Kehoe, J. J. (2016). Heat-Induced Denaturation, Aggregation and Gelation of Whey Proteins. In Paul L. H. McSweeney & J. A. O'Mahony (Eds.), *Advanced Dairy Chemistry: Volume 1B: Proteins: Applied Aspects* (pp. 155–178). Springer New York. https://doi.org/10.1007/978-1-4939-2800-2_6

Brodkorb, A., Egger, L., Alminger, M., Alvito, P., Assunção, R., Ballance, S., Bohn, T., Bourlieu-Lacanal, C., Boutrou, R., Carrière, F., Clemente, A., Corredig, M., Dupont, D., Dufour, C., Edwards, C., Golding, M., Karakaya, S., Kirkhus, B., Le Feunteun, S., … Recio, I. (2019). INFOGEST static in vitro simulation of gastrointestinal food digestion. *Nature Protocols*, *14*(4), 991–1014. https://doi.org/10.1038/s41596-018-0119-1

Brown, J. (2016). *Nutrition Through the Life Cycle* (6th ed.). CENGAGE Learning Custom Publishing.

Broyard, C., & Gaucheron, F. (2015). Modifications of structures and functions of caseins: A scientific and technological challenge. *Dairy Science & Technology*, *95*(6), 831–862.

Brulé, G., Maubois, J. L., & Fauquant, J. (1974). Étude de la teneur en éléments minéraux des produits obtenus lors de l'ultrafiltration du lait sur membrane. *Le Lait*, *54*(539–540), 600–615.

Buggy, A. K., McManus, J. J., Brodkorb, A., Carthy, N. M., & Fenelon, M. A. (2017). Stabilising effect of α-lactalbumin on concentrated infant milk formula emulsions heat treated pre- or post-homogenisation. *Dairy Science & Technology*, *96*(6), 845–859. https://doi.org/10.1007/s13594-016-0306-1

Butler, J. (1994). Indigenous antimicrobial agents of milk. Recent developments. *Indigenous Antimicrobial Agents of Milk: Recent Developments*.

Bylund, G. (1995). Milk powder. In *Dairy Processing Handbook*. Tetra Pak Processing Systems AB.

Calapaj, G. G. (1968). An electron microscope study of the ultrastructure of bovine and human casein micelles in fresh and acidified milk. *Journal of Dairy Research*, *35*(1), 1–6. https://doi.org/10.1017/S0022029900018719

Calbet, J. A. L., & Holst, J. J. (2004). Gastric emptying, gastric secretion and enterogastrone response after administration of milk proteins or their peptide hydrolysates in humans. *European Journal of Nutrition*, *43*(3), 127–139. https://doi.org/10.1007/s00394-004-0448-4

Calvo, M. M., Leaver, J., & Banks, J. M. (1993). Influence of other whey proteins on the heat-induced aggregation of α-lactalbumin. *International Dairy Journal*, *3*(8), 719–727. https://doi.org/10.1016/0958-6946(93)90085-E

Carbonaro, M., Cappelloni, M., Sabbadini, S., & Carnovale, E. (1997). Disulfide Reactivity and In Vitro Protein Digestibility of Different Thermal-Treated Milk Samples and Whey Proteins. *Journal of Agricultural and Food Chemistry*, *45*(1), 95–100. https://doi.org/10.1021/jf950828i

Castellino, J., Fish, W., & Kenneth, G. (1970). Studies on Bovine Lactoferrin. *The Journal of Biological Chemistry*, *245*(17), 4269–4275.

Castellote, C., Casillas, R., Ramírez-Santana, C., Pérez-Cano, F. J., Castell, M., Moretones, M. G., López-Sabater, M. C., & Franch, À. (2011). Premature Delivery Influences the Immunological Composition of Colostrum and Transitional and Mature Human Milk. *The Journal of Nutrition*, *141*(6), 1181–1187. https://doi.org/10.3945/jn.110.133652

Castillo, E., Pérez, M. D., Franco, I., Calvo, M., & Sánchez, L. (2012). Kinetic and thermodynamic parameters for heat denaturation of human recombinant lactoferrin from rice [1] This article is part of a Special Issue entitled Lactoferrin and has undergone the Journal's usual peer review process. *Biochemistry and Cell Biology*, *90*(3), 389–396. https://doi.org/10.1139/o11-073

Cattaneo, A., Burmaz, T., Arendt, M., Nilsson, I., Mikiel-Kostyra, K., Kondrate, I., Communal, M. J., Massart, C., Chapin, E., & Fallon, M. (2010). Protection, promotion and support of breast-feeding in Europe: Progress from 2002 to 2007. *Public Health Nutrition*, *13*(06), 751–759. https://doi.org/10.1017/S1368980009991844

Cavallarin, E. B. (2011). Effect of two pasteurization methods on the protein content of human milk Cristina Baro1, Marzia Giribaldi1, Sertac Arslanoglu2, Maria Gabriella Giuffrida1, Giuseppina Dellavalle1, Amedeo Conti1, Paola Tonetto2, 3, Augusto Biasini2, 4, Alessandra Coscia3, Claudio Fabris3, Guido Eugenio Moro2, 5, Laura. *Frontiers in Bioscience*, *3*, 818–829.

Cavell, B. (1983). Postprandial gastric acid secretion in infants. *Acta Paediatrica*, *72*(6), 857–860. https://doi.org/10.1111/j.1651-2227.1983.tb09830.x

Cavkll, B. (1981). Gastric emptying in infants fed human milk or infant formula. *Acta Paediatrica*, *70*(5), 639–641. https://doi.org/10.1111/j.1651-2227.1981.tb05760.x

Ceja-Medina, L. I., Jiménez-Fernández, M., Andrade-González, I., Navarrete-Guzmán, A., Chacón-López, M. A., García-Magaña, M. L., Bonilla-Cárdenas, J. A., & Ortiz-Basurto, R. I. (2020). Microbiological stability and general sensory acceptance of microfiltered skim milk with agave fructans of a high degree of polymerization added. *Journal of Food Safety*, *n/a*(n/a), e12844. https://doi.org/10.1111/jfs.12844

Chaplin, L. C., & Lyster, R. L. J. (1986). Irreversible heat denaturation of bovine α-lactalbumin. *Journal of Dairy Research*, *53*(2), 249–258. Cambridge Core. https://doi.org/10.1017/S0022029900024857

Chatterton, Dereck E.W., Nguyen, D. N., Bering, S. B., & Sangild, P. T. (2013). Anti-inflammatory mechanisms of bioactive milk proteins in the intestine of newborns. *The International Journal of Biochemistry & Cell Biology*, *45*(8), 1730–1747. https://doi.org/10.1016/j.biocel.2013.04.028

Chatterton, D.E.W, Rasmussen, J. T., Heegaard, C. W., Sørensen, E. S., & Petersen, T. E. (2004). In vitro digestion of novel milk protein ingredients for use in infant formulas: Research on biological functions. *Trends in Food Science & Technology*, *15*(7–8), 373–383. https://doi.org/10.1016/j.tifs.2003.12.004

Cheison, S. C., Lai, M.-Y., Leeb, E., & Kulozik, U. (2011). Hydrolysis of β-lactoglobulin by trypsin under acidic pH and analysis of the hydrolysates with MALDI–TOF–MS/MS. *Food Chemistry*, *125*, 1241–1248. https://doi.org/10.1016/j.foodchem.2010.10.042

Chierici, R., Sawatzki, G., Tamisari, L., Volpato, S., & Vigi, V. (1992). Supplementation of an adapted formula with bovine lactoferrin. 2. Effects on serum iron, ferritin and zinc levels. *Acta Paediatrica*, *81*(6–7), 475–479. https://doi.org/10.1111/j.1651-2227.1992.tb12277.x

Chierici, R., & Vigi, V. (1994). Lactoferrin in infant formulae. *Acta Paediatrica*, *83*(s402), 83–88. https://doi.org/10.1111/j.1651-2227.1994.tb13367.x

Church, F. C., Swaisgood, H. E., Porter, D. H., & Catignani, G. L. (1983). Spectrophotometric assay using o-phthaldialdehyde for determination of proteolysis in milk and isolated milk proteins. *Journal of Dairy Science*, *66*(6), 1219–1227.

Cleghorn, G., Durie, P., Benjamin, L., & Dati, F. (1988). The Ontogeny of Serum Immunoreactive Pancreatic Lipase and Cationic Trypsinogen in the Premature Human Infant. *Neonatology*, *53*(1), 10–16. https://doi.org/10.1159/000242756

Codex Alimentarius Commission. (1981). *Standard For Infant Formula And Formulas For Special Medical Purposes Intended For Infants*. FAO/WHO.

Conesa, C., Calvo, M., & Sánchez, L. (2010). Recombinant human lactoferrin: A valuable protein for pharmaceutical products and functional foods. *Biotechnology Advances*, *28*(6), 831–838. https://doi.org/10.1016/j.biotechadv.2010.07.002

Córdova-Dávalos, L. E., Jiménez, M., & Salinas, E. (2019). Glycomacropeptide Bioactivity and Health: A Review Highlighting Action Mechanisms and Signaling Pathways. *Nutrients*, *11*(3), 598. PubMed. https://doi.org/10.3390/nu11030598

Corredig, M., Dalgleish, D.G. (1999). The mechanisms of the heat-induced interaction of whey proteins with casein micelles in milk. *International Dairy Journal*, *9*, 233–236. https://doi.org/10.1016/S0958-6946(99)00066-7

Corzo-Martínez, M., Soria, A. C., Belloque, J., Villamiel, M., & Moreno, F. J. (2010). Effect of glycation on the gastrointestinal digestibility and immunoreactivity of bovine β-lactoglobulin. *International Dairy Journal*, *20*(11), 742–752. https://doi.org/10.1016/j.idairyj.2010.04.002

Costa, F. F., Vasconcelos Paiva Brito, M. A., Moreira Furtado, M. A., Martins, M. F., Leal de Oliveira, M. A., Mendonça de Castro Barra, P., Amigo Garrido, L., & Siqueira de Oliveira dos Santos, A. (2014). Microfluidic chip electrophoresis investigation of major milk proteins: Study of buffer effects and quantitative approaching. *Analytical Methods*, *6*(6), 1666–1673. https://doi.org/10.1039/C3AY41706A

Creamer, L., Loveday, S., & Sawyer, L. (2011). Beta-lactoglobulin. In *Encyclopedia of Dairy Sciences* (Vol. 3, pp. 787–794).

Croguennec, T., Leng, N., Hamon, P., Rousseau, F., Jeantet, R., & Bouhallab, S. (2014). Caseinomacropeptide modifies the heat-induced denaturation–aggregation process of β-lactoglobulin. *International Dairy Journal*, *36*(1), 55–64. https://doi.org/10.1016/j.idairyj.2014.01.004

Croguennec, T., Li, N., Phelebon, L., Garnier-Lambrouin, F., & Gésan-Guiziou, G. (2012). Interaction between lactoferrin and casein micelles in skimmed milk. *International Dairy Journal*, *27*(1–2), 34–39. https://doi.org/10.1016/j.idairyj.2012.06.003

Crowley, S. V., Dowling, A. P., Caldeo, V., Kelly, A. L., & O'Mahony, J. A. (2016). Impact of α-lactalbumin:β-lactoglobulin ratio on the heat stability of model infant milk formula protein systems. *Food Chemistry*, *194*, 184–190. https://doi.org/10.1016/j.foodchem.2015.07.077

Cuillière, M. L., Trégoat, V., Béné, M. C., Faure, G., & Montagne, P. (1999). Changes in the kappa-casein and beta-casein concentrations in human milk during lactation. *Journal of Clinical Laboratory Analysis*, *13*(5), 213–218. PubMed. https://doi.org/10.1002/(SICI)1098-2825(1999)13:5<213::AID-JCLA4>3.0.CO;2-F

Dalgleish, D.G., & Banks, J. M. (1991). The formation of complexes between serum proteins and fat globules during heating of whole milk. *Milchwissenschaft*, *46*(2), 75–78.

Dalgleish, D.G., Horne, D. S., & Law, A. J. R. (1989). Size-related differences in bovine casein micelles. *Biochimica et Biophysica Acta (BBA) - General Subjects*, *991*(3), 383–387. https://doi.org/10.1016/0304-4165(89)90061-5

Dalgleish, Douglas G., Senaratne, V., & Francois, S. (1997). Interactions between α-lactalbumin and β-lactoglobulin in the early stages of heat denaturation. *Journal of Agricultural and Food Chemistry*, *45*(9), 3459–3464.

Dallas, D. C., Guerrero, A., Khaldi, N., Borghese, R., Bhandari, A., Underwood, M. A., Lebrilla, C. B., German, J. B., & Barile, D. (2014). A peptidomic analysis of human milk digestion in the infant stomach reveals protein-specific degradation patterns. *The Journal of Nutrition*, *144*(6), 815–820. PubMed. https://doi.org/10.3945/jn.113.185793

Dallas, D. C., Guerrero, A., Khaldi, N., Castillo, P. A., Martin, W. F., Smilowitz, J. T., Bevins, C. L., Barile, D., German, J. B., & Lebrilla, C. B. (2013). Extensive in vivo human milk peptidomics reveals specific proteolysis yielding protective antimicrobial peptides. *Journal of Proteome Research*, *12*(5), 2295–2304. PubMed. https://doi.org/10.1021/pr400212z

Dallas, D. C., Guerrero, A., Parker, E. A., Garay, L. A., Bhandari, A., Lebrilla, C. B., Barile, D., & German, J. B. (2014). Peptidomic Profile of Milk of Holstein Cows at Peak Lactation. *Journal of Agricultural and Food Chemistry*, *62*(1), 58–65. https://doi.org/10.1021/jf4040964

Dallas, D. C., Murray, N. M., & Gan, J. (2015). Proteolytic Systems in Milk: Perspectives on the Evolutionary Function within the Mammary Gland and the Infant. *Journal of Mammary Gland Biology and Neoplasia*, *20*(3–4), 133–147. PubMed. https://doi.org/10.1007/s10911-015-9334-3

Dangin, M., Boirie, Y., Guillet, C., & Beaufrère, B. (2002). Influence of the Protein Digestion Rate on Protein Turnover in Young and Elderly Subjects. *The Journal of Nutrition*, *132*(10), 3228S-3233S. https://doi.org/10.1093/jn/131.10.3228S

Dangin, M., Guillet, C., Garcia-Rodenas, C., Gachon, P., Bouteloup-Demange, C., Reiffers-Magnani, K., Fauquant, J., Ballèvre, O., & Beaufrère, B. (2003). The rate of protein digestion affects protein gain differently during aging in humans. *The Journal of Physiology*, *549*(Pt 2), 635–644. PubMed. https://doi.org/10.1113/jphysiol.2002.036897

Daniel, H. (2004). Molecular and Integrative Physiology of Intestinal Peptide Transport. *Annual Review of Physiology*, *66*(1), 361–384. https://doi.org/10.1146/annurev.physiol.66.032102.144149

Dannenberg, F., & Kessler, H.-G. (1988). Reaction kinetics of the denaturation of whey proteins in milk. *Journal of Food Science*, *53*(1), 258–263.

Darmawan, K. K., Karagiannis, T. C., Hughes, J. G., Small, D. M., & Hung, A. (2020). High temperature induced structural changes of apo-lactoferrin and interactions with β-lactoglobulin and α-lactalbumin for potential encapsulation strategies. *Food Hydrocolloids*, *105*, 105817. https://doi.org/10.1016/j.foodhyd.2020.105817

Darragh, A. J., & Moughan, P. J. (1998). The amino acid composition of human milk corrected for amino acid digestibility. *British Journal of Nutrition*, *80*(1), 25–34. Cambridge Core. https://doi.org/10.1017/S0007114598001731

Davidson, G. P., Daniels, E., Nunan, H., Moore, A. G., Whyte, P. B. D., Franklin, K., Mccloud, P. I., & Moore, D. J. (1989). Passive immunisation of children with bovine colostrum containing antibodies to human rotavirus. *Originally Published as Volume 2, Issue 8665*, *334*(8665), 709–712. https://doi.org/10.1016/S0140-6736(89)90771-X

Davidson, L. A., & Lönnerdal, B. (1987). Persistence of Human Milk Proteins in the Breast-Fed Infant. *Acta Paediatrica*, *76*(5), 733–740. https://doi.org/10.1111/j.1651-2227.1987.tb10557.x

Davidson, L. A., & Lonnerdal, B. (1988). Specific binding of lactoferrin to brush-border membrane: Ontogeny and effect of glycan chain. *American Journal of Physiology-Gastrointestinal and Liver Physiology*, *254*(4), G580–G585. https://doi.org/10.1152/ajpgi.1988.254.4.G580

Davies, M. G., & Thomas, A. J. (1973). An investigation of hydrolytic techniques for the amino acid analysis of foodstuffs. *Journal of the Science of Food and Agriculture*, *24*(12), 1525–1540. https://doi.org/10.1002/jsfa.2740241208

Davis, A. M., Harris, B. J., Lien, E. L., Pramuk, K., & Trabulsi, J. (2008). α-Lactalbumin-rich infant formula fed to healthy term infants in a multicenter study: Plasma essential amino acids and gastrointestinal tolerance. *European Journal of Clinical Nutrition*, *62*(11), 1294–1301. https://doi.org/10.1038/sj.ejcn.1602848

de Figueiredo Furtado, G., Pereira, R. N. C., Vicente, A. A., & Cunha, R. L. (2018). Cold gel-like emulsions of lactoferrin subjected to ohmic heating. *Food Research International*, *103*, 371–379. https://doi.org/10.1016/j.foodres.2017.10.061

de Guibert, D., Hennetier, M., Martin, F., Six, T., Gu, Y., Le Floch-Fouéré, C., Delaplace, G., & Jeantet, R. (2020). Flow process and heating conditions modulate the characteristics of whey protein aggregates. *Journal of Food Engineering*, *264*, 109675. https://doi.org/10.1016/j.jfoodeng.2019.07.022

de Haan, P., Ianovska, M. A., Mathwig, K., van Lieshout, G. A. A., Triantis, V., Bouwmeester, H., & Verpoorte, E. (2019). Digestion-on-a-chip: A continuous-flow modular microsystem recreating enzymatic digestion in the gastrointestinal tract. *Lab on a Chip*, *19*(9), 1599–1609. https://doi.org/10.1039/C8LC01080C

de Kruif, C. G. (1997). Skim Milk Acidification. *Journal of Colloid and Interface Science*, *185*(1), 19–25. https://doi.org/10.1006/jcis.1996.4548

de la Fuente, M. A., Singh, H., & Hemar, Y. (2002). Recent advances in the characterisation of heat-induced aggregates and intermediates of whey proteins. *Trends in Food Science & Technology*, *13*(8), 262–274. https://doi.org/10.1016/S0924-2244(02)00133-4

De oliveira, S. C. (2016). *Impact de la pasteurisation et de l'homogénéisation sur la digestion du lait maternel chez le nouveau-né: Etudes in vitro et in vivo*. http://www.theses.fr/2016NSARB284/document

de Oliveira, S. C., Deglaire, A., Ménard, O., Bellanger, A., Rousseau, F., Henry, G., Dirson, E., Carrière, F., Dupont, D., & Bourlieu, C. (2016). Holder pasteurization impacts the proteolysis, lipolysis and disintegration of human milk under in vitro dynamic term newborn digestion. *Food Research International*, *88*, 263–275. https://doi.org/10.1016/j.foodres.2015.11.022

de Wit, J. N. (1998). Nutritional and Functional Characteristics of Whey Proteins in Food Products. *Journal of Dairy Science*, *81*(3), 597–608. https://doi.org/10.3168/jds.S0022-0302(98)75613-9

de Wit, J. N. (2009). Thermal behaviour of bovine β-lactoglobulin at temperatures up to 150°C. a review. *Trends in Food Science & Technology*, *20*(1), 27–34. https://doi.org/10.1016/j.tifs.2008.09.012

Debye, P. (1944). Light Scattering in Solutions. *Journal of Applied Physics*, *15*, 338. https://doi.org/10.1063/1.1707436

Deeth, H., & Bansal, N. (2019). Chapter 1—Whey Proteins: An Overview. In H. C. Deeth & N. Bansal (Eds.), *Whey Proteins* (pp. 1–50). Academic Press. https://doi.org/10.1016/B978-0-12-812124-5.00001-1

Deglaire, Amélie, Bos, C., Tomé, D., & Moughan, P. J. (2009). Ileal digestibility of dietary protein in the growing pig and adult human. *British Journal of Nutrition*, *102*(12), 1752–1759. Cambridge Core. https://doi.org/10.1017/S0007114509991267

Deglaire, Amélie, De Oliveira, S. C., Jardin, J., Briard-Bion, V., Emily, M., Ménard, O., Bourlieu, C., & Dupont, D. (2016). Impact of human milk pasteurization on the kinetics of peptide release during in vitro dynamic term newborn digestion. *ELECTROPHORESIS*, *37*(13), 1839–1850. https://doi.org/10.1002/elps.201500573

Deglaire, Amélie, Fromentin, C., Fouillet, H., Airinei, G., Gaudichon, C., Boutry, C., Benamouzig, R., Moughan, P. J., Tomé, D., & Bos, C. (2009). Hydrolyzed dietary casein as compared with the intact protein reduces postprandial peripheral, but not whole-body, uptake of nitrogen in humans. *The American Journal of Clinical Nutrition*, *90*(4), 1011–1022. https://doi.org/10.3945/ajcn.2009.27548

Deglaire, Amelie, & Moughan, P. J. (2012). Animal models for determining amino acid digestibility in humans – a review. *British Journal of Nutrition*, *108*(S2), S273–S281. Cambridge Core. https://doi.org/10.1017/S0007114512002346

Deglaire, Amélie, Oliveira, S. D., Jardin, J., Briard-Bion, V., Kroell, F., Emily, M., Ménard, O., Bourlieu, C., & Dupont, D. (2019). Impact of human milk pasteurization on the kinetics of peptide release during in vitro dynamic digestion at the preterm newborn stage. *Food Chemistry*, *281*, 294–303. https://doi.org/10.1016/j.foodchem.2018.12.086

Delachaume-Salem, E., & Sarles, H. (1970). Evolution en fonction de l'age de la secretion pancreatique humaine normale. *Biol Gastroenterol*, *2*, 135–146.

Delplace, F., Leuliet, J. C., & Leviex, D. (1997). A reaction engineering approach to the analysis of fouling by whey proteins of a six-channels-per-pass plate heat exchanger. *Journal of Food Engineering*, *34*(1), 91–108. https://doi.org/10.1016/S0260-8774(97)00068-X

Delplanque, B., Du, Q., Agnani, G., Le Ruyet, P., & Martin, J. C. (2013). A dairy fat matrix providing alpha-linolenic acid (ALA) is better than a vegetable fat mixture to increase brain DHA accretion in young rats. *The Tenth Fatty Acids and Cell Signalling Meeting (FACS-10)*, *88*(1), 115–120. https://doi.org/10.1016/j.plefa.2012.07.004

Dey, T. (2011). Fennema's Food Chemistry, Fourth Edition, Edited by Srinivasan Damodaran, Kirk L. Parkin and Owen R. Fennema. *Journal of Dispersion Science and Technology - J DISPER SCI TECH*. https://doi.org/10.1080/01932691.2011.584482

Dickinson, E. (2013). Stabilising emulsion-based colloidal structures with mixed food ingredients. *Journal of the Science of Food and Agriculture*, *93*(4), 710–721. https://doi.org/10.1002/jsfa.6013

Dissanayake, M., Ramchandran, L., Donkor, O. N., & Vasiljevic, T. (2013). Denaturation of whey proteins as a function of heat, pH and protein concentration. *International Dairy Journal*, *31*(2), 93–99. Scopus. https://doi.org/10.1016/j.idairyj.2013.02.002

Dissanayake, Muditha, Ramchandran, L., Piyadasa, C., & Vasiljevic, T. (2013). Influence of heat and pH on structure and conformation of whey proteins. *International Dairy Journal*, *28*(2), 56–61. https://doi.org/10.1016/j.idairyj.2012.08.014

Donangelo, C. M., & Trugo, N. M. F. (2003). Lactation | Human Milk: Composition and Nutritional Value. In B. Caballero (Ed.), *Encyclopedia of Food Sciences and Nutrition (Second Edition)* (pp. 3449–3458). Academic Press. https://doi.org/10.1016/B0-12-227055-X/01356-0

Donato, L., Alexander, M., & Dalgleish, D. G. (2007). Acid Gelation in Heated and Unheated Milks: Interactions between Serum Protein Complexes and the Surfaces of Casein Micelles. *Journal of Agricultural and Food Chemistry*, *55*(10), 4160–4168. https://doi.org/10.1021/jf063242c

Donato, L., & Guyomarc'h, F. (2009). Formation and properties of the whey protein/κ-casein complexes in heated skim milk—A review. *Dairy Science & Technology*, *89*(1), 3–29. https://doi.org/10.1051/dst:2008033

Donato, L., Guyomarc'h, F., Amiot, S., & Dalgleish, D. G. (2007). Formation of whey protein/κ-casein complexes in heated milk: Preferential reaction of whey protein with κ-casein in the casein micelles. *International Dairy Journal*, *17*(10), 1161–1167. https://doi.org/10.1016/j.idairyj.2007.03.011

Douglas, F. W., Greenberg, R., Farrell, H. M., & Edmondson, L. F. (1981). Effects of ultra-high-temperature pasteurization on milk proteins. *Journal of Agricultural and Food Chemistry*, *29*(1), 11–15. https://doi.org/10.1021/jf00103a004

Draher, J., & White, N. (2019). HPLC Determination of Total Tryptophan in Infant Formula and Adult/Pediatric Nutritional Formula Following Enzymatic Hydrolysis: Single-Laboratory Validation, First Action 2017.03. *Journal of AOAC INTERNATIONAL*, *101*(3), 824–830. https://doi.org/10.5740/jaoacint.17-0257

Dumpler, J., Wohlschläger, H., & Kulozik, U. (2017). Dissociation and coagulation of caseins and whey proteins in concentrated skim milk heated by direct steam injection. *Dairy Science & Technology*, *96*(6), 807–826. https://doi.org/10.1007/s13594-016-0304-3

Dupont, D., Boutrou, R., Menard, O., Jardin, J., Tanguy, G., Schuck, P., Haab, B. B., & Leonil, J. (2010). Heat Treatment of Milk During Powder Manufacture Increases Casein Resistance to Simulated Infant Digestion. *Food Digestion*, *1*(1–2), 28–39. https://doi.org/10.1007/s13228-010-0003-0

Dupont, D., Mandalari, G., Mollé, D., Jardin, J., Rolet-Répécaud, O., Duboz, G., Léonil, J., Mills, C. E. N., & Mackie, A. R. (2010). Food processing increases casein resistance to simulated infant digestion. *Molecular Nutrition & Food Research*, *54*(11), 1677–1689. https://doi.org/10.1002/mnfr.200900582

Ebina, T., Sato, A., Umezu, K., Ishida, N., Ohyama, S., Oizumi, A., Aikawa, K., Katagiri, S., Katsushima, N., Imai, A., Kitaoka, S., Suzuki, H., & Konno, T. (1985). Prevention of rotavirus infection by oral administration of cow colostrum containing antihumanrotavirus antibody. *Medical Microbiology and Immunology*, *174*(4), 177–185. https://doi.org/10.1007/BF02123694

Ebner, K. E., Denton, W. L., & Brodbeck, U. (1966). The substitution of a-lactalbumin for the B protein of lactose synthetase. *Biochemical and Biophysical Research Communications*, *24*(2), 232–236. https://doi.org/10.1016/0006-291X(66)90725-X

Egger, L., Ménard, O., Baumann, C., Duerr, D., Schlegel, P., Stoll, P., Vergères, G., Dupont, D., & Portmann, R. (2019). Digestion of milk proteins: Comparing static and dynamic in vitro digestion systems with in vivo data. *The 5th International Conference on Food Digestion*, *118*, 32–39. https://doi.org/10.1016/j.foodres.2017.12.049

Egger, L., Schlegel, P., Baumann, C., Stoffers, H., Guggisberg, D., Brügger, C., Dürr, D., Stoll, P., Vergères, G., & Portmann, R. (2017). Physiological comparability of the harmonized INFOGEST in vitro digestion method to in vivo pig digestion. *Food Research International*, *102*, 567–574. https://doi.org/10.1016/j.foodres.2017.09.047

Elashoff, J. D., Reedy, T. J., & Meyer, J. H. (1982). Analysis of Gastric Emptying Data. *Gastroenterology*, *83*(6), 1306–1312. https://doi.org/10.1016/S0016-5085(82)80145-5

Elfagm, A. A., & Wheelock, J. V. (1978). Interaction of bovine α-lactalbumin and β-lactoglobulin during heating. *Journal of Dairy Science*, *61*(1), 28–32.

Engfer, M. B., Stahl, B., Finke, B., Sawatzki, G., & Daniel, H. (2000). Human milk oligosaccharides are resistant to enzymatic hydrolysis in the upper gastrointestinal tract. *The American Journal of Clinical Nutrition*, *71*(6), 1589–1596. https://doi.org/10.1093/ajcn/71.6.1589

Eugenia Lucena, M., Alvarez, S., Menéndez, C., Riera, F. A., & Alvarez, R. (2006). Beta-lactoglobulin removal from whey protein concentrates. *Separation and Purification Technology*, *52*(2), 310–316. https://doi.org/10.1016/j.seppur.2006.05.006

European Childhood Obesity Trial Study Group, Koletzko, B., von Kries, R., Closa, R., Escribano, J., Scaglioni, S., Giovannini, M., Beyer, J., Demmelmair, H., Gruszfeld, D., Dobrzanska, A., Sengier, A., Langhendries, J.-P., Rolland Cachera, M.-F., & Grote, V. (2009). Lower protein in infant formula is associated with lower weight up to age 2 y: A randomized clinical trial. *The American Journal of Clinical Nutrition*, *89*(6), 1836–1845. https://doi.org/10.3945/ajcn.2008.27091

European commission. (2000). *Commission Directive 2000/45/EC of 6 July 2000 establishingCommunity methods of analysis for the determination of vitamin A, vitamin E and tryptophan in feedingstuffs*. http://data.europa.eu/eli/dir/2000/45/oj/fra

European Commission. (2006). Commission Directive 2006/141/EC of 26 December 2006 on infant formulae and follow-on formulae. *Official Journal of European Union*.

European Food Safety Authority. (2012). *EFSA Panel on Dietetic Products, Nutrition and Allergies (NDA): Scientific Opinion on bovine lactoferrin* (10(7):2811). https://efsa.onlinelibrary.wiley.com/doi/pdf/10.2903/j.efsa.2012.2811

European Union. (2016). *Commission delegated regulation (EU) 2016/127 of 25 September 2015 supplementing Regulation (EU) No 609/2013 of the European Parliament and of the Council as regards the specific compositional and information requirements for infant formula and follow-on formula and as regards requirements on information relating to infant and young child feeding*. European commission.

Fagnani, R., Mexia, M. M., Puppio, A. A. N., & Battaglini, A. P. P. (2016). Sanitary aspects and technological challenges of whole milk microfiltration at low temperatures. *Pesquisa Agropecuária Brasileira*, *51*(8), 990–997. https://doi.org/10.1590/S0100-204X2016000800011

Fairweather-Tait, S. J., Balmer, S. E., Scott, P. H., & Minski, M. J. (1987). Lactoferrin and Iron Absorption in Newborn Infants. *Pediatric Research*, *22*(6), 651–654. https://doi.org/10.1203/00006450-198712000-00007

Fan, F., Liu, M., Shi, P., Xu, S., Lu, W., & Du, M. (2019). Effects of thermal treatment on the physicochemical properties and osteogenic activity of lactoferrin. *Journal of Food Processing and Preservation*, *43*(9), e14068. https://doi.org/10.1111/jfpp.14068

Fan, F., Liu, M., Shi, P., Xu, X., Lu, W., Wang, Z., & Du, M. (2018). Protein cross-linking and the Maillard reaction decrease the solubility of milk protein concentrates. *Food Science & Nutrition*, *6*(5), 1196–1203. https://doi.org/10.1002/fsn3.657

Farrell, Harold M., Behe, M. J., & Enyeart, J. A. (1987). Binding of p-Nitrophenyl Phosphate and Other Aromatic Compounds by β-Lactoglobulin. *Journal of Dairy Science*, *70*(2), 252–258. https://doi.org/10.3168/jds.S0022-0302(87)80004-8

Farrell, H.M., Jimenez-Flores, R., Bleck, G. T., Brown, E. M., Butler, J. E., Creamer, L. K., Hicks, C. L., Hollar, C. M., Ng-Kwai-Hang, K. F., & Swaisgood, H. E. (2004). Nomenclature of the Proteins of Cows' Milk—Sixth Revision. *Journal of Dairy Science*, *87*(6), 1641–1674. https://doi.org/10.3168/jds.S0022-0302(04)73319-6

Farrell, J., Harold, Kumosinski, T., Malin, E., & Brown, E. (2002). The Caseins of Milk as Calcium-Binding Proteins. *Methods in Molecular Biology (Clifton, N.J.)*, *172*, 97–140. https://doi.org/10.1385/1-59259-183-3:097

Fazzolari-Nesci, A., Domianello, D., Sotera, V., & Räihä, N. (1992). Tryptophan fortification of adapted formula increases plasma tryptophan concentrations to levels not different from those found in breast-fed infants. *Journal of Pediatric Gastroenterology and Nutrition*, *14*(4), 456–459. PubMed. https://doi.org/10.1097/00005176-199205000-00014

Fenelon, M. A., Hickey, R. M., Buggy, A., McCarthy, N., & Murphy, E. G. (2019). Chapter 12—Whey Proteins in Infant Formula. In H. C. Deeth & N. Bansal (Eds.), *Whey Proteins* (pp. 439–494). Academic Press. https://doi.org/10.1016/B978-0-12-812124-5.00013-8

Fernández, A., & Riera, F. (2013). β-Lactoglobulin tryptic digestion: A model approach for peptide release. *Biochemical Engineering Journal*, *70*, 88–96. https://doi.org/10.1016/j.bej.2012.10.001

Ferron-Baumy, C., Maubois, J. L., Garric, G., & Quiblier, J. P. (1991). Coagulation présure du lait et des rétentats d'ultrafiltration. Effets de divers traitements thermiques. *Le Lait*, *71*(4), 423–434. https://doi.org/10.1051/lait:1991432

Fox, P. F., & McSweeney, P. L. H. (1998). *Dairy Chemistry and Biochemistry* (1st ed.). Springer.

Fox, P. F., Uniacke-Lowe, T., McSweeney, P. L. H., & O'Mahony, J. A. (2015). Lactose. In P. F. Fox, T. Uniacke-Lowe, P. L. H. McSweeney, & J. A. O'Mahony (Eds.), *Dairy Chemistry and Biochemistry* (pp. 21–68). Springer International Publishing. https://doi.org/10.1007/978-3-319-14892-2_2

Fox, P., Uniacke-Lowe, T., McSweeney, P., & O'Mahony, J. (2015). Milk proteins. In *Dairy Chemistry and Biochemistry* (2nd ed.).

FranceAgriMer. (2018). *La transformation laitière française: Évolutions récentes* (Les Études de FranceAgriMer). https://www.franceagrimer.fr/filiere-lait/Actualites/2018/La-transformation-laitiere-francaise-evolutions-recentes-donnees-2017

Franco, I., Pérez, M. D., Conesa, C., Calvo, M., & Sánchez, L. (2018). Effect of technological treatments on bovine lactoferrin: An overview. *Food Research International*, *106*, 173–182. https://doi.org/10.1016/j.foodres.2017.12.016

Fraunhofer, W., & Winter, G. (2004). The use of asymmetrical flow field-flow fractionation in pharmaceutics and biopharmaceutics. *The International Association of Pharmaceutical Technology (APV)*, *58*(2), 369–383. https://doi.org/10.1016/j.ejpb.2004.03.034

Furlund, C. B., Ulleberg, E. K., Devold, T. G., Flengsrud, R., Jacobsen, M., Sekse, C., Holm, H., & Vegarud, G. E. (2013). Identification of lactoferrin peptides generated by digestion with human gastrointestinal enzymes. *Journal of Dairy Science*, *96*(1), 75–88. https://doi.org/10.3168/jds.2012-5946

García-Montoya, I. A., Cendón, T. S., Arévalo-Gallegos, S., & Rascón-Cruz, Q. (2012). Lactoferrin a multiple bioactive protein: An overview. *Transferrins: Molecular Mechanisms of Iron Transport and Disorders*, *1820*(3), 226–236. https://doi.org/10.1016/j.bbagen.2011.06.018

Gaspard, S. J., Auty, M. A. E., Kelly, A. L., O'Mahony, J. A., & Brodkorb, A. (2017). Isolation and characterisation of κ-casein/whey protein particles from heated milk protein concentrate and role of κ-casein in whey protein aggregation. *International Dairy Journal*, *73*, 98–108. https://doi.org/10.1016/j.idairyj.2017.05.012

Gauthier, S. F., Vachon, C., Jones, J. D., & Savoie, L. (1982). Assessment of Protein Digestibility by In Vitro Enzymatic Hydrolysis with Simultaneous Dialysis. *The Journal of Nutrition*, *112*(9), 1718–1725. https://doi.org/10.1093/jn/112.9.1718

Givens, D. I., Allison, R., Cottrill, B., & Blake, J. S. (2004). Enhancing the selenium content of bovine milk through alteration of the form and concentration of selenium in the diet of the dairy cow. *Journal of the Science of Food and Agriculture*, *84*(8), 811–817. https://doi.org/10.1002/jsfa.1737

Glantz, M., Håkansson, A., Lindmark Månsson, H., Paulsson, M., & Nilsson, L. (2010). Revealing the Size, Conformation, and Shape of Casein Micelles and Aggregates with Asymmetrical Flow Field-Flow Fractionation and Multiangle Light Scattering. *Langmuir*, *26*(15), 12585–12591. https://doi.org/10.1021/la101892x

Gnoth, M., Kunz, C., Kinne-Saffran, E., & Rudloff, S. (2000). Human Milk Oligosaccharides Are Minimally Digested In Vitro. *The Journal of Nutrition*, *130*, 3014–3020. https://doi.org/10.1093/jn/130.12.3014

Godfrey, J., & Lawrence, R. (2010). Toward optimal health: The maternal benefits of breastfeeding. Journal of Women's Health. *Journal of Women's Health*, *19*(9). https://doi.org/10.1089/jwh.2010.2290

Goedhart, A. C., & Bindels, J. G. (1994). The Composition of Human Milk as a Model for the Design of Infant Formulas: Recent Findings and Possible Applications. *Nutrition Research Reviews*, *7*(1), 1–23. Cambridge Core. https://doi.org/10.1079/NRR19940004

Goldsmith, S. J., Dickson, J. S., Barnhart, H. M., Toledo, R. T., & Eiten-Miller, R. R. (1983). IgA, IgG, IgM and Lactoferrin Contents of Human Milk During Early Lactation and the Effect of Processing and Storage. *Journal of Food Protection*, *46*(1), 4–7. https://doi.org/10.4315/0362-028X-46.1.4

Gotham, S. M., Fryer, P. J., & Pritchard, A. M. (1992). β-lactoglobulin denaturation and aggregation reactions and fouling deposit formation: A DSC study. *International Journal of Food Science & Technology*, *27*(3), 313–327. Scopus. https://doi.org/10.1111/j.1365-2621.1992.tb02033.x

Goulart, A. J., Bassan, J. C., Barbosa, O. A., Marques, D. P., Silveira, C. B., Santos, A. F., Garrido, S. S., Resende, F. A., Contiero, J., & Monti, R. (2014). Transport of amino acids from milk whey by Caco-2 cell monolayer after hydrolytic action of gastrointestinal enzymes. *XVI IUFoST World Congress*, *63*, 62–70. https://doi.org/10.1016/j.foodres.2014.01.037

Gouseti, O., Bornhorst, G., Bakalis, S., & Mackie, A. (2019). *Interdisciplinary Approaches to Food Digestion*. Springer.

Graveland-Bikker, J. F., & Anema, S. G. (2003). Effect of individual whey proteins on the rheological properties of acid gels prepared from heated skim milk. *International Dairy Journal*, *13*(5), 401–408. https://doi.org/10.1016/S0958-6946(02)00190-5

Griep, E. R., Cheng, Y., & Moraru, C. I. (2018). Efficient removal of spores from skim milk using cold microfiltration: Spore size and surface property considerations. *Journal of Dairy Science*, *101*(11), 9703–9713. https://doi.org/10.3168/jds.2018-14888

Groves, M. L. (1960). The Isolation of a Red Protein from Milk2. *Journal of the American Chemical Society*, *82*(13), 3345–3350. https://doi.org/10.1021/ja01498a029

Guerra, A., Etienne-Mesmin, L., Livrelli, V., Denis, S., Blanquet-Diot, S., & Alric, M. (2012). Relevance and challenges in modeling human gastric and small intestinal digestion. *Trends in Biotechnology*, *30*(11), 591–600. https://doi.org/10.1016/j.tibtech.2012.08.001

Guilloteau, P., Le Meuth-Metzinger, V., Morisset, J., & Zabielski, R. (2006). Gastrin, cholecystokinin and gastrointestinal tract functions in mammals. *Nutrition Research Reviews*, *19*(2), 254–283. Cambridge Core. https://doi.org/10.1017/S0954422407334082

Guo, M. R., Fox, P. F., Flynn, A., & Kindstedt, P. S. (1995). Susceptibility of β-Lactoglobulin and Sodium Caseinate to Proteolysis by Pepsin and Trypsin. *Journal of Dairy Science*, *78*(11), 2336–2344. https://doi.org/10.3168/jds.S0022-0302(95)76860-6

Gutiérrez-Castrellón, P., Mora-Magaña, I., Díaz-García, L., Jiménez-Gutiérrez, C., Ramirez-Mayans, J., & Solomon-Santibáñez, G. A. (2007). Immune response to nucleotide-supplemented infant formulae: Systematic review and meta-analysis. *British Journal of Nutrition*, *98*(S1), S64–S67. Cambridge Core. https://doi.org/10.1017/S000711450783296X

Guyomarc'h, F. (2006). Formation of heat-induced protein aggregates in milk as a means to recover the whey protein fraction in cheese manufacture, and potential of heat-treating milk at alkaline pH values in order to keep its rennet coagulation properties. A review. *Le Lait*, *86*(1), 1–20. https://doi.org/10.1051/lait:2005046

Guyomarc'h, F., Jemin, M., Le Tilly, V., Madec, M.-N., & Famelart, M.-H. (2009). Role of the Heat-Induced Whey Protein/κ-Casein Complexes in the Formation of Acid Milk Gels: A Kinetic Study Using Rheology and Confocal Microscopy. *Journal of Agricultural and Food Chemistry*, *57*(13), 5910–5917. https://doi.org/10.1021/jf804042k

Guyomarc'h, F., Law, A. J. R., & Dalgleish, D. G. (2003). Formation of Soluble and Micelle-Bound Protein Aggregates in Heated Milk. *Journal of Agricultural and Food Chemistry*, *51*(16), 4652–4660. https://doi.org/10.1021/jf0211783

Guyomarc'h, F., Queguiner, C., Law, A. J. R., Horne, D. S., & Dalgleish, D. G. (2003). Role of the Soluble and Micelle-Bound Heat-Induced Protein Aggregates on Network Formation in Acid Skim Milk Gels. *Journal of Agricultural and Food Chemistry*, *51*(26), 7743–7750. https://doi.org/10.1021/jf030201x

Hambraeus, L., & Lonnerdal, B. (2003). *Advanced Dairy Chemistry* (pp. 605–645). https://doi.org/10.1007/978-1-4419-8602-3_18

Hanning, R. M., Paes, B., & Atkinson, S. A. (1992). Protein metabolism and growth of term infants in response to a reduced-protein, 40:60 whey: Casein formula with added tryptophan. *The American Journal of Clinical Nutrition*, *56*(6), 1004–1011. https://doi.org/10.1093/ajcn/56.6.1004

Hansen, M., Sandström, B., & Lönnerdal, B. (1996). The Effect of Casein Phosphopetides on Zinc and Calcium Absorption from High Phytate Infant Diets Assessed in Rat Pups and Caco-2 Cells. *Pediatric Research*, *40*(4), 547–552. https://doi.org/10.1203/00006450-199610000-00006

Harouna, S., Carramiñana, J. J., Navarro, F., Pérez, M. D., Calvo, M., & Sánchez, L. (2015). Antibacterial activity of bovine milk lactoferrin on the emerging foodborne pathogen Cronobacter sakazakii: Effect of

media and heat treatment. *Food Control*, *47*, 520–525. https://doi.org/10.1016/j.foodcont.2014.07.061

Harris, W. R. (1986). Estimation of the ferrous—Transferrin binding constants based on thermodynamic studies of nickel(II)—Transferrin. *Journal of Inorganic Biochemistry*, *27*(1), 41–52. https://doi.org/10.1016/0162-0134(86)80107-6

Havea, P., Singh, H., & Creamer, L. K. (2002). Heat-Induced Aggregation of Whey Proteins: Comparison of Cheese WPC with Acid WPC and Relevance of Mineral Composition. *Journal of Agricultural and Food Chemistry*, *50*(16), 4674–4681. https://doi.org/10.1021/jf011583e

He, L., Yin, Y., Li, T., Huang, R., Xie, M., Wu, Z., & Wu, G. (2013). Use of the Ussing chamber technique to study nutrient transport by epithelial tissues. *Frontiers in Bioscience (Landmark Edition)*, *18*, 1266–1274. PubMed. https://doi.org/10.2741/4178

Heertje, I., Visser, J., & Smits, P. (1985). Structure Formation in Acid Milk Gels. *Food Microstructure*, *4*, 267–277.

Heine, W. E. (1999). The Significance of Tryptophan in Infant Nutrition. In G. Huether, W. Kochen, T. J. Simat, & H. Steinhart (Eds.), *Tryptophan, Serotonin, and Melatonin: Basic Aspects and Applications* (pp. 705–710). Springer US. https://doi.org/10.1007/978-1-4615-4709-9_91

Heine, W. E., Klein, P. D., & Reeds, P. J. (1991). The Importance of α-Lactalbumin in Infant Nutrition. *The Journal of Nutrition*, *121*(3), 277–283. https://doi.org/10.1093/jn/121.3.277

Heine, W., Radke, M., Wutzke, K., Peters, E., & Kundt, G. (1996). α-Lactalbumin-enriched low-protein infant formulas: A comparison to breast milk feeding. *Acta Paediatrica*, *85*(9), 1024–1028. https://doi.org/10.1111/j.1651-2227.1996.tb14210.x

Henderson, T. R., Hamosh, M., Armand, M., Mehta, N. R., & Hamosh, P. (2001). Gastric Proteolysis in Preterm Infants Fed Mother's Milk or Formula. In David S. Newburg (Ed.), *Bioactive Components of Human Milk* (pp. 403–408). Springer US. https://doi.org/10.1007/978-1-4615-1371-1_50

Hernández-Ledesma, B., Quirós, A., Amigo, L., & Recio, I. (2007). Identification of bioactive peptides after digestion of human milk and infant formula with pepsin and pancreatin. *International Dairy Journal*, *17*(1), 42–49. https://doi.org/10.1016/j.idairyj.2005.12.012

Hill, A. R. (1989). The β-Lactoglobulin-χ-Casein Complex. *Canadian Institute of Food Science and Technology Journal*, *22*(2), 120–123. https://doi.org/10.1016/S0315-5463(89)70345-X

Hillier, R. M., Lyster, R. L. J., & Cheeseman, G. C. (1979). Thermal denaturation of α-lactalbumin and β-lactoglobulin in cheese whey: Effect of total solids concentration and pH. *Journal of Dairy Research*, *46*(1), 103–111. Scopus. https://doi.org/10.1017/S0022029900016903

Hines, M. E., & Foegeding, E. Allen. (1993). Interactions of .alpha.-lactalbumin and bovine serum albumin with .beta.-lactoglobulin in thermally induced gelation. *Journal of Agricultural and Food Chemistry*, *41*(3), 341–346. https://doi.org/10.1021/jf00027a001

Hodgkinson, A. J., Wallace, O. A. M., Smolenski, G., & Prosser, C. G. (2019). Gastric digestion of cow and goat milk: Peptides derived from simulated conditions of infant digestion. *Food Chemistry*, *276*, 619–625. https://doi.org/10.1016/j.foodchem.2018.10.065

Hoffmann, M. A. M., Roefs, S. P. F. M., Verheul, M., Van Mil, P. J. J. M., & De Kruif, K. G. (1996). Aggregation of β-lactoglobulin studied by in situ light scattering. *Journal of Dairy Research*, *63*(3), 423–440. Scopus.

Hollar, C. M., Parris, N., Hsieh, A., & Cockley, K. D. (1995). Factors Affecting the Denaturation and Aggregation of Whey Proteins in Heated Whey Protein Concentrate Mixtures1. *Journal of Dairy Science*, *78*(2), 260–267. https://doi.org/10.3168/jds.S0022-0302(95)76633-4

Houlihan, A. V., Goddard, P. A., Kitchen, B. J., & Masters, C. J. (1992). Changes in structure of the bovine milk fat globule membrane on heating whole milk. *Journal of Dairy Research*, *59*(3), 321–329. Cambridge Core. https://doi.org/10.1017/S0022029900030594

Huërou-Luron, I. L. (2002). Chapter 16 Production and gene expression of brush border disaccharidases and peptidases during development in pigs and calves. In *Biology of Growing Animals* (Vol. 1, pp. 491–513). Elsevier. https://doi.org/10.1016/S1877-1823(09)70132-8

Huppertz, T., & Lambers, T. T. (2020). Influence of micellar calcium phosphate on in vitro gastric coagulation and digestion of milk proteins in infant formula model systems. *International Dairy Journal*, *107*, 104717. https://doi.org/10.1016/j.idairyj.2020.104717

Hur, S. J., Lim, B. O., Decker, E. A., & McClements, D. J. (2011). In vitro human digestion models for food applications. *Food Chemistry*, *125*(1), 1–12. https://doi.org/10.1016/j.foodchem.2010.08.036

Hurley, W. L., & Theil, P. K. (2013). Immunoglobulins in Mammary Secretions. In Paul L. H. McSweeney & P. F. Fox (Eds.), *Advanced Dairy Chemistry: Volume 1A: Proteins: Basic Aspects, 4th Edition* (pp. 275–294). Springer US. https://doi.org/10.1007/978-1-4614-4714-6_9

Hyde, G. A., Jr. (1968). Gastric secretions following neonatal surgery. *Journal of Pediatric Surgery*, *3*(6), 691–695. https://doi.org/10.1016/0022-3468(68)90900-7

Innis, S. M. (1993). Essential fatty acid requirements in human nutrition. *Canadian Journal of Physiology and Pharmacology*, *71*(9), 699–706. https://doi.org/10.1139/y93-104

Inouye, K., & Fruton, J. S. (1967). Studies on the Specificity of Pepsin [*]. *Biochemistry*, *6*(6), 1765–1777. https://doi.org/10.1021/bi00858a027

International Dairy Federation. (1993). *Determination of Nitrogen Content, IDF Standard No. 20B:1993, ,IDF,*. Brussels, Belgium.

Iversen, C., & Forsythe, S. (2004). Isolation of Enterobacter sakazakii and other Enterobacteriaceae from powdered infant formula milk and related products. *Food Microbiology*, *21*(6), 771–777. https://doi.org/10.1016/j.fm.2004.01.009

Iwaniak, A., Minkiewicz, P., Darewicz, M., Sieniawski, K., & Starowicz, P. (2016). BIOPEP database of sensory peptides and amino acids. *Food Research International*, *85*, 155–161. https://doi.org/10.1016/j.foodres.2016.04.031

Iyer, S., & Lonnerdal, B. (1993). Lactoferrin, lactoferrin receptors and iron metabolism. *European Journal of Clinical Nutrition*, *47*(4), 232–241. Scopus.

Jakopovic, K., Barukčić, I., & Božanić, R. (2016). Physiological significance, structure and isolation of alpha-lactalbumin. *Mljekarstvo / Dairy*, *66*, 3–11.

Jang, H. D., & Swaisgood, H. E. (1990). Disulfide Bond Formation Between Thermally Denatured β-Lactoglobulin and κ-Casein in Casein Micelles. *Journal of Dairy Science*, *73*(4), 900–904. https://doi.org/10.3168/jds.S0022-0302(90)78746-2

Jean, P. (1969). Dosage du phosphore dans le lait. *Le Lait*, *49*(483–484), 175–188.

Jeantet, R., Croguennec, T., Schuck, P., & Brulé, G. (2016). Inactivation of Food Modifying Agents. In *Handbook of Food Science and Technology 2*. 10.1002/9781119285229.ch4

Jenkins, J. A., Breiteneder, H., & Mills, E. N. C. (2007). Evolutionary distance from human homologs reflects allergenicity of animal food proteins. *Journal of Allergy and Clinical Immunology*, *120*(6), 1399–1405. https://doi.org/10.1016/j.jaci.2007.08.019

Jenness, R. (1979). The composition of human milk. *Seminars in Perinatology*, *3*(3), 225–239. PubMed.

Jensen, G., & Thompson, M. (1995). Nitrogenous components of milk. In *Handbook of milk composition*. Academic Press.

Jensen, M. L., Sangild, P. T., Lykke, M., Schmidt, M., Boye, M., Jensen, B. B., & Thymann, T. (2013). Similar efficacy of human banked milk and bovine colostrum to decrease incidence of necrotizing enterocolitis in preterm piglets. *American Journal of Physiology-Regulatory, Integrative and Comparative Physiology*, *305*(1), R4–R12. https://doi.org/10.1152/ajpregu.00094.2013

Jeyarajah, S., & Allen, J. C. (1994). Calcium binding and salt-induced structural changes of native and preheated .beta.-lactoglobulin. *Journal of Agricultural and Food Chemistry*, *42*(1), 80–85. https://doi.org/10.1021/jf00037a012

Ji, Y. Y., & Xiao, D. C. (2006). GIT physicochemical modeling—A critical review. *International Journal of Food Engineering*, *2*.

Jiang, R., Liu, L., Du, X., & Lönnerdal, B. (2020). Evaluation of Bioactivities of the Bovine Milk Lactoferrin–Osteopontin Complex in Infant Formulas. *Journal of Agricultural and Food Chemistry*, *68*(22), 6104–6111. https://doi.org/10.1021/acs.jafc.9b07988

Jiang, Y. J., & Guo, M. (2014). 8—Processing technology for infant formula. In M. Guo (Ed.), *Human Milk Biochemistry and Infant Formula Manufacturing Technology* (pp. 211–229). Woodhead Publishing. https://doi.org/10.1533/9780857099150.2.211

Johnston, S. I. (2015). Narrating myths: Story and belief in ancient Greece. *Arethusa*, *48*(2), 173–218. Scopus. https://doi.org/10.1353/are.2015.0011

Jones, T. F., Ingram, L. A., Fullerton, K. E., Marcus, R., Anderson, B. J., McCarthy, P. V., Vugia, D., Shiferaw, B., Haubert, N., Wedel, S., & Angulo, F. J. (2006). A Case-Control Study of the Epidemiology of Sporadic Salmonella Infection in Infants. *Pediatrics*, *118*(6), 2380. https://doi.org/10.1542/peds.2006-1218

Joyce, A. M., Brodkorb, A., Kelly, A. L., & O'Mahony, J. A. (2017). Separation of the effects of denaturation and aggregation on whey-casein protein interactions during the manufacture of a model infant formula. *Dairy Science & Technology*, *96*(6), 787–806. https://doi.org/10.1007/s13594-016-0303-4

Keil, B. (1992). *Specificity of proteolysis* (1st ed.). Springer-Verlag Berlin-Heidelberg-New York.

Kelly, A. L., O'Connell, J. E., & Fox, P. F. (2003). Manufacture and Properties of Milk Powders. In P. F. Fox & P. L. H. McSweeney (Eds.), *Advanced Dairy Chemistry—1 Proteins: Part A / Part B* (pp. 1027–1061). Springer US. https://doi.org/10.1007/978-1-4419-8602-3_29

Kelly, A. L., O'Flaherty, F., & Fox, P. F. (2006). Indigenous proteolytic enzymes in milk: A brief overview of the present state of knowledge. *First IDF Symposium on Indigenous Enzymes in Milk*, *16*(6), 563–572. https://doi.org/10.1016/j.idairyj.2005.10.019

Kent, R. M., Fitzgerald, G. F., Hill, C., Stanton, C., & Ross, R. P. (2015). Novel approaches to improve the intrinsic microbiological safety of powdered infant milk formula. *Nutrients*, *7*(2), 1217–1244. PubMed. https://doi.org/10.3390/nu7021217

Kessler, H.-G., & Beyer, H.-J. (1991). Thermal denaturation of whey proteins and its effect in dairy technology. *International Journal of Biological Macromolecules*, *13*(3), 165–173. https://doi.org/10.1016/0141-8130(91)90043-T

Kim, J. C., & Lund, D. B. (1998). Milk protein/stainless steel interaction relevant to the initial stage of fouling in thermal processing. *Journal of Food Process Engineering*, *21*(5), 369–386. https://doi.org/10.1111/j.1745-4530.1998.tb00459.x

Kim, Y. S., Birtwhistle, W., & Kim, Y. W. (1972). Peptide hydrolases in the bruch border and soluble fractions of small intestinal mucosa of rat and man. *The Journal of Clinical Investigation*, *51*(6), 1419–1430. PubMed. https://doi.org/10.1172/JCI106938

Kinsella, J. E., & Whitehead, D. M. (1989). Proteins in Whey: Chemical, Physical, and Functional Properties. In John E. Kinsella (Ed.), *Advances in Food and Nutrition Research* (Vol. 33, pp. 343–438). Academic Press. https://doi.org/10.1016/S1043-4526(08)60130-8

Kitabatake, N., & Kinekawa, Y.-I. (1998). Digestibility of Bovine Milk Whey Protein and β-Lactoglobulin in Vitro and in Vivo. *Journal of Agricultural and Food Chemistry*, *46*(12), 4917–4923. https://doi.org/10.1021/jf9710903

Koletzko, B. (2008). Basic concepts in nutrition: Nutritional needs of children and adolescents. *E-SPEN, the European e-Journal of Clinical Nutrition and Metabolism*, *3*(4), e179–e184. https://doi.org/10.1016/j.eclnm.2008.04.007

Koletzko, B., Agostoni, C., Bergmann, R., Ritzenthaler, K., & Shamir, R. (2011). Physiological aspects of human milk lipids and implications for infant feeding: A workshop report: Human milk lipids. *Acta Paediatrica*, *100*(11), 1405–1415. https://doi.org/10.1111/j.1651-2227.2011.02343.x

Koletzko, B., Baker, S., Cleghorn, G., Neto, U. F., Gopalan, S., Hernell, O., Hock, Q. S., Jirapinyo, P., Lonnerdal, B., Pencharz, P., Pzyrembel, H., Ramirez-Mayans, J., Shamir, R., Turck, D., Yamashiro, Y., & Zong-Yi, D. (2005). Global Standard for the Composition of Infant Formula: Recommendations of an ESPGHAN Coordinated International Expert Group. *Journal of Pediatric Gastroenterology and Nutrition*, *41*(5). https://journals.lww.com/jpgn/Fulltext/2005/11000/Global_Standard_for_the_Composition_of_Infant.6.aspx

Koletzko, B., Demmelmair, H., Grote, V., & Totzauer, M. (2019). Optimized protein intakes in term infants support physiological growth and promote long-term health. *Neonatal Nutrition*, *43*(7), 151153. https://doi.org/10.1053/j.semperi.2019.06.001

Kong, F., & Singh, R. P. (2010). A Human Gastric Simulator (HGS) to Study Food Digestion in Human Stomach. *Journal of Food Science*, *75*(9), E627–E635. https://doi.org/10.1111/j.1750-3841.2010.01856.x

Krissansen, G. W. (2007). Emerging Health Properties of Whey Proteins and Their Clinical Implications. *Journal of the American College of Nutrition*, *26*(6), 713S-723S. https://doi.org/10.1080/07315724.2007.10719652

Kumar, R. (2009). Role of naturally occurring osmolytes in protein folding and stability. *Archives of Biochemistry and Biophysics*, *491*(1), 1–6. https://doi.org/10.1016/j.abb.2009.09.007

Kumosinski, T. F., & Timasheff, S. N. (1966). Molecular Interactions in β-Lactoglobulin. X. The Stoichiometry of the β-Lactoglobulin Mixed Tetramerization1. *Journal of the American Chemical Society*, *88*(23), 5635–5642. https://doi.org/10.1021/ja00975a051

Kunz, C., Rudloff, S., Baier, W., Klein, N., & Strobel, S. (2000). Oligosaccharides in Human Milk: Structural, Functional, and Metabolic Aspects. *Annual Review of Nutrition*, *20*(1), 699–722. https://doi.org/10.1146/annurev.nutr.20.1.699

Kunz, Clemens, & Lönnerdal, B. (1992). Re-evaluation of the whey protein/casein ratio of human milk. *Acta Paediatrica*, *81*(2), 107–112. https://doi.org/10.1111/j.1651-2227.1992.tb12184.x

Kussendrager, K. D. (1994). Effects of heat treatment on structure and iron-binding capacity of bovine lactoferrin. *IDF Bulletin: Indigenous Antimicrobial Agents of Milk: Recent Developments*, 133–146.

Labropoulos, A. E., Palmer, J. K., & LOPEZ, A. (1981). Whey protein denaturation of uht processed milk and its effect on rheology of yogurt. *Journal of Texture Studies*, *12*(3), 365–374. https://doi.org/10.1111/j.1745-4603.1981.tb00545.x

Lacroix, M., Bon, C., Bos, C., Léonil, J., Benamouzig, R., Luengo, C., Fauquant, J., Tomé, D., & Gaudichon, C. (2008). Ultra High Temperature Treatment, but Not Pasteurization, Affects the Postprandial Kinetics of Milk Proteins in Humans. *The Journal of Nutrition*, *138*(12), 2342–2347. https://doi.org/10.3945/jn.108.096990

Lai, K. (2001). Enterobacter sakazakii Infections among Neonates, Infants, Children, and Adults: Case Reports and a Review of the Literature. *Medicine*, *80*(2). https://journals.lww.com/md-journal/Fulltext/2001/03000/Enterobacter_sakazakii_Infections_among_Neonates,.4.aspx

Law, A. J. R., & Leaver, J. (1997). Effect of Protein Concentration on Rates of Thermal Denaturation of Whey Proteins in Milk. *Journal of Agricultural and Food Chemistry*, *45*(11), 4255–4261. https://doi.org/10.1021/jf970242r

Law, A.J.R. (1995). Heat denaturation of bovine, caprine and ovine whey proteins. *Milchwissenschaft*.

Le Huërou-Luron, I., Bouzerzour, K., Ferret-Bernard, S., Ménard, O., Le Normand, L., Perrier, C., Le Bourgot, C., Jardin, J., Bourlieu, C., Carton, T., Le Ruyet, P., Cuinet, I., Bonhomme, C., & Dupont, D. (2018). A mixture of milk and vegetable lipids in infant formula changes gut digestion, mucosal immunity and microbiota composition in neonatal piglets. *European Journal of Nutrition*, *57*(2), 463–476. https://doi.org/10.1007/s00394-016-1329-3

Le Roux, L. (2019). *De la fabrication à la digestion in vitro de formules infantiles innovantes en partie composées de protéines végétales: Une approche multi-échelle*.

Le Roux, L., Chacon, R., Dupont, D., Jeantet, R., Deglaire, A., & Nau, F. (2020). In vitro static digestion reveals how plant proteins modulate model infant formula digestibility. *Food Research International*, *130*, 108917. https://doi.org/10.1016/j.foodres.2019.108917

Le Roux, L., Ménard, O., Chacon, R., Dupont, D., Jeantet, R., Deglaire, A., & Nau, F. (2020). Are Faba Bean and Pea Proteins Potential Whey Protein Substitutes in Infant Formulas? An In Vitro Dynamic Digestion Approach. *Foods (Basel, Switzerland)*, *9*(3), 362. PubMed. https://doi.org/10.3390/foods9030362

Lebenthal, E., & Lee, P. C. (1980). Development of Functional Response in Human Exocrine Pancreas. *Pediatrics*, *66*(4), 556.

Lebenthal, E., Lee, P. C., & Heitlinger, L. A. (1983). Impact of development of the gastrointestinal tract on infant feeding. *The Journal of Pediatrics*, *102*(1), 1–9. https://doi.org/10.1016/S0022-3476(83)80276-5

Lee, A. P., Barbano, D. M., & Drake, M. A. (2017). The influence of ultra-pasteurization by indirect heating versus direct steam injection on skim and 2% fat milks. *Journal of Dairy Science*, *100*(3), 1688–1701. https://doi.org/10.3168/jds.2016-11899

Leeb, E., Götz, A., Letzel, T., Cheison, S. C., & Kulozik, U. (2015). Influence of denaturation and aggregation of β-lactoglobulin on its tryptic hydrolysis and the release of functional peptides. *Food Chemistry*, *187*, 545–554. https://doi.org/10.1016/j.foodchem.2015.04.034

Leiros, H.-K. S., Brandsdal, B. O., Andersen, O. A., Os, V., Leiros, I., Helland, R., Otlewski, J., Willassen, N. P., & Smalås, A. O. (2004). Trypsin specificity as elucidated by LIE calculations, X-ray structures, and association constant measurements. *Protein Science*, *13*(4), 1056–1070. PubMed. https://doi.org/10.1110/ps.03498604

Lemaire, M., Dou, S., Cahu, A., Formal, M., Le Normand, L., Romé, V., Nogret, I., Ferret-Bernard, S., Rhimi, M., Cuinet, I., Canlet, C., Tremblay-Franco, M., Le Ruyet, P., Baudry, C., Gérard, P., Le Huërou-Luron, I., & Blat, S. (2018). Addition of dairy lipids and probiotic Lactobacillus fermentum in infant formula programs gut microbiota and entero-insular axis in adult minipigs. *Scientific Reports*, *8*(1), 11656. https://doi.org/10.1038/s41598-018-29971-w

Lewis, M. J., & Deeth, H. C. (2009). Heat Treatment of Milk. In *Milk Processing and Quality Management*.

Li, N., Richoux, R., Boutinaud, M., Martin, P., & Gagnaire, V. (2014). Role of somatic cells on dairy processes and products: A review. *Dairy Science & Technology*, *94*. https://doi.org/10.1007/s13594-014-0176-3

Li, Q., & Zhao, Z. (2018). Interaction between lactoferrin and whey proteins and its influence on the heat-induced gelation of whey proteins. *Food Chemistry*, *252*, 92–98. https://doi.org/10.1016/j.foodchem.2018.01.114

Li-Chan, E., & Nakai, S. (1989). Enzymic dephosphorylation of bovine casein to improve acid clotting properties and digestibility for infant formula. *Journal of Dairy Research*, *56*(3), 381–390. Cambridge Core. https://doi.org/10.1017/S0022029900028843

Lieberman, J. (1966). Proteolytic Enzyme Activity in Fetal Pancreas and Meconium: Demonstration of plasminogen and trypsinogen activators in pancreatic tissue. *Gastroenterology*, *50*(2), 183–190. https://doi.org/10.1016/S0016-5085(66)80051-3

Lien, E. L. (2003). Infant formulas with increased concentrations of α-lactalbumin. *The American Journal of Clinical Nutrition*, *77*(6), 1555S-1558S. https://doi.org/10.1093/ajcn/77.6.1555S

Lin, S. H. C., Dewan, R. K., Bloomfield, V. A., & Morr, C. V. (1971). Inelastic light-scattering study of the size distribution of bovine milk casein micelles. *Biochemistry*, *10*(25), 4788–4793. https://doi.org/10.1021/bi00801a029

Lin, S. H. C., Leong, S. L., Dewan, R. K., Bloomfield, V. A., & Morr, C. V. (1972). Effect of calcium ion on the structure of native bovine casein micelles. *Biochemistry*, *11*(10), 1818–1821. https://doi.org/10.1021/bi00760a013

Lin, Y., Kelly, A., O'Mahony, J., & Guinee, T. (2017). Effect of heat treatment during skim milk powder manufacture on the compositional and processing characteristics of reconstituted skim milk and concentrate. *International Dairy Journal*, *78*. https://doi.org/10.1016/j.idairyj.2017.10.007

Lipkie, T. E., Banavara, D., Shah, B., Morrow, A. L., McMahon, R. J., Jouni, Z. E., & Ferruzzi, M. G. (2014). Caco-2 accumulation of lutein is greater from human milk than from infant formula despite similar bioaccessibility. *Molecular Nutrition & Food Research*, *58*(10), 2014–2022. https://doi.org/10.1002/mnfr.201400126

Liu, D. Z., Dunstan, D. E., & Martin, G. J. O. (2012). Evaporative concentration of skimmed milk: Effect on casein micelle hydration, composition, and size. *Food Chemistry*, *134*(3), 1446–1452. https://doi.org/10.1016/j.foodchem.2012.03.053

Liu, G., Carøe, C., Qin, Z., Munk, D. M. E., Crafack, M., Petersen, M. A., & Ahrné, L. (2020). Comparative study on quality of whole milk processed by high hydrostatic pressure or thermal pasteurization treatment. *LWT*, *127*, 109370. https://doi.org/10.1016/j.lwt.2020.109370

Liu, H., Boggs, I., Weeks, M., Li, Q., Wu, H., Harris, P., Ma, Y., & Day, L. (2020). Kinetic modelling of the heat stability of bovine lactoferrin in raw whole milk. *Journal of Food Engineering*, *280*, 109977. https://doi.org/10.1016/j.jfoodeng.2020.109977

Livney, Y. D., Verespej, E., & Dalgleish, D. G. (2003). Steric Effects Governing Disulfide Bond Interchange during Thermal Aggregation in Solutions of β-Lactoglobulin B and α-Lactalbumin. *Journal of Agricultural and Food Chemistry*, *51*(27), 8098–8106. Scopus. https://doi.org/10.1021/jf034582q

Liyanaarachchi, W. S., Ramchandran, L., & Vasiljevic, T. (2015). Controlling heat induced aggregation of whey proteins by casein inclusion in concentrated protein dispersions. *International Dairy Journal*, *44*, 21–30. https://doi.org/10.1016/j.idairyj.2014.12.010

Liyanaarachchi, W. S., & Vasiljevic, T. (2018). Caseins and their interactions that modify heat aggregation of whey proteins in commercial dairy mixtures. *International Dairy Journal*, *83*, 43–51. https://doi.org/10.1016/j.idairyj.2018.03.006

Loiseleux, T., Rolland-Sabaté, A., Garnier, C., Croguennec, T., Guilois, S., Anton, M., & Riaublanc, A. (2018). Determination of hydro-colloidal characteristics of milk protein aggregates using Asymmetrical Flow Field-Flow Fractionation coupled with Multiangle Laser Light Scattering and Differential Refractometer (AF4-MALLS-DRi). *Food Hydrocolloids*, *74*, 197–206. https://doi.org/10.1016/j.foodhyd.2017.08.012

Lombardini, B., & Azuma, J. (1992). *Taurine: Nutritional Value and Mechanisms of Action* (Vol. 315). https://doi.org/10.1007/978-1-4615-3436-5

Lönnerdal, B, & Atkinson, S. (1995). CHAPTER 5—Nitrogenous Components of Milk: A. Human Milk Proteins. In R.G Jensen (Ed.), *Handbook of Milk Composition* (pp. 351–368). Academic Press. https://doi.org/10.1016/B978-012384430-9/50016-0

Lönnerdal, B, Forsum, E., & Hambraeus, L. (1976). A longitudinal study of the protein, nitrogen, and lactose contents of human milk from Swedish well-nourished mothers. *The American Journal of Clinical Nutrition*, *29*(10), 1127–1133. https://doi.org/10.1093/ajcn/29.10.1127

Lönnerdal, Bo. (2003). Nutritional and physiologic significance of human milk proteins. *The American Journal of Clinical Nutrition*, *77*(6), 1537S-1543S. https://doi.org/10.1093/ajcn/77.6.1537S

Lönnerdal, Bo. (2013). Bioactive proteins in breast milk. *Journal of Paediatrics and Child Health*, *49*(S1), 1–7. https://doi.org/10.1111/jpc.12104

Lönnerdal, Bo. (2014). Infant formula and infant nutrition: Bioactive proteins of human milk and implications for composition of infant formulas. *The American Journal of Clinical Nutrition*, *99*(3), 712S-717S. https://doi.org/10.3945/ajcn.113.071993

Lönnerdal, Bo. (2016). Human Milk: Bioactive Proteins/Peptides and Functional Properties. In J. Bhatia, R. Shamir, & Y. Vandenplas (Eds.), *Nestlé Nutrition Institute Workshop Series* (Vol. 86, pp. 97–107). S. Karger AG. https://doi.org/10.1159/000442729

Lönnerdal, Bo, Erdmann, P., Thakkar, S. K., Sauser, J., & Destaillats, F. (2017). Longitudinal evolution of true protein, amino acids and bioactive proteins in breast milk: A developmental perspective. *The Journal of Nutritional Biochemistry*, *41*, 1–11. https://doi.org/10.1016/j.jnutbio.2016.06.001

Lorenzen, P. C., & Schrader, K. (2006). A comparative study of the gelation properties of whey protein concentrate and whey protein isolate. *Le Lait*, *86*(4), 259–271. https://doi.org/10.1051/lait:2006008

Loveday, S. M., Peram, M. R., Singh, H., Ye, A., & Jameson, G. B. (2014). Digestive diversity and kinetic intrigue among heated and unheated β-lactoglobulin species. *Food & Function*, *5*(11), 2783–2791. https://doi.org/10.1039/C4FO00362D

Lucey, J. A., Teo, C. T., Munro, P. A., & Singh, H. (1997). Rheological properties at small (dynamic) and large (yield) deformations of acid gels made from heated milk. *Journal of Dairy Research*, *64*(4), 591–600. Cambridge Core. https://doi.org/10.1017/S0022029997002380

Lucey, John A., Tamehana, M., Singh, H., & Munro, P. A. (1998). Effect of interactions between denatured whey proteins and casein micelles on the formation and rheological properties of acid skim milk gels. *Journal of Dairy Research*, *65*(4), 555–567. https://doi.org/10.1017/S0022029998003057

Lucey, John A., Teo, C. T., Munro, P. A., & Singh, H. (1998). Microstructure, permeability and appearance of acid gels made from heated skim milk. *Food Hydrocolloids*, *12*(2), 159–165. https://doi.org/10.1016/S0268-005X(98)00012-5

Maathuis, A., Havenaar, R., He, T., & Bellmann, S. (2017). Protein Digestion and Quality of Goat and Cow Milk Infant Formula and Human Milk Under Simulated Infant Conditions: *Journal of Pediatric Gastroenterology and Nutrition*, *65*(6), 661–666. https://doi.org/10.1097/MPG.0000000000001740

Macierzanka, A., Sancho, A., E.N.C, M., Rigby, N., & Mackie, A. (2009). Emulsification alters simulated gastrointestinal proteolysis of β-casein and β-lactoglobulin. *Soft Matter*, *5*, 538–550. https://doi.org/10.1039/B811233A

Maharlouei, N., MD, Pourhaghighi, A., Medical student, Raeisi Shahraki, H., PhD, Zohoori, D., MD, & Lankarani, K. B., MD. (2018). Factors Affecting Exclusive Breastfeeding, Using Adaptive LASSO Regression. *International Journal of Community Based Nursing and Midwifery*, *6*(3), 260–271. PubMed.

Majka, G., Śpiewak, K., Kurpiewska, K., Heczko, P., Stochel, G., Strus, M., & Brindell, M. (2013). A high-throughput method for the quantification of iron saturation in lactoferrin preparations. *Analytical and Bioanalytical Chemistry*, *405*(15), 5191–5200. https://doi.org/10.1007/s00216-013-6943-9

Marangoni, A. G., Barbut, S., McGauley, S. E., Marcone, M., & Narine, S. S. (2000). On the structure of particulate gels—The case of salt-induced cold gelation of heat-denatured whey protein isolate. *Food Hydrocolloids*, *14*(1), 61–74. https://doi.org/10.1016/S0268-005X(99)00046-6

Martin, G., Williams, R., & Dunstan, D. (2007). Comparison of Casein Micelles in Raw and Reconstituted Skim Milk. *Journal of Dairy Science*, *90*, 4543–4551. https://doi.org/10.3168/jds.2007-0166

Marze, S., Algaba, H., & Marquis, M. (2014). A microfluidic device to study the digestion of trapped lipid droplets. *Food & Function*, *5*(7), 1481–1488. https://doi.org/10.1039/C4FO00010B

Mason, S. (1962). Some Aspects of Gastric Function in the Newborn. *Archives of Disease in Childhood*, *37*(194), 387–391. https://doi.org/10.1136/adc.37.194.387

Matsumoto, T. (2011). Mitigation of the allergenic activity of beta-lactoglobulin by electrolysis. *Pediatric Allergy and Immunology*, *22*(2), 235–242. https://doi.org/10.1111/j.1399-3038.2010.01069.x

Mayayo, C., Montserrat, M., Ramos, S. J., Martínez-Lorenzo, M. J., Calvo, M., Sánchez, L., & Pérez, M. D. (2014). Kinetic parameters for high-pressure-induced denaturation of lactoferrin in human milk. *International Dairy Journal*, *39*(2), 246–252. https://doi.org/10.1016/j.idairyj.2014.07.001

McClean, P., & Weaver, L. T. (1993). Ontogeny of human pancreatic exocrine function. *Archives of Disease in Childhood*, *68*(1 Spec No), 62–65. https://doi.org/10.1136/adc.68.1_Spec_No.62

McKenna, B. M., & O'Sullivan, A. C. (1971). Whey Protein Denaturation in Concentrated Skimmilks. *Journal of Dairy Science*, *54*(7), 1075–1077. https://doi.org/10.3168/jds.S0022-0302(71)85973-8

McKenzie, H. A., Ralston, G. B., & Shaw, D. C. (1972). Location of sulfhydryl and disulfide groups in bovine .beta.-lactoglobulins and effects of urea. *Biochemistry*, *11*(24), 4539–4547. https://doi.org/10.1021/bi00774a017

McKenzie, H. A., & Sawyer, W. H. (1967). Effect of pH on β-Lactoglobulins. *Nature*, *214*(5093), 1101–1104. https://doi.org/10.1038/2141101a0

McMahon, D. J., Du, H., McManus, W. R., & Larsen, K. M. (2009). Microstructural changes in casein supramolecules during acidification of skim milk. *Journal of Dairy Science*, *92*(12), 5854–5867. https://doi.org/10.3168/jds.2009-2324

McSweeney, P. L. H., & O'Mahony, J. A. (2016). Milk proteins. In *Advanced Dairy Chemistry, Volume 1B: Proteins: Applied Aspects* (4th ed.). Springer, New York, NY. https://doi.org/10.1007/978-1-4939-2800-2

McSweeney, S. L., Mulvihill, D. M., & O'Callaghan, D. M. (2004). The influence of pH on the heat-induced aggregation of model milk protein ingredient systems and model infant formula emulsions stabilized by milk protein ingredients. *Food Hydrocolloids*, *18*(1), 109–125. https://doi.org/10.1016/S0268-005X(03)00049-3

Mediwaththe, A., Bogahawaththa, D., Grewal, M. K., Chandrapala, J., & Vasiljevic, T. (2018). Structural changes of native milk proteins subjected to controlled shearing and heating. *Food Research International*, *114*, 151–158. https://doi.org/10.1016/j.foodres.2018.08.001

Meltretter, J., Schmidt, A., Humeny, A., Becker, C.-M., & Pischetsrieder, M. (2008). Analysis of the Peptide Profile of Milk and Its Changes during Thermal Treatment and Storage. *Journal of Agricultural and Food Chemistry*, *56*, 2899–2906. https://doi.org/10.1021/jf073479o

Ménard, O., Bourlieu, C., De Oliveira, S. C., Dellarosa, N., Laghi, L., Carrière, F., Capozzi, F., Dupont, D., & Deglaire, A. (2018). A first step towards a consensus static in vitro model for simulating full-term infant digestion. *Food Chemistry*, *240*, 338–345. https://doi.org/10.1016/j.foodchem.2017.07.145

Ménard, Olivia, Cattenoz, T., Guillemin, H., Souchon, I., Deglaire, A., Dupont, D., & Picque, D. (2014). Validation of a new in vitro dynamic system to simulate infant digestion. *Food Chemistry*, *145*, 1039–1045. https://doi.org/10.1016/j.foodchem.2013.09.036

Ménard, Olivia, & Dupont, D. (2014). *Atouts et limites des modèles de digestion gastro-intestinale: De l'in vitro à l'in vivo*.

Ménard, Olivia, Picque, D., & Dupont, D. (2015). The DIDGI® System. In K. Verhoeckx, P. Cotter, I. López-Expósito, C. Kleiveland, T. Lea, A. Mackie, T. Requena, D. Swiatecka, & H. Wichers (Eds.), *The Impact of Food Bioactives on Health* (pp. 73–81). Springer International Publishing. https://doi.org/10.1007/978-3-319-16104-4_8

Michaelsen, K. F., & Greer, F. R. (2014). Protein needs early in life and long-term health. *The American Journal of Clinical Nutrition*, *99*(3), 718S-722S. https://doi.org/10.3945/ajcn.113.072603

Michalski, M. C., Briard, V., Michel, F., Tasson, F., & Poulain, P. (2005). Size Distribution of Fat Globules in Human Colostrum, Breast Milk, and Infant Formula. *Journal of Dairy Science*, *88*(6), 1927–1940. https://doi.org/10.3168/jds.S0022-0302(05)72868-X

Michalski, M. C., Cariou, R., Michel, F., & Garnier, C. (2002). Native vs. Damaged Milk Fat Globules: Membrane Properties Affect the Viscoelasticity of Milk Gels. *Journal of Dairy Science*, *85*(10), 2451–2461. https://doi.org/10.3168/jds.S0022-0302(02)74327-0

Michalski, M.-C. (2009). Specific molecular and colloidal structures of milk fat affecting lipolysis, absorption and postprandial lipemia. *European Journal of Lipid Science and Technology*, *111*(5), 413–431. https://doi.org/10.1002/ejlt.200800254

Miller, L., & Houghton, J. A. (1945). The microKjeldahl determination of the nitrogen content of amino acids and proteins. *Journal of Biological Chemistry*, *169*, 373–383. CABDirect.

Minekus, M., Alminger, M., Alvito, P., Ballance, S., Bohn, T., Bourlieu, C., Carrière, F., Boutrou, R., Corredig, M., Dupont, D., Dufour, C., Egger, L., Golding, M., Karakaya, S., Kirkhus, B., Le Feunteun, S., Lesmes, U., Macierzanka, A., Mackie, A., … Brodkorb, A. (2014). A standardised static in vitro digestion method suitable for food – an international consensus. *Food & Function*, *5*(6), 1113–1124. https://doi.org/10.1039/C3FO60702J

Minekus, M., Smeets-Peeters, M., Bernalier, A., Marol-Bonnin, S., Havenaar, R., Marteau, P., Alric, M., Fonty, G., & Huis in't Veld, J. H. J. (1999). A computer-controlled system to simulate conditions of the large intestine with peristaltic mixing, water absorption and absorption of fermentation products. *Applied Microbiology and Biotechnology*, *53*(1), 108–114. https://doi.org/10.1007/s002530051622

Minekus, Mans. (2015). The TNO Gastro-Intestinal Model (TIM). In K. Verhoeckx, P. Cotter, I. López-Expósito, C. Kleiveland, T. Lea, A. Mackie, T. Requena, D. Swiatecka, & H. Wichers (Eds.), *The Impact of Food Bioactives on Health: In vitro and ex vivo models* (pp. 37–46). Springer International Publishing. https://doi.org/10.1007/978-3-319-16104-4_5

Minekus, Mans, Marteau, P., Havenaar, R., & Veld, J. (1995). A multicompartmental dynamic computer-controlled model simulating the stomach and small intestine. ATLA Altern Lab Anim. *Alternatives to Laboratory Animals: ATLA*, *23*, 197–209.

Miranda, G., & Pelissier, J.-P. (1981). In vivo studies on the digestion of bovine caseins in the rat stomach. *Journal of Dairy Research*, *48*(2), 319–326. https://doi.org/10.1017/S0022029900021749

Møller, H. K., Thymann, T., Fink, L. N., Frokiaer, H., Kvistgaard, A. S., & Sangild, P. T. (2011). Bovine colostrum is superior to enriched formulas in stimulating intestinal function and necrotising enterocolitis resistance in preterm pigs. *British Journal of Nutrition*, *105*(1), 44–53. Cambridge Core. https://doi.org/10.1017/S0007114510003168

Molly, K., Vande Woestyne, M., & Verstraete, W. (1993). Development of a 5-step multi-chamber reactor as a simulation of the human intestinal microbial ecosystem. *Applied Microbiology and Biotechnology*, *39*(2), 254–258. https://doi.org/10.1007/BF00228615

Mondino, A., Bongiovanni, G., Fumero, S., & Rossi, L. (1972). An improved method of plasma deproteination with sulphosalicylic acid for determining amino acids and related compounds. *Journal of Chromatography A*, *74*(2), 255–263.

Montagne, D., Dael, P., Skanderby, M., & Hugelshofer, W. (2009). Infant Formulae – Powders and Liquids. In *Dairy Powders and Concentrated Products* (A.Tamime). John Wiley and Sons.

Moore, S. A., Anderson, B. F., Groom, C. R., Haridas, M., & Baker, E. N. (1997). Three-dimensional structure of diferric bovine lactoferrin at 2.8 Å resolution11Edited by D. Rees. *Journal of Molecular Biology*, *274*(2), 222–236. https://doi.org/10.1006/jmbi.1997.1386

Moore, S., Spackman, D., & Stein, W. (1958). Chromatography of Amino Acids on Sulfonated Polystyrene Resins. *Analytical Chemistry*, 1186–1190. https://doi.org/10.1021/ac60139a005

Morell, P., Fiszman, S., Llorca, E., & Hernando, I. (2017). Designing added-protein yogurts: Relationship between in vitro digestion behavior and structure. *Food Hydrocolloids*, *72*, 27–34. https://doi.org/10.1016/j.foodhyd.2017.05.026

Morgan, P. E., Treweek, T. M., Lindner, R. A., Price, W. E., & Carver, J. A. (2005). Casein Proteins as Molecular Chaperones. *Journal of Agricultural and Food Chemistry*, *53*(7), 2670–2683. https://doi.org/10.1021/jf048329h

Moscovici, A. M., Joubran, Y., Briard-Bion, V., Mackie, A., Dupont, D., & Lesmes, U. (2014). The impact of the Maillard reaction on the in vitro proteolytic breakdown of bovine lactoferrin in adults and infants. *Food Funct.*, *5*(8), 1898–1908. https://doi.org/10.1039/C4FO00248B

Mounsey, J. S., & O'Kennedy, B. T. (2010). Heat-stabilisation of β-lactoglobulin through interaction with sodium caseinate. *Milchwissenschaft*, *65*(1), 79–83. CABDirect.

Mulet-Cabero, A.-I., Egger, L., Portmann, R., Ménard, O., Marze, S., Minekus, M., Le Feunteun, S., Sarkar, A., Grundy, M. M.-L., Carrière, F., Golding, M., Dupont, D., Recio, I., Brodkorb, A., & Mackie, A. (2020). A standardised semi-dynamic in vitro digestion method suitable for food – an international consensus. *Food & Function*, *11*(2), 1702–1720. https://doi.org/10.1039/C9FO01293A

Mulet-Cabero, A.-I., Mackie, A. R., Wilde, P. J., Fenelon, M. A., & Brodkorb, A. (2019). Structural mechanism and kinetics of in vitro gastric digestion are affected by process-induced changes in bovine milk. *Food Hydrocolloids*, *86*, 172–183. https://doi.org/10.1016/j.foodhyd.2018.03.035

Mullally, M. M., Mehra, R., & FitzGerald, R. (1998). Thermal effects on the conformation and susceptibility of β-lactoglobulin to hydrolysis by gastric and pancreatic endoproteinases. *Irish Journal of Agricultural and Food Research*, *37*, 51–60.

Müller, D., Cattaneo, S., Meier, F., Welz, R., & de Mello, A. J. (2015). Nanoparticle separation with a miniaturized asymmetrical flow field-flow fractionation cartridge. *Frontiers in Chemistry*, *3*. https://doi.org/10.3389/fchem.2015.00045

Mulvihill, D. M., & Donovan, M. (1987). Whey Proteins and Their Thermal Denaturation—A Review. *Irish Journal of Food Science and Technology*, *11*(1), 43–75. JSTOR.

Nasirpour, A., Scher, J., & Desobry, S. (2006). Baby Foods: Formulations and Interactions (A Review). *Critical Reviews in Food Science and Nutrition*, *46*(8), 665–681. https://doi.org/10.1080/10408390500511896

Nazarowec-White, M., & Farber, J. M. (1999). Phenotypic and genotypic typing of food and clinical is0lates of Enterobacter sakazakii. *Journal of Medical Microbiology*, *48*(6). https://doi.org/10.1099/00222615-48-6-559

Nebbia, S., Giribaldi, M., Cavallarin, L., Bertino, E., Coscia, A., Briard-Bion, V., Ossemond, J., Henry, G., Ménard, O., Dupont, D., & Deglaire, A. (2020). Differential impact of Holder and High Temperature Short Time pasteurization on the dynamic in vitro digestion of human milk in a preterm newborn model. *Food Chemistry*, *328*, 127126. https://doi.org/10.1016/j.foodchem.2020.127126

Neu, J. (2007). Gastrointestinal maturation and implications for infant feeding. *Selected Proceedings of the Neonatal Update 2007*, *83*(12), 767–775. https://doi.org/10.1016/j.earlhumdev.2007.09.009

Newburg, D.S, & Neubauer, S. H. (1995). CHAPTER 4—Carbohydrates in Milks: Analysis, Quantities, and Significance. In R.G Jensen (Ed.), *Handbook of Milk Composition* (pp. 273–349). Academic Press. https://doi.org/10.1016/B978-012384430-9/50015-9

Nguyen, H.A., Wong, W., Anema, S.G., Havea, P., Guyomarc'h, F. (2012). Effects of adding low levels of a disulfide reducing agent on the disulfide interactions of β-lactoglobulin and κ-casein in skim milk. *Journal of Agricultural and Food Chemistry*, 2337–2342. https://doi.org/10.1021/jf205297p

Nguyen, N. H. A., Streicher, C., & Anema, S. G. (2018). The effect of thiol reagents on the denaturation of the whey protein in milk and whey protein concentrate solutions. *International Dairy Journal*, *85*, 285–293. https://doi.org/10.1016/j.idairyj.2018.06.012

Nguyen, T. P. T. (2017). *Digestibility and structural changes of ingredients in infant formulae during the gastrointestinal digestion*.

Nguyen, T. T. P., Bhandari, B., Cichero, J., & Prakash, S. (2015). Gastrointestinal digestion of dairy and soy proteins in infant formulas: An in vitro study. *Food Research International*, *76*, 348–358. https://doi.org/10.1016/j.foodres.2015.07.030

Nicoleta, S., Van der Plancken, I., Rotaru, G., & Hendrickx, M. (2008). Denaturation impact in susceptibility of beta-lactoglobulin to enzymatic hydrolysis: A kinetic study. *Revue Roumaine de Chimie*, *53*.

Nielsen, L. R., Lund, M. N., Davies, M. J., Nielsen, J. H., & Nielsen, S. B. (2018). Effect of free cysteine on the denaturation and aggregation of holo α-lactalbumin. *International Dairy Journal*, *79*, 52–61. https://doi.org/10.1016/j.idairyj.2017.11.014

Nielsen, Søren D., Beverly, R. L., Underwood, M. A., & Dallas, D. C. (2018). Release of functional peptides from mother's milk and fortifier proteins in the premature infant stomach. *PLOS ONE*, *13*(11), e0208204. https://doi.org/10.1371/journal.pone.0208204

Nielsen, Søren Drud, Beverly, R. L., Qu, Y., & Dallas, D. C. (2017). Milk bioactive peptide database: A comprehensive database of milk protein-derived bioactive peptides and novel visualization. *Food Chemistry*, *232*, 673–682. https://doi.org/10.1016/j.foodchem.2017.04.056

Nilsson, L. (2013). Separation and characterization of food macromolecules using field-flow fractionation: A review. *Food Hydrocolloids*, *30*(1), 1–11. https://doi.org/10.1016/j.foodhyd.2012.04.007

Norman, A., Strandvik, B., & Ojamäe, Ö. (1972). Bile acids and pancreatic enzymes during absorption in the newborn. *Acta Paediatrica*, *61*(5), 571–576. https://doi.org/10.1111/j.1651-2227.1972.tb15947.x

Nowak-Wegrzyn, A., & Fiocchi, A. (2009). Rare, medium, or well done? The effect of heating and food matrix on food protein allergenicity. *Current Opinion in Allergy and Clinical Immunology*, *9*(3). https://journals.lww.com/co-allergy/Fulltext/2009/06000/Rare,_medium,_or_well_done__The_effect_of_heating.11.aspx

Nunes, L., Martins, E., Perrone, Í., & Carvalho, A. (2019). The Maillard Reaction in Powdered Infant Formula. *Journal of Food and Nutrition Research*, *7*, 33–40. https://doi.org/10.12691/jfnr-7-1-5

Obladen, M. (2014). From Swill Milk to Certified Milk: Progress in Cow's Milk Quality in the 19th Century. *Annals of Nutrition and Metabolism*, *64*(1), 80–87. https://doi.org/10.1159/000363069

O'Callaghan, D. M., O'Mahony, J. A., Ramanujam, K. S., & Burgher, A. M. (2011). Dehydrated Dairy Products | Infant Formulae. In J. W. Fuquay (Ed.), *Encyclopedia of Dairy Sciences (Second Edition)* (pp. 135–145). Academic Press. https://doi.org/10.1016/B978-0-12-374407-4.00124-2

Office of Food Additive Safety. (2016). *GRAS notice GRN 669. Food and Drug Administration. Generally Recognized As Safe (GRAS) Notice: The Use ofBovine Milk-derived Lactoferrin In Term Milk-based Infant Formulas and Toddler Formulas.* https://www.fda.gov/media/124472/download

O'Kennedy, B. T., & Mounsey, J. S. (2006). Control of Heat-Induced Aggregation of Whey Proteins Using Casein. *Journal of Agricultural and Food Chemistry*, *54*(15), 5637–5642. https://doi.org/10.1021/jf0607866

Oldfield, D. J., Singh, H., & Taylor, M. W. (2005). Kinetics of heat-induced whey protein denaturation and aggregation in skim milks with adjusted whey protein concentration. *Journal of Dairy Research*, *72*(3), 369–378. https://doi.org/10.1017/S002202990500107X

Oldfield, D. J., Singh, H., Taylor, M. W., & Pearce, K. N. (1998). Kinetics of Denaturation and Aggregation of Whey Proteins in Skim Milk Heated in an Ultra-high Temperature (UHT) Pilot Plant. *International Dairy Journal*, *8*(4), 311–318. https://doi.org/10.1016/S0958-6946(98)00089-2

O'Loughlin, I. B., Murray, B. A., Kelly, P. M., FitzGerald, R. J., & Brodkorb, A. (2012). Enzymatic Hydrolysis of Heat-Induced Aggregates of Whey Protein Isolate. *Journal of Agricultural and Food Chemistry*, *60*(19), 4895–4904. https://doi.org/10.1021/jf205213n

Osborn, DA, Sinn, JKH, & Jones, L. (2018). Infant formulas containing hydrolysed protein for prevention of allergic disease. *Cochrane Database of Systematic Reviews*, *10*. https://doi.org/10.1002/14651858.CD003664.pub6

Packard, V. S. (1982). 1—Macronutrients and Energy. In V. S. Packard (Ed.), *Human Milk and Infant Formula* (pp. 7–28). Academic Press. https://doi.org/10.1016/B978-0-12-543420-1.50006-5

Passannanti, F., Nigro, F., Gallo, M., Tornatore, F., Frasso, A., Saccone, G., Budelli, A., Barone, M. V., & Nigro, R. (2017). In vitro dynamic model simulating the digestive tract of 6-month-old infants. *PloS One*, *12*(12), e0189807–e0189807. PubMed. https://doi.org/10.1371/journal.pone.0189807

Patel, H. A., Singh, H., Anema, S. G., & Creamer, L. K. (2006). Effects of Heat and High Hydrostatic Pressure Treatments on Disulfide Bonding Interchanges among the Proteins in Skim Milk. *Journal of Agricultural and Food Chemistry*, *54*(9), 3409–3420. https://doi.org/10.1021/jf052834c

Patocka, G., Jelen, P., & Kalab, M. (1993). Thermostability of skimmilk with modified casein/whey protein content. *International Dairy Journal*, *3*(1), 35–48. https://doi.org/10.1016/0958-6946(93)90074-A

Paulsson, M. A., Svensson, U., Kishore, A. R., & Satyanarayan Naidu, A. (1993). Thermal Behavior of Bovine Lactoferrin in Water and Its Relation to Bacterial Interaction and Antibacterial Activity. *Journal of Dairy Science*, *76*(12), 3711–3720. https://doi.org/10.3168/jds.S0022-0302(93)77713-9

Peram, M. R., Loveday, S. M., Ye, A., & Singh, H. (2013). In vitro gastric digestion of heat-induced aggregates of β-lactoglobulin. *Journal of Dairy Science*, *96*(1), 63–74. https://doi.org/10.3168/jds.2012-5896

Pérez, M. D., & Calvo, M. (1995). Interaction of β-Lactoglobulin with Retinol and Fatty Acids and Its Role as a Possible Biological Function for This Protein: A Review. *Journal of Dairy Science*, *78*(5), 978–988. https://doi.org/10.3168/jds.S0022-0302(95)76713-3

Peters, T. (1985). Serum Albumin. In C. B. Anfinsen, J. T. Edsall, & F. M. Richards (Eds.), *Advances in Protein Chemistry* (Vol. 37, pp. 161–245). Academic Press. https://doi.org/10.1016/S0065-3233(08)60065-0

Petit, J., Herbig, A.-L., Moreau, A., & Delaplace, G. (2011). Influence of calcium on β-lactoglobulin denaturation kinetics: Implications in unfolding and aggregation mechanisms. *Journal of Dairy Science*, *94*(12), 5794–5810. https://doi.org/10.3168/jds.2011-4470

Philippe, M., Legraet, Y., & Gaucheron, F. (2005). The effects of different cations on the physicochemical characteristics of casein micelles. *Food Chemistry*, *90*(4), 673–683. https://doi.org/10.1016/j.foodchem.2004.06.001

Picariello, G., Ferranti, P., & Addeo, F. (2016). Use of brush border membrane vesicles to simulate the human intestinal digestion. *The 4th International Conference on Food Digestion*, *88*, 327–335. https://doi.org/10.1016/j.foodres.2015.11.002

Picariello, G., Ferranti, P., Fierro, O., Mamone, G., Caira, S., Di Luccia, A., Monica, S., & Addeo, F. (2010). Peptides surviving the simulated gastrointestinal digestion of milk proteins: Biological and toxicological implications. *Journal of Chromatography B*, *878*(3), 295–308. https://doi.org/10.1016/j.jchromb.2009.11.033

Picariello, G., Iacomino, G., Mamone, G., Ferranti, P., Fierro, O., Gianfrani, C., Di Luccia, A., & Addeo, F. (2013). Transport across Caco-2 monolayers of peptides arising from in vitro digestion of bovine milk proteins. *Food Chemistry*, *139*(1), 203–212. https://doi.org/10.1016/j.foodchem.2013.01.063

Picariello, G., Miralles, B., Mamone, G., Sanchez-Rivera, L., Recio, I., Addeo, F., & Ferranti, P. (2015). Role of intestinal brush border peptidases in the simulated digestion of milk proteins. *Molecular Nutrition & Food Research*, *59*. https://doi.org/10.1002/mnfr.201400856

Pierce, A., Colavizza, D., Benaissa, M., Maes, P., Tartar, A., Montreuil, J., & Spik, G. (1991). Molecular cloning and sequence analysis of bovine lactotransferrin. *European Journal of Biochemistry*, *196*(1), 177–184. https://doi.org/10.1111/j.1432-1033.1991.tb15801.x

Piper, D. W., & Fenton, B. H. (1965). PH stability and activity curves of pepsin with special reference to their clinical importance. *Gut*, *6*(5), 506–508. https://doi.org/10.1136/gut.6.5.506

Plock, J., Spiegel, T., & Kessler, H. G. (1998). Influence of the lactose concentration on the denaturation kinetics of whey proteins in concentrated sweet whey. *Milchwissenschaft*, *53*(7), 389–392. Scopus.

Plowman, J. E., & Creamer, L. K. (1995). Restrained molecular dynamics study of the interaction between bovine κ-casein peptide 98–111 and bovine chymosin and porcine pepsin. *Journal of Dairy Research*, *62*(3), 451–467. Cambridge Core. https://doi.org/10.1017/S0022029900031150

Poon, S., Clarke, A. E., & Schultz, C. J. (2001). Effect of denaturants on the emulsifying activity of proteins. *Journal of Agricultural and Food Chemistry*, *49*(1), 281–286. Scopus. https://doi.org/10.1021/jf000179x

Poquet, L., & Wooster, T. J. (2016). Infant digestion physiology and the relevance of in vitro biochemical models to test infant formula lipid digestion. *Molecular Nutrition & Food Research*, *60*(8), 1876–1895. https://doi.org/10.1002/mnfr.201500883

Puyol, P., Perez, M. D., Ena, J. M., & Calvo, M. (1991). Interaction of Bovine β-Lactoglobulin and Other Bovine and Human Whey Proteins with Retinol and Fatty Acids. *Agricultural and Biological Chemistry*, *55*(10), 2515–2520. https://doi.org/10.1080/00021369.1991.10871001

Qi, P. X. (2007). Studies of casein micelle structure: The past and the present. *Le Lait*, *87*(4–5), 363–383. https://doi.org/10.1051/lait:2007026

Qian, F., Sun, J., Cao, D., Tuo, Y., Jiang, S., & Mu, G. (2017). Experimental and Modelling Study of the Denaturation of Milk Protein by Heat Treatment. *Korean Journal for Food Science of Animal Resources*, *37*(1), 44–51. https://doi.org/10.5851/kosfa.2017.37.1.44

Raikos, V. (2010). Effect of heat treatment on milk protein functionality at emulsion interfaces. A review. *Food Hydrocolloids*, *24*(4), 259–265. https://doi.org/10.1016/j.foodhyd.2009.10.014

Rao, M. A. (2010). *Rheology of fluid and semisolid foods: Principles and applications* (Springer Science&Business Media).

Rastogi, N., Nagpal, N., Alam, H., Pandey, S., Gautam, L., Sinha, M., Shin, K., Manzoor, N., Virdi, J. S., Kaur, P., Sharma, S., & Singh, T. P. (2014). Preparation and Antimicrobial Action of Three Tryptic Digested Functional Molecules of Bovine Lactoferrin. *PLoS ONE*, *9*(3), e90011. https://doi.org/10.1371/journal.pone.0090011

Rastogi, N., Singh, A., Pandey, S. N., Sinha, M., Bhushan, A., Kaur, P., Sharma, S., & Singh, T. P. (2014). Structure of the iron-free true C-terminal half of bovine lactoferrin produced by tryptic digestion and its functional significance in the gut. *FEBS Journal*, *281*(12), 2871–2882. https://doi.org/10.1111/febs.12827

Rene, F., & Lalande, M. (1988). Description and Measurements of Fouling of Heat Exchangers. Example of Milk Thermal Treatment. *Entropie Paris*, *24*(139), 13–23. Scopus.

Roman, C., Carriere, F., Villeneuve, P., Pina, M., Millet, V., Simeoni, U., & Sarles, J. (2007). Quantitative and Qualitative Study of Gastric Lipolysis in Premature Infants: Do MCT-Enriched Infant Formulas Improve Fat Digestion? *Pediatric Research*, *61*(1), 83–88. https://doi.org/10.1203/01.pdr.0000250199.24107.fb

Rowan, A. M., Moughan, P. J., Wilson, M. N., Maher, K., & Tasman-Jones, C. (1994). Comparison of the ileal and faecal digestibility of dietary amino acids in adult humans and evaluation of the pig as a model animal for digestion studies in man. *British Journal of Nutrition*, *71*(1), 29–42. Cambridge Core. https://doi.org/10.1079/BJN19940108

Rowley, B. O., & Richardson, T. (1985). Protein-Lipid Interactions in Concentrated Infant Formula. *Journal of Dairy Science*, *68*(12), 3180–3188. https://doi.org/10.3168/jds.S0022-0302(85)81225-X

Rudloff, S., & Kunz, C. (1997). Protein and Nonprotein Nitrogen Components in Human Milk, Bovine Milk, and Infant Formula: Quantitative and Qualitative Aspects in Infant Nutrition. *Journal of Pediatric*

Gastroenterology and Nutrition, *24*(3). https://journals.lww.com/jpgn/Fulltext/1997/03000/Protein_and_Nonprotein_Nitrogen_Components_in.17.aspx

Rüegg, M., Moor, U., & Blanc, B. (1977). A calorimetric study of the thermal denaturation of whey proteins in simulated milk ultrafiltrate. *Journal of Dairy Research*, *44*(3), 509–520. Scopus. https://doi.org/10.1017/S002202990002046X

Rutherfurd, S. M., Darragh, A. J., Hendriks, W. H., Prosser, C. G., & Lowry, D. (2006). True Ileal Amino Acid Digestibility of Goat and Cow Milk Infant Formulas. *Journal of Dairy Science*, *89*(7), 2408–2413. https://doi.org/10.3168/jds.S0022-0302(06)72313-X

Sakurai, K., Oobatake, M., & Goto, Y. (2001). Salt-dependent monomer-dimer equilibrium of bovine beta-lactoglobulin at pH 3. *Protein Science : A Publication of the Protein Society*, *10*(11), 2325–2335. PubMed. https://doi.org/10.1110/ps.17001

Sánchez, L., Peiró, J. M., Castillo, H., Pérez, M. D., Ena, J. M., & Calvo, M. (1992). Kinetic Parameters for Denaturation of Bovine Milk Lactoferrin. *Journal of Food Science*, *57*(4), 873–879. https://doi.org/10.1111/j.1365-2621.1992.tb14313.x

Sánchez-Rivera, L., Ménard, O., Recio, I., & Dupont, D. (2015). Peptide mapping during dynamic gastric digestion of heated and unheated skimmed milk powder. *FOOD BIOACTIVE COMPOUNDS: QUALITY CONTROL AND BIOACTIVITY*, *77*, 132–139. https://doi.org/10.1016/j.foodres.2015.08.001

Sanchón, J., Fernández-Tomé, S., Miralles, B., Hernández-Ledesma, B., Tomé, D., Gaudichon, C., & Recio, I. (2018). Protein degradation and peptide release from milk proteins in human jejunum. Comparison with in vitro gastrointestinal simulation. *Food Chemistry*, *239*, 486–494. https://doi.org/10.1016/j.foodchem.2017.06.134

Sandström, O., Lönnerdal, B., Graverholt, G., & Hernell, O. (2008). Effects of α-lactalbumin–enriched formula containing different concentrations of glycomacropeptide on infant nutrition. *The American Journal of Clinical Nutrition*, *87*(4), 921–928. https://doi.org/10.1093/ajcn/87.4.921

Santos, O., Nylander, T., Schillén, K., Paulsson, M., & Trägårdh, C. (2006). Effect of surface and bulk solution properties on the adsorption of whey protein onto steel surfaces at high temperature. *Journal of Food Engineering*, *73*(2), 174–189. https://doi.org/10.1016/j.jfoodeng.2005.01.018

Sarles, J., Moreau, H., & Verger, R. (1992). Human gastric lipase: Ontogeny and variations in children. *Acta Paediatrica*, *81*(6-7), 511–513. https://doi.org/10.1111/j.1651-2227.1992.tb12284.x

Sarwar, G., Peace, R. W., & Botting, H. G. (1989). Differences in protein digestibility and quality of liquid concentrate and powder forms of milk-based infant formulas fed to rats. *The American Journal of Clinical Nutrition*, *49*(5), 806–813. https://doi.org/10.1093/ajcn/49.5.806

Sato, R., Noguchi, T., & Naito, H. (1986). Casein phosphopeptide (CPP) enhances calcium absorption from the ligated segment of rat small intestine. *Journal of Nutritional Science and Vitaminology*, *32*(1), 67–76. https://doi.org/10.3177/jnsv.32.67

Sawyer, L. (2013). β-Lactoglobulin. In Paul L. H. McSweeney & P. F. Fox (Eds.), *Advanced Dairy Chemistry: Volume 1A: Proteins: Basic Aspects, 4th Edition* (pp. 211–259). Springer US. https://doi.org/10.1007/978-1-4614-4714-6_7

Sawyer, W. H. (1969). Complex between β-lactoglobulin and κ-casein. A review. *Journal of Dairy Science*, *52*(9), 1347–1355.

Schmitt, C., Bovay, C., Rouvet, M., Shojaei-Rami, S., & Kolodziejczyk, E. (2007). Whey Protein Soluble Aggregates from Heating with NaCl: Physicochemical, Interfacial, and Foaming Properties. *Langmuir*, *23*(8), 4155–4166. https://doi.org/10.1021/la0632575

Schokker, E. P., Singh, H., & Creamer, L. K. (2000). Heat-induced aggregation of -lactoglobulin A and B with -lactalbumin. *International Dairy Journal*, 11.

Senterre, T., Rigo, J., Symonds, M., & Ramsay, M. (2010). Macronutrients for lactation and infant growth. In *Maternal-Fetal Nutrition During Pregnancy and Lactation* (p. 64).

Shani-Levi, C., Alvito, P., Andrés, A., Assunção, R., Barberá, R., Blanquet-Diot, S., Bourlieu, C., Brodkorb, A., Cilla, A., Deglaire, A., Denis, S., Dupont, D., Heredia, A., Karakaya, S., Giosafatto, C. V. L., Mariniello, L., Martins, C., Ménard, O., El, S. N., ... Lesmes, U. (2017). Extending in vitro digestion models to specific human populations: Perspectives, practical tools and bio-relevant information. *Special Issues from the 29th EFFoST International Conference*, *60*, 52–63. https://doi.org/10.1016/j.tifs.2016.10.017

Shani-Levi, C., Levi-Tal, S., & Lesmes, U. (2013). Comparative performance of milk proteins and their emulsions under dynamic in vitro adult and infant gastric digestion. *Food Hydrocolloids*, *32*(2), 349–357. https://doi.org/10.1016/j.foodhyd.2013.01.017

Sharma, S., Sinha, M., Kaushik, S., Kaur, P., & Singh, T. P. (2013). C-Lobe of Lactoferrin: The Whole Story of the Half-Molecule. *Biochemistry Research International*, *2013*, 1–8. https://doi.org/10.1155/2013/271641

Shimazaki, K.-I., Kawaguchi, A., Sato, T., Ueda, Y., Tomimura, T., & Shimamura, S. (1993). Analysis of human and bovine milk lactoferrins by rotofor and chromatofocusing. *International Journal of Biochemistry*, *25*(11), 1653–1658. https://doi.org/10.1016/0020-711X(93)90524-I

Signer, E., Murphy, G. M., Edkins, S., & Anderson, C. M. (1974). Role of bile salts in fat malabsorption of premature infants. *Archives of Disease in Childhood*, *49*(3), 174–180. PubMed. https://doi.org/10.1136/adc.49.3.174

Singh, H, & Creamer, L. K. (1993). In vitro Digestibility of Whey Protein/K-Casein Complexes Isolated from Heated Concentrated Milk. *Journal of Food Science*, *58*(2), 299–302. https://doi.org/10.1111/j.1365-2621.1993.tb04260.x

Singh, H., & Havea, P. (2003). Thermal Denaturation, Aggregation and Gelation of Whey Proteins. In P. F. Fox & P. L. H. McSweeney (Eds.), *Advanced Dairy Chemistry—1 Proteins: Part A / Part B* (pp. 1261–1287). Springer US. https://doi.org/10.1007/978-1-4419-8602-3_34

Singh, Harjinder. (2004). Heat stability of milk. *International Journal of Dairy Technology*, *57*(2-3), 111–119. https://doi.org/10.1111/j.1471-0307.2004.00143.x

Singh, Harjinder. (2007). Interactions of milk proteins during the manufacture of milk powders. *Http://Dx.Doi.Org/10.1051/Lait:2007014*, *87*. https://doi.org/10.1051/lait:2007014

Singh, Harjinder, & Creamer, L. K. (1991). Denaturation, aggregation and heat stability of milk protein during the manufacture of skim milk powder. *Journal of Dairy Research*, *58*(3), 269–283. https://doi.org/10.1017/S002202990002985X

Singh, Harjinder, & Creamer, L. K. (1993). In vitro Digestibility of Whey Protein/ $_K$ -Casein Complexes Isolated from Heated Concentrated Milk. *Journal of Food Science*, *58*(2), 299–302. https://doi.org/10.1111/j.1365-2621.1993.tb04260.x

Singh, T., Kihlman Oiseth, S., Lundin, L., & Day, L. (2014). Influence of heat and shear induced protein aggregation on the in vitro digestion rate of whey proteins. *Food & Function*, *5*. https://doi.org/10.1039/C4FO00454J

Singhal, A., Macfarlane, G., Macfarlane, S., Lanigan, J., Kennedy, K., Elias-Jones, A., Stephenson, T., Dudek, P., & Lucas, A. (2008). Dietary nucleotides and fecal microbiota in formula-fed infants: A randomized controlled trial. *The American Journal of Clinical Nutrition*, *87*(6), 1785–1792. https://doi.org/10.1093/ajcn/87.6.1785

Smith, A. M., Picciano, M. F., & Milner, J. A. (1982). Selenium intakes and status of human milk and formula fed infants. *The American Journal of Clinical Nutrition*, *35*(3), 521–526. https://doi.org/10.1093/ajcn/35.3.521

Stănciuc, N., Aprodu, I., Râpeanu, G., van der Plancken, I., Bahrim, G., & Hendrickx, M. (2013). Analysis of the Thermally Induced Structural Changes of Bovine Lactoferrin. *Journal of Agricultural and Food Chemistry*, *61*(9), 2234–2243. https://doi.org/10.1021/jf305178s

Stelwagen, K., Carpenter, E., Haigh, B., Hodgkinson, A., & Wheeler, T. T. (2009). Immune components of bovine colostrum and milk1. *Journal of Animal Science*, *87*(suppl_13), 3–9. https://doi.org/10.2527/jas.2008-1377

Stender, E. G. P., Koutina, G., Almdal, K., Hassenkam, T., Mackie, A., Ipsen, R., & Svensson, B. (2018). Isoenergic modification of whey protein structure by denaturation and crosslinking using transglutaminase. *Food & Function*, *9*(2), 797–805. https://doi.org/10.1039/C7FO01451A

Sturman, J. A. (1988). Taurine in Development. *The Journal of Nutrition*, *118*(10), 1169–1176. https://doi.org/10.1093/jn/118.10.1169

Su, M.-Y., Broadhurst, M., Liu, C.-P., Gathercole, J., Cheng, W.-L., Qi, X.-Y., Clerens, S., Dyer, J. M., Day, L., & Haigh, B. (2017). Comparative analysis of human milk and infant formula derived peptides following in vitro digestion. *Food Chemistry*, *221*, 1895–1903. https://doi.org/10.1016/j.foodchem.2016.10.041

Sutariya, S. G., Huppertz, T., & Patel, H. A. (2017). Influence of milk pre-heating conditions on casein–whey protein interactions and skim milk concentrate viscosity. *International Dairy Journal*, *69*, 19–22. https://doi.org/10.1016/j.idairyj.2017.01.007

Svedberg, J., de Haas, J., Leimenstoll, G., Paul, F., & Teschemacher, H. (1985). Demonstration of β-casomorphin immunoreactive materials in in vitro digests of bovine milk and in small intestine contents after bovine milk ingestion in adult humans. *Peptides*, *6*(5), 825–830. https://doi.org/10.1016/0196-9781(85)90308-0

Tam, J. J., & Whitaker, J. R. (1972). Rates and Extents of Hydrolysis of Several Caseins by Pepsin, Rennin, Endothia parasitica Protease and Mucor pusillus Protease. *Journal of Dairy Science*, *55*(11), 1523–1531. https://doi.org/10.3168/jds.S0022-0302(72)85714-X

Tercinier, L., Ye, A., Anema, S. G., Singh, A., & Singh, H. (2014). Interactions of Casein Micelles with Calcium Phosphate Particles. *Journal of Agricultural and Food Chemistry*, *62*(25), 5983–5992. https://doi.org/10.1021/jf5018143

Thompkinson, D. K., & Kharb, S. (2007). Aspects of Infant Food Formulation. *Comprehensive Reviews in Food Science and Food Safety*, *6*(4), 79–102. https://doi.org/10.1111/j.1541-4337.2007.00020.x

Timby, N., Hernell, O., Vaarala, O., Melin, M., Lönnerdal, B., & Domellöf, M. (2015). Infections in Infants Fed Formula Supplemented With Bovine Milk Fat Globule Membranes. *Journal of Pediatric Gastroenterology and Nutrition*, *60*(3). https://journals.lww.com/jpgn/Fulltext/2015/03000/Infections_in_Infants_Fed_Formula_Supplemented.24.aspx

Tobey, N., Heizer, W., Yeh, R., Huang, T.-I., & Hoffner, C. (1985). Human Intestinal Brush Border Peptidases. *Gastroenterology*, *88*(4), 913–926. https://doi.org/10.1016/S0016-5085(85)80008-1

Tolkach, A., & Kulozik, U. (2007). Reaction kinetic pathway of reversible and irreversible thermal denaturation of β-lactoglobulin. *Le Lait*, *87*(4–5), 301–315. https://doi.org/10.1051/lait:2007012

Tomita, M., Wakabayashi, H., Yamauchi, K., Teraguchi, S., & Hayasawa, H. (2002). Bovine lactoferrin and lactoferricin derived from milk: Production and applications. *Biochemistry and Cell Biology*, *80*(1), 109–112. Scopus. https://doi.org/10.1139/o01-230

Tomita, Mamoru, Bellamy, W., Takase, M., Yamauchi, K., Wakabayashi, H., & Kawase, K. (1991). Potent Antibacterial Peptides Generated by Pepsin Digestion of Bovine Lactoferrin. *Journal of Dairy Science*, *74*(12), 4137–4142. https://doi.org/10.3168/jds.S0022-0302(91)78608-6

Townend, R., Herskovits, T. T., Timasheff, S. N., & Gorbunoff, M. J. (1969). The state of amino acid residues in β-lactoglobulin. *Archives of Biochemistry and Biophysics*, *129*(2), 567–580. https://doi.org/10.1016/0003-9861(69)90216-1

Tran, H., Datta, N., Lewis, M. J., & Deeth, H. C. (2008). Predictions of some product parameters based on the processing conditions of ultra-high-temperature milk plants. *International Dairy Journal*, *18*(9), 939–944. https://doi.org/10.1016/j.idairyj.2008.01.006

Tunick, M. H., Ren, D. X., Van Hekken, D. L., Bonnaillie, L., Paul, M., Kwoczak, R., & Tomasula, P. M. (2016). Effect of heat and homogenization on in vitro digestion of milk. *Journal of Dairy Science*, *99*(6), 4124–4139. https://doi.org/10.3168/jds.2015-10474

Turck, D., Vidailhet, M., Bocquet, A., Bresson, J., Briend, A., Chouraquif, J., Darmaun, D., Dupont, C., Frelut, M.-L., Girardet, J., Goulet, O., Hankard, R., Rieu, D., & Simeoni, U. (2013). Breastfeeding: Health benefits for child and mother. *Archives de Pédiatrie*, *20*, 529–548.

Turner, R. B., & Kelsey, D. K. (1993). Passive immunization for prevention of rotavirus illness in healthy infants. *The Pediatric Infectious Disease Journal*, *12*(9). https://journals.lww.com/pidj/Fulltext/1993/09000/Passive_immunization_for_prevention_of_rotavirus.3.aspx

Uauy, R., Quan, R., & Gil, A. (1994). Role of Nucleotides in Intestinal Development and Repair: Implications for Infant Nutrition. *The Journal of Nutrition*, *124*(suppl_8), 1436S-1441S. https://doi.org/10.1093/jn/124.suppl_8.1436S

UNICEF. (2018). *Breastfeeding; a mother's gift, for every child*. https://www.unicef.org/publications/files/UNICEF_Breastfeeding_A_Mothers_Gift_for_Every_Child.pdf

UNICEF, & WHO. (2017). *Global breastfeeding scorecard: Tracking progress for breastfeeding policies and programmes*. https://www.who.int/nutrition/publications/infantfeeding/global-bf-scorecard-2017.pdf?ua=1

Van Boekel, M. A. J. S. (1998). Effect of heating on Maillard reactions in milk. *Food Chemistry*, *62*(4), 403–414. https://doi.org/10.1016/S0308-8146(98)00075-2

van de Looij, Y., Ginet, V., Chatagner, A., Toulotte, A., Somm, E., Hüppi, P. S., & Sizonenko, S. V. (2014). Lactoferrin during lactation protects the immature hypoxic-ischemic rat brain. *Annals of Clinical and Translational Neurology*, *1*(12), 955–967. https://doi.org/10.1002/acn3.138

Vardhanabhuti, B., & Foegeding, E. A. (1999). Rheological Properties and Characterization of Polymerized Whey Protein Isolates. *Journal of Agricultural and Food Chemistry*, *47*(9), 3649–3655. https://doi.org/10.1021/jf981376n

Vasbinder, A. J., Alting, A. C., & de Kruif, K. G. (2003). Quantification of heat-induced casein–whey protein interactions in milk and its relation to gelation kinetics. *Colloids and Surfaces B: Biointerfaces*, *31*(1–4), 115–123. https://doi.org/10.1016/S0927-7765(03)00048-1

Vasbinder, A. J., & de Kruif, C. G. (2003). Casein–whey protein interactions in heated milk: The influence of pH. *International Dairy Journal*, *13*(8), 669–677. https://doi.org/10.1016/S0958-6946(03)00120-1

Vasbinder, A.J., Van Mil, P.J.J.M., Bot, A., de Kruif, K.G. (2001). Acid-induced gelation of heat-treated milk studied by diffusing wave spectroscopy. *Colloids and Surfaces B: Biointerfaces*, *21*, 245–250. https://doi.org/10.1016/S0927-7765(01)00177-1

Verheul, M., Roefs, S. P. F. M., & De Kruif, K. G. (1998). Kinetics of Heat-Induced Aggregation of βLactoglobulin. *Journal of Agricultural and Food Chemistry*, *46*(3), 896–903. Scopus. https://doi.org/10.1021/jf970751t

Verruck, S., Sartor, S., Marenda, F., Barros, E., Camelo-Silva, C., Canella, M. H., & Prudencio, E. (2019). *Influence of Heat Treatment and Microfiltration on the Milk Proteins Properties*. *5*, 54–66. https://doi.org/10.17140/AFTNSOJ-5-157

Victora, C. G., Bahl, R., Barros, A. J. D., França, G. V. A., Horton, S., Krasevec, J., Murch, S., Sankar, M. J., Walker, N., & Rollins, N. C. (2016). Breastfeeding in the 21st century: Epidemiology, mechanisms, and lifelong effect. *The Lancet*, *387*(10017), 475–490. https://doi.org/10.1016/S0140-6736(15)01024-7

Villa, C., Costa, J., Oliveira, M. B. P. P., & Mafra, I. (2018). Bovine Milk Allergens: A Comprehensive Review: Bovine milk allergens…. *Comprehensive Reviews in Food Science and Food Safety*, *17*(1), 137–164. https://doi.org/10.1111/1541-4337.12318

Vors, C., Capolino, P., Guérin, C., Meugnier, E., Pesenti, S., Chauvin, M.-A., Monteil, J., Peretti, N., Cansell, M., Carrière, F., & Michalski, M.-C. (2012). Coupling in vitro gastrointestinal lipolysis and Caco-2 cell cultures for testing the absorption of different food emulsions. *Food & Function*, *3*, 537–546. https://doi.org/10.1039/c2fo10248j

Wack, R. P., Lien, E. L., Taft, D., & Roscelli, J. D. (1997). Electrolyte composition of human breast milk beyond the early postpartum period. *Nutrition*, *13*(9), 774–777. https://doi.org/10.1016/S0899-9007(97)00187-1

Wada, Y., & Lönnerdal, B. (2014). Effects of Different Industrial Heating Processes of Milk on Site-Specific Protein Modifications and Their Relationship to in Vitro and in Vivo Digestibility. *Journal of Agricultural and Food Chemistry*, *62*(18), 4175–4185. https://doi.org/10.1021/jf501617s

Wada, Y., & Lönnerdal, B. (2015). Bioactive peptides released from in vitro digestion of human milk with or without pasteurization. *Pediatric Research*, *77*(4), 546–553. https://doi.org/10.1038/pr.2015.10

Wada, Y., Phinney, B. S., Weber, D., & Lönnerdal, B. (2017). In vivo digestomics of milk proteins in human milk and infant formula using a suckling rat pup model. *Peptides*, *88*, 18–31. https://doi.org/10.1016/j.peptides.2016.11.012

Wagner, S., Kersuzan, C., Gojard, S., Tichit, C., Nicklaus, S., Geay, B., Humeau, P., Thierry, X., Charles, M.-A., & Lioret, S. (2015). *Durée de l'allaitement en France selon les caractéristiques des parents et de la naissance. Résultats de l'étude longitudinale française Elfe, 2011*. 22.

Wakabayashi, H., Yamauchi, K., & Takase, M. (2006). Lactoferrin research, technology and applications. *Technological and Health Aspects of Bioactive Components of Milk*, *16*(11), 1241–1251. https://doi.org/10.1016/j.idairyj.2006.06.013

Wal, J.-M. (2002). Cow's milk proteins/allergens. *Annals of Allergy, Asthma & Immunology*, *89*(6, Supplement), 3–10. https://doi.org/10.1016/S1081-1206(10)62115-1

Wang, J., Wu, P., Liu, M., Liao, Z., Wang, Y., Dong, Z., & Chen, X. (2019). An advanced near real dynamic in vitro human stomach system to study gastric digestion and emptying of beef stew and cooked rice. *Food & Function*, *10*. https://doi.org/10.1039/C8FO02586J

Wang, M. (2016). Iron Deficiency and Other Types of Anemia in Infants and Children. *American Family Physician*, *93*, 270–278.

Wang, T., & Lucey, J. A. (2003). Use of Multi-Angle Laser Light Scattering and Size-Exclusion Chromatography to Characterize the Molecular Weight and Types of Aggregates Present in Commercial Whey Protein Products. *Journal of Dairy Science*, *86*(10), 3090–3101. https://doi.org/10.3168/jds.S0022-0302(03)73909-5

Wang, X., Ye, A., Lin, Q., Han, J., & Singh, H. (2018). Gastric digestion of milk protein ingredients: Study using an in vitro dynamic model. *Journal of Dairy Science*, *101*(8), 6842–6852. https://doi.org/10.3168/jds.2017-14284

Watanabe, K., & Klostermeyer, H. (1976). Heat-induced changes in sulphydryl and disulphide levels of β-lactoglobulin A and the formation of polymers. *Journal of Dairy Research*, *43*(3), 411–418. Cambridge Core. https://doi.org/10.1017/S0022029900015995

Wazed, & Farid. (2019). Hypoallergenic and Low-Protein Ready-to-Feed (RTF) Infant Formula by High Pressure Pasteurization: A Novel Product. *Foods*, *8*(9), 408. https://doi.org/10.3390/foods8090408

Wazed, M. A., Ismail, M., & Farid, M. (2020). Pasteurized ready-to-feed (RTF) infant formula fortified with lactoferrin: A potential niche product. *Journal of Food Engineering*, *273*, 109810. https://doi.org/10.1016/j.jfoodeng.2019.109810

Weber, M., Grote, V., Closa-Monasterolo, R., Escribano, J., Langhendries, J.-P., Dain, E., Giovannini, M., Verduci, E., Gruszfeld, D., Socha, P., Koletzko, B., & for The European Childhood Obesity Trial Study Group. (2014). Lower protein content in infant formula reduces BMI and obesity risk at school age: Follow-up of a randomized trial. *The American Journal of Clinical Nutrition*, *99*(5), 1041–1051. https://doi.org/10.3945/ajcn.113.064071

Wehbi, Z., Pérez, M.-D., Sánchez, L., Pocoví, C., Barbana, C., & Calvo, M. (2005). Effect of Heat Treatment on Denaturation of Bovine α-Lactalbumin: Determination of Kinetic and Thermodynamic Parameters. *Journal of Agricultural and Food Chemistry*, *53*(25), 9730–9736. https://doi.org/10.1021/jf050825y

WHO. (2007). *Safe Preparation, Storage and Handling of Powdered Infant Formula Guidlines*.

Wijayanti, H. B., Bansal, N., & Deeth, H. C. (2014). Stability of Whey Proteins during Thermal Processing: A Review. *Comprehensive Reviews in Food Science and Food Safety*, *13*(6), 1235–1251. https://doi.org/10.1111/1541-4337.12105

Wijayanti, H. B., Brodkorb, A., Hogan, S. A., & Murphy, E. G. (2019). Chapter 6—Thermal Denaturation, Aggregation, and Methods of Prevention. In H. C. Deeth & N. Bansal (Eds.), *Whey Proteins* (pp. 185–247). Academic Press. https://doi.org/10.1016/B978-0-12-812124-5.00006-0

Wittgren, B., Borgström, J., Piculell, L., & Wahlund, K. G. (1998). Conformational change and aggregation of κ-carrageenan studied by flow field-flow fractionation and multiangle light scattering. *Biopolymers*, *45*(1). https://doi.org/10.1002/(SICI)1097-0282(199801)45:1<85::AID-BIP7>3.0.CO;2-V

Wolz, M., & Kulozik, U. (2015). Thermal denaturation kinetics of whey proteins at high protein concentrations. *International Dairy Journal*, *49*, 95–101. https://doi.org/10.1016/j.idairyj.2015.05.008

World Health Organization. (2006). *Enterobacter sakazakii and Salmonella in powdered infant formula: Meeting report*. WHO IRIS. https://apps.who.int/iris/handle/10665/43547

World Health Organization, & UNICEF. (2003). *Global Strategy for Infant and Young Child Feeding*. http://apps.who.int/iris/bitstream/10665/42590/1/9241562218.pdf?ua=1&ua=1

Wu, S., Grimm, R., German, J. B., & Lebrilla, C. B. (2011). Annotation and Structural Analysis of Sialylated Human Milk Oligosaccharides. *Journal of Proteome Research*, *10*(2), 856–868. https://doi.org/10.1021/pr101006u

Ye, A., Cui, J., Carpenter, E., Prosser, C., & Singh, H. (2019). Dynamic in vitro gastric digestion of infant formulae made with goat milk and cow milk: Influence of protein composition. *International Dairy Journal*, *97*, 76–85. https://doi.org/10.1016/j.idairyj.2019.06.002

Ye, A., Cui, J., Dalgleish, D., & Singh, H. (2016). Formation of a structured clot during the gastric digestion of milk: Impact on the rate of protein hydrolysis. *Food Hydrocolloids*, *52*, 478–486. https://doi.org/10.1016/j.foodhyd.2015.07.023

Ye, A., Cui, J., Dalgleish, D., & Singh, H. (2017). Effect of homogenization and heat treatment on the behavior of protein and fat globules during gastric digestion of milk. *Journal of Dairy Science*, *100*(1), 36–47. https://doi.org/10.3168/jds.2016-11764

Ye, A., Liu, W., Cui, J., Kong, X., Roy, D., Kong, Y., Han, J., & Singh, H. (2019). Coagulation behaviour of milk under gastric digestion: Effect of pasteurization and ultra-high temperature treatment. *Food Chemistry*, *286*, 216–225. https://doi.org/10.1016/j.foodchem.2019.02.010

Ye, A., Roy, D., & Singh, H. (2020). Chapter 19—Structural changes to milk protein products during gastrointestinal digestion. In M. Boland & H. Singh (Eds.), *Milk Proteins (Third Edition)* (pp. 671–700). Academic Press. https://doi.org/10.1016/B978-0-12-815251-5.00019-0

Ye, A., Singh, H., Taylor, M. W., & Anema, S. (2004). Interactions of whey proteins with milk fat globule membrane proteins during heat treatment of whole milk. *Le Lait*, *84*(3), 269–283. https://doi.org/10.1051/lait:2004004

Yogman, M. W., Zeisel, S. H., & Roberts, C. (1982). Assessing effects of serotonin precursors on newborn behavior. *Journal of Psychiatric Research*, *17*(2), 123–133. https://doi.org/10.1016/0022-3956(82)90014-0

Zenker, H. E., van Lieshout, G. A. A., van Gool, M. P., Bragt, M. C. E., & Hettinga, K. A. (2020). Lysine blockage of milk proteins in infant formula impairs overall protein digestibility and peptide release. *Food & Function*, *11*(1), 358–369. https://doi.org/10.1039/C9FO02097G

Zhang, H., & Lyden, D. (2019). Asymmetric-flow field-flow fractionation technology for exomere and small extracellular vesicle separation and characterization. *Nature Protocols*, *14*(4), 1027–1053. https://doi.org/10.1038/s41596-019-0126-x

Zhang, Q., Cundiff, J., Maria, S., McMahon, R., Wickham, M., Faulks, R., & Tol, E. (2014). Differential Digestion of Human Milk Proteins in a Simulated Stomach Model. *Journal of Proteome Research*, *13*, 1055–1064. https://doi.org/10.1021/pr401051u

Zhang, S., & Vardhanabhuti, B. (2014). Effect of initial protein concentration and pH on in vitro gastric digestion of heated whey proteins. *Food Chemistry*, *145*, 473–480. https://doi.org/10.1016/j.foodchem.2013.08.076

Zhang, X., Fu, X., Zhang, H., Liu, C., Jiao, W., & Chang, Z. (2005). Chaperone-like activity of β-casein. *The International Journal of Biochemistry & Cell Biology*, *37*(6), 1232–1240. https://doi.org/10.1016/j.biocel.2004.12.004

Zhang, Z., Arrighi, V., Campbell, L., Lonchamp, J., & Euston, S. R. (2016). Properties of partially denatured whey protein products 2: Solution flow properties. *Food Hydrocolloids*, *56*, 218–226. https://doi.org/10.1016/j.foodhyd.2015.12.012

Zhao, H., Brown, P. H., & Schuck, P. (2011). On the Distribution of Protein Refractive Index Increments. *Biophysical Journal*, *100*(9), 2309–2317. https://doi.org/10.1016/j.bpj.2011.03.004

Zimm, B. H. (1948). The Scattering of Light and the Radial Distribution Function of High Polymer Solutions. *Journal of Chemical Physics*, *16*, 1093. https://doi.org/10.1063/1.1746738

Zoppi, G., Andreotti, G., Pajno-Ferrara, F., Bellini, P., & Gaburro, D. (1973). The Development of Specific Responses of the Exocrine Pancreas to Pancreozymin and Secretin Stimulation in Newborn Infants. *Pediatric Research*, *7*(4), 198–203. https://doi.org/10.1203/00006450-197304000-00023

Zúñiga, R. N., Tolkach, A., Kulozik, U., & Aguilera, J. M. (2010). Kinetics of formation and physicochemical characterization of thermally-induced β-Lactoglobulin aggregates. *Journal of Food Science*, *75*(5), E261–E268. Scopus. https://doi.org/10.1111/j.1750-3841.2010.01617.x